Appendix A
Phase 1 Modeling Preliminary Results

BAYOU LAFOURCHE DIVERSION STUDY
PHASE I MODELING RESULTS

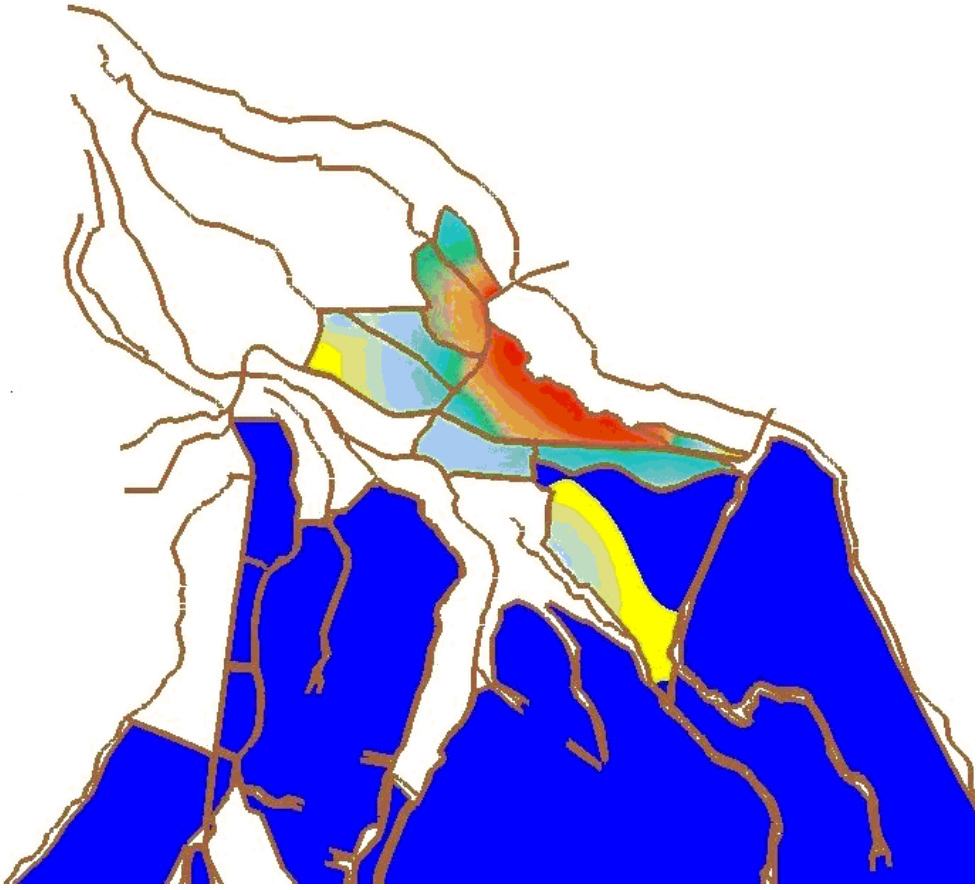

August 11, 2005

BAYOU LAFOURCHE DIVERSION STUDY
PHASE I MODELING RESULTS

Prepared for the

Louisiana Department of Natural Resources,
Coastal Restoration Division

under subcontract with
CH2M Hill
1515 Poydras, Suite 2110
New Orleans, LA 70112

Prepared by

FTN Associates, Ltd.
3 Innwood Circle, Suite 220
Little Rock, AR 72211

August 11, 2005

EXECUTIVE SUMMARY

The areas benefited by the Bayou Lafourche Division project as identified in "Evaluation of Bayou Lafourche Wetlands Restoration Project" (United States Environmental Protection Agency, 1998) (Figure 1.2) were re-evaluated given the limitations of the previous modeling. Marsh surveys required for accurate determination of salinity reductions for the identified benefited areas would have been cost prohibitive. Consequently, a new model that more accurately represented the forces driving flows in the Terrebonne and Barataria basins was developed to determine the benefit areas. This work constituted Phase I of a two-phase approach that was adopted so that project survey funds could be used judiciously. In Phase II, new surveys will be made to improve the model.

Examination of the tide records for stations in the area (Figure 1.3) showed that tides peak higher and earlier from west to east (Figure 1.4). This causes flow in the Gulf Intracoastal Waterway (GIWW) to flow from west to east, except during storms when the normal tidal forcing can be reversed. During the 8 month period over which hourly data was collected the flow was in an easterly direction 93% of the time (Figure 1.5). This observation coupled with the flow, stage, and salinity record available at the only connection between the two basins (intersection of the GIWW and Bayou Lafourche) allowed the computational mesh to be reduced to represent only the Terrebonne basin, thus reducing simulation times from weeks to days. This allowed the model to be quickly calibrated to observed flow, water surface elevation (WSEL), and salinity data from May – June, 2004.

Several tracer simulations were run that showed the movement of Bayou Lafourche water. These simulations showed that very little of the tracer moved south of the GIWW. Flow moving south down the Company Canal or Bayou Lafourche is largely captured by the GIWW and moved eastward due to the larger conveyance capacity and eastward momentum of the GIWW.

The model will be improved in Phase II by collecting survey data in several marsh areas and used to evaluate several operational scenarios. In Phase II, the model can also be used to

investigate channel improvements that would be required to move freshwater flows south of the GIWW.

TABLE OF CONTENTS

TABLE OF CONTENTS (CONTINUED)

LIST OF APPENDICES

LIST OF TABLES

LIST OF FIGURES

1.0 INTRODUCTION

The Coastal Wetlands Planning Protection and Restoration Act (CWPPRA) Program is assessing the benefit of diverting Mississippi River flows into Bayou Lafourche while maintaining or potentially increasing current water levels in the bayou. Numerical modeling is being used to evaluate the different alternatives for this project, the Mississippi River Water Reintroduction into Bayou Lafourche Project (Louisiana Department of Natural Resources (LDNR) (Project). This report describes the modeling effort for Phase I of two phases of work to be completed for the project.

1.1 Study Approach

The original Louisiana LDNR Scope of Services for the Project was based on the previous modeling which showed that some of the benefited areas were in the southernmost portions of the Barataria and Terrebonne basins. The survey effort to develop the detailed bathymetry required to accurately model an area that large would have been cost-prohibitive.

In addition, a review of the modeling upon which the benefits were based (LDNR 1999) revealed that the one-dimensional (1D) dynamic wave model UNET (HEC 2001) simulations were made in steady state mode without any representation of the interaction between the channels and marsh areas and without any water quality transport. By running only steady state flows and constant boundary elevations in the model, the effect of tides that move water in and out of the system on a diurnal basis were not accounted for. The model also excluded complex interactions of flow between the channels and marshes in the area that affects the distribution of flows in the interconnecting canals. The net effect of not including these components in the model was to inaccurately represent the movement of the freshwater in the channels and bias the interpretation of benefited areas. The benefited areas identified by the previous modeling (United States Environmental Protection Agency (USEPA) 1998) are shown in Figure 1.2.

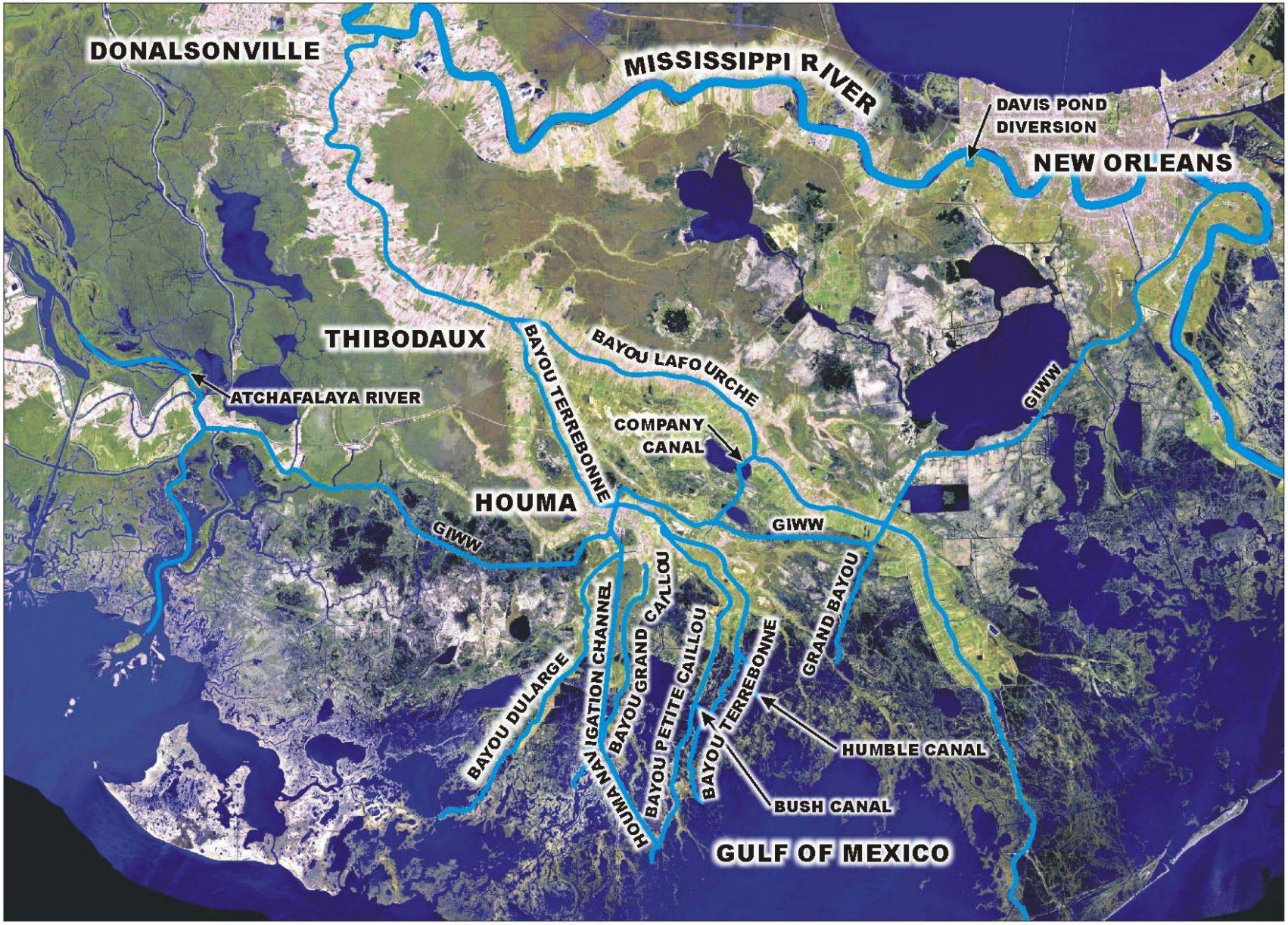

Figure 1.1. Vicinity map showing major waterways within the system modeled.

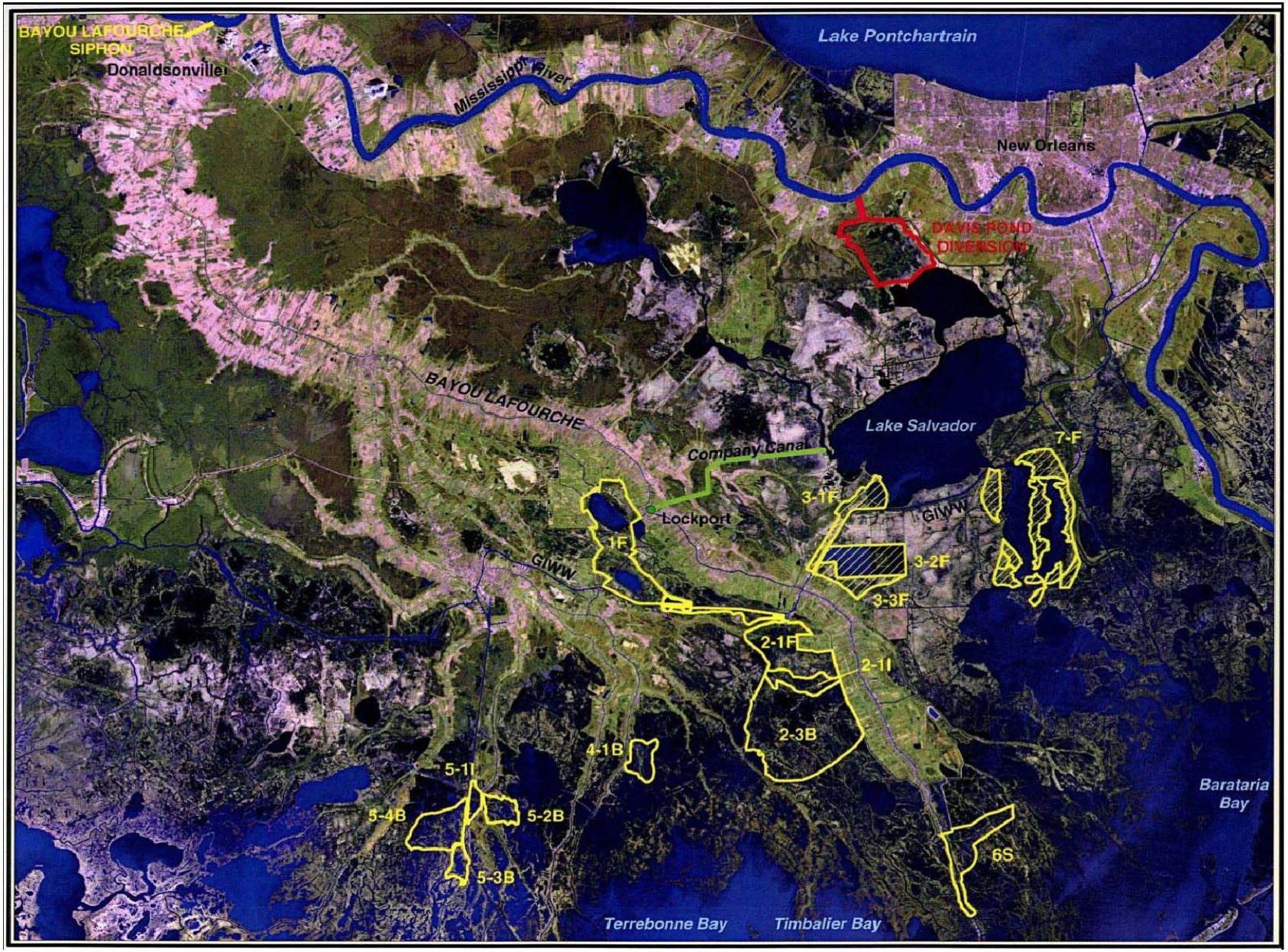

Figure 1.2. Benefit areas from US EPA (1998).

Without including water quality transport, benefits were assumed to occur wherever flow increases were predicted. However, flow increases could be due to displaced ambient or Gulf water, not to the transport of freshwater. The previous modeling did not show where the freshwater was transported.

Consequently, an alternative Scope of Services was developed. The modeling was divided into two phases. Preliminary modeling was conducted in Phase I with limited new channel surveys and only existing marsh topographic data. The purpose of the Phase I modeling was to identify the marsh areas that actually receive the freshwater flows (i.e., from the diversion or the displaced flows from the Gulf Intracoastal Waterway (GIWW)). Once the marsh areas are identified that receive the freshwater flows, surveys will be augmented as necessary in Phase II. Then in Phase II, the model will be improved by incorporating the surveys into the marsh bathymetry so that the amount of freshening can be quantified.

This two-phased approach will eliminate collecting expensive survey information in the remote areas of the project area where freshwater does not reach. It will also potentially reduce the area to be modeled, saving in the analysis effort. Another advantage of the phased approach is that minimal effort is required over that specified in the original Scope of Services except for two additional simulations to determine where the freshwater flows.

1.2 Description of the Project Area

Bayou Lafourche divides the portions of the two basins that comprise the study area: the Barataria and Terrebonne basins (Figure 1.1). The Barataria basin lies to the east of Bayou Lafourche with the Terrebonne basin to the west. The study area boundaries are roughly the Mississippi River to the north and east, Bayou duLarge to the west, and the Gulf of Mexico to the south. The only hydrologic interconnections between the Terrebonne and Barataria basins are at the GIWW and Company Canal.

The forces that drive flow within the system are

- Gulf tides,
- Mississippi River diversion flows at the Davis Pond Diversion Structure,
- Flow that is pumped into the headwater of Bayou Lafourche,
- Wind,

- Precipitation, and
- Atchafalaya River flows that move into the system via the GIWW.

Direct precipitation was included for model calibration; runoff from adjacent areas is negligible and was not included.

Examination of the tide records for stations in the area (Figure 1.3) showed that tides peak higher and earlier from west to east (Figure 1.4). This causes flow in the GIWW to flow from west to east, except during storms when the normal tidal forcing may be reversed. During the 8 month period over which hourly data was collected (January through August 2004) the flow was in an easterly direction 93% of the time (Figure 1.5).

The GIWW acts as an interceptor for the five main waterways that convey flow north and south within the Terrebonne basin (the Houma Navigation Canal (HNC), Grand Bayou, Bayou Petite Caillou, Bayou Grand Caillou, and Bayou Terrebonne).

Forced drainage areas (leveed areas under pump) are common in the Terrebonne basin and are generally attached to the natural levees along the bayous and extend into the adjacent marsh. As such, they are hydraulically isolated and were not included in the study.

Relatively shallow marshes and channels dominate both basins. The marshes exhibit little vertical variation in velocity, density and salinity and can be considered two-dimensional (2D). The channels in the Terrebonne basin generally can be considered 1D since no significant vertical or lateral variation occurs hydrodynamically. In the Barataria basin the main north-south flow path is a series of wide interconnected lakes and generally can be considered 2D with only small variations vertically. The only exception to this characterization is when salt wedges move upstream in deeper channels (e.g., the HNC) causing a vertically stratified flow regime. However, this generally only occurs during extreme headwater low flow conditions, a condition that will not be considered in the Phase 1 portion of the study.

Figure 1.3. Tidal gage locations.

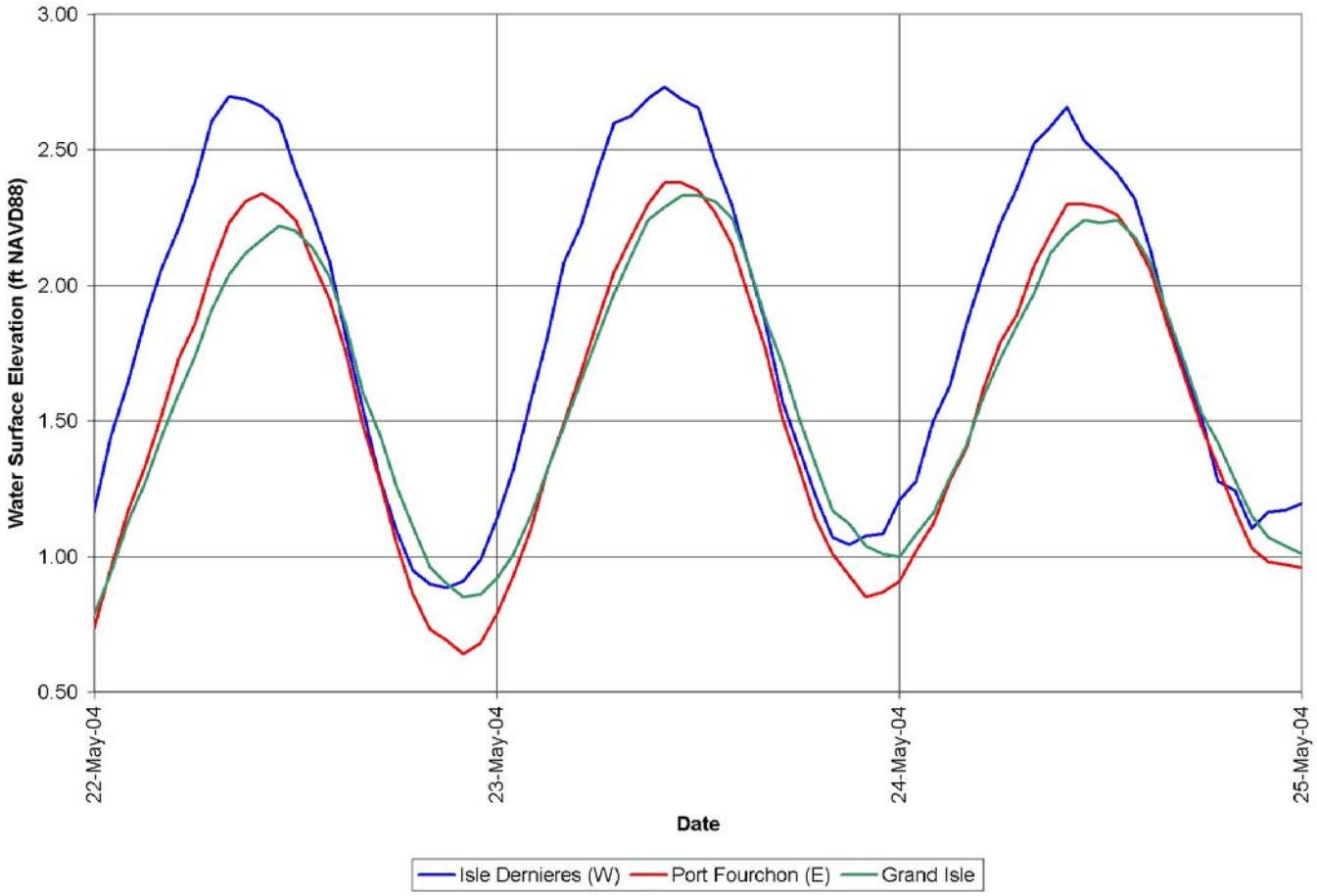

Figure 1.4. Tidal cycles with peaks occurring earlier and higher at the western tidal stations.

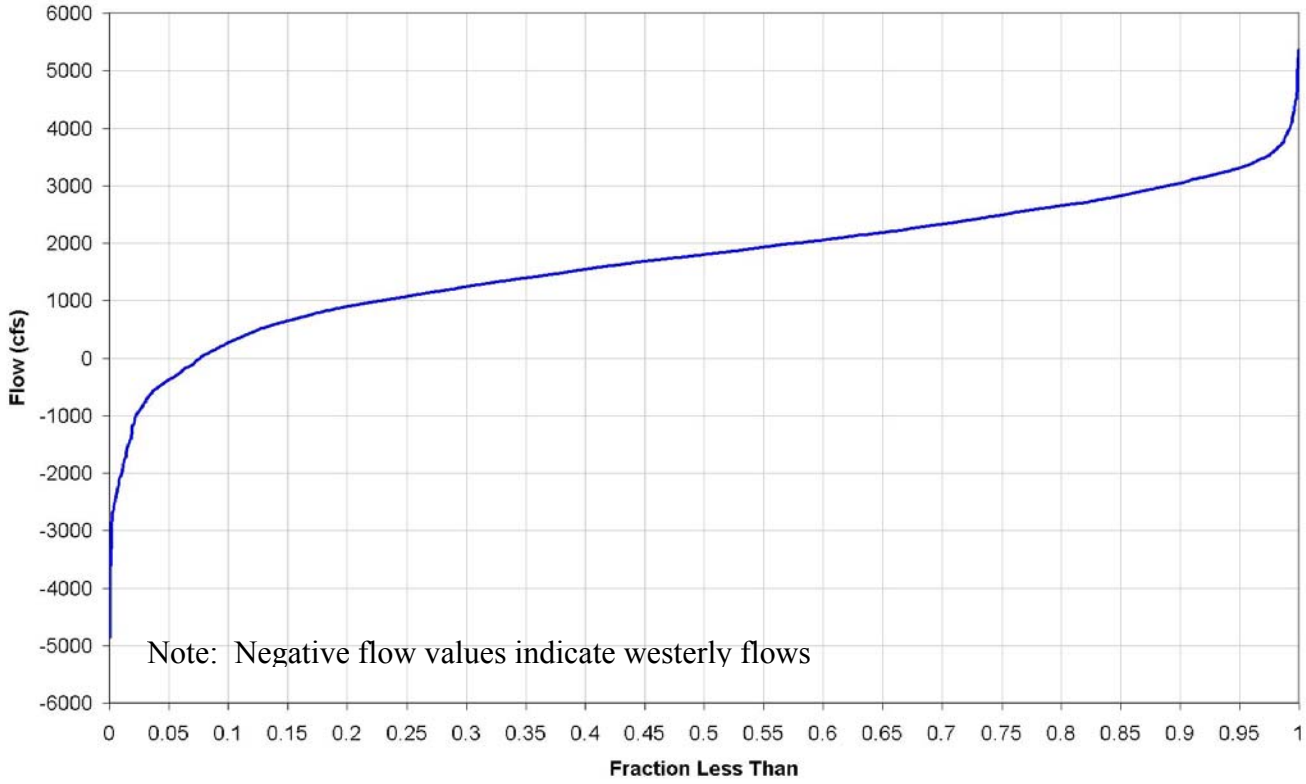

Figure 1.5. Cumulative frequency distribution of hourly flows in the GIWW at Larose.

2.0 MODEL DESCRIPTION

2.1 Model Selection

A 2D vertically-averaged hydrodynamic transport model was deemed appropriate for representing the Terrebonne and Barataria basins (Section 1.2). Although, at times, portions of the system may be three-dimensional (3D), they are the exception rather than the rule and are not representative of the conditions to be modeled.

Modeling was initiated using the TABS-MD modeling system (RMA-2 and RMA-4) (US Army Corps of Engineers Engineering Research and Development Center, 2000) and the Surface Water Modeling System (SMS) (Brigham Young University, 2004). TABS-MD is distributed by the Engineering Research Development Center (ERDC) (formerly the Waterways Experiment Station) of the US Army Corps of Engineers. SMS is a pre/post-processing interface developed by ERDC and the Environmental Modeling Research Laboratory at Brigham Young University. However, this study required that several unique features be added that were not in the ERDC version of TABS-MD. Consequently, Dr. Ian King's version of the RMA modeling suite (RMA-2 hydrodynamic and RMA-11 water quality models) (King 2005) was used. Dr. King was co-author of the code the ERDC version of TABS-MD is based on. His latest version was selected because:

- Dr. King was available to add the necessary project-specific features (Section 3.2) to the model code in a short time frame (he is one of the original model's developers), and
- Dr. King's version had other enhancements that promoted model stability and allowed greater flexibility in modeling the system (Sections 3.5.3 and 3.5.4).

2.2 Assumptions and Limitations

RMA-2/RMA-11 is a finite element model designed for simulation of flow and water quality in rivers, estuaries, and coastal systems. RMA-2 solves the vertically averaged equations of continuity and momentum using the Galerkin Method of weighted residuals to calculate time-varying velocities, elevations, and flows. A 1D representation of system geometry is also accommodated using the area-integrated 1D shallow water equations. Flow is assumed to be

subcritical with a free water surface; vertical accelerations are assumed negligible. The model incorporates a fully non-linear solution of the governing equations including terms for bed friction, turbulent viscosity, wind stresses, pressure gradient, and Coriolis forces.

This means that the model cannot represent:

- Stratified flows (e.g., salt wedge movement),
- Supercritical flows (high velocity, shallow depth flows that may occur near spillway outlets, in steep sloped channels, or in some areas where large constrictions in the channel may occur),
- Flows in long culverts or tunnels flowing full, or
- Flows in the immediate vicinity (near-field) of a pump station intake as well as other situations where the flow varies significantly with depth.

It also means that observed water surface elevation, velocity, and salinity data are required to calibrate the various model coefficients.

The finite element solution method allows the user to specify an irregular mesh of quadrilateral and triangular elements of varying sizes over the 2D areas of the system so spatial resolution may vary. In contrast, a finite difference grid for the same system would have many more elements to achieve the same resolution in the area of interest by the requirement that the grid be of uniform size, which results in a larger computational burden and longer simulation times.

One-dimensional elements (usually channels) may be connected to 2D elements to allow a transition from riverine to estuarine environments and to allow the representation of overbank flooding into areas where depth-averaged 2D circulation patterns are needed.

In this application, the following assumptions were also made:

- Winds are accounted for implicitly in the boundary conditions.
- The calibration data collected (Section 3.3) is representative of conditions to be evaluated in future simulations.
- The assumed bathymetry for the marsh areas in the Terrebonne basin is representative.

3.0 MODEL INPUT

The data required for model input are the finite element mesh, topography of the study area, flows or water surface elevations at the edges of the study area (boundary condition data), and model coefficients. In addition, several model options must be specified in order to properly represent the system.

3.1 Finite Element Mesh

The finite element mesh defines where results will be calculated and reported spatially within the system. The finite element mesh used for the project area is shown in Figure 3.1. This is the largest and most complex TABS model that has ever been constructed[1].

The finite element mesh for the Barataria basin was obtained from the New Orleans District (NOD) office of the US Army Corps of Engineers. It was developed for a TABS-MD model to evaluate the Myrtle Grove Siphon Project.

The finite element mesh for the Terrebonne basin was developed by FTN Associates, Ltd. (FTN) using 1998 georeferenced digital ortho quarter-quadrangle aerial photos as a guide to marsh boundaries and channel centerlines. It should be noted that numerous large areas (forced drainage areas) are excluded from the mesh because they are separated from the marsh by levees and are drained by pump stations (Section 1.2).

[1] Personal Communication, Ian King, PhD, author of RMA-2 and RMA-11, based on number of computational nodes, degree of wetting and drying of mesh, and length of marsh-channel exchange zones.

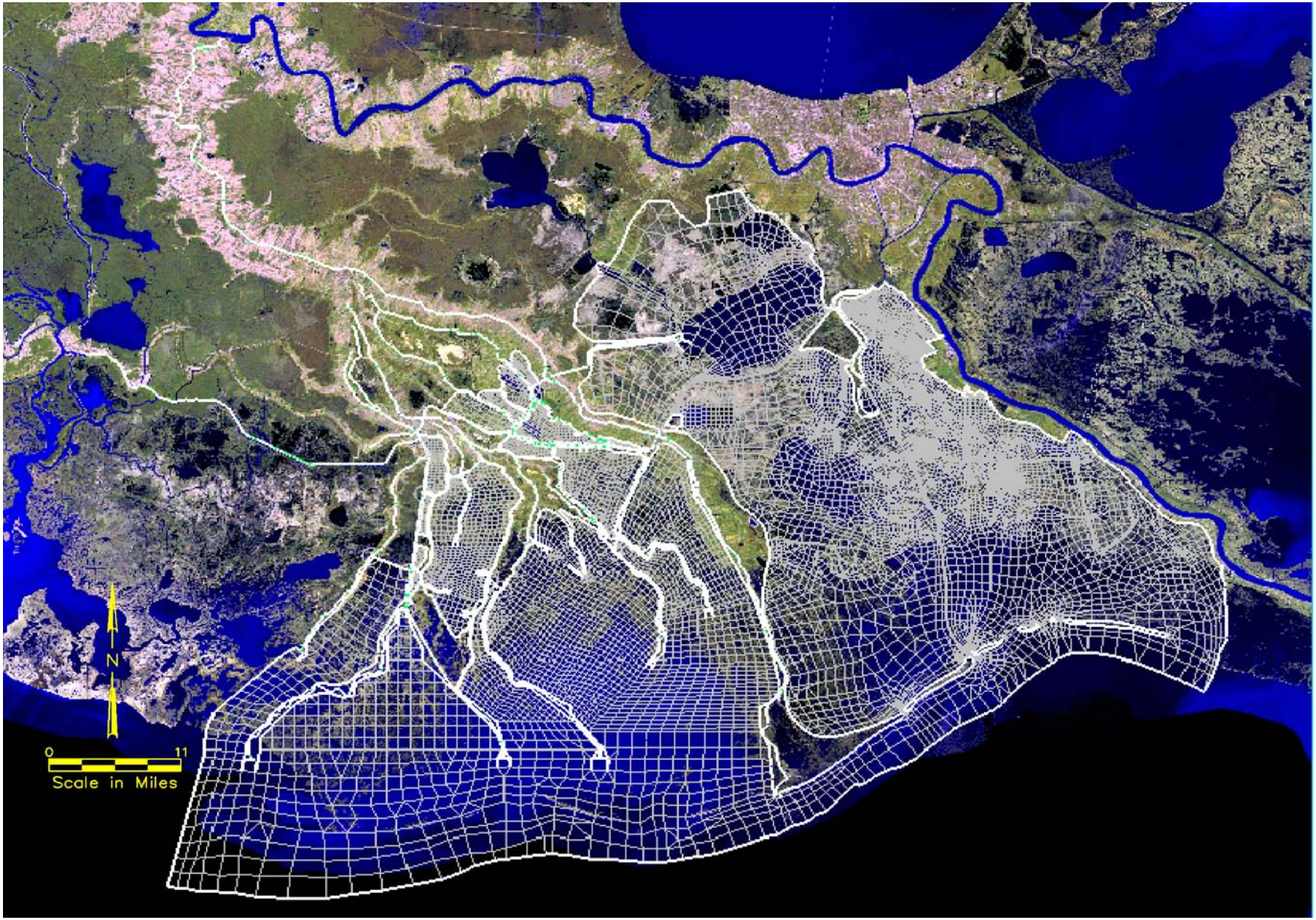

Figure 3.1. Initial finite element mesh for the study area.

3.2 System Topography

In terms of topography, the system has two distinct features, namely canals and marshes. In the model the canals are represented using over 120 newly surveyed cross sections for Bayou Lafourche, Company Canal, the GIWW, and portions of Grand Bayou. Topography for the rest of the channels was represented using 740 surveyed cross sections from the US Army Corps of Engineers' Morganza to the Gulf Feasibility Study (US Army Corps of Engineers NOD 2000) UNET model. These sections were adjusted vertically as necessary to tie them into the Louisiana Coastal Zone Primary GPS network. New marsh surveys were not included in Phase I as explained in Section 1.1 - only data from existing models and surveys were used. Existing data were only available for the Barataria basin; consequently, bathymetry had to be assumed for the Terrebonne basin. A sensitivity analysis was performed to determine the effect of this assumption on model results (Section 4.2.2).

In Phase I it was critical that the flow distributions at channel intersections be modeled properly. In Phase II water surface elevations in the upper reaches of Bayou Lafourche will need to be accurately modeled to assess the impact of increased flows from the introduction of freshwater. These requirements meant the capabilities of the existing RMA-2 program would need revision. Previously in RMA-2, 1D channels could only be represented by certain regular shapes (e.g., trapezoidal, triangular, rectangular). In this study, however, preliminary testing (Section 4.1.2) showed that improved computed water surface elevations and flows would result from refined representation of the channels. Representing the channels with 2D elements would add considerable computational overhead and stability problems. Therefore, RMA-2 was modified to read in tables of elevation versus cross-sectional area and top widths that were computed using detailed cross section points for 1D elements. The tables were computed using the same algorithms used in HEC-RAS (HEC 2002) and in the UNET (HEC 2001) preprocessor program CSECT.

The only available useful topographic data for the marsh areas was in the Barataria basin. This consisted of bathymetry from another RMA-2 model created by the NOD to evaluate the Myrtle Grove Siphon Project. LDNR collected eight transects in the large open water areas of the

basin for the Barataria Basin Feasibility Study. The NOD Barataria basin bathymetry was updated in these areas.

3.3 Boundary Conditions

The hydrodynamics and the salinity transport in a modeled system are driven by the forces applied to the system via flow and salinity entering or leaving it at the boundaries. Continuous readings of water surface elevations and salinity data were collected over a period of 8 months at several locations in and around the study area. Figure 3.2 shows the locations and station identifiers of the gages where data was collected. Table 3.1 summarizes characteristics of the collected data sets.

The recorded data from the boundary gages (4, 10, and 18) were used to provide boundary input to the model. Data recorded at the internal gages (1 through 3, 5 through 8, and 15 through 17) were not part of the input to the model but were used to compare against simulated values produced by the model. Most of the newly installed gages were active during the period from February 2004 through August 2004 except for a few days or hours for some gages.

Before processing the observed data into the format readable by the RMA-2 modeling program, it was visually inspected to identify any artificial or erroneous values, revealed in most cases by spikes on the plots. Any spikes that were unrealistic were smoothed out.

Daily rainfall data were obtained from the Louisiana State University (LSU) Agricultural Center in Houma, Louisiana. These data were used as time-varying input to the model.

The original tidal gage locations were at Cocodrie, Dulac, and Grand Isle. However, it was determined that the Cocodrie and Dulac (data collection location 16 and 15 respectively) recorded water surface elevations did not accurately represent the tidal fluctuations along the Gulf of Mexico boundary in the Terrebourne basin. After investigating potential new sources of tidal gage data, gage data at Isle Dernieres and Port Fourchon provided by the LSU Coastal Studies Institute and the National Oceanic and Atmospheric Administration National Data Buoy Center, respectively, were obtained for use in the model instead. The location of the tidal stations are shown in Figure 1.3. The Isle Dernieres elevations were applied at the westernmost point of

the southern boundary. Port Fourchon data were applied near the outlet of Bayou Lafourche. The Grand Isle data were applied at the easternmost point. RMA-2 linearly interpolated between the three locations along the southern boundary. These interpolated data proved to provide the best representation of tidal forcing along the southern boundary.

Figure 1.4 shows that the tides peak earlier and higher from west to east. This differential drives flows in the GIWW from west to east, and is the reason why 93% of the observed hourly data over an 8 month period shows eastward flows in the GIWW (Figure 1.5).

3.4 Model Coefficients

Three important coefficients must be specified that affect model results. First, bottom and bank friction within the prototype is represented using Mannings 'n' roughness coefficients. Second, eddy viscosity represents the resistance of flow to changes in applied force. Third, the dispersion coefficient defines the spreading of a constituent due to differential shear within the water column. They vary spatially and were assigned initially based on engineering judgment and adjusted through the calibration process.

3.5 Model Options

3.5.1 One-dimensional Channels

As described in Section 3.2, a new capability was added to RMA-2 and used irregular cross sections instead of trapezoidal approximations to better represent channel geometry and allow more accurate water surface profiles and flow distributions to be calculated.

3.5.2 Channel Junctions

At channel intersections, junction elements were coded to use matching water surface elevations (element type 901) since the momentum conservation method (element type 903) proved to produce unrealistically large water surface elevation and flow differences at the intersections; this was due to the tendency for flows to change directions given the tidal influence of the Gulf.

3.5.3 Channel and Marsh/Swamp Interconnections

In the ERDC version of RMA-2, connections between 1D (channel) and 2D (marsh) elements is done using special "Transition Elements." For the dozens of miles of connectivity within this system these elements proved to be time-consuming to code and introduced stability and mass conservation problems in preliminary simulations.

Consequently, for this study, a new type of 1D to 2D connection technique was used in RMA-2 as described in King and Williams (1999). The technique forces elevations to match along the line of the 1D channel nodes and then treats these levels as elevation boundary conditions for the 2D portion of the mesh. The advantages of this technique are that the bounding 1D nodes are connected to the 2D nodes with a new quadrilateral element that 1) significantly reduces the mass conservation problems that can occur with Transition Elements, and 2) allows the full length of the overflow area to be represented.

3.5.4 Mesh Wetting/Drying

The Marsh Porosity option was used for handling element wetting and drying issues. This is a technique that allows a smooth transition computationally when shoreline elements vary between wet and dry states. This was used instead of the Element Elimination Method that requires much more refinement of the mesh in the shoreline areas in order for the solution to converge. This would result in significantly longer simulation times.

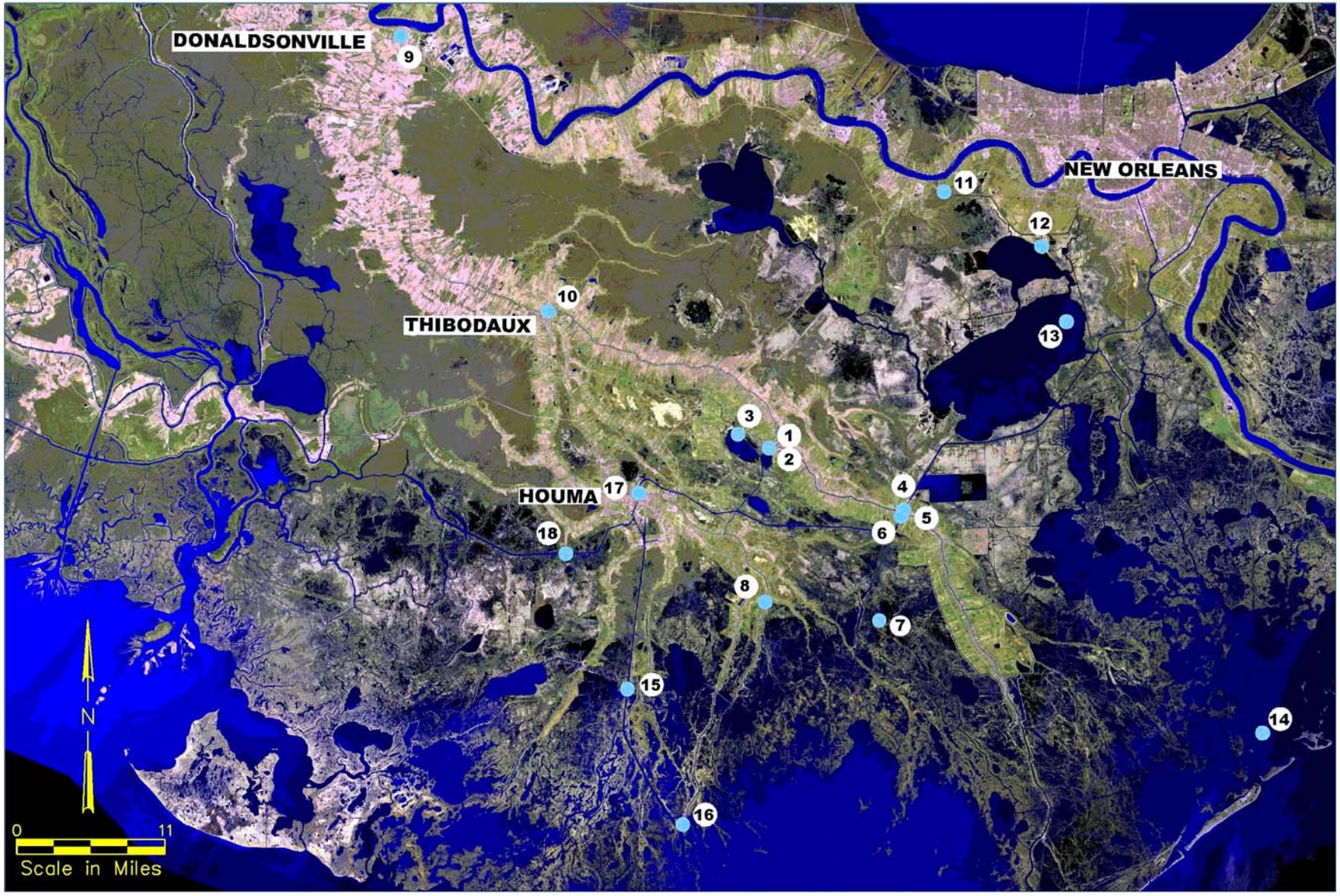

Figure 3.2. Data collection locations.

Table 3.1. Calibration data: stations, sampling duration and intervals.

Station No	Station Description	Starting Date	Ending Date	Sampling Interval	Collected Parameter[2]	Comments
1	Bayou Lafourche north of Company Canal	02/19/04	08/05/04	15MIN	ZCV	New installation
2	Company Canal at Highway 1 near Lockport	01/01/04	08/30/04	15MIN	ZC	USGS ID 7381350
3	Lake Fields	02/16/04	08/05/04	15MIN/1HR	ZC	New installation
4	GIWW East of Bayou Lafourche at Larose	02/15/04	08/06/04	15MIN	ZCV	New installation
5	Bayou Lafourche south of GIWW	02/12/04	08/06/04	15MIN	ZCV	New installation
6	GIWW West of Bayou Lafourche at Larose	01/01/04	08/30/04	15MIN	ZCVQ	USGS ID 7381235
7	Grand Bayou Marsh	02/16/04	08/06/04	15MIN	ZC	New installation
8	Bayou Terrebonne Southeast of Houma	02/13/04	08/06/04	15MIN	ZCV	New installation
9	Bayou Lafourche at Donaldsonville	01/01/04	08/30/04	15MIN	ZCVQ	USGS ID 7380401
10	Bayou Lafourche at Thibodaux	01/01/04	08/30/04	15MIN	ZVQ	USGS ID 7381000
11	Davis Pond Freshwater Diversion	01/01/04	08/30/04	15MIN	ZCVQ	USGS ID 90190400
12	Lake Cataouatche	01/01/04	08/30/04	15MIN	C	USGS ID 90901217
13	Lake Salvador	01/26/04	08/30/04	15MIN	ZC	USGS ID 73802375
14	Barataria Pass East of Grand Isle	01/01/04	08/30/04	15MIN	ZCQ	USGS ID 73802515
15	Houma Navigation Canal at Dulac	01/01/04	08/30/04	15MIN	ZCV	USGS ID 7381328
16	Bayou Petit Caillou at Cocodrie	01/01/04	08/18/04	1HR	ZCV	LUMCON
17	GIWW at Houma	01/01/04	08/30/04	15MIN	ZCVQ	USGS ID 7381331
18	GIWW at Minors Canal	02/19/04	08/10/04	15MIN/1HR	ZC	USACE
19	Bayou des Allemands at Highway 90	01/01/04	06/30/04	15MIN	ZC	LDNR ID BAFS-03

[2] Key: Z = Water Surface Elevation
C = Salinity Concentration
V = Velocity
Q = Discharge

4.0 MODEL TESTING AND SENSITIVITY ANALYSES

4.1 Model Testing

Model testing has been an integral and continuous part of the model development, starting with small simplified test cases during the initial model development and continuing through to initial calibration simulations with the full model mesh. Just a few of the many purposes for model testing include:

- Checking model convergence,
- Evaluating the implications of representing the 1D channel geometry with a simplified shape,
- Testing newly added model capabilities,
- Comparing different modeling methodologies or formulations, and
- Revealing problems with the mesh that cause mass not to be conserved locally.

4.1.1 Convergence

Since the model uses the Newton-Raphson iterative solution technique, convergence criteria must be specified that define when to stop the iterations and move to the next computational time step (i.e., the maximum acceptable change between computed values of depth and velocity components between iterations). For all the model simulations, convergence criteria of 0.005 ft were used for depth and 0.001 ft/sec for both the x- and y-velocity components. Using a 15-minute timestep, the solution usually converged within 20 iterations initially and then within 8 to 10 iterations as the simulations progressed.

4.1.2 Channel Geometry Representation

Some of the earliest model testing conducted for this project involved testing the effects of the trapezoidal shape to approximate the channel cross sections in RMA-2. A simplified test case was developed consisting of a small network of 1D channels and interconnected storage areas. The UNET model was used for comparing flows and water surface elevations using irregular cross section geometry from Bayou Lafourche along with vertical-walled storage areas.

Lateral weir (UNET "LA" and "WD") records were used to represent the connections between the 1D channels and the storage areas with UNET.

For RMA-2, the geometry included 1D trapezoidal representations of the irregular cross sections for the channels and simplified 2D meshes representing the same storage areas defined in the UNET input test case. Transition Elements were first used to connect the 1D channels to the 2D mesh to allow for the interaction of flow between the channels and storage areas; however, these proved problematic and a new method for connecting the channels and marsh was used (Section 4.1.4).

The same boundary conditions were specified for both models. Various runs were performed with both steady state and dynamic boundary conditions, and the results from the two models were compared at selected locations. Computed water surface elevations typically were within 0.5 ft or less, and computed flows were within 20%. However, this was not deemed accurate enough, which gave rise to the need for the representation of irregular channels in RMA-2 (Section 3.2).

After adding the irregular channel capability to RMA-2, RMA-2 computed water surface elevations matched those from UNET to within 0.2 ft with flows matching within 5%.

4.1.3 One-dimensional Junction Formulation

Another example of model testing conducted with a simple test case involved the comparison of available 1D junction node types in RMA-2. RMA-2 includes the following three types of junction nodes: type 901, which forces equal water surface elevation at the ends of all the reaches forming the junction; type 902, which matches total head (water surface elevation + velocity head) at the ends of all the reaches forming the junction; and type 903, which conserves momentum at the junction. For the type 903 junction, it is necessary to specify which reaches represent the "main channel" at the junction. It seems reasonable to assume that any differences between these formulations would be highly dependent upon the magnitudes of flow velocities in the reaches at the junction and upon the differences in velocity among the reaches forming the junction. These expectations were confirmed with a small test case consisting of three 1D

reaches creating a simple T-shaped junction. The different formulations were tested by comparing the flow distribution and computed water surface elevations at the junction.

When velocities in the reaches were low, there was practically no difference between the three formulations. For higher velocities, more pronounced differences were observed. These results confirmed that the momentum conservation method (type 903) produced unrealistic results.

4.1.4 Lateral Weir 1D-2D Connections

A fairly recent addition to the King's version of RMA-2 is the type 999 lateral connection element between 1D and 2D elements (King and Williams 1999). This capability was added to the RMA-2 model to simulate the lateral flow exchange between a river channel and leveed overbank areas during flood events. Conceptually, the same type of flow exchange occurs between the channels and adjacent marsh areas in the project area.

To use the type 999 lateral flow exchange feature, the 2D elements along the edge of a mesh that abuts a 1D channel reach where flow exchange can occur must be aligned and nodes spaced to be adjacent to end nodes of 1D elements on the channel. Internally, the model matches water surface elevation in the channel to the adjacent 2D element and matches flow entering or leaving a 1D element as inflow to or outflow from the adjacent 2D element. In effect, the 1D channel becomes a boundary condition for the 2D mesh. This formulation allows for the exchange of flow between 1D and 2D elements in either direction. The connection between a 1D and 2D element is specified by creating a quadrilateral element from the corner nodes of adjacent 1D and 2D elements with the element type 999.

Because accurate representation of the interaction between the channels and adjacent marsh areas is such a critical component of this project, it was decided to prepare a simple test case to test the type 999 lateral flow exchange formulation. The purpose of this test was to determine their effect on computation times. According to Dr. Ian King, the primary drawback of the type 999 lateral connections is increased computation times. Because manageable simulation times are critical to meeting project deadlines, it was essential to know how the type 999 elements would affect simulation times to decide whether or not to use them.

Two simple test cases were set up with a 1D channel reach connected to a 2D mesh; one with traditional Transition Elements and one with the type 999 elements. While both formulations gave similar results, the runs with the type 999 elements took about twice as long. The decision was initially made not to use the type 999 lateral connections, and to code all lateral connections with traditional Transition Elements based on these test results.

However, it was later decided that the best possible formulation for the type of continuous connection between the channels and marshes in the project area was the type 999 element. At issue was the preservation of lateral weir length along the channel that controlled the exchange between the channel and adjacent marsh areas. (Too short a length meant that flows into or out of the marsh would be underestimated). With the Transition Elements it was difficult to conserve the weir length due to the discrete nature of the connection from a single 1D node to a 2D element. At best, the Transition Elements could give only a rough, discretized approximation of the weir length. When tests were run with type 999 elements implemented in the full model network, it was found that their impact on computation times was minimal.

It is believed that the earlier simplified tests with the type 999 elements led to a flawed conclusion about simulation times due to the scale of the original test. In the original test, only one reach and two adjacent marsh areas were tested. Due to the small number of nodes and elements in the test network, the type 999 elements had a substantial influence on the simulation times. The full model simulation times are more heavily influenced by the very large total number of elements, so the type 999 elements have much less influence. For this particular case, the original model testing led to a misleading conclusion.

4.1.5 Continuity

One of the fundamental tests of acceptability for any model is adequate continuity and conservation of mass. For a model mesh this large, it is critical to ascertain whether mass is being created or lost in the model. Therefore, continuity checks are one of the most important kinds of model testing. In fact, the goal of the acceptable continuity error has driven the development and refinement of this model more than any other single factor.

4.1.5.1 One-Dimensional Reach Continuity

Due to the density and sheer numbers of 1D nodes in this model, it was originally difficult to quantify continuity in the 1D reaches. The majority of visualization tools for interpreting output data from RMA-2 are specific to 2D elements (e.g., contouring). To eliminate the laborious task of tracking flows by 1D node numbers in the model output file, Dr. Ian King developed a tool for the RMAPLT program that graphically displays flows at 1D nodes. This tool proved invaluable in finding areas of poor continuity in the 1D reaches. These areas typically occurred around bridges or other significant changes in the channel geometry (e.g., cross-sectional area, invert). The solution for these continuity errors in most cases was simply to refine the spacing of the 1D nodes. Additional 1D nodes do not exact a computational time penalty on the model simulations, so the 1D elements can be made very dense at locations where extra resolution is needed.

4.1.5.2 Two-Dimensional Continuity – Flow Through a Marsh

Two-dimensional continuity was tested by establishing continuity lines at inflow, outflow, and interior points of the 2D mesh. The total inflow versus outflow could then be tracked, giving an estimate of the mass created or lost in the mesh. Continuity was tested for small marsh areas as well as the entire Barataria Basin. Under steady state conditions, the entire mesh showed good continuity at all continuity lines, with less than 5% loss at any given location.

4.2 Sensitivity Analyses

Several sensitivity analyses have been performed on the full model. These include investigation of the effects of computational time step, the marsh elevations in the Terrebonne Basin, and the 1D junction node types.

4.2.1 Computational Time Step

The computational time step used for all dynamic runs performed for this project has typically been one hour. To test the effect of the time step, two identical runs were performed, one with a one hour time step and one with a 30-minute time step. As expected, the run with the

30-minute time step took almost twice as long to run, and the results of the two simulations were judged close enough to not be worth incurring the longer run times associated with the shorter time step. However, subsequent runs with a 15-minute timestep allowed the model to converge faster so all calibration and tracer runs were made using a 15-minute timestep.

4.2.2 Terrebonne Basin Marsh Elevations

Because of the lack of bathymetry data in the Terrebonne basin, all marsh invert elevations north of the Gulf were initially set at –5 ft NAVD88 based on limited data. Because of concerns of artificially deep depths affecting flows and velocities in the marshes, a simulation was performed with all marsh elevations increased to –2 ft NAVD88. Because this change did not have a significant impact on the computed marsh velocities, it was decided to keep the marsh elevations at –5 ft NAVD88. The Terrebonne basin bathymetry will be further refined if and when the additional bathymetric data for the basin is obtained.

4.2.3 One-dimensional Junction Nodes

As described in Section 3.5.2, RMA-2 allows a choice of 1D junction node types. The model for this project was initially developed using the default junction node type (type 901). In response to questions about the flow distribution at 1D nodes, the junction nodes at the Bayou LaFourche/Company Canal and Bayou LaFourche/GIWW junctions were changed to a type that conserved momentum (type 903). This change had a negligible impact on the flow distributions at these junctions due to the low velocities in the channels. Thus, the flow distribution is more significantly impacted by head differential than momentum for the conditions tested. Later simulations showed, however, that the momentum junction (type 903) produced unrealistically large head and flow differentials at the junctions due to the tidally-induced reversing flows. Consequently, they were all changed back to equal elevation (type 901) junctions.

5.0 MODEL MESH MODIFICATION

After the model testing phase, several modifications were performed to the geometry to improve results and reduce simulation times without significantly compromising model resolution. The final mesh used for the calibration and tracer simulations is shown in Figures 5.1.a and 5.1.b.

5.1 Mesh Refinement

As stated in Section 3.5.3 (Channel and Marsh/Swamp Interconnections), the connections between 1D (channel) and 2D (marsh) elements were done using a new quadrilateral element type 999. The 2D marsh areas to which the type 999 elements are connected were refined further to more accurately compute the flow exchange between 1D channels and 2D marsh.

The nodal elevations for all 2D elements connected to type 999 elements were held constant so that there was no slope across the 2D elements. Additionally, a second tier of 2D elements adjacent to the weir connections was coded with a constant elevation to create a flat "shelf" at the overbank weir elevation. These shelves were coded to help smooth the transition of flow between the 1D channels and 2D marsh areas. For marshes connected to 1D channels, nodal elevations for perimeter nodes not included in a weir connection were increased to +5.0 ft NAVD88.

5.2 Mesh Truncation

Flow data at Bayou Lafourche at Donaldsonville had periods of missing and invalid data, so use of these data was discontinued as the upstream boundary condition on Bayou Lafourche. Furthermore, it was determined that for the calibration and tracer runs, there was no need to extend the 1D portion of Bayou Lafourche all the way north to Donaldsonville. Therefore, the northern end of Bayou Lafourche was eliminated from the mesh and the model boundary was instituted at Thibodaux instead. The measured flow data at Bayou Lafourche at Thibodaux data was used in lieu of the Donaldsonville data as the upstream flow boundary condition for Bayou Lafourche.

In addition, because the observed data show flow in the GIWW at Bayou Lafourche moving eastward 93% of the time for the 8 month period over which data was collected (Figure 1.5), it was decided to eliminate the Barataria portion of the mesh for the Phase I study only. The resulting mesh is shown in Figures 5.1.a and 5.1.b. Consequently, only the Isle Dernieres and Port Fourchon tidal records were used with the truncated mesh. Figure 5.2 shows the location of the final boundary condition locations used in the truncated model. The modified model provided the information and results needed, and reduced the model complexity and run times.

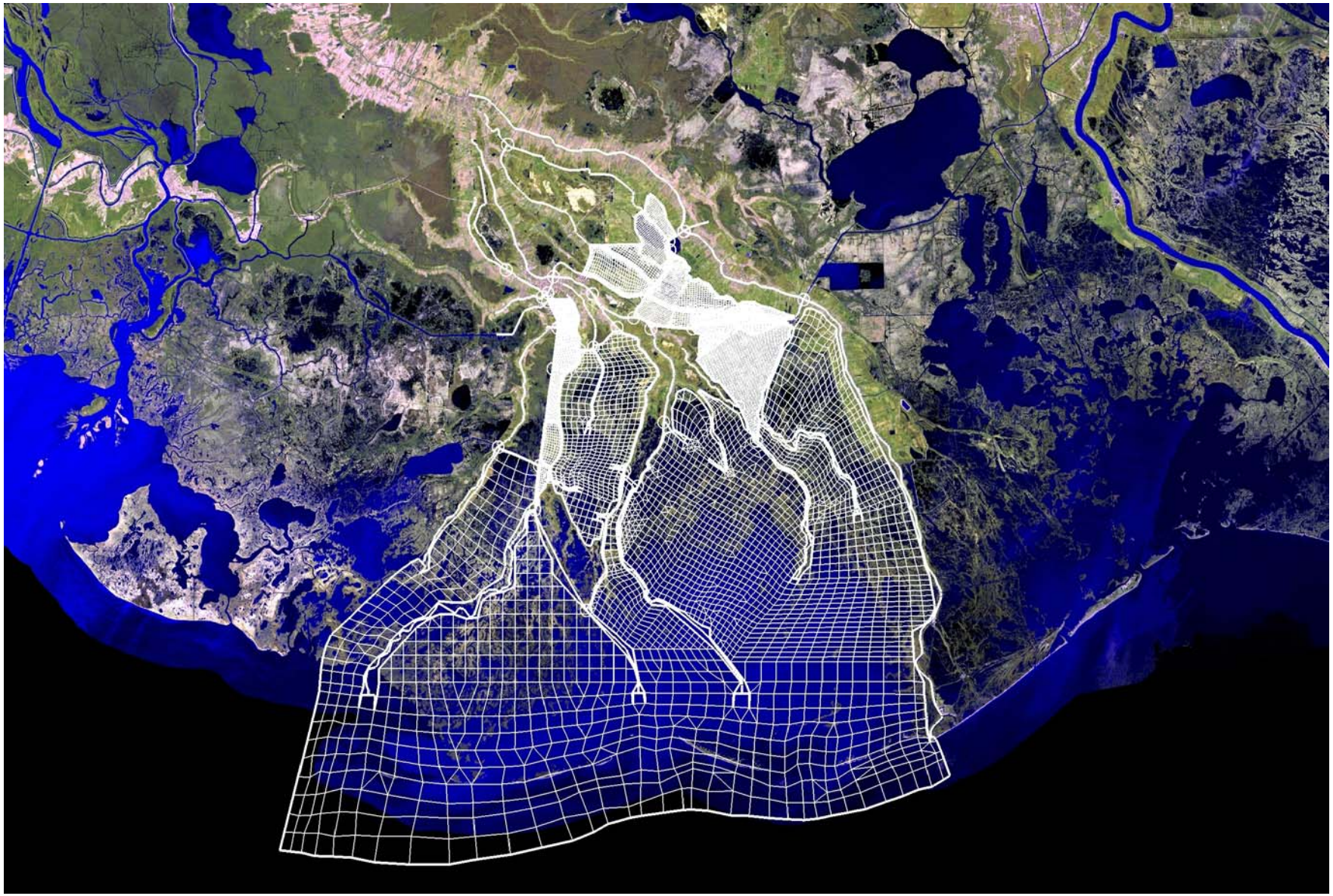

Figure 5.1.a. Final calibration and tracer mesh.

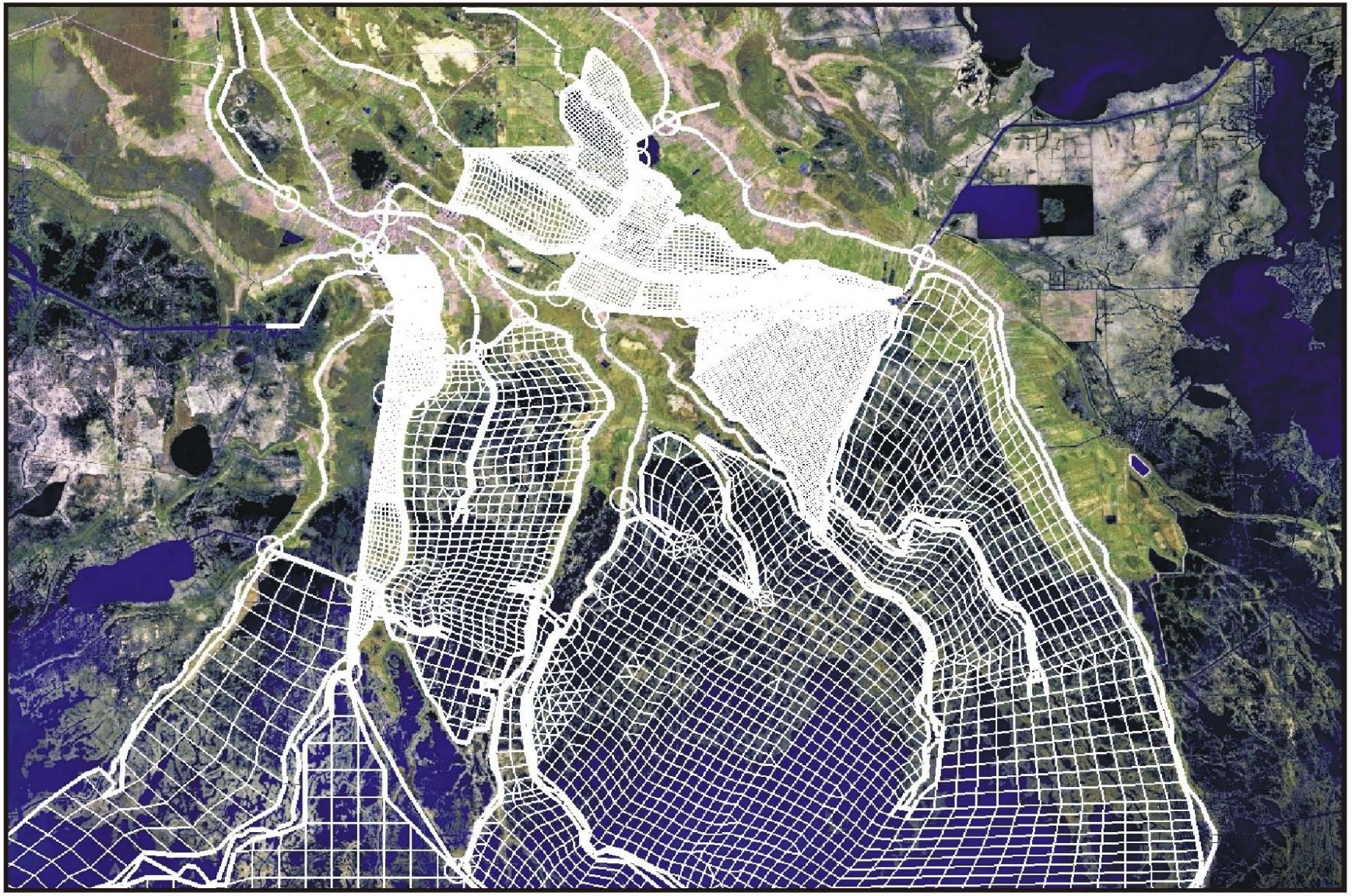

Figure 5.1.b. Detail from the dense mesh area shown in Figure 5.1.a.

Figure 5.2. Final boundary condition locations shown in yellow.

6.0 MODEL CALIBRATION

6.1 RMA-2 Calibration

Water surface elevation, flows, velocities, and salinity were calibrated to observed gage data. An initial RMA-2 simulation was run for an 8-week period to establish a baseline condition to which other calibration simulations could be compared. After this baseline was determined, a series of five different runs was executed for a 4-week period, all using a different combination of Manning's 'n' values for the 1D channels and 2D marshes. The 4-week period was long enough to compare to the baseline, allowing one set of calibration parameters to be chosen over the others. All the models were run with a computational time step of 15 minutes. The five different calibration runs were as follows:

1. Global increase in Manning's 'n' from 0.020 to 0.035 for all 1D channels;
2. Increase Manning's 'n' for open water areas from 0.040 to 0.15;
3. Increase Manning's 'n' in all channels except Bayou Lafourche, GIWW, Company Canal, and HNC from 0.020 to 0.05;
4. Decrease Manning's 'n' for open water/marsh area 2D elements from 0.04 to 0.02; and
5. Increase Manning's 'n' for open water/marsh area 2D elements from 0.04 to 0.100.

After these simulations were run for a 4-week period, it was determined that the last run best reproduced observed water surface elevation and flow data, so it was run for a total of eight weeks. The final water surface elevation, velocity, and flow calibration results for the various gages are shown in Figures A.1 through A.16 in Appendix A, and the final calibration parameters are shown in Table 6.1 below and Figure 6.1.

Table 6.1. Final RMA-2 calibration parameters.

Water Body	Element Type	Eddy viscosity associated with X-direction & u velocity	Eddy viscosity associated with Y-direction & u velocity	Eddy viscosity associated with X-direction & v velocity	Eddy viscosity associated with X-direction & v velocity	Manning's 'n'
Overbanks	29	Scaled	Scaled	Scaled	Scaled	0.50
Marsh areas connected to Gulf	30	Scaled	Scaled	Scaled	Scaled	0.10
Gulf of Mexico	32	Scaled	Scaled	Scaled	Scaled	0.10
Isolated marsh areas with connections to channels	33	Scaled	Scaled	Scaled	Scaled	0.20
All 1D Channels	1 through 28	20.0	20.0	20.0	20.0	0.02

The computed water surface elevations showed good agreement with the observed data for most of the observed gage locations. In instances where elevations were not matching in magnitude, the computed results reproduced observed trends.

Of all the locations where computed elevations matched observed, the poorest matches were found at the following three locations: Bayou Terrebonne southeast of Houma (Station 8), HNC at Dulac (Station 15), and GIWW at Houma south of Bayou Terrebonne (Station 17). This may be due to the fact that the overbank elevations along the GIWW and the HNC are suspect, having been determined using approximate methods. Consequently, the volume of flow entering and leaving the marshes in these areas is not being accounted for accurately. It was also observed that the computed flows passing through Humble Canal and Bush Canal were suspect, and thus could account for poor results in Bayou Terrebonne.

Another possible source of error could have been a problem with the datum for the HNC at Dulac gage (Station 15). This is indicated by the fact that the computed elevations there match up quite well with the observed elevations at the Bayou Petit Caillou at Cocodrie gage (Station 16) that is located relatively close to the gage on the HNC.

6.2 RMA-11 Calibration

Several simulations were carried out to calibrate the model at various monitoring gages by systematically varying dispersion coefficients.

As a first step, specific portions of the southern mesh were assigned different element types to account for the variation in mixing characteristics of the various wetland regions. The southern segments of the canals were also assigned different element types than those of the northern portion. This allowed higher dispersion coefficients to be set in the southern areas where the primary mechanism of transport is mixing and dispersion. Figure 6.2 shows the various element types of the mesh.

In RMA-11, one can either specify the absolute value of the dispersion coefficient or a dispersion coefficient scaling parameter for a given element type. When a scaling parameter is specified, the program computes dispersion coefficients based on the size of the element and the average velocity at that element. The scaling parameter approach was used for the present calibration; the final values are tabulated in Table 6.2.

Numerous simulations were carried out to calibrate the model. The final salinity calibration results are presented in Figures B.1 through B.9 in Appendix B. The observed salinity data at Gages 1, 3, 7, 10 and 17 show constant low values without any spikes during the calibration period. The model also behaved similarly and predicted that no salinity was being transported towards these areas.

It should be noted that the entire grid was initialized to the same initial concentration in all RMA-11 simulations; therefore, model results for the first 2-3 weeks will result in a poor match with the observed data.

The model predictions matched the salinity spike observed at Gage 5 (Figure B.3).

Table 6.2. Final RMA-11 calibration parameters.

Water Body	Element Type	Dispersion scale factor in X-direction	Dispersion scale factor in Y-direction	Minimum Dispersion in X-direction (m^2/s)	Minimum Dispersion in Y-direction (m^2/s)
Humble Canal	27	100	100	0.5	0.5
Marsh south HNC-Bayou Dularge junction	30	20	20	0.5	0.5
Marsh south Point-aux-Chenes canal	32	250	250	0.5	0.5
Marsh to the east of Grand Bayou	34	20	20	0.5	0.5
Southern segment of Bayou Dularge	35	500	500	0.5	0.5
HNC	36	500	500	0.5	0.5
HNC	37	500	500	0.5	0.5
B. Terrebonne	38	500	500	0.5	0.5
Gulf of Mexico	39	500	500	0.5	0.5
Grand Bayou	40	100	100	0.5	0.5
Gulf of Mexico	41	500	500	0.5	0.5
All other marshes and channels	1 - 26, 28, 29, 31, 33	1	1	0.5	0.5

For Gage 7, the model shows a poor match between the observed and predicted salinity (Figure B.4). Upon further investigation of model results in this area, it was noted that the salinity profile in the nearby Grand Bayou canal showed a distinct rise-fall trend. Based on this observation, review of the aerial imagery and field reconnaissance of the area, we believe that the measured salinity at this gage is influenced by advection through the numerous channels that penetrate into the area. This is shown by results for an adjacent channel node as indicated by "model_canal" in Figure B4. The Phase I model does not have sufficient detail to represent such an intricate network of channels in the geometry (and such representation is beyond the scope of Phase I).

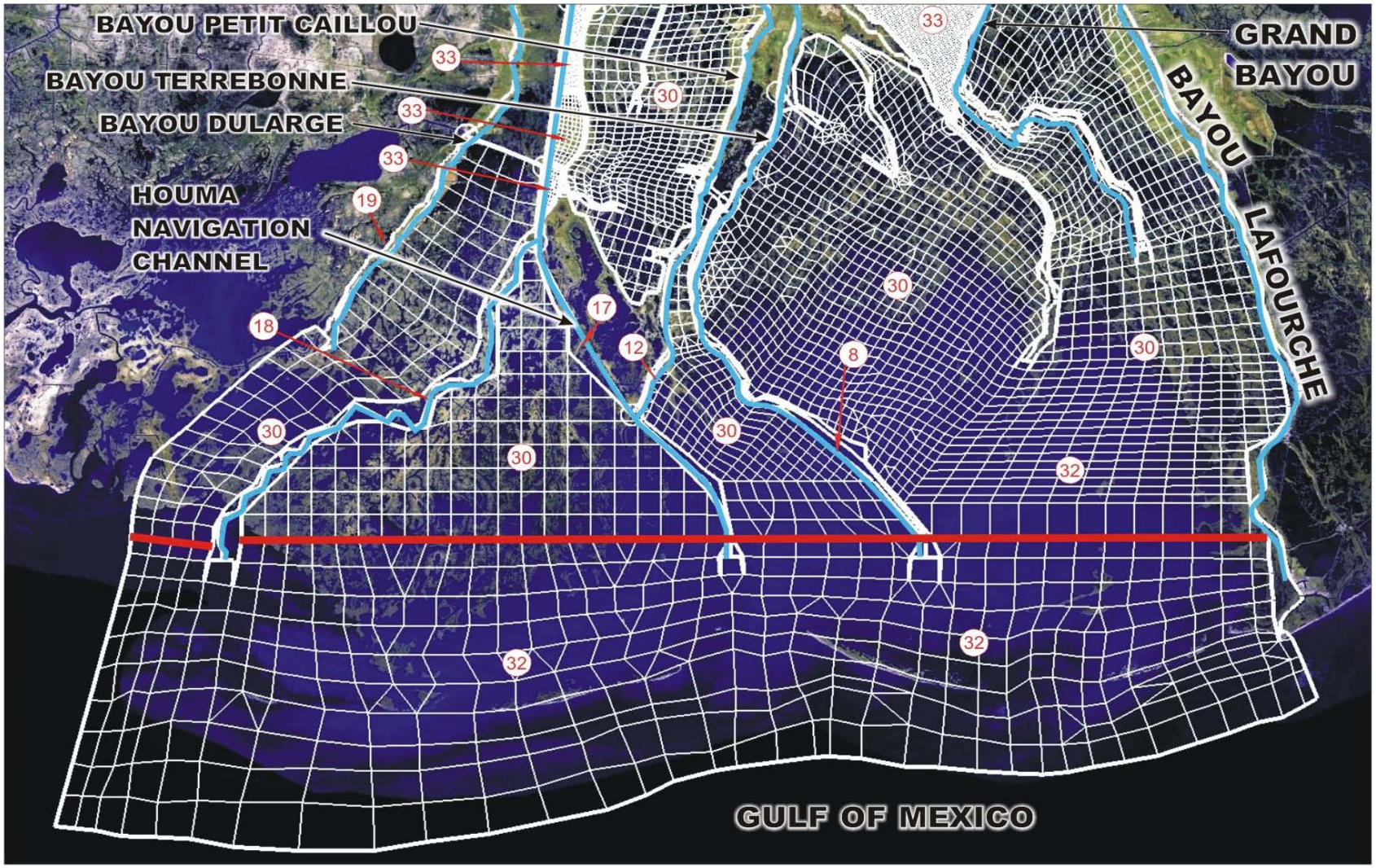

Figure 6.1 Location of RMA-2 element types in the mesh.

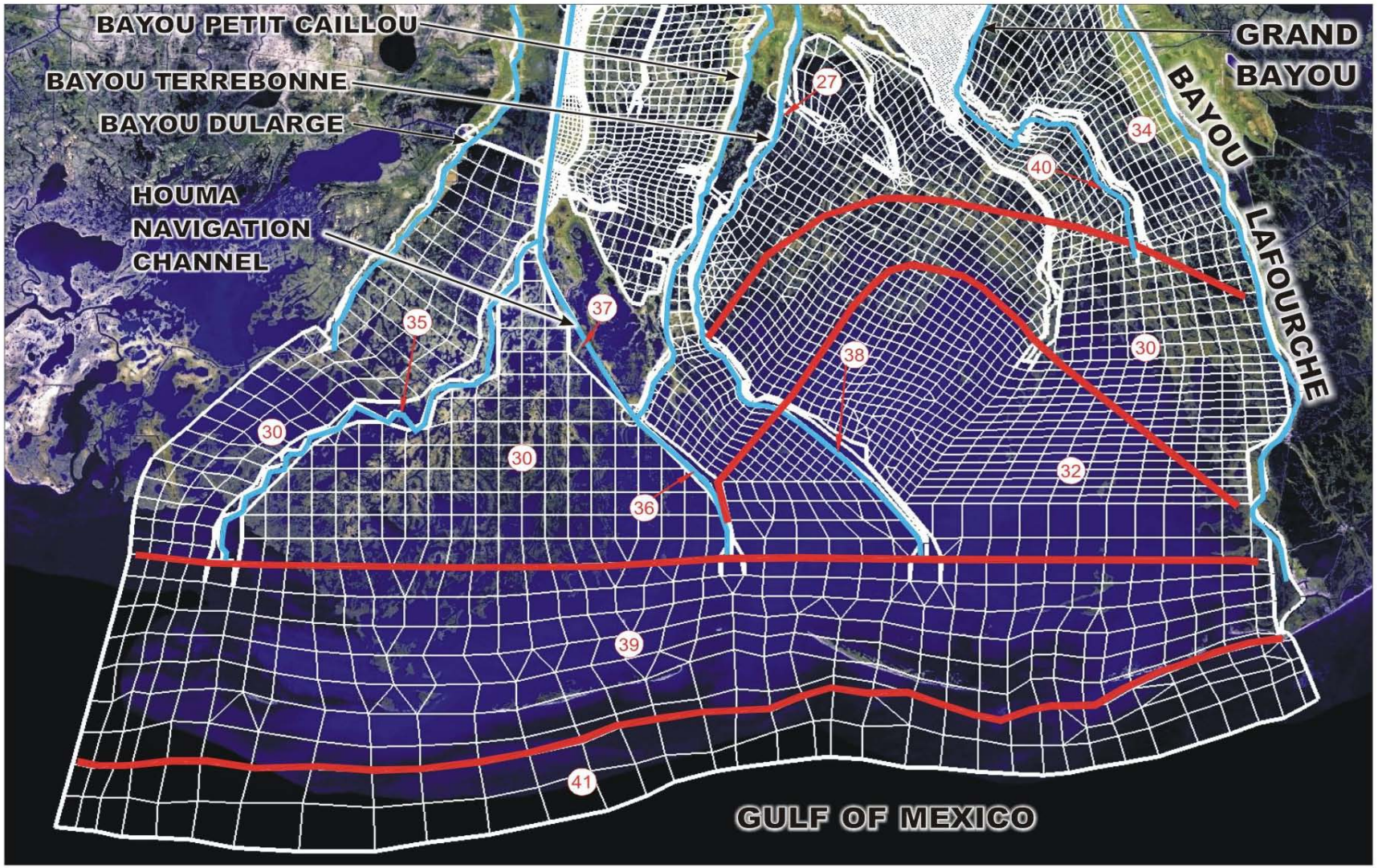

Figure 6.2. Location of RMA-11 element types in the mesh.

The measured salinity at Gage 8 was mostly constant low values except for two spikes as seen in the Figure B.5. The model did not predict these spikes. The RMA-2 predictions need to be refined further to improve Gage 8 results. The salinity spikes at this station may be caused by flows coming in from the Humble Canal or by transport northwards in Bayou Terrebonne.

Model predictions matched very well with the observed salinity at Gage 15 (Figure B.7). The excellent match for the first set of spikes suggests that the model is reasonably able to capture the transport processes in the HNC. The model does not predict the second set of spikes in salinity at the gage but increases were predicted in the lower portions of the reach, indicating that the velocities may be too low in the RMA-2 model.

At Gage 16 (Figure B.8) the model matches the observed salinity.

Once the model was calibrated, it offered good confidence for its further application.

7.0 TRACER SIMULATIONS

7.1 RMA-2 Tracer Simulations

After calibration, the next task was to use the model to identify the areas where the freshwater would travel once it was introduced at Thibodaux at the northern end of Bayou Lafourche. The areas where the freshwater would travel would be analyzed more in-depth to determine whether any benefits could be derived from the addition of freshwater.

Two different diversion flows were simulated: 1,000 cfs and 2,000 cfs. With exception of the inflow at the northern end of Bayou Lafourche, these freshwater diversions were modeled using the same boundary conditions that were used in the final calibration simulation from May 4, 2004 through June 30, 2004. Final calibration simulation results were used as a baseline condition for comparison purposes.

Before the salinity tracer run was attempted, the flow results of the RMA-2 simulation were analyzed for reasonableness. The results give a good estimate as to the flow path of the freshwater. These results are shown in Figures A.17 through A.38 in Appendix A.

Under the baseline conditions, on average, the general trend is for flows to travel south-southeast down Bayou Lafourche. Flows in the GIWW travel from west to east toward the Barataria Basin, and flow travels in a north-northeasterly direction in Company Canal from the GIWW towards Bayou Lafourche.

For the 1,000 cfs simulation, the freshwater flow travels southeast down Bayou Lafourche from Thibodaux, and upon reaching the junction with Company Canal, on average, approximately 50% splits and travels to the southwest down Company Canal while the remaining 50% continues southeasterly down Bayou Lafourche. This is significant in that the freshwater flow is of high enough magnitude that it reverses the flow in Company Canal when compared to the baseline case. The flows down Company Canal are lost into the marshes along Company Canal and Bayou L'eau Bleu, while the remainder splits both east, west, and south upon reaching the GIWW. The 50% flow that makes it past Company Canal on Bayou Lafourche is almost completely diverted into the GIWW to the northeast and carried into the Barataria Basin. For the 2,000 cfs diversion, the flow patterns are similar, but increase in magnitude.

Figures 7.1 and 7.2 show the percentage of the total Bayou Lafourche diversion flows (1,000 cfs and 2,000 cfs, respectively) averaged over the 8-week tracer simulation period at the junctions of Bayou Lafourche, Company Canal, and the GIWW based on an accounting of tracer material mass passing locations near junctions. Note that these values represent averages over the entire 8-week period; there are instances where flows occur in the opposite directions from what is shown in the figures, but these are of short enough duration and as such, do not change the overall average values. The reduction in values shown between the north and south portion of Company Canal between Bayou Lafourche and the GIWW is due to flow that leaves Company Canal and moves into adjacent marshes and down Bayou L'eau Bleu. The "lost" flow is recovered as flows from the marshes and Bayou L'eau Bleu re-enter the GIWW.

Upon further analysis, it was determined that an unrealistic hydraulic gradient from west to east was imposed. In Bayou Lafourche, the eastern boundary on the GIWW at Larose was the elevation observed for lower baseline flow conditions. Under higher flow conditions the elevations would be expected to be slightly higher. Consequently, the imposed gradient caused a significant amount of flow to move eastward in the GIWW and into the Barataria Basin.

As a result, a third diversion simulation was performed. A run was made with a 1,000 cfs diversion flow and observed water levels at the eastern boundary increased by 0.25. Since no long-term elevation-flow records exist in the GIWW, a 0.25-ft value was chosen because it was within the range of differences experienced during the study and was observed in HEC-RAS results obtained for early screening simulations for a 1,000 cfs diversion.

For the third diversion simulation with the elevated eastern boundary, flow down Bayou Lafourche was the same, but flow in the GIWW was predominately from east to west. Consequently, flows southward in Company Canal split to the south and west upon reaching the junction with the GIWW, instead of traveling eastward as was the case in previous simulations. So it is apparent that the GIWW captures a large portion of the Bayou Lafourche flows, as might be expected given its larger channel conveyance and momentum.

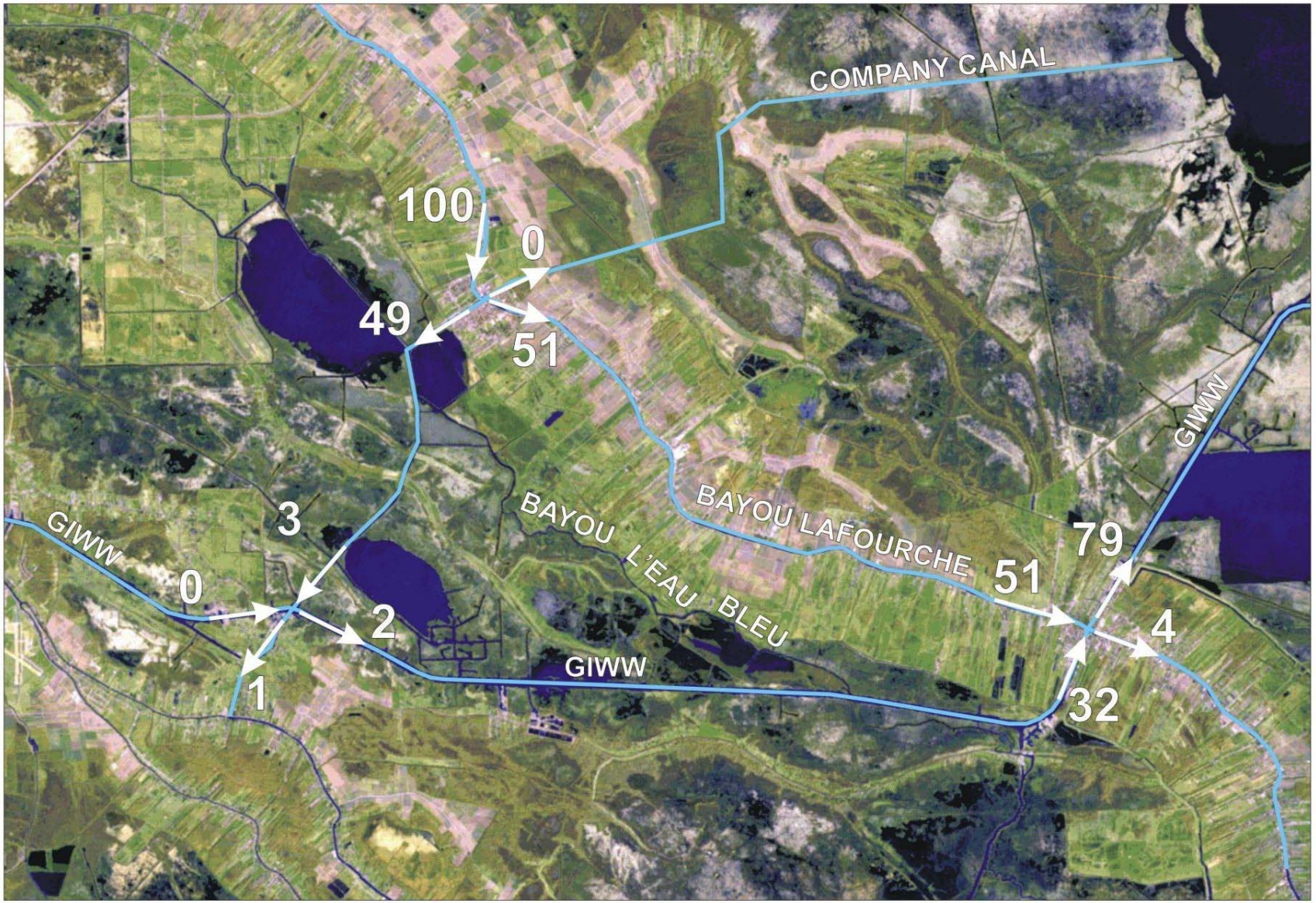

Figure 7.1. Average flow distribution resulting from 1,000 cfs Bayou Lafourche diversion flow tracer simulations. Values shown are percent of diversion flow at each location averaged over the two month simulation duration.

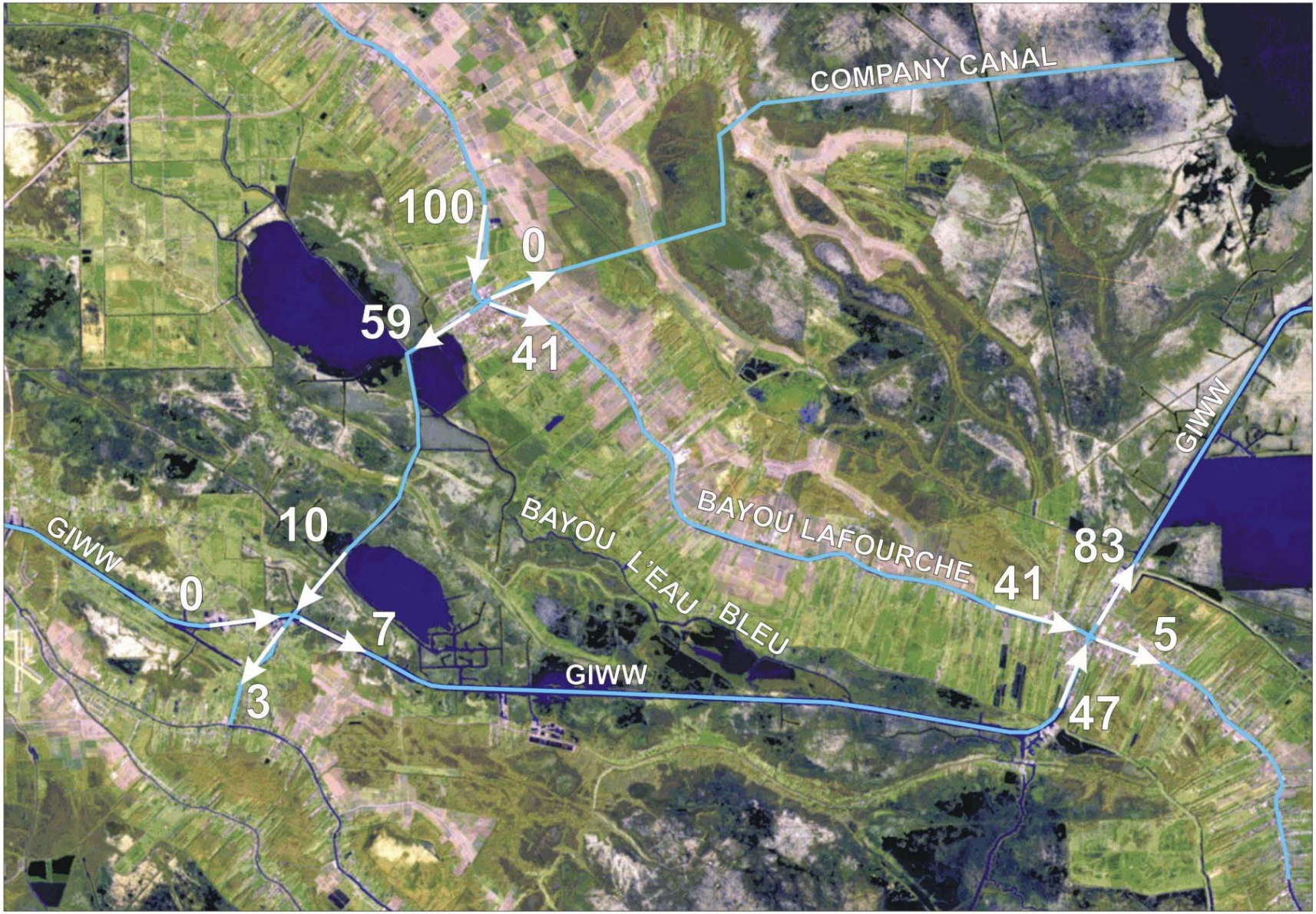

Figure 7.2. Average flow distribution resulting from 2,000 cfs Bayou Lafourche diversion flow tracer simulations. Values shown are percent of diversion flow at each location averaged over the two month simulation duration.

7.2 RMA-11 Tracer Simulations

For the tracer simulations, the general strategy was to initialize the entire system to an arbitrary low tracer concentration, 0.15 ppt in this case, and then introduce the diversion flows at 100 ppt tracer concentration at the upper end of Bayou Lafourche. The tracer movement was then tracked as it moved throughout the system. The tracer was assumed to be a conservative substance (i.e., would not decay over time). Table 7.1 describes the different conditions associated with the tracer simulations.

Table 7.1. Tracer simulation conditions.

Simulation Run No.	Diversion Flow	Diversion Concentration	Initial Condition	Boundary Salinity	GIWW Flow
1	1,000 cfs	100.0 ppt	0.15 ppt	0.15 ppt Constant	Observed, Easterly
2	2,000 cfs	100.0 ppt	0.15 ppt	0.15 ppt Constant	Observed, Easterly
3	1,000 cfs	0.0 ppt	Observed (0.15 ppt)	Observed dynamic	Observed, Easterly
4	2,000 cfs	0.0 ppt	Observed (0.15 ppt)	Observed dynamic	Observed, Easterly
5	1,000 cfs	100.0 ppt	0.15 ppt	0.15 ppt Constant	Westerly (GIWW Easterly +0.25 ft)

As stated before, the purpose of first two simulations was to identify areas where the diversion water would travel. Simulations 3 and 4 were performed using ambient salinity concentrations that would likely be experienced within the system coupled with a zero salinity diversion flow to see what salinity concentrations would likely result. Simulation 5 was carried out to investigate the effect of a predominately westerly flowing GIWW imposed by an increased eastern elevation boundary on the distribution of the diversion flow.

To analyze the results, tracer time series data were plotted in all the major canals and the adjoining marshes. Figure 7.3 shows locations for which the tracer time series profiles were plotted. Figures B.10 through B.14 are the plots of the time series resulting from diversion of 1,000 cfs (Run 1) and Figures B.15 through B.19 are the corresponding results for 2,000 cfs

(Run 2). Since the salinity concentrations in the system were very low to begin with, reductions in salinity caused by the diversion flows (Runs 3 and 4) were imperceptible and were not plotted.

Results for the last simulation (Run 5) are presented in Figures B.20 through B.24. The time series are listed generally from north to south and east to west for a given waterway since these are the directions the tracer front is likely to move. For the figures showing tracer concentrations in the marshes, nodes closer to the waterway have been selected to avoid bias from the effects of marsh dispersion on tracer concentrations.

The time series plots provide two pieces of information. First, they show the approximate time taken by the diversion flow to reach various areas of the system. Note that, as explained in previous sections, the diversion flow was introduced at Thibodaux and not at Donaldsonville. Second, they show how the boundary conditions influence the diversion flow distribution. For example, Figure B.10 shows that during westerly GIWW flows, the water is pushed to the north of the GIWW in Bayou Lafourche for one to two miles during the periods of May 12-16, 2004 and May 31 to June 1, 2004.

In Figures B.25 through B.32, concentration time series plots for Runs 1 and 5 are compared. They show an example of the effects of GIWW flow direction on the distribution of diversion flows.

Another way to view the results is by looking at “snapshots” in time of the tracer distribution throughout the system. Figures B.33 through B.40 show the snapshots at the end of the first through the eighth week for the 1,000 cfs diversion (Run 1) while similar snapshots for the 2,000 cfs diversion (Run 2) are shown in Figures B.41 through B.48. Note that the scale shown is not linear. These snapshots show that the Bayou Lafourche water is confined primarily to the area bounded by Bayou Lafourche, Company Canal, and the GIWW. However, some tracer is shown in the HNC as the result of short periods of westerly flows in the GIWW which results in flow moving down the HNC.

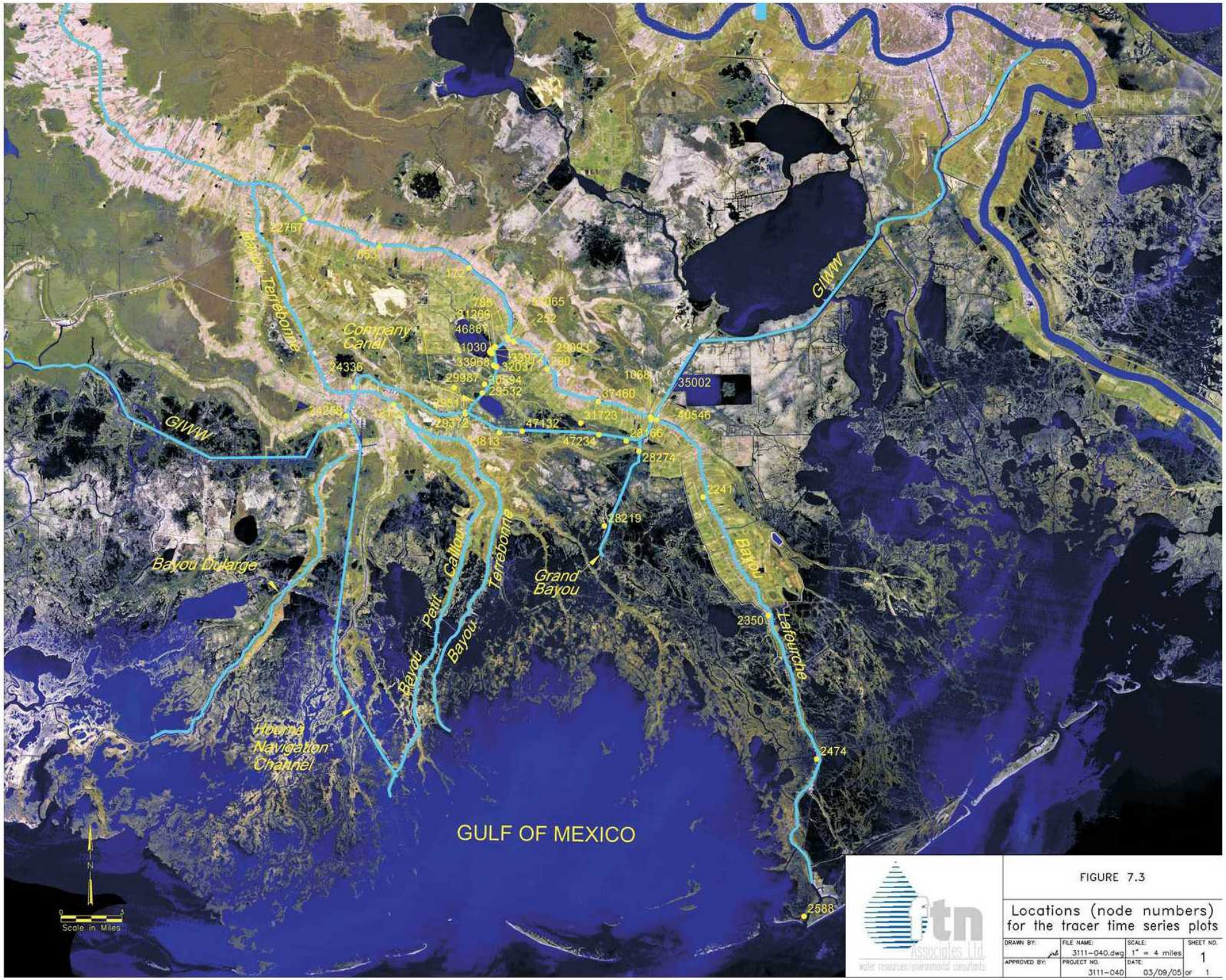

FIGURE 7.3

Locations (node numbers) for the tracer time series plots

DRAWN BY:	FILE NAME:	SCALE:	SHEET NO.
	3111-040.dwg	1" = 4 miles	1
APPROVED BY:	PROJECT NO.	DATE:	of 1
	3111-040	03/09/05	

For the westward GIWW flow hydrology (Run 5), tracer distribution plots are shown in Figures B.49 through B.56. These tracer distribution plots show where the diversion water moves under each of the boundary condition scenarios. The model parameters have been set such that tracer transport in the canals is primarily advective (mass movement) and not dispersive. However, some dispersion exists. Therefore, the lower tracer concentrations shown, say below 5 ppt, represent very small diversion flow contributions.

8.0 CONCLUSIONS AND RECOMMENDATIONS

A computationally-efficient and stable model that is capable of predicting salinities and water surface elevations for the Terrebonne Basin was developed. The model was first calibrated to observed data (Section 6.0) and then tracer simulations were applied to identify the marsh areas that actually receive freshwater from flows diverted into Bayou Lafourche (Section 7.0).

It was apparent from the modeling that the GIWW captures the Bayou Lafourche diversion flows due to its larger conveyance and momentum. The GIWW flow is driven by differential tide peaks and timing that forces flows from west to east except during storms (Section 1.2). As a result, the marsh areas to the south of the GIWW receive a very small percentage of the diversion flows.

In Phase II, the model will be improved in the following ways:

1. Incorporating new survey data into the marsh bathymetry and overbanks to better represent the exchange between 1D channels and 2D marsh,
2. Connecting portions of the southern reaches of the 1D channels to adjacent marsh/open water areas,
3. Refining element types for marsh/open water areas, and
4. Examining cross-sections/Manning's 'n' for Bush Canal and Humble Canal because the computed flows in those channels seem excessively high.

In addition, in Phase II the model can be used to evaluate channel improvements that would allow a larger amount of freshwater to flow to areas south of the GIWW, particularly in the Company Canal between the GIWW and Bayou Terrebonne and Grand Bayou at its northern terminus with the GIWW.

9.0 REFERENCES

Brigham Young University. 2004. Surface Water Modeling System (SMS) Reference Manual, Version 8.1. Provo, UT. 84602.

King, I. P. and D. K. Williams. 1999. Proceedings of the 6th International Conference on Estuarine and Coastal Modeling. November 3-5, New Orleans, Louisiana. M.L. Spaulding, L. Butler (eds). American Society of Civil Engineers. 1801 Alexander Bell Drive, Reston, VA. 20191.

King, I. P. 2005. RMA Modeling Suite for Flow in Estuaries and Streams. Version 7.3c. Resource Modeling Associates. 9 Dumaresq St. Gordon, New South Wales, Australia. 2072.

Louisiana Louisiana Department of Natural Resources. 1999. Review of New Orleans District Corps of Engineers UNET Modeling of Bayou Lafourche. FTN Associates letter report dated June 14, 1999. PO Box 94396, Baton Rouge, LA. 70804.

US Army Corps of Engineers Hydrologic Engineering Center. 2001. UNET One-Dimensional Unsteady Flow Through a Full Network of Open Channels. 609 Second Street, Davis, CA. 95616.

US Army Corps of Engineers Hydrologic Engineering Center. 2002. HEC-RAS River Analysis System User's Manual. 609 Second Street, Davis, CA. 95616.

US Army Corps of Engineers Engineer Research and Development Center. 2000. Users Guide to RMA2 WES Version 4.5. 3909 Halls Ferry Road. Vicksburg, MS. 39180.

US Army Corps of Engineers New Orleans District. 2000. Mississippi River and Tributaries, Morganza, Louisiana to the Gulf of Mexico Hurricane Protection Feasibility Report. PO Box 60267, New Orleans, LA. 70160.

US Environmental Protection Agency. 1998. Evaluation of Bayou Lafourche Wetlands Restoration Project, Coastal Wetlands Planning, Protection and Restoration Act Project PBA-20 Summary Report. Region 6 Office, 1445 Ross Avenue, 6EN-X, Dallas, TX. 75202-2733.

APPENDIX A

RMA-2 Calibration and Flushing Simulations Results

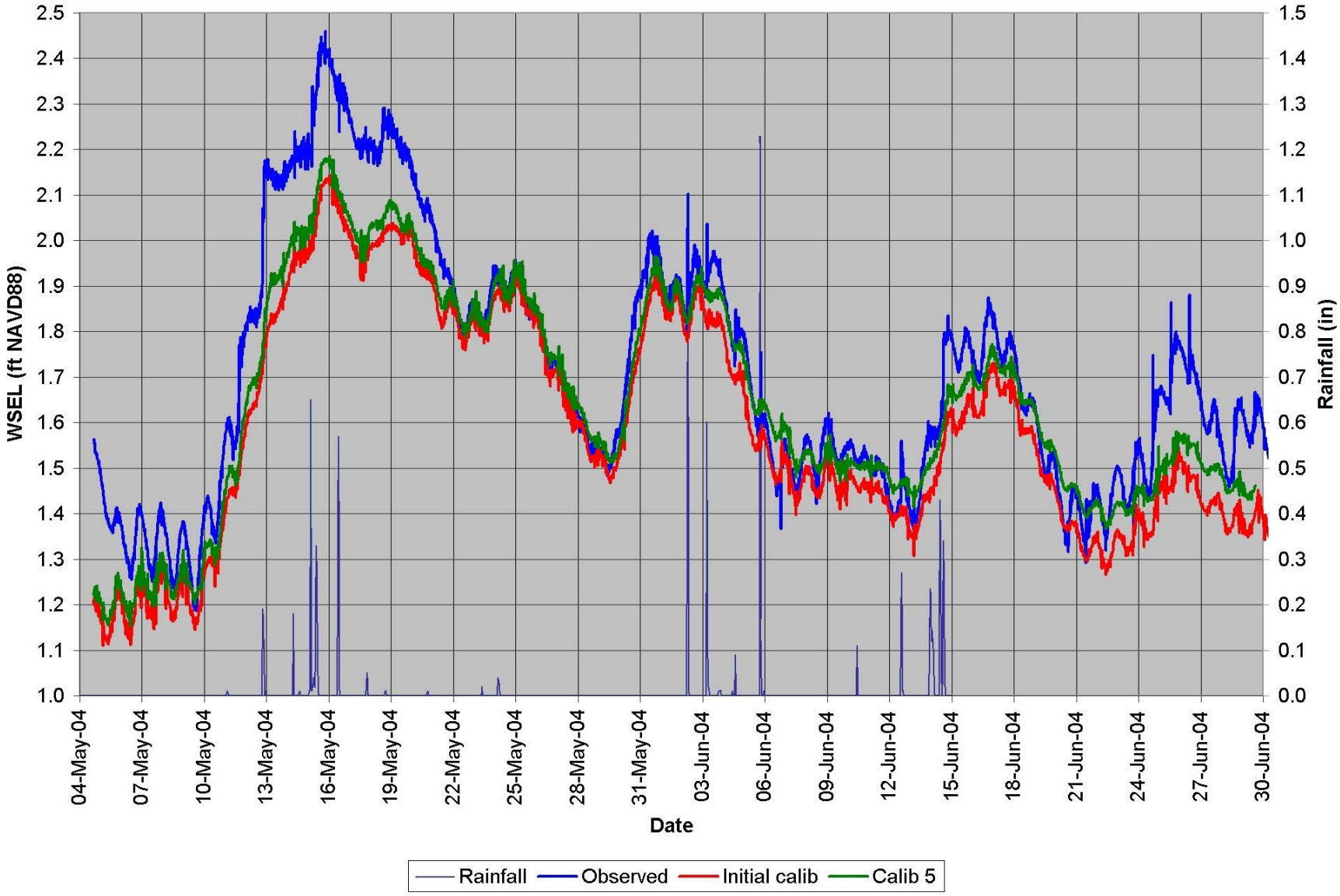

Figure A.1. Final RMA-2 Water Surface Elevation Calibration (Gage 1).

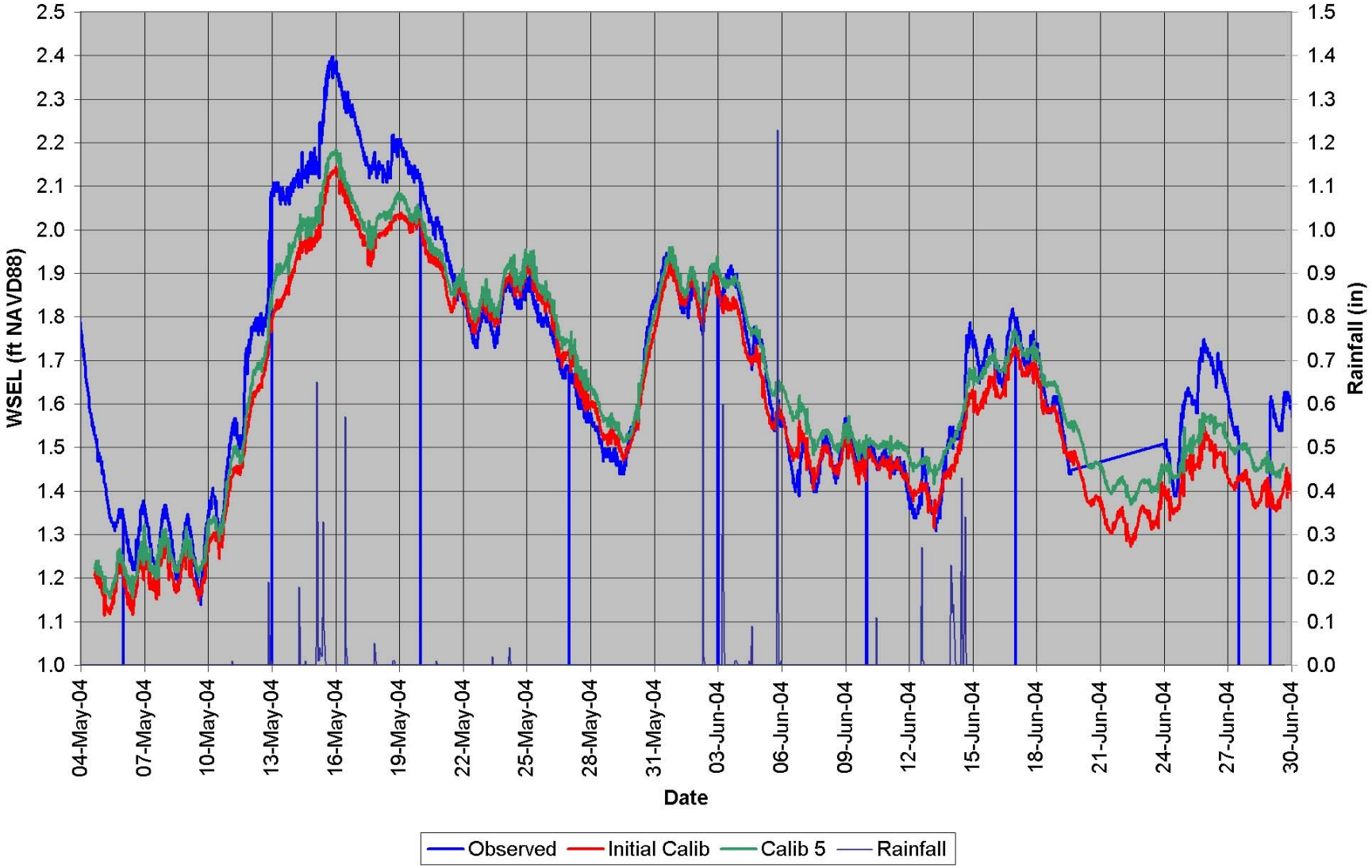

Figure A.2. Final RMA-2 Water Surface Elevation Calibration (Gage 2).

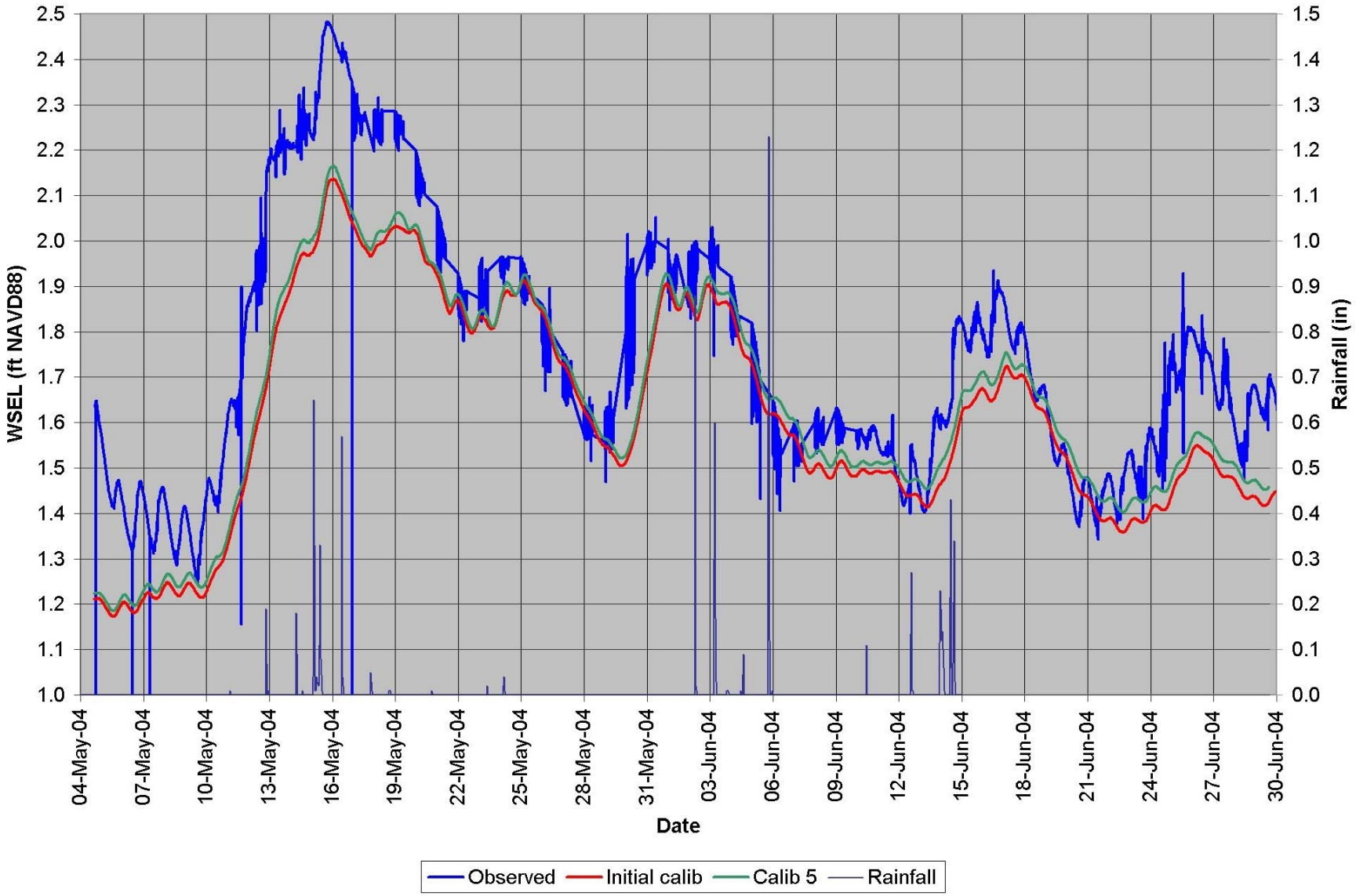

Figure A.3. Final RMA-2 Water Surface Elevation Calibration (Gage 3).

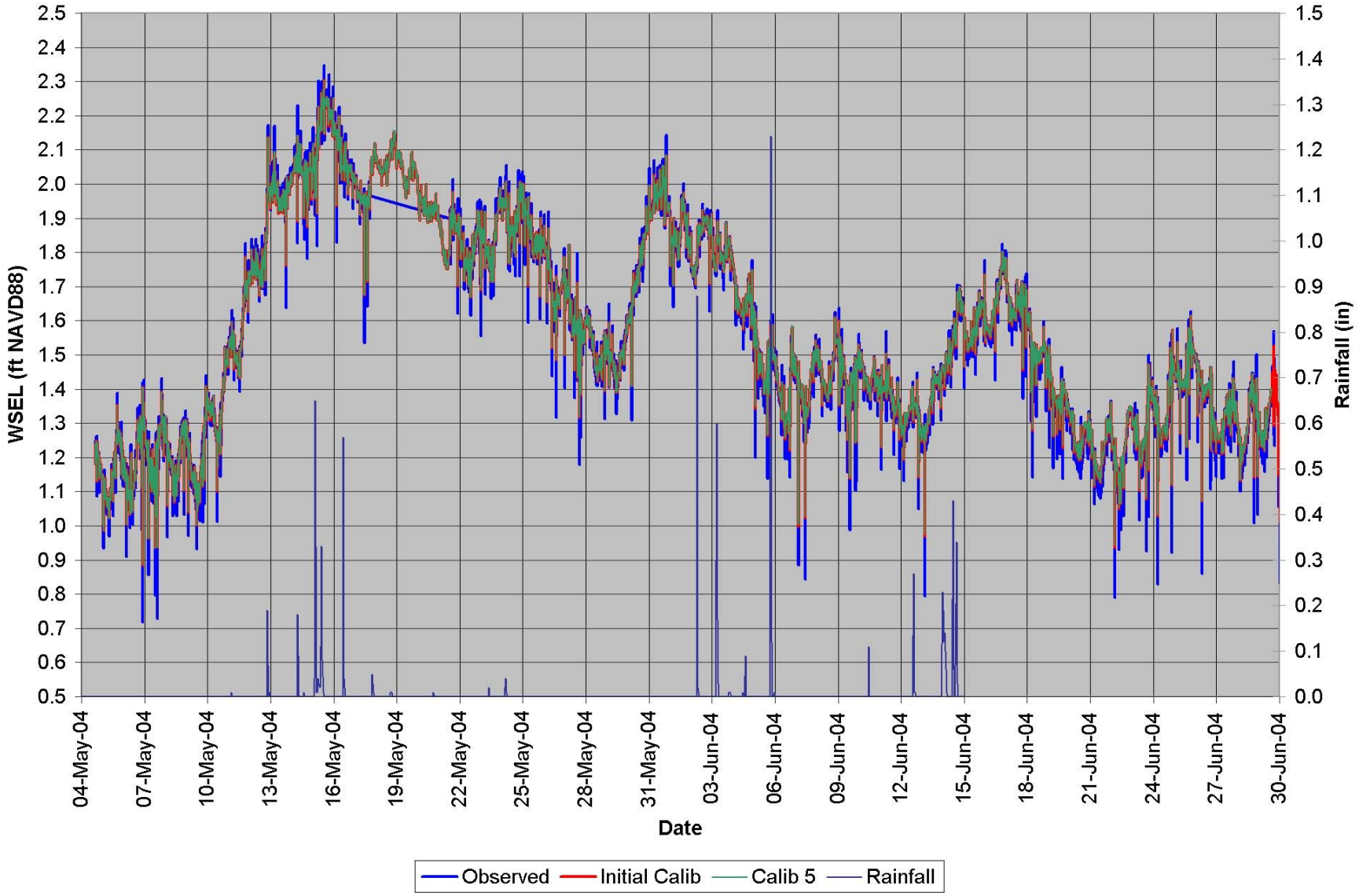

Figure A.4. Final RMA-2 Water Surface Elevation Calibration (Gage 4).

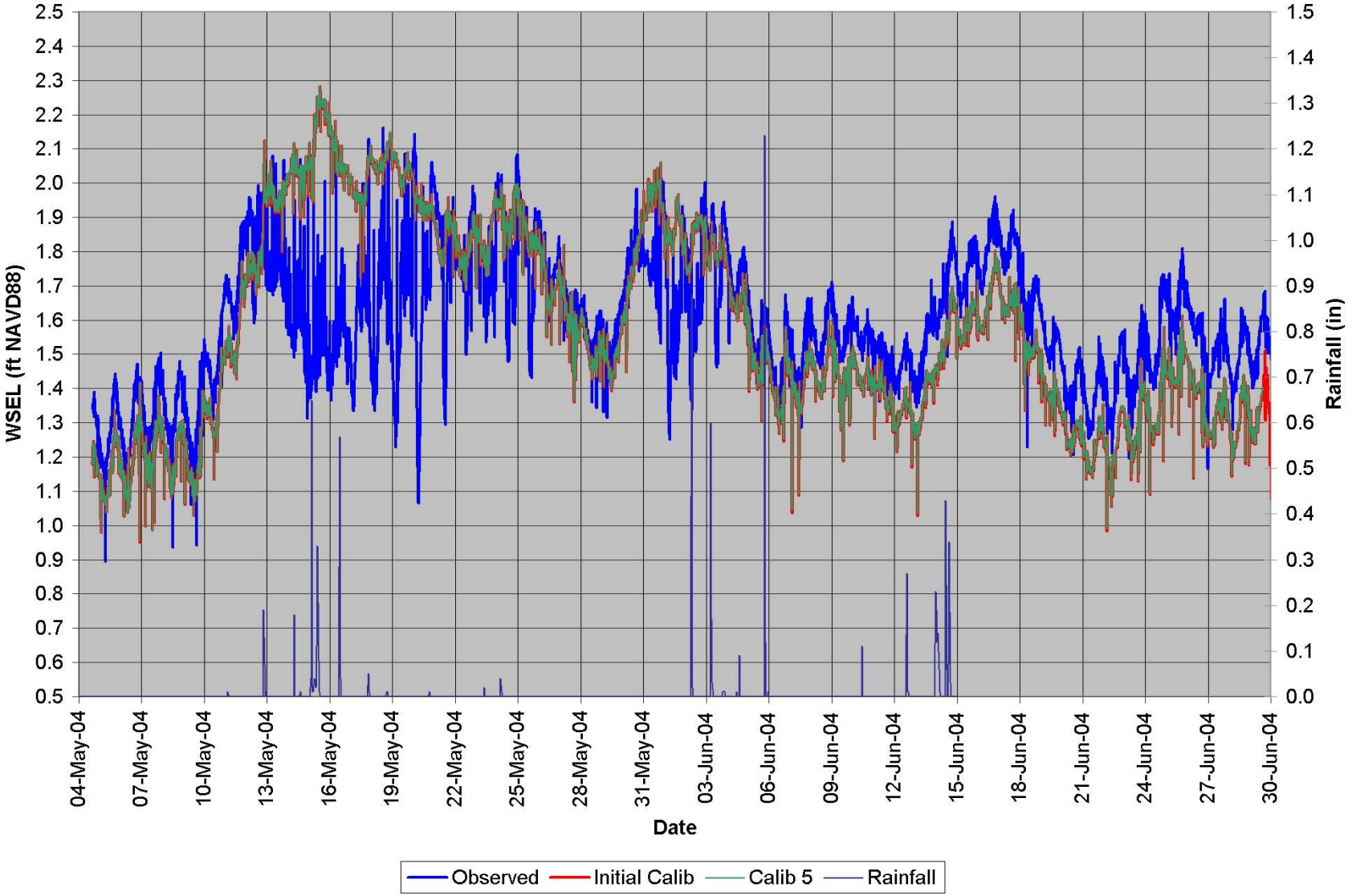

Figure A.5. Final RMA-2 Water Surface Elevation Calibration (Gage 5).

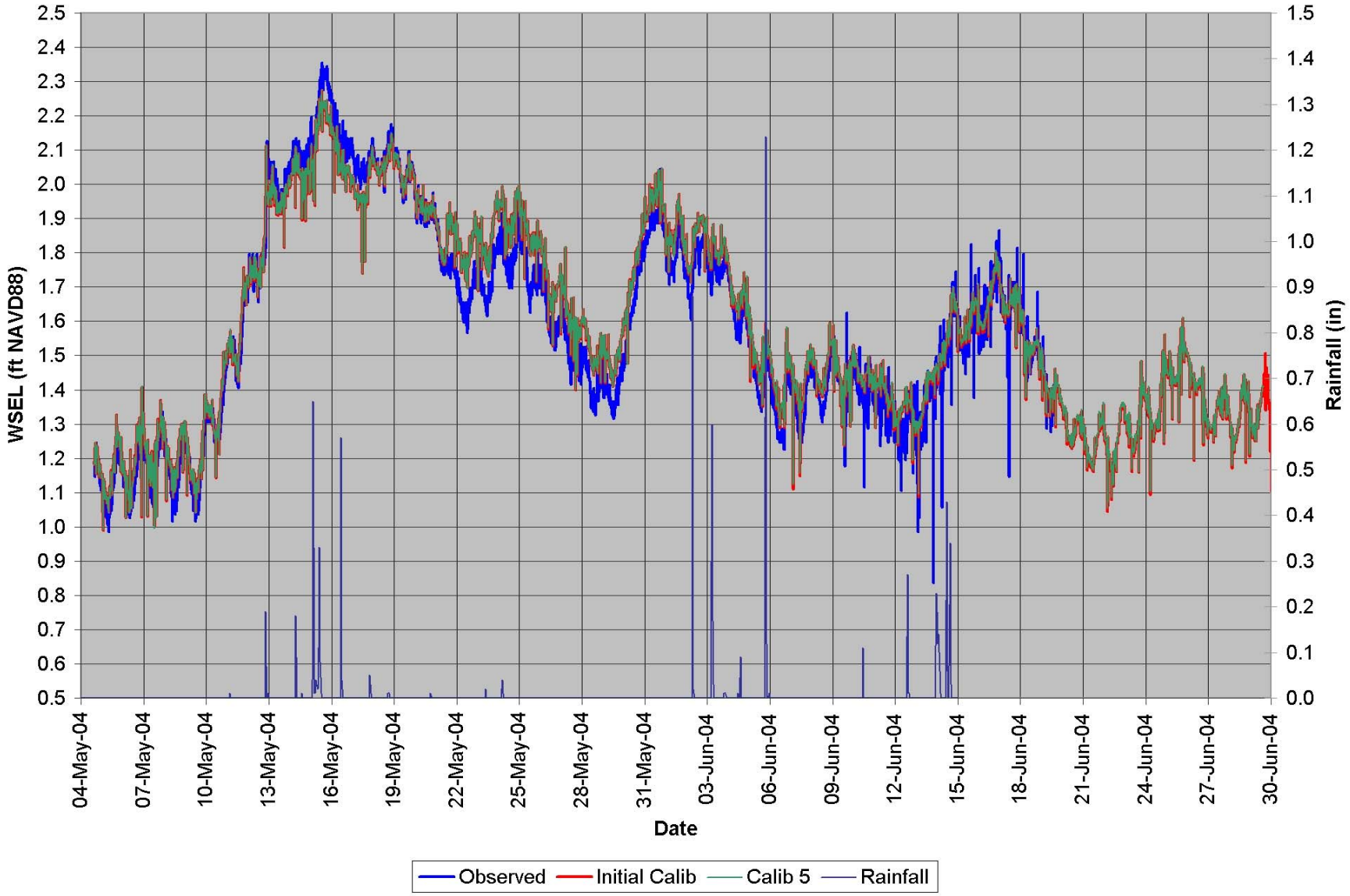

Figure A.6. Final RMA-2 Water Surface Elevation Calibration (Gage 6).

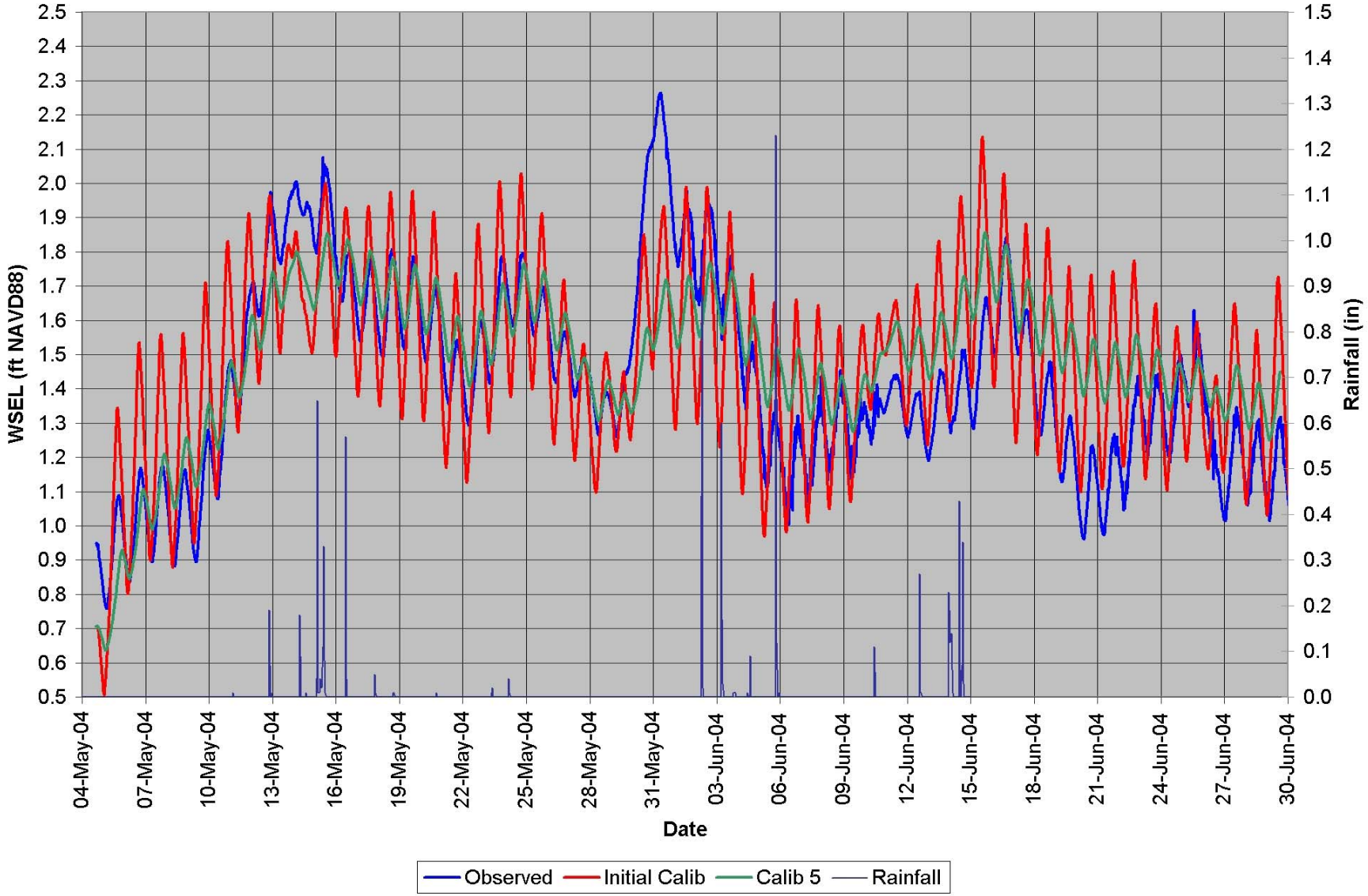

Figure A.7. Final RMA-2 Water Surface Elevation Calibration (Gage 7).

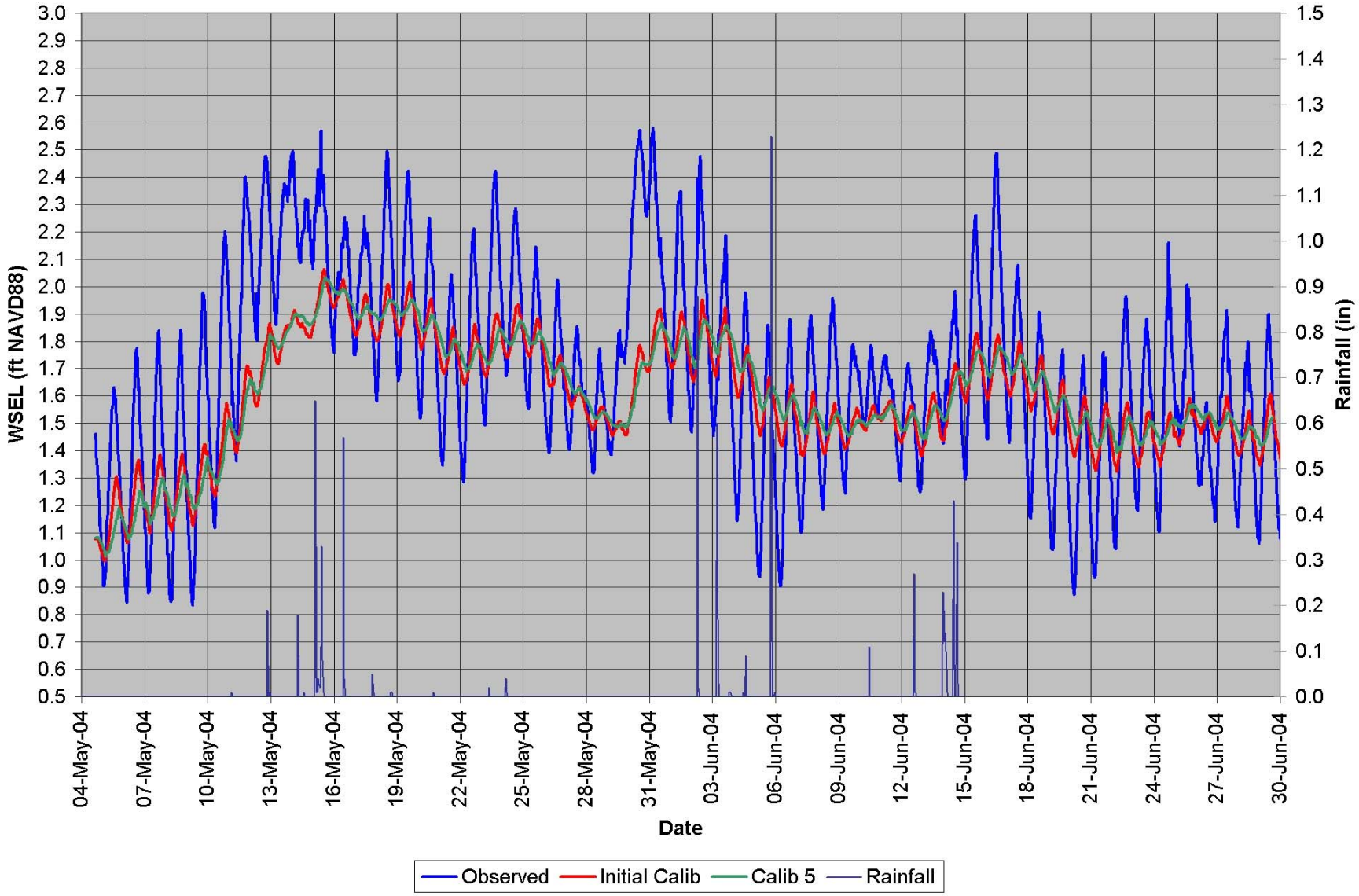

Figure A.8. Final RMA-2 Water Surface Elevation Calibration (Gage 8).

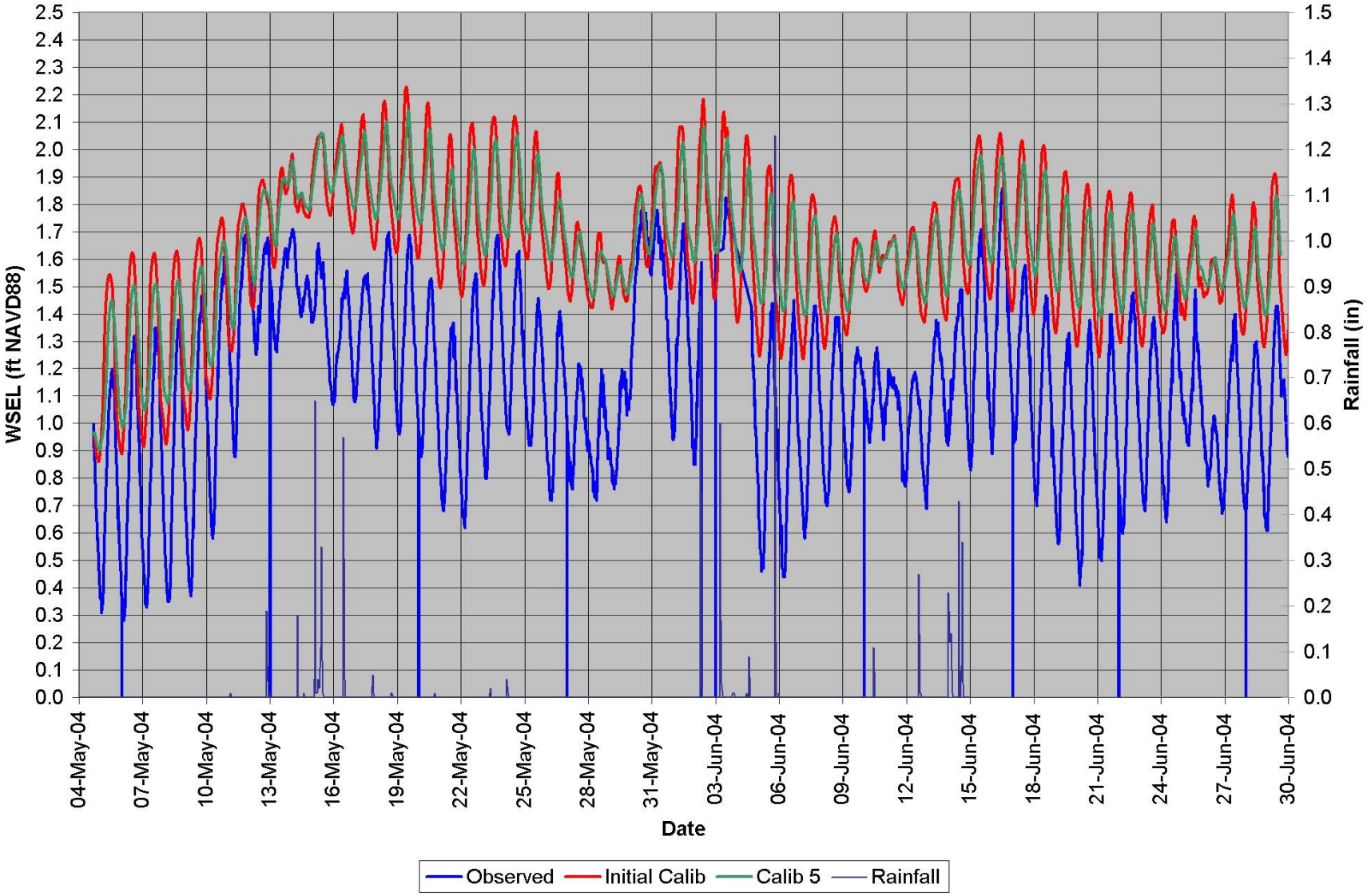

Figure A.9. Final RMA-2 Water Surface Elevation Calibration (Gage 15).

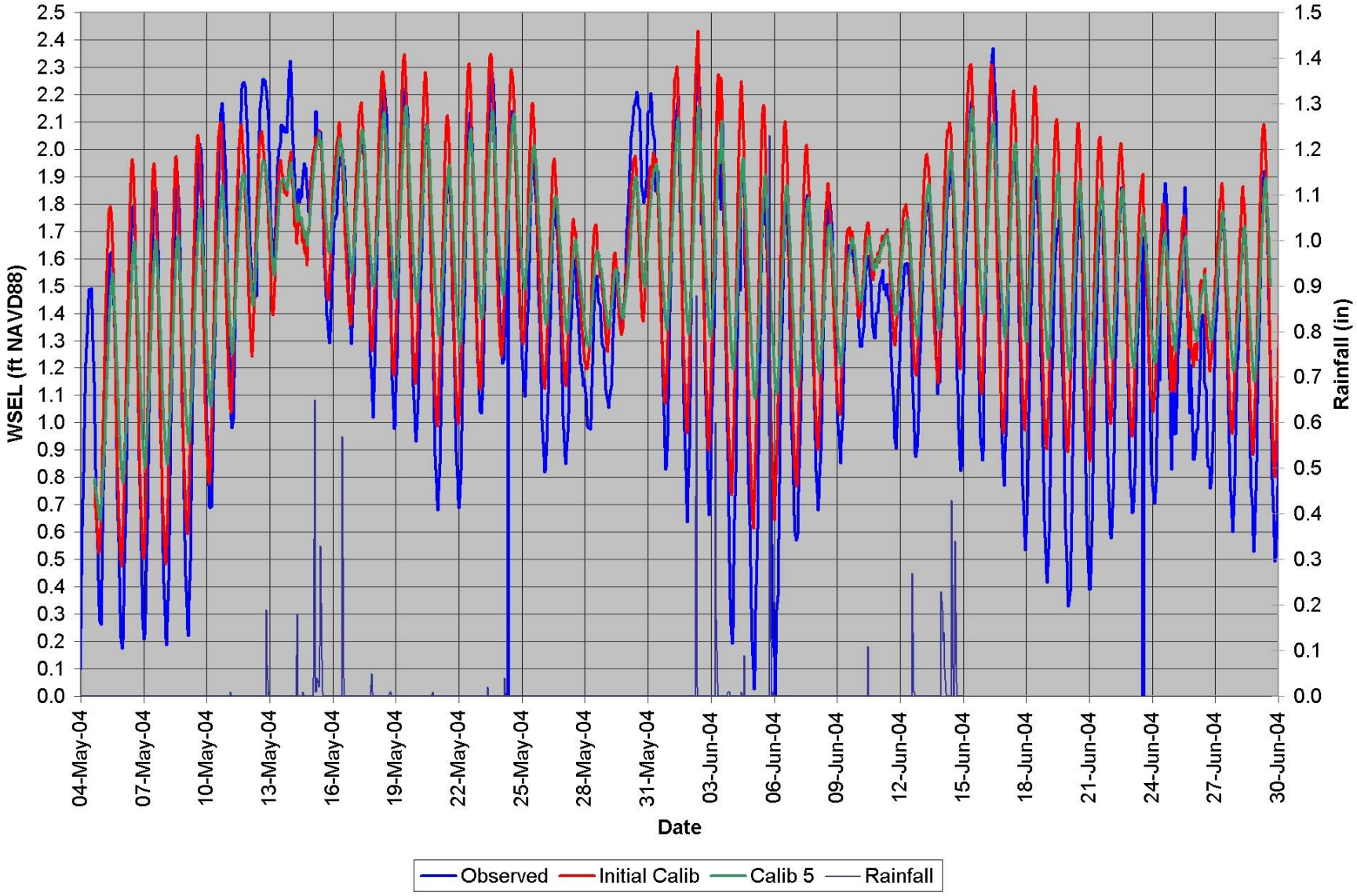

Figure A.10. Final RMA-2 Water Surface Elevation Calibration (Gage 16).

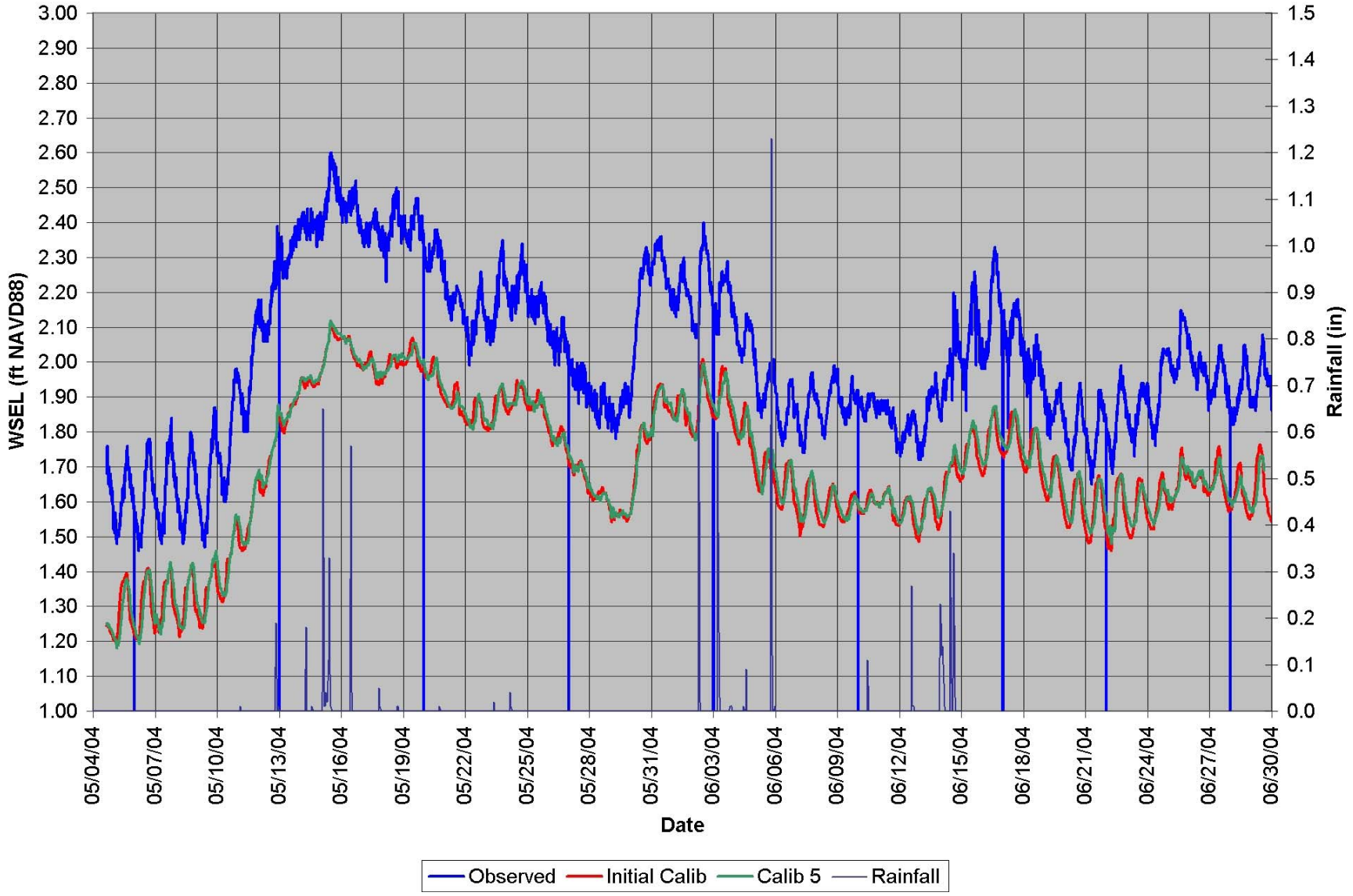

Figure A.11. Final RMA-2 Water Surface Elevation Calibration (Gage 17).

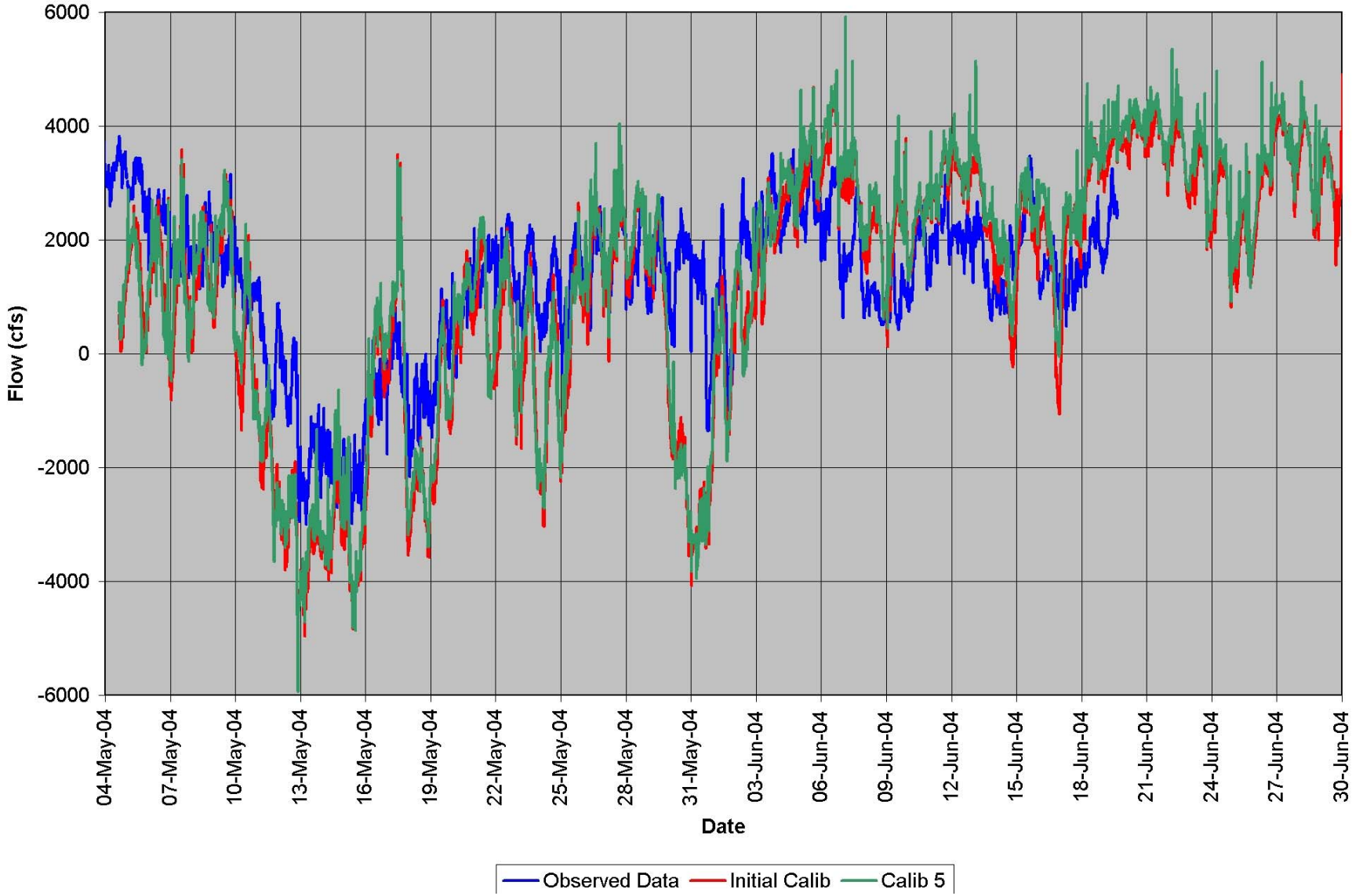

Figure A.12. Final RMA-2 Flow Calibration (Gage 6).

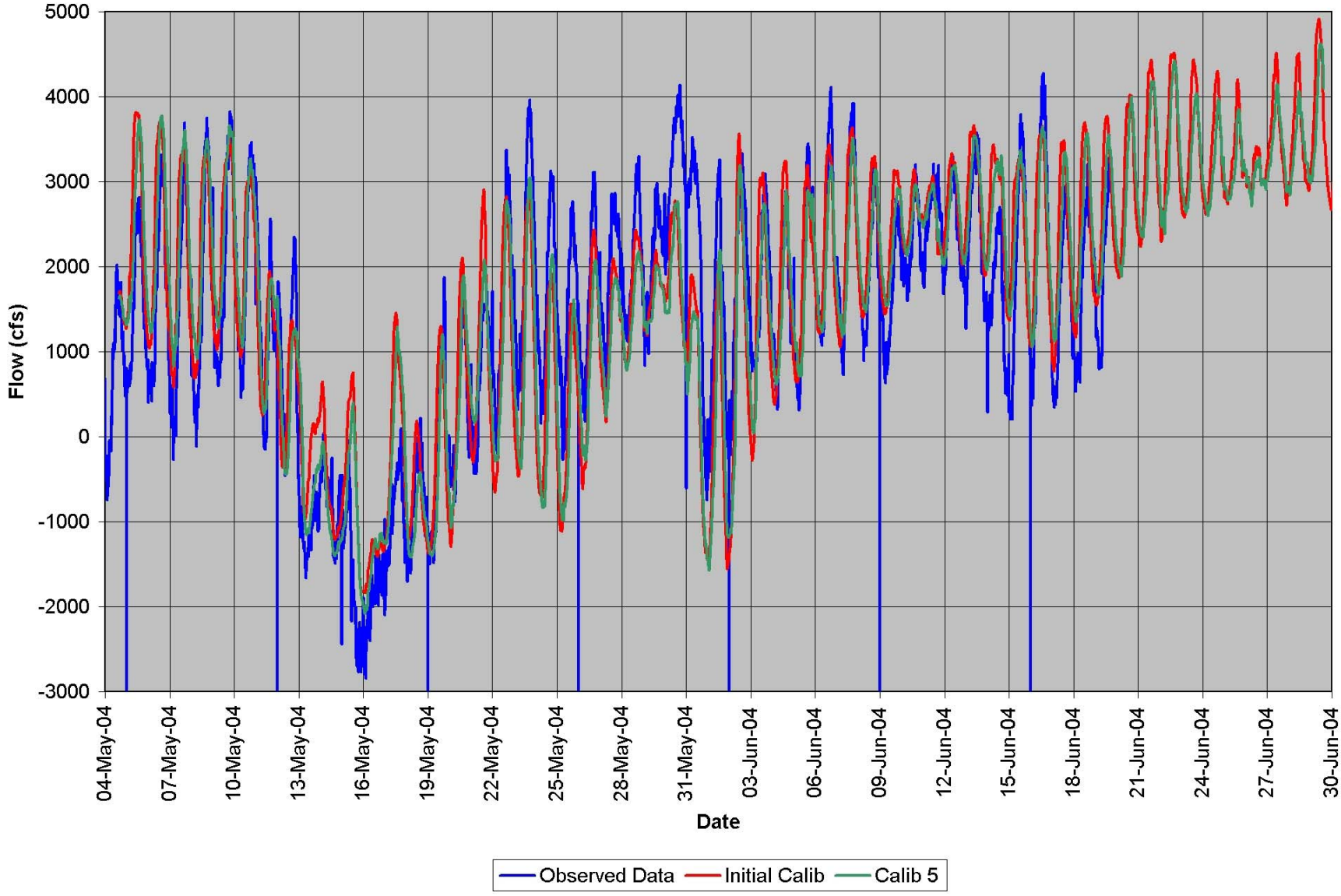

Figure A.13. Final RMA-2 Flow Calibration (Gage 17).

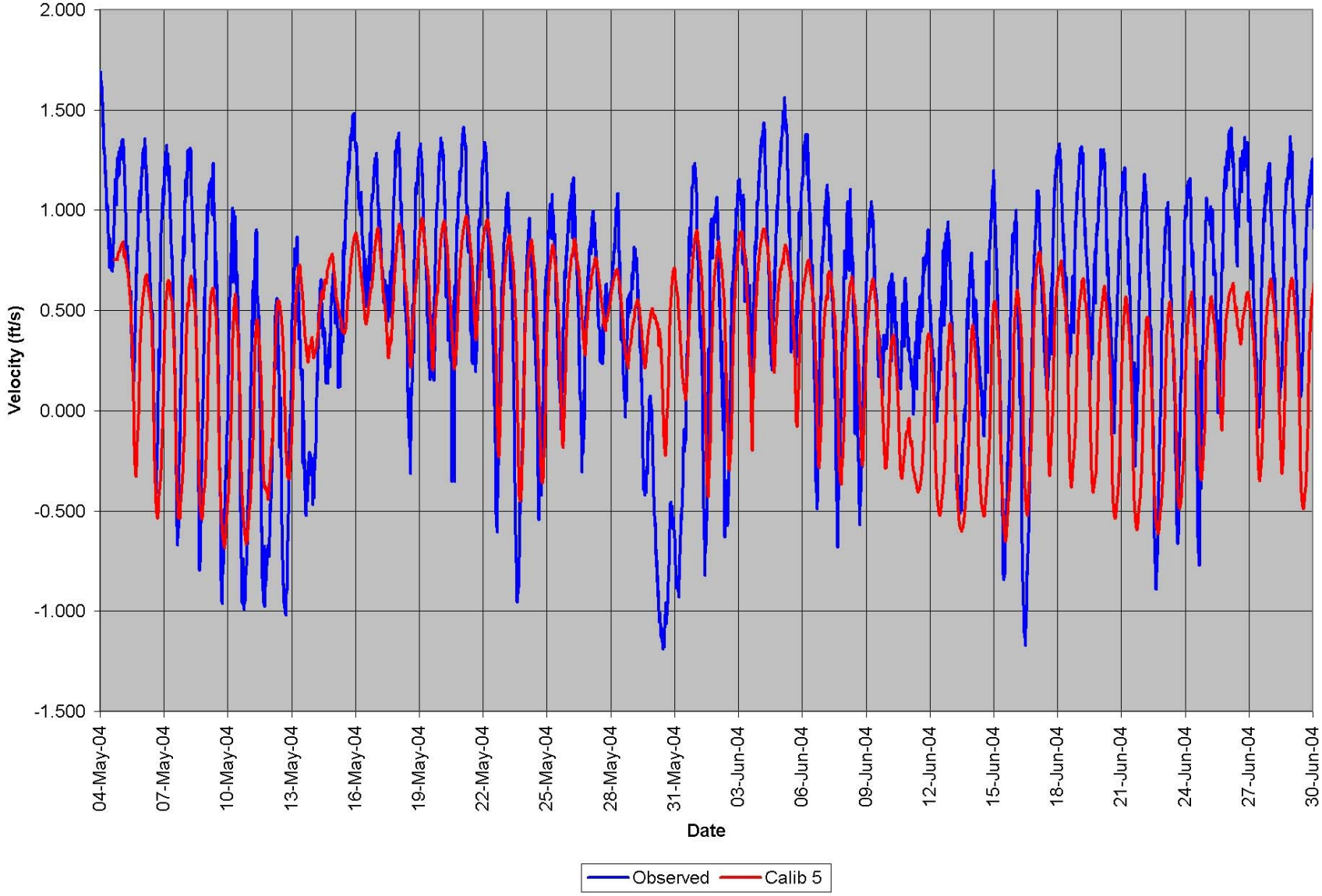

Figure A.14. Final RMA-2 Velocity Calibration (Gage 8).

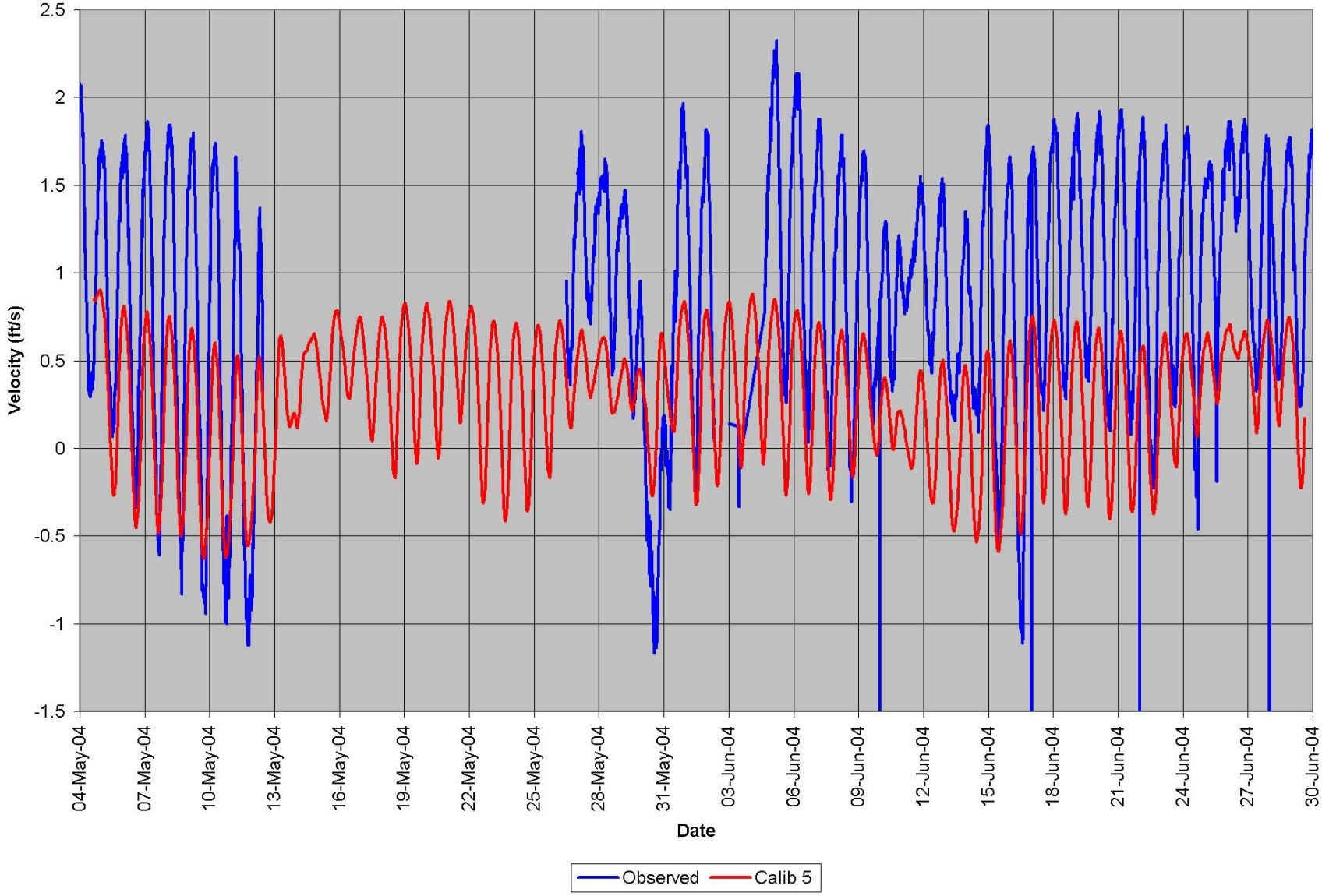

Figure A.15. Final RMA-2 Velocity Calibration (Gage 15).

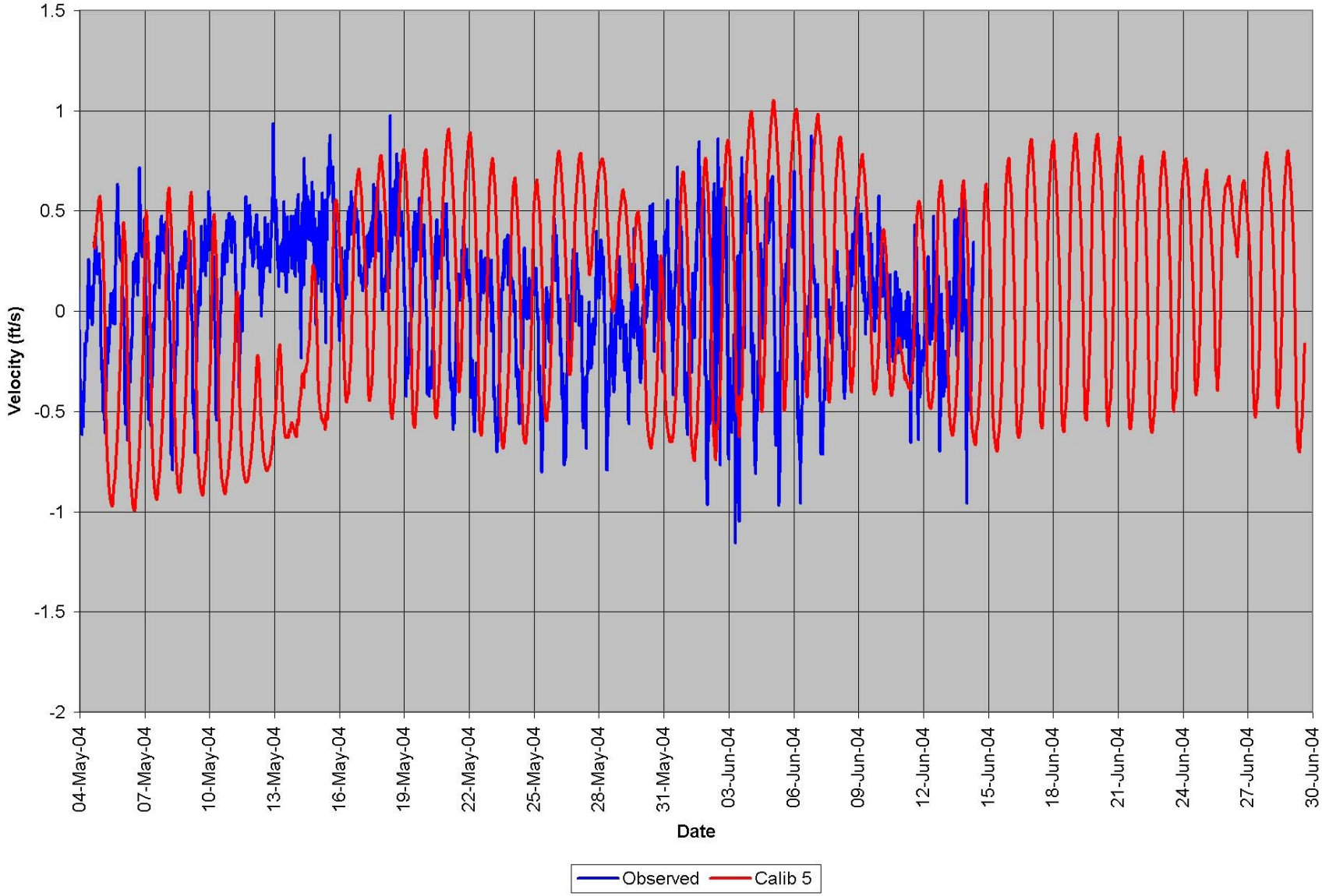

Figure A.16. Final RMA-2 Velocity Calibration (Gage 16).

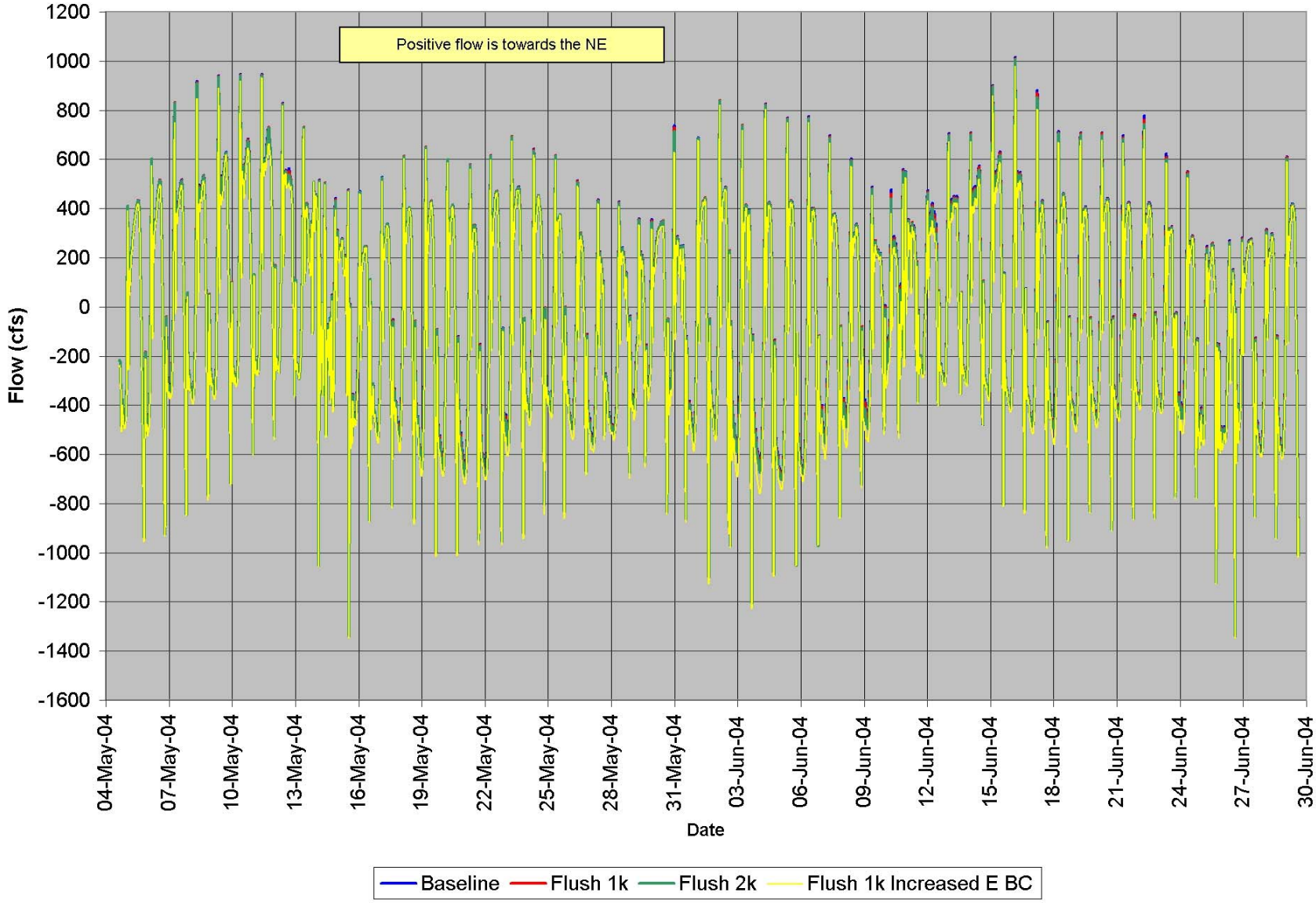

Figure A.17. RMA-2 Computed Flow for Flushing Simulations: Southern end of Bayou Dularge.

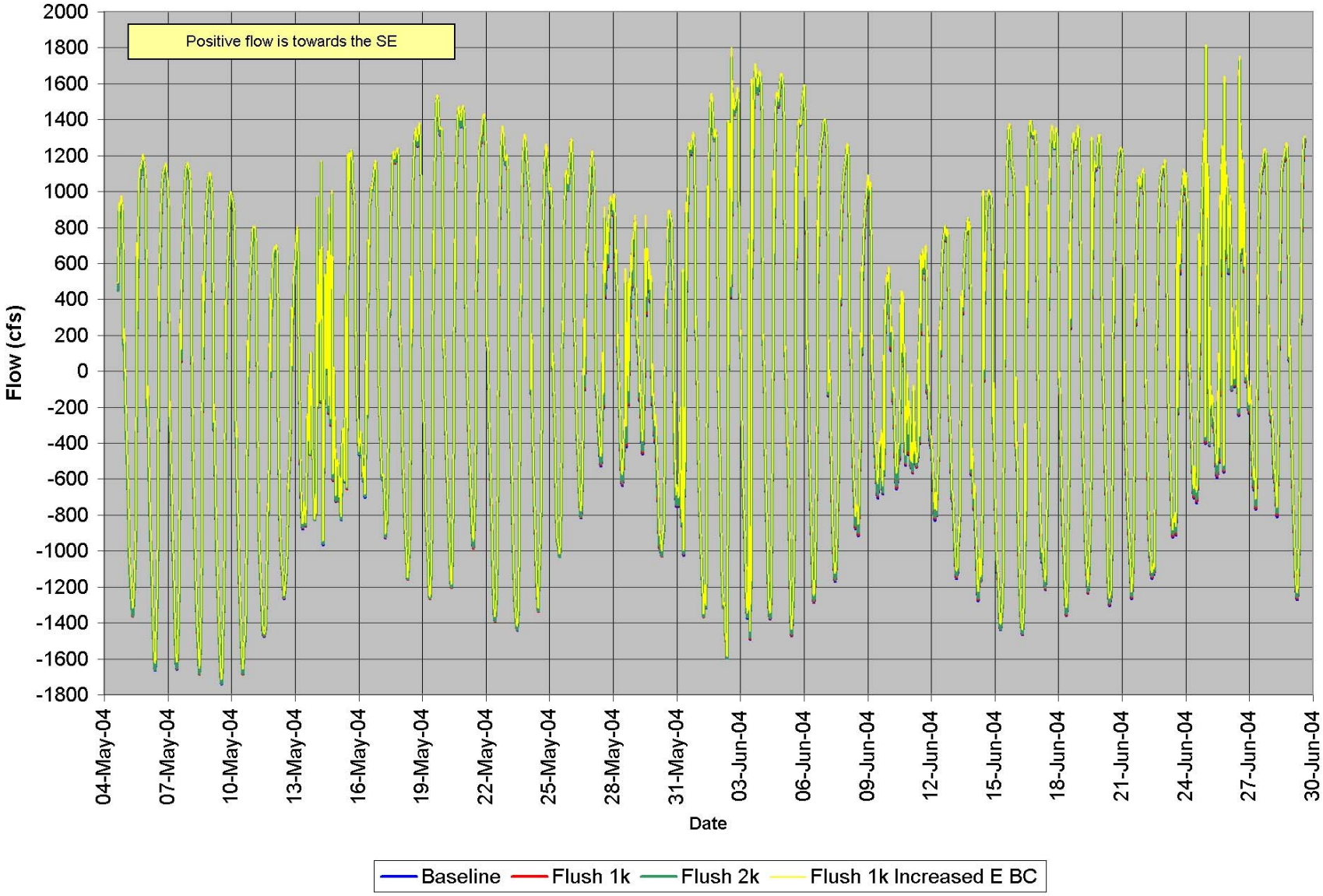

Figure A.18. RMA-2 Computed Flows for Flushing Simulations: Southern end of Grand Caillou.

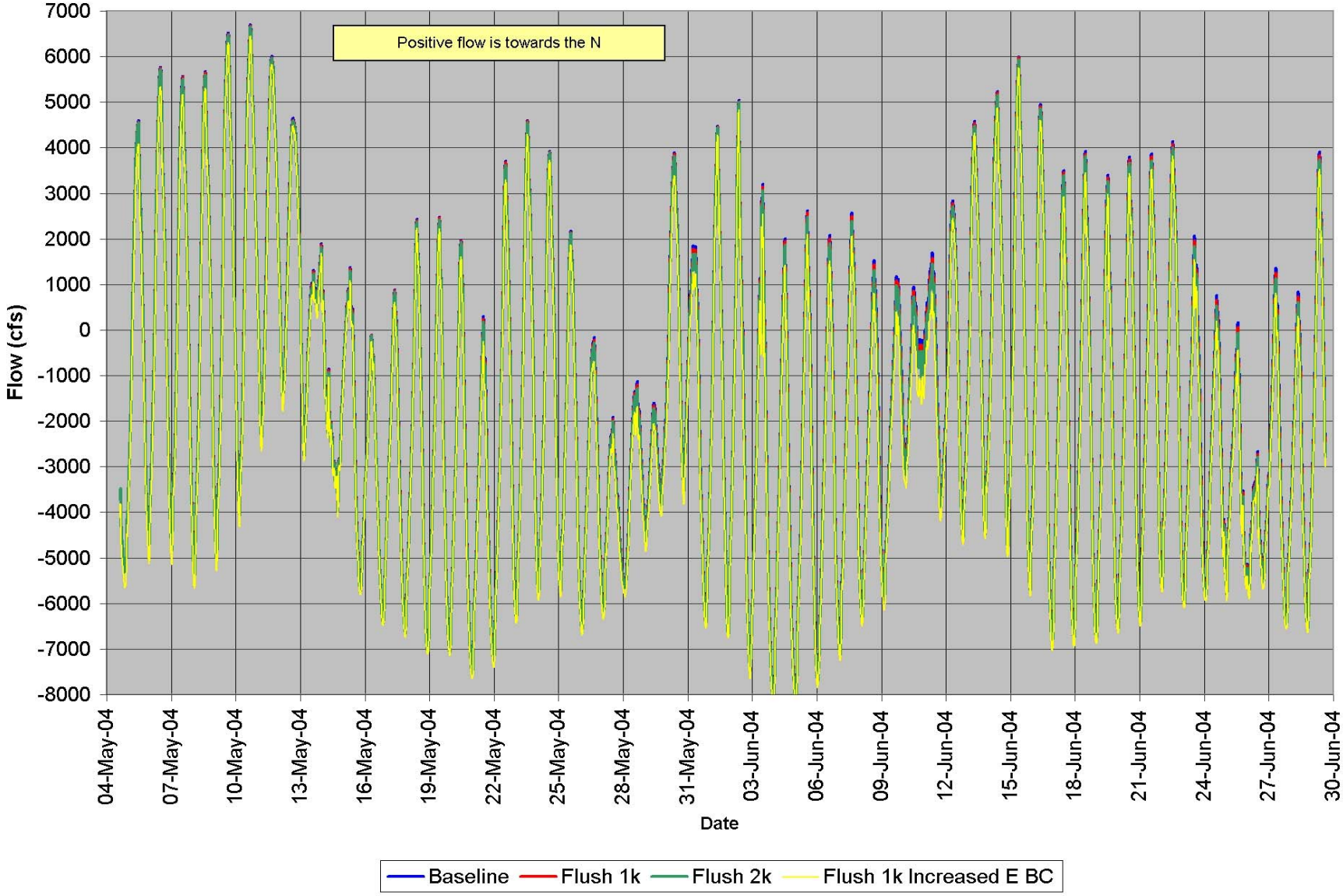

Figure A.19. RMA-2 Computed Flows for Flushing Simulations: Southern end of Houma Navigation Canal.

Figure A.20. RMA-2 Computed Flows for Flushing Simulations: Southern end of Bayou Terrebonne.

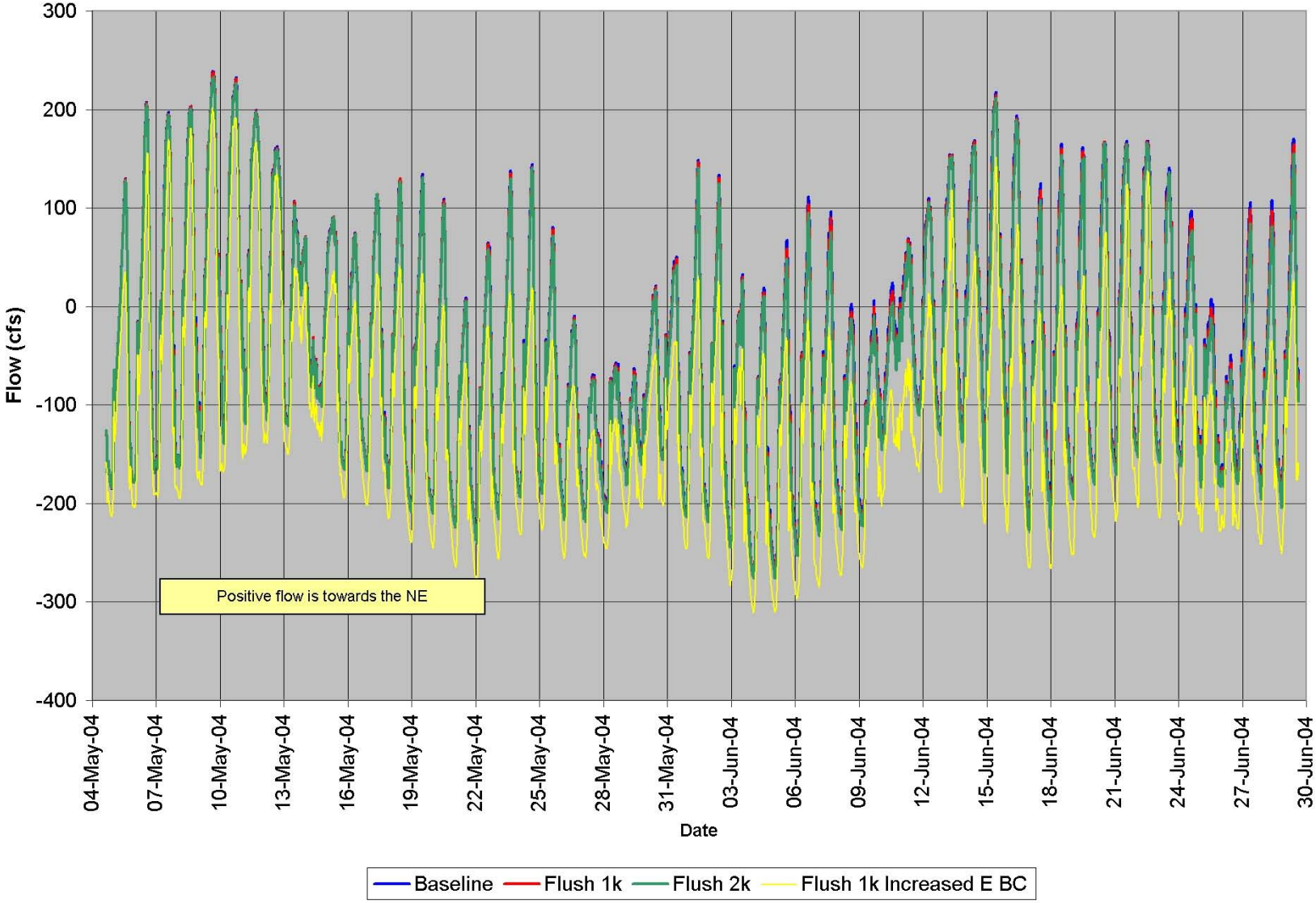

Figure A.21. RMA-2 Computed Flows for Flushing Simulations: Southern end of Bayou Point Au Chien.

Figure A.22. RMA-2 Computed Flows for Flushing Simulations: Southern end of Grand Bayou.

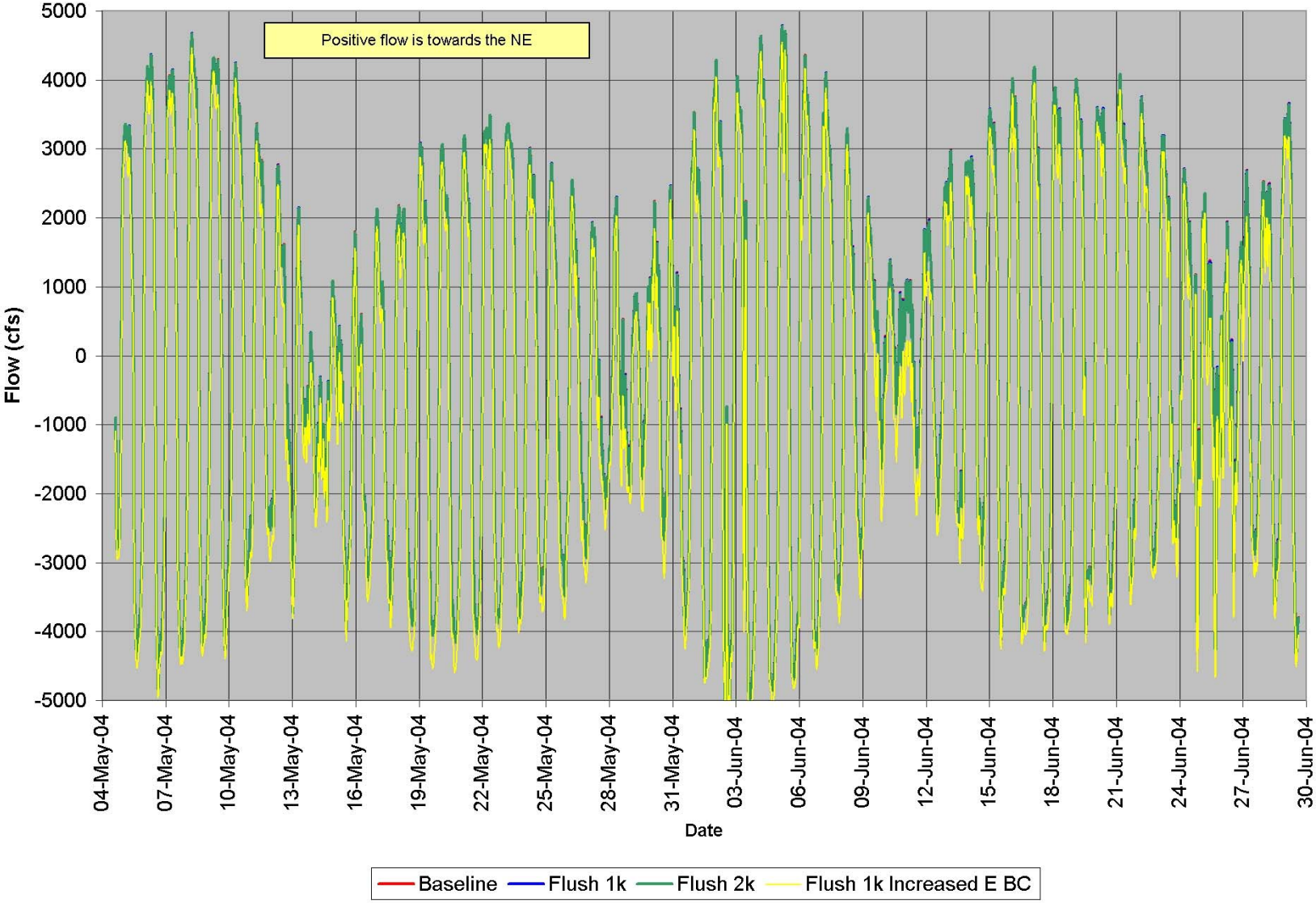

Figure A.23. RMA-2 Computed Flows for Flushing Simulation: Southern end of Bayou Lafourche.

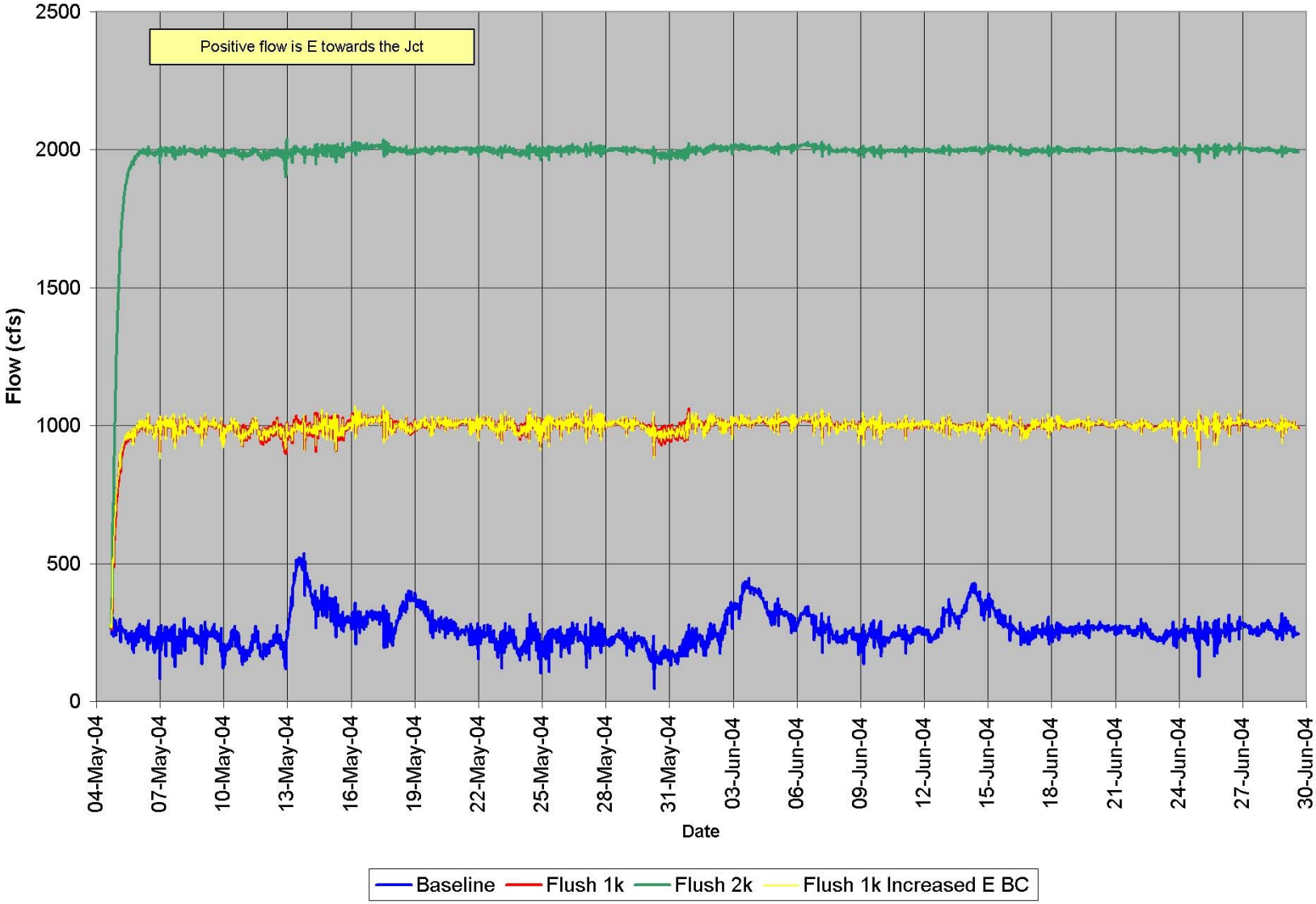

Figure A.24. RMA-2 Computed Flows for Flushing Simulations: Bayou Lafourche West of Junction with Company Canal.

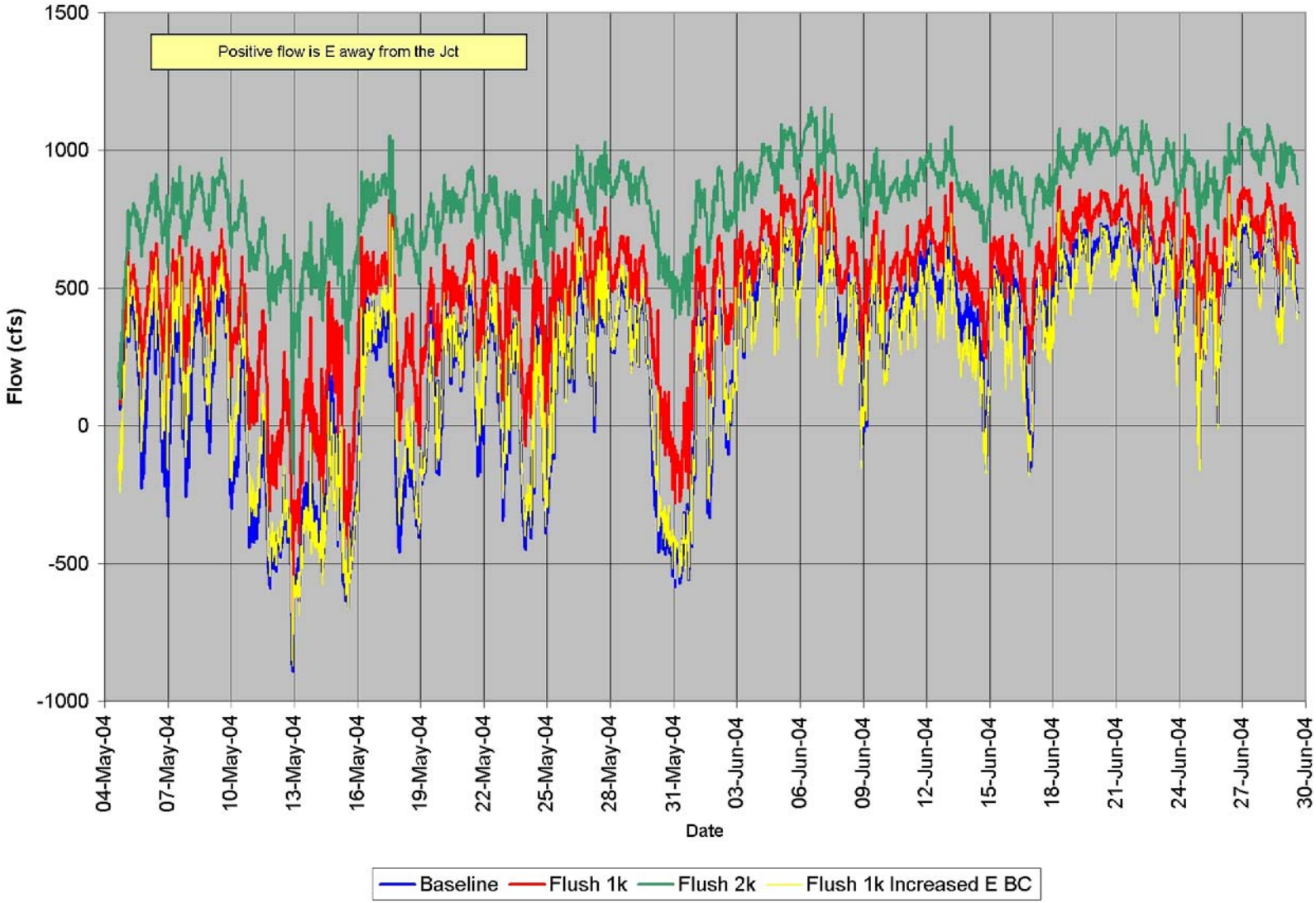

Figure A.25. RMA-2 Computed Flows for Flushing Simulations: Bayou Lafourche East of Junction with Company Canal.

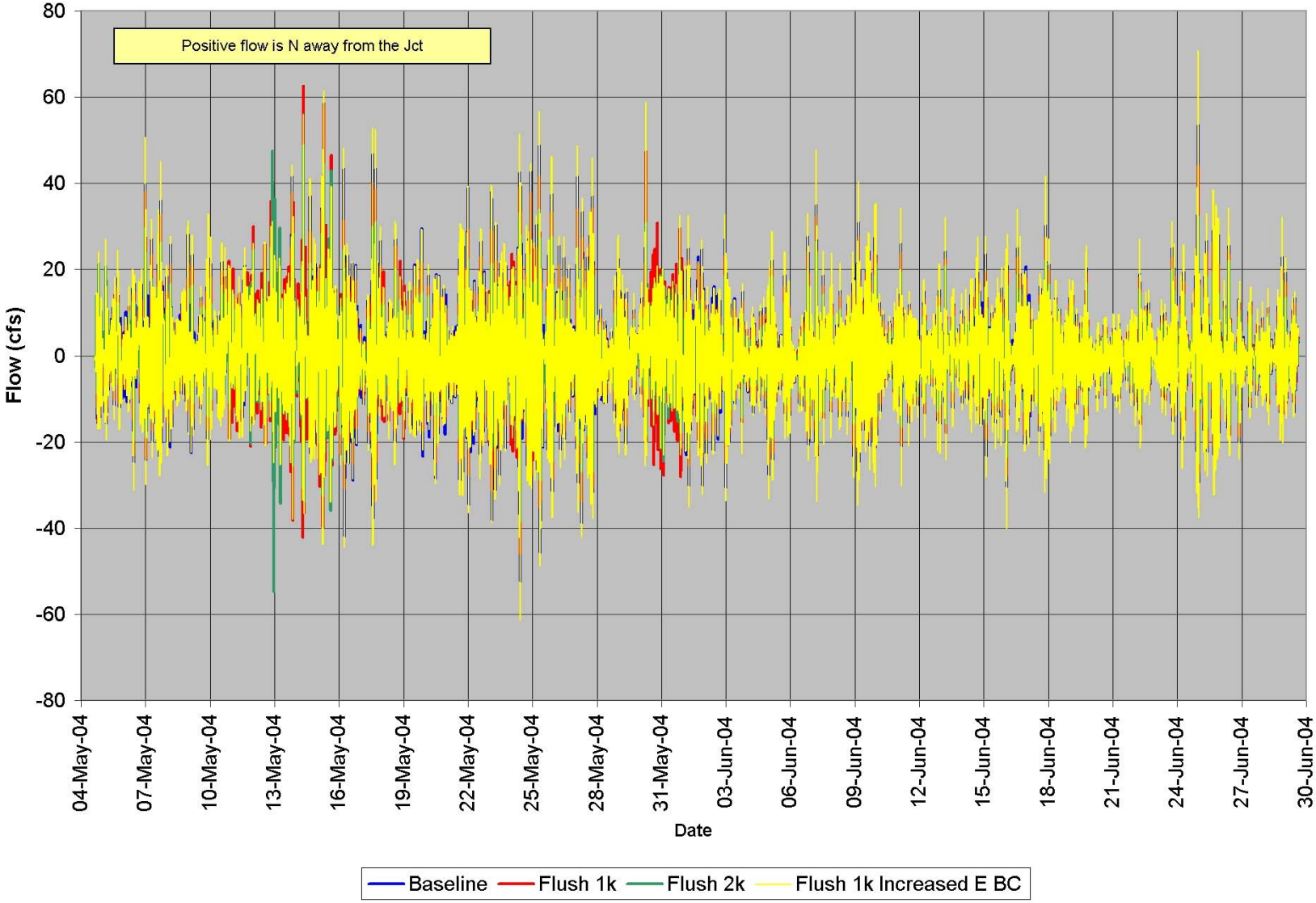

Figure A.26. RMA-2 Computed Flows for Flushing Simulations: Company Canal North of Junction with Bayou Lafourche.

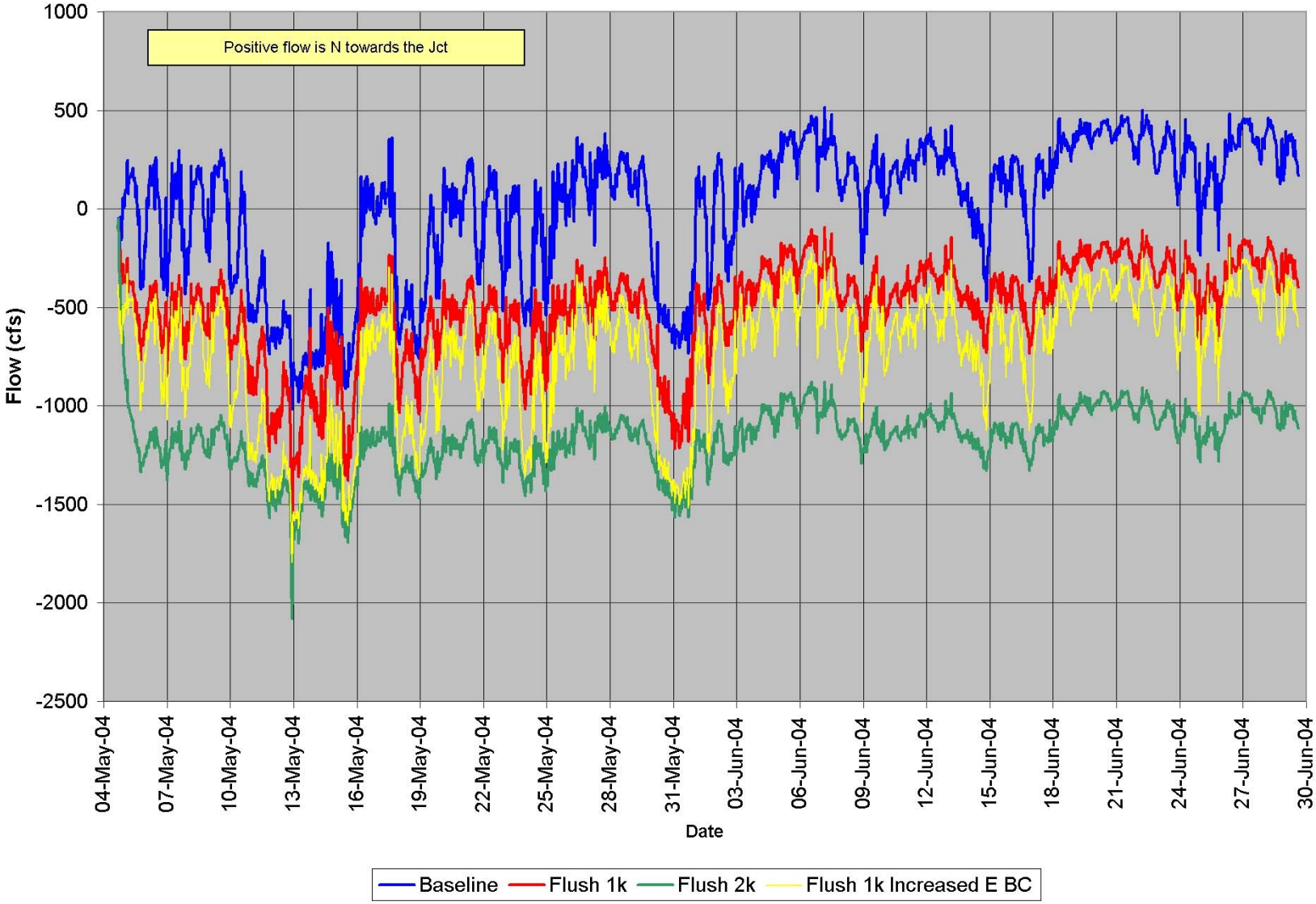

Figure A.27. RMA-2 Computed Flows for Flushing Simulations: Company Canal South of Junction with Bayou Lafourche.

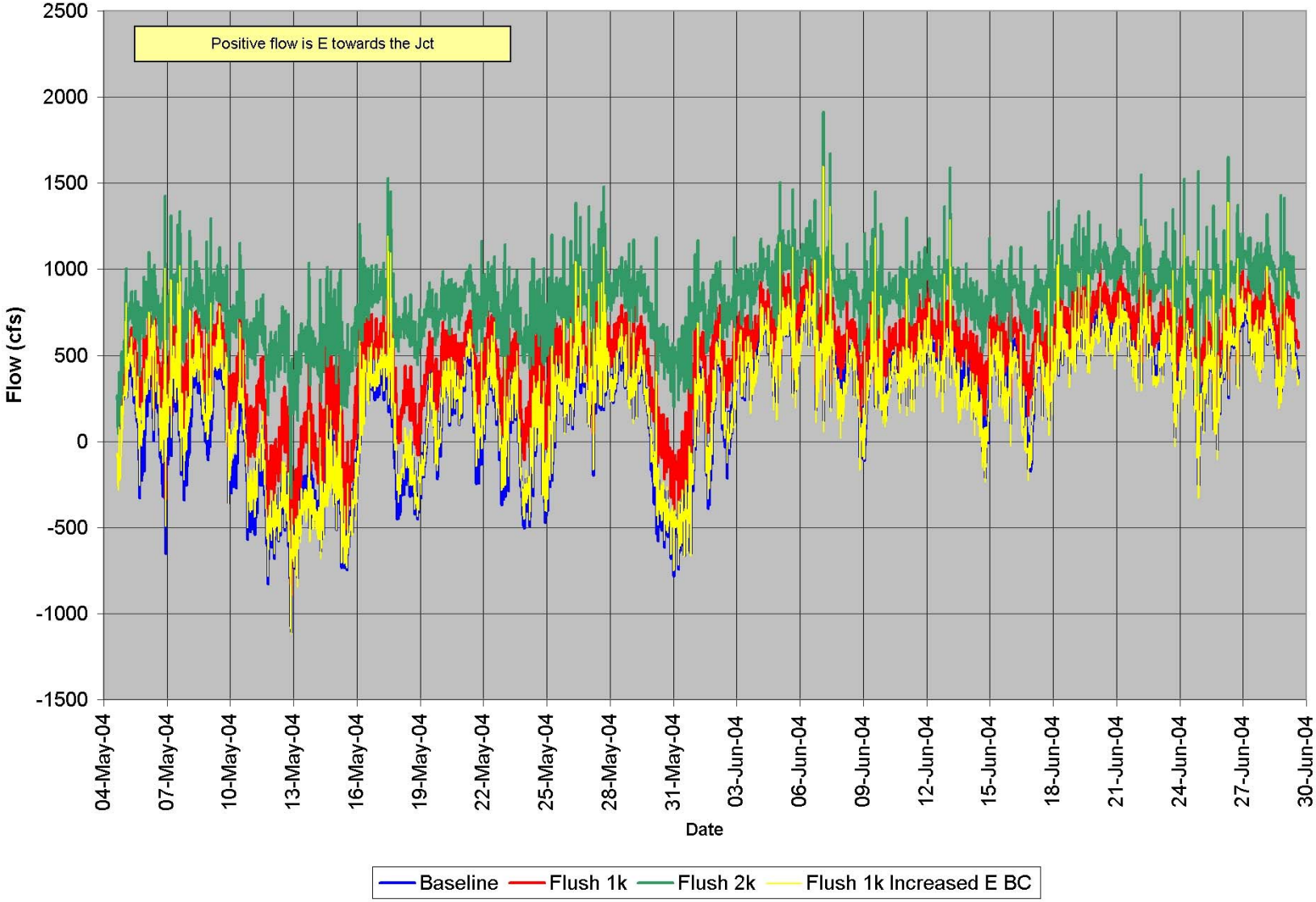

Figure A.28. RMA-2 Computed Flows for Flushing Simulations: Bayou Lafourche West of Junction with the GIWW.

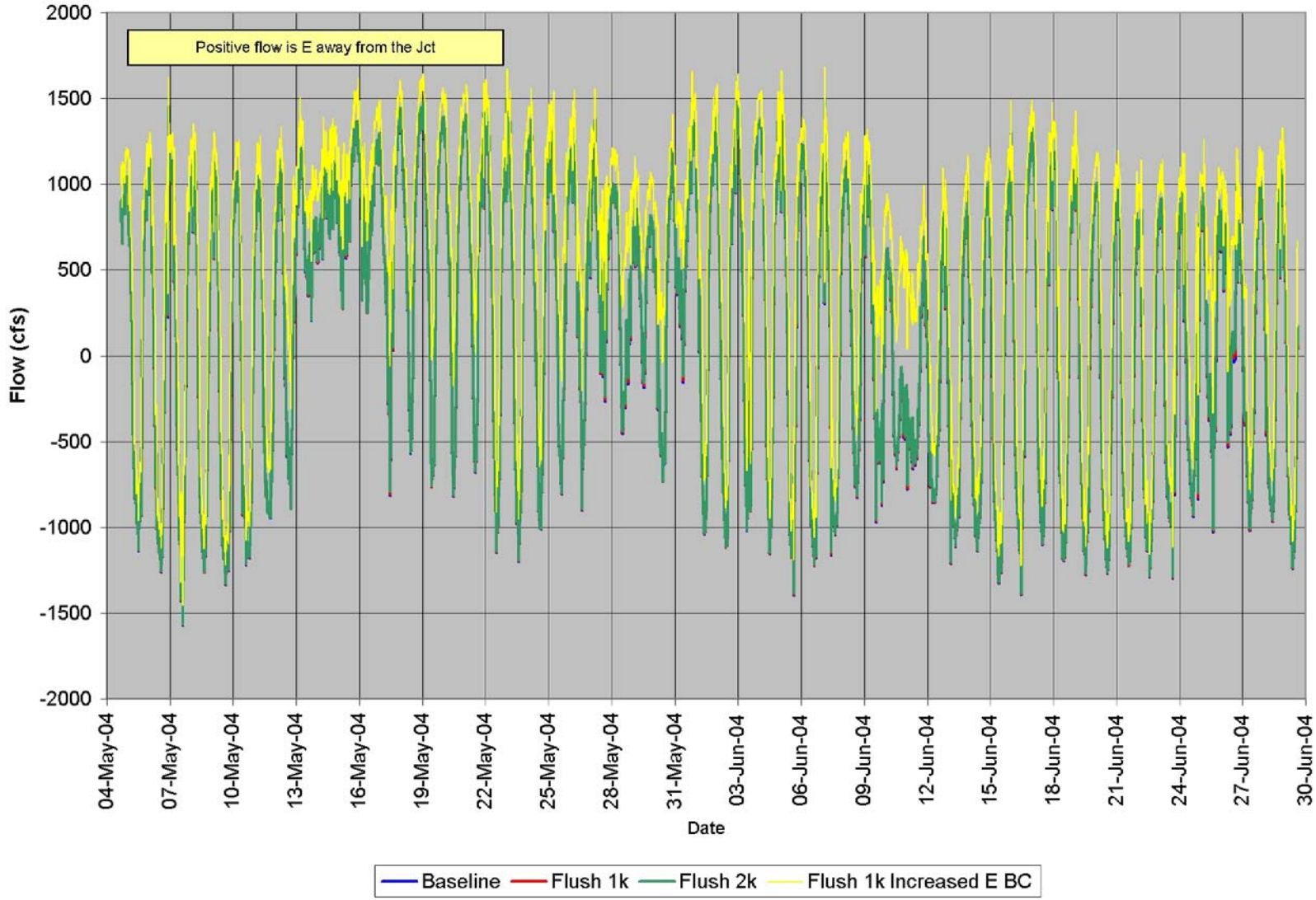

Figure A.29. RMA-2 Computed Flows for Flushing Simulations: Bayou Lafourche East of Junction with the GIWW.

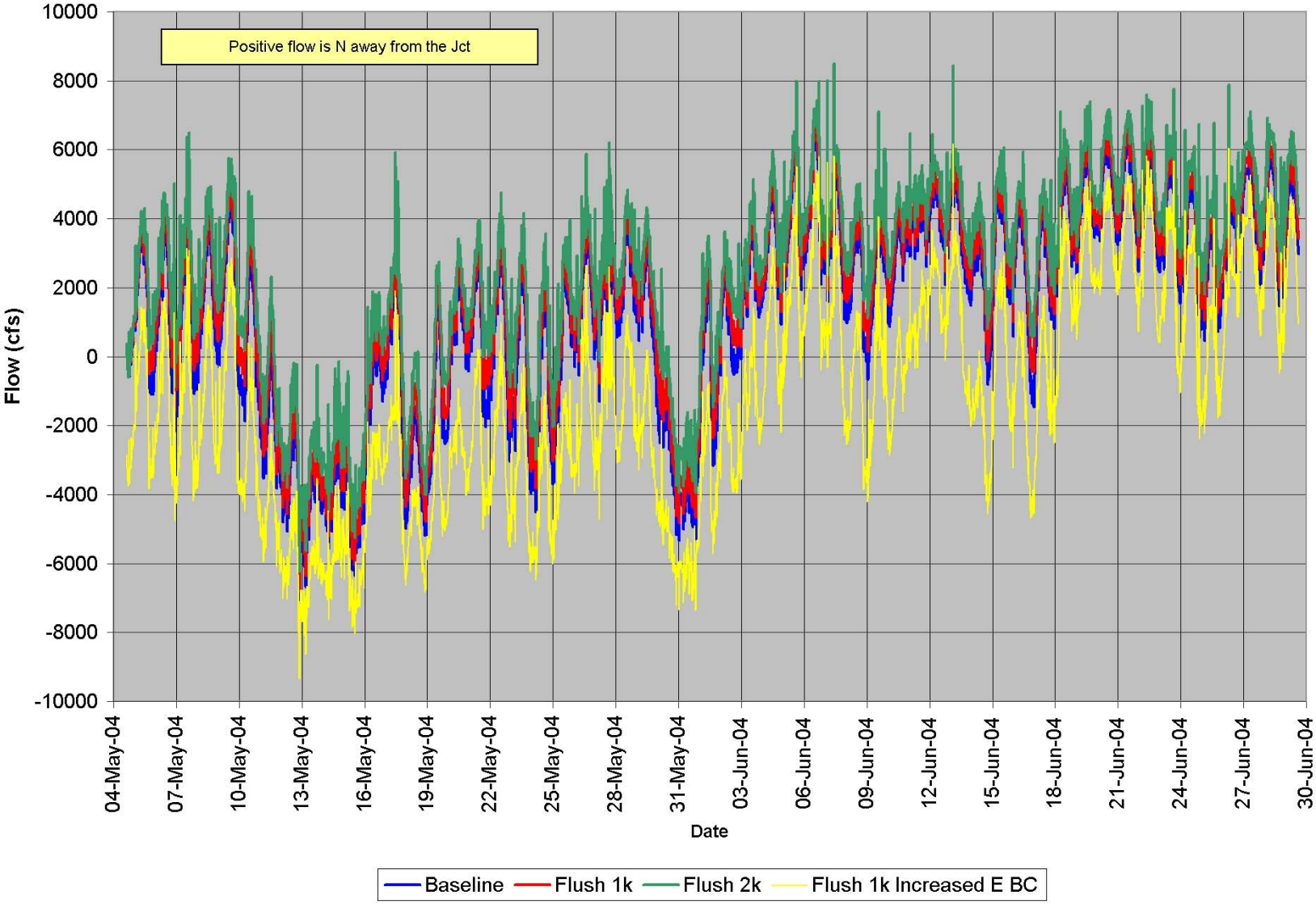

Figure A.30. RMA-2 Computed Flows for Flushing Simulations: GIWW North of Junction with Bayou Lafourche.

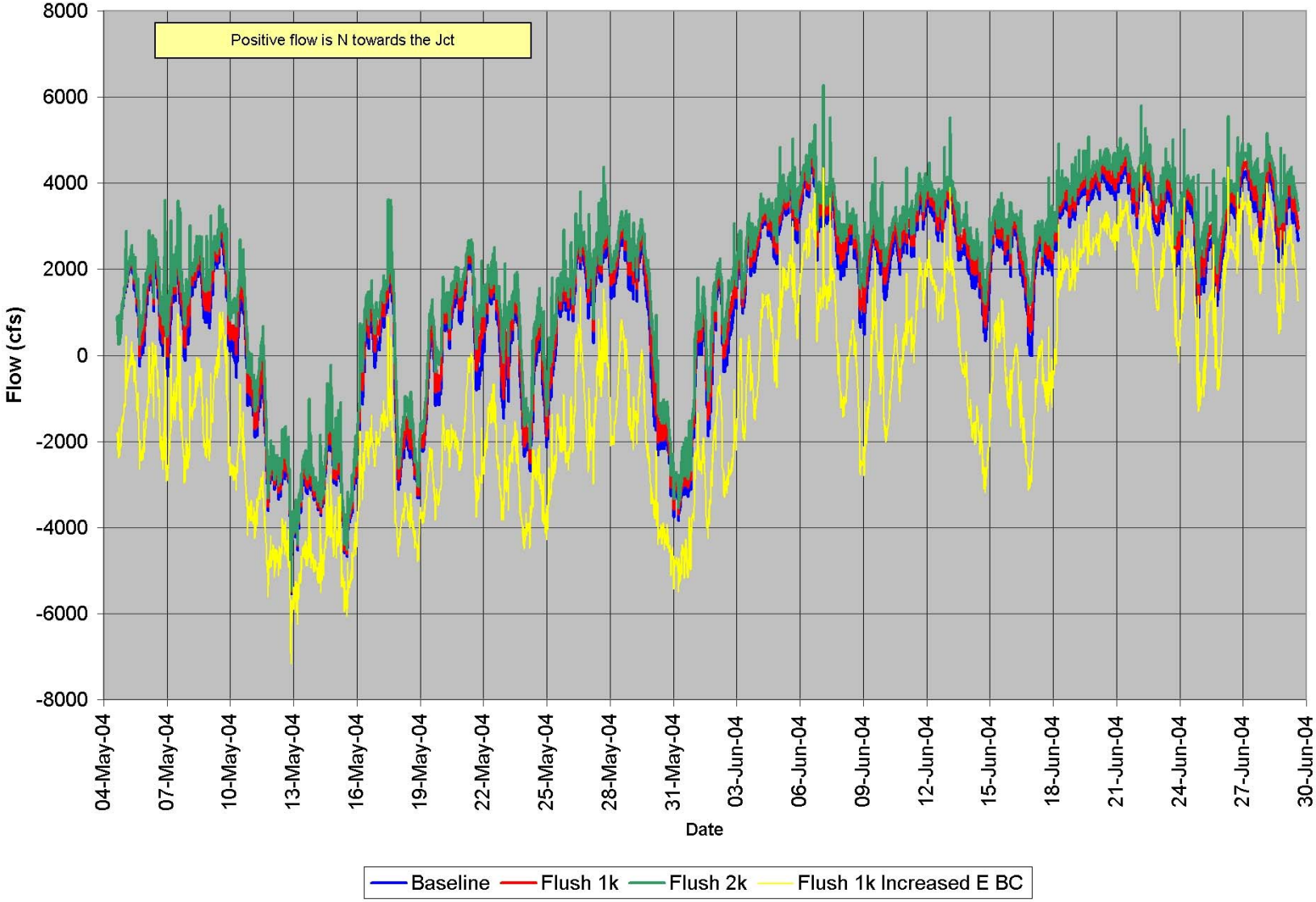

Figure A.31. RMA-2 Computed Flows for Flushing Simulations: GIWW South of Junction with Bayou Lafourche.

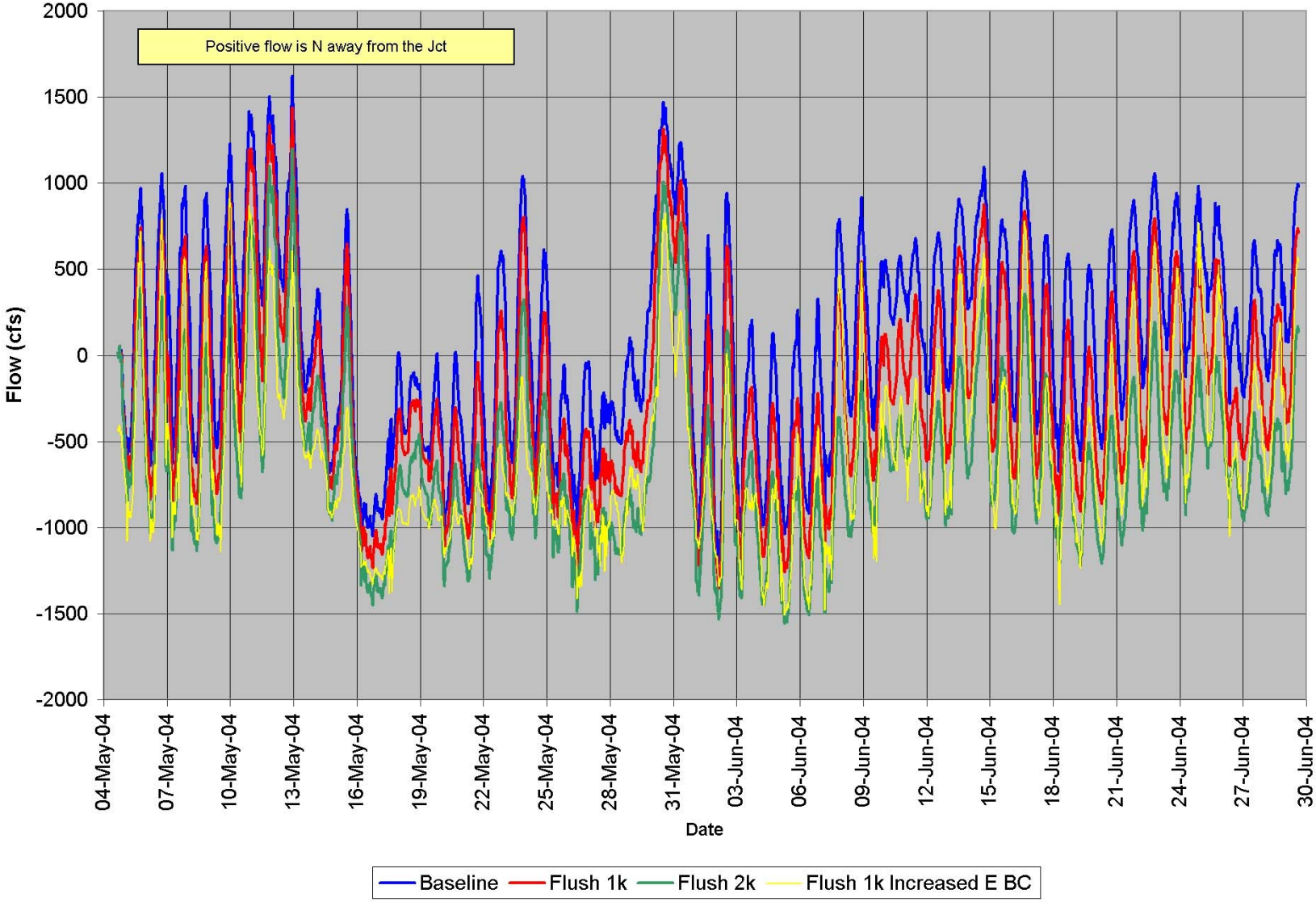

Figure A.32. RMA-2 Computed Flows for Flushing Simulations: Company Canal North of Junction with the GIWW.

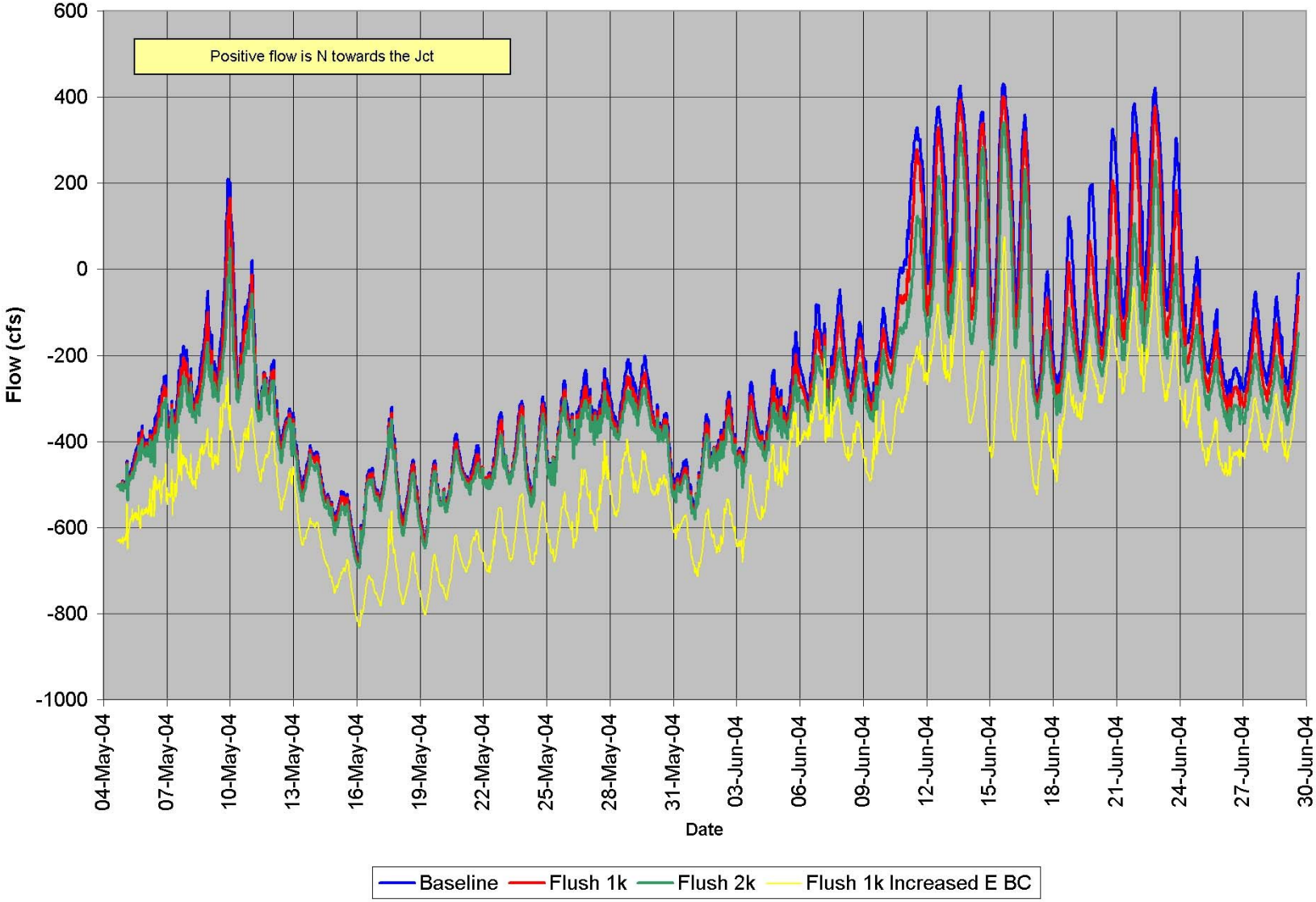

Figure A.33. RMA-2 Computed Flows for Flushing Simulations: Company Canal South of Junction with the GIWW.

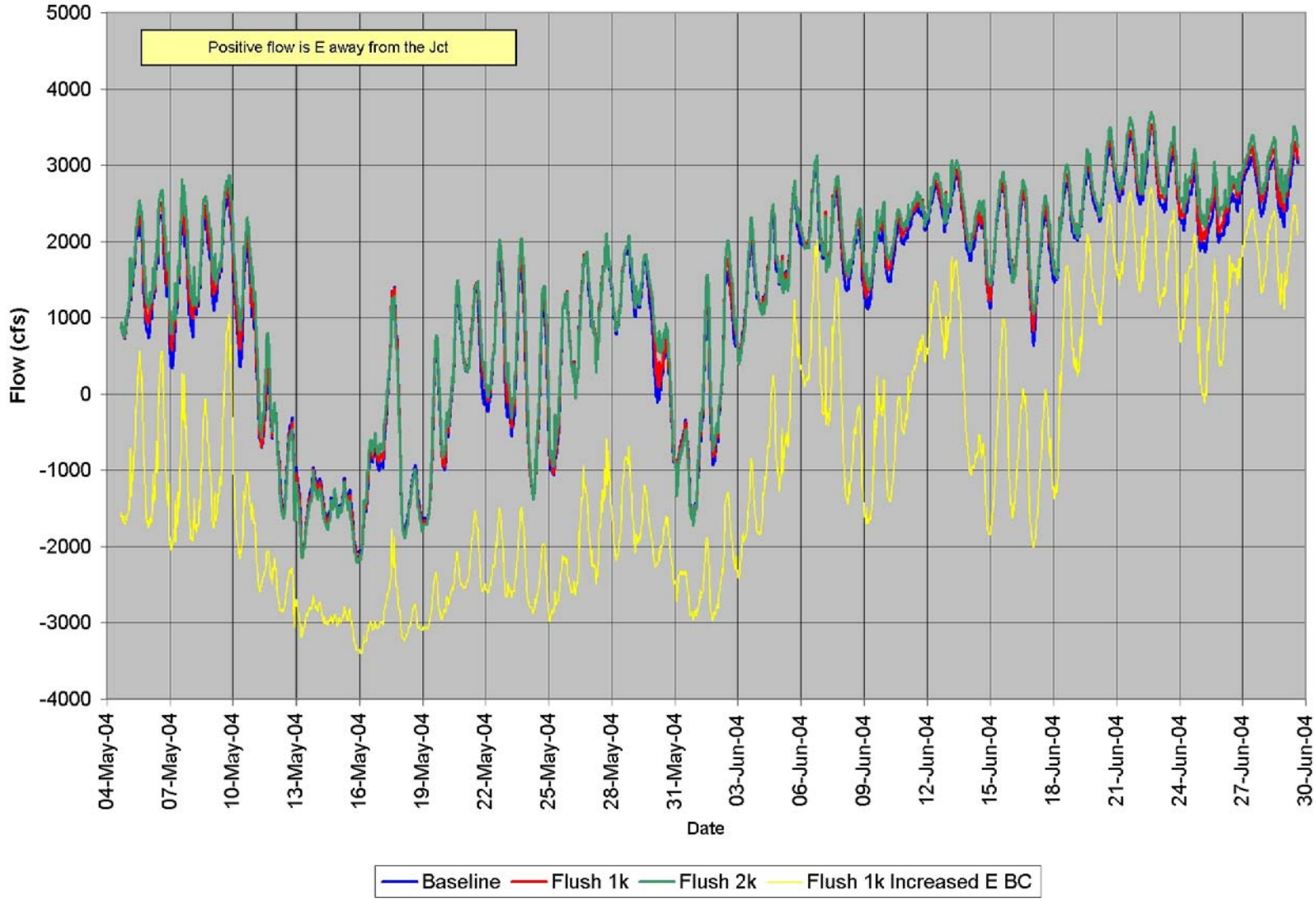

Figure A.34. RMA-2 Computed Flows for Flushing Simulations: GIWW East of Junction with Company Canal.

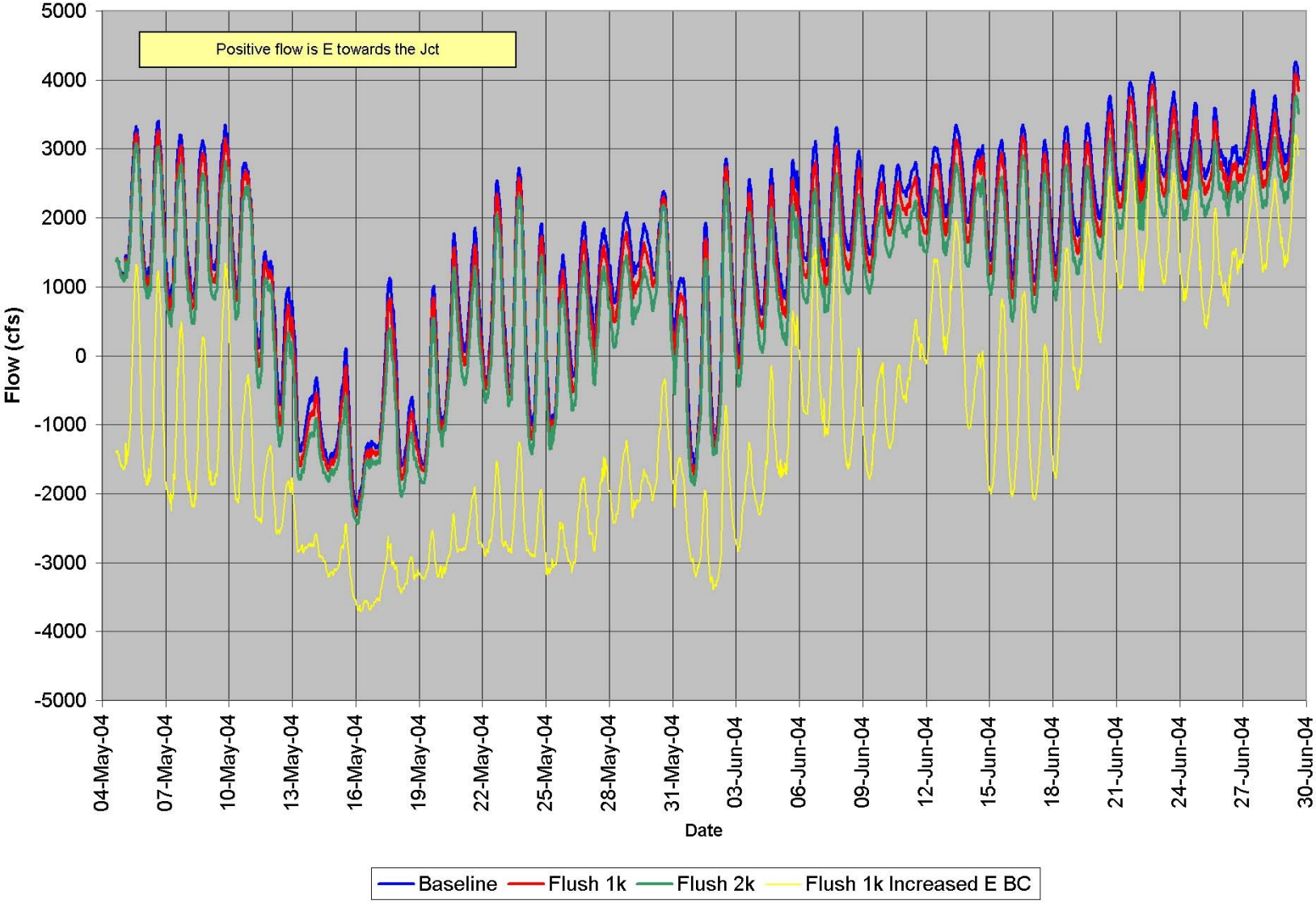

Figure A.35. RMA-2 Computed Flows for Flushing Simulations: GIWW West of Junction with Company Canal.

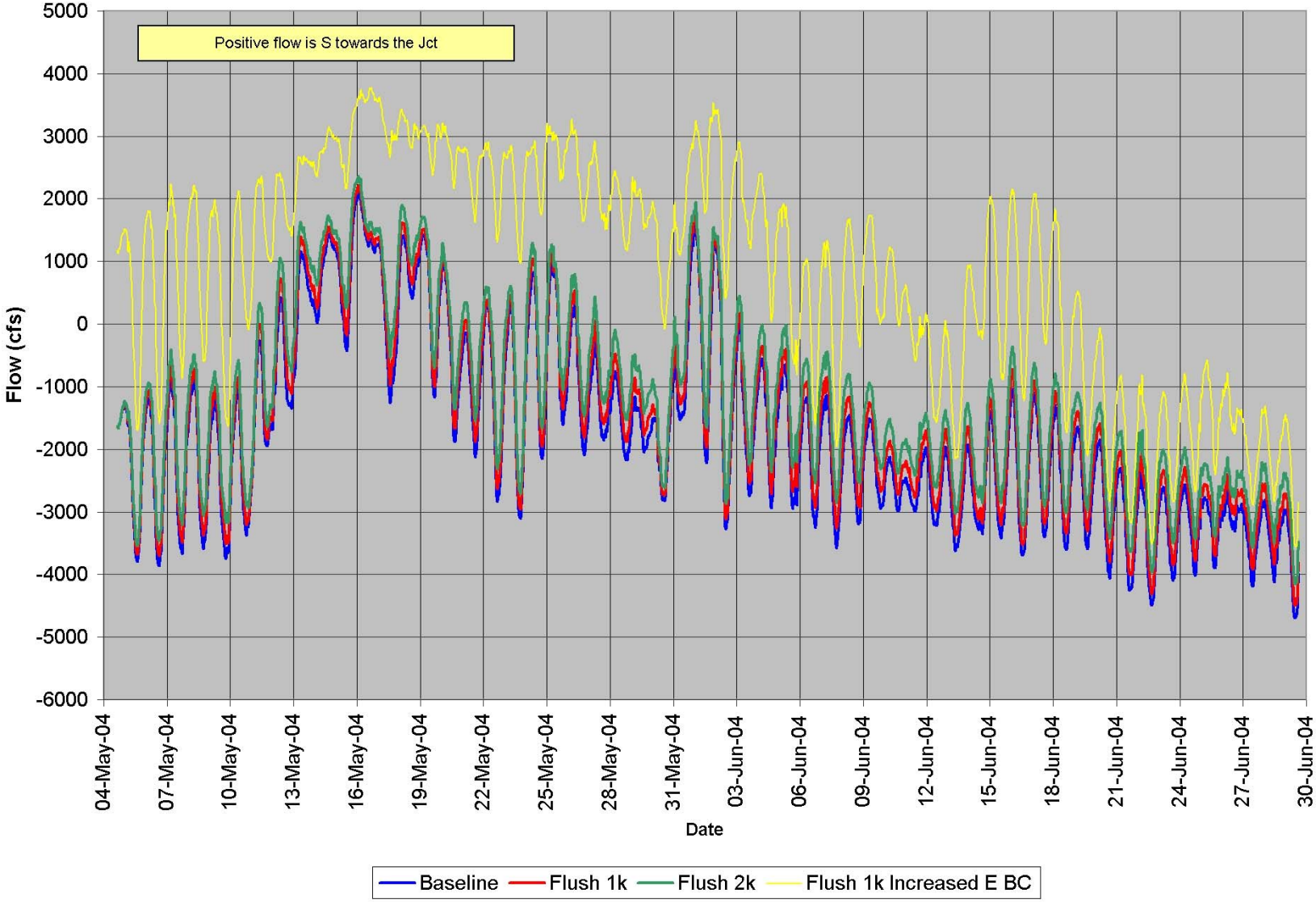

Figure A.36. RMA-2 Computed Flows for Flushing Simulations: GIWW North of Junction with Houma Navigation Canal.

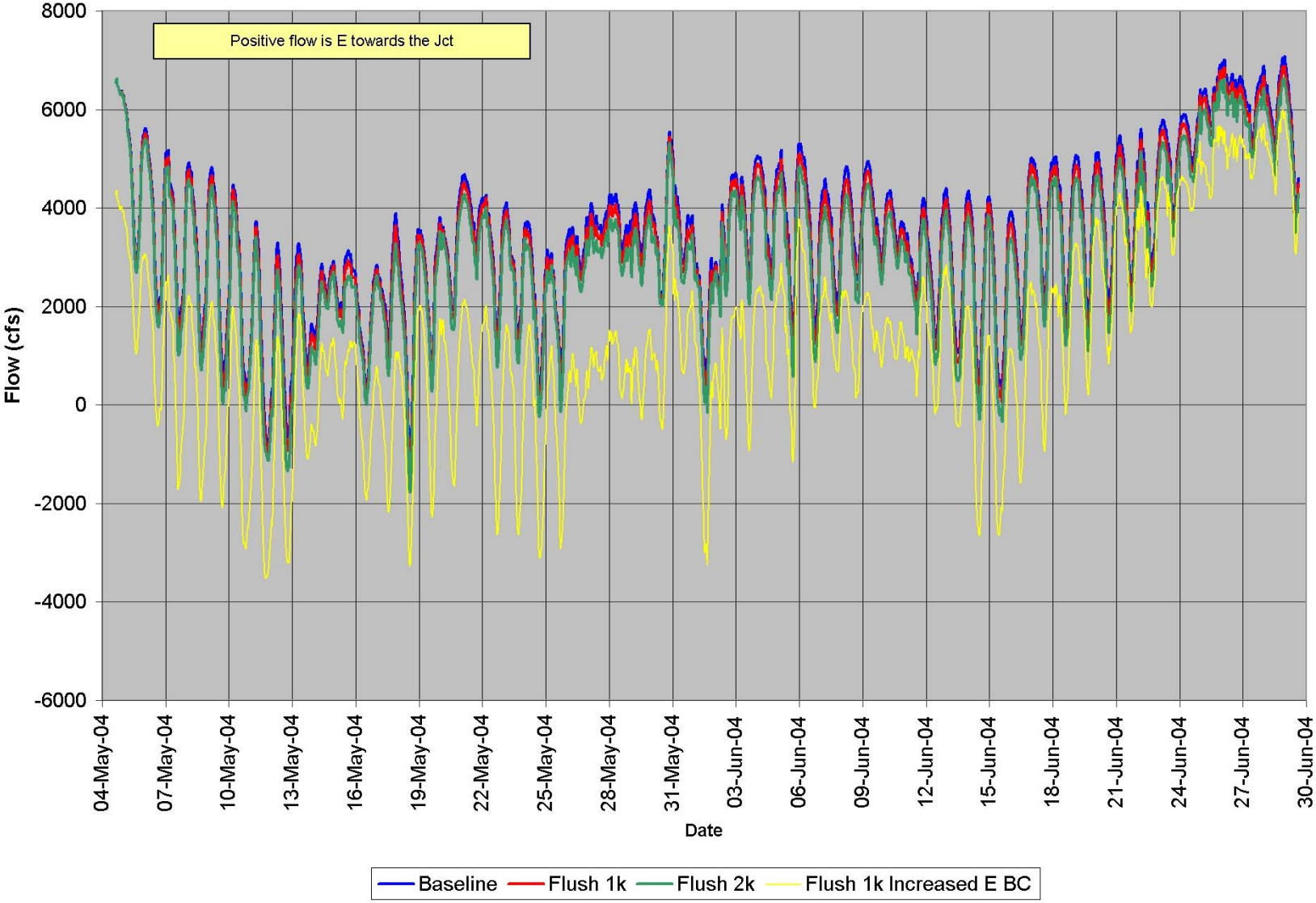

Figure A.37. RMA-2 Computed Flows for Flushing Simulations: GIWW West of Junction with Houma Navigation Canal.

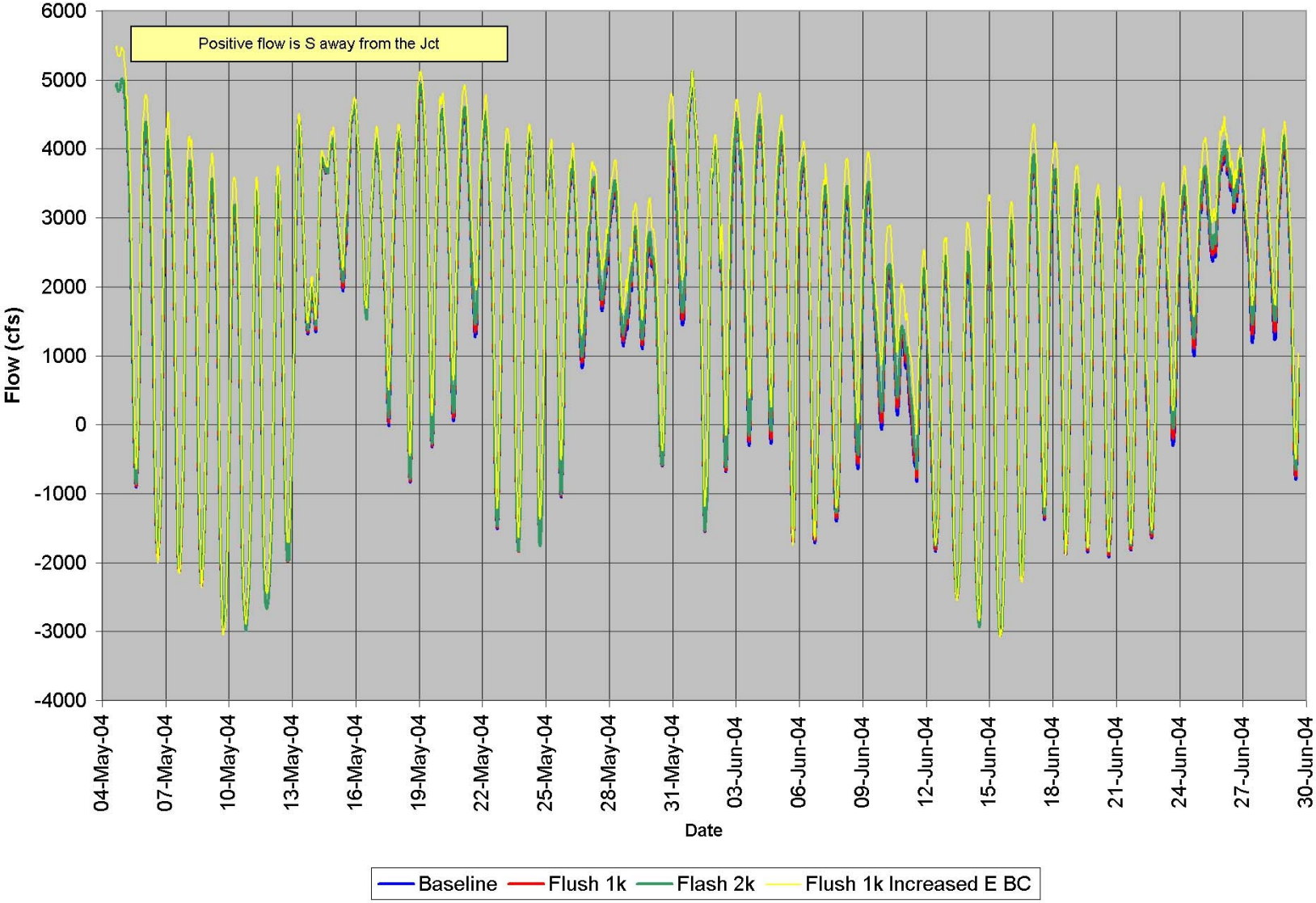

Figure A.38. RMA-2 Computed Flows for Flushing Simulations: Houma Navigation Canal South of Junction with the GIWW.

APPENDIX B

RMA-11 Calibration and Flushing Simulations Results

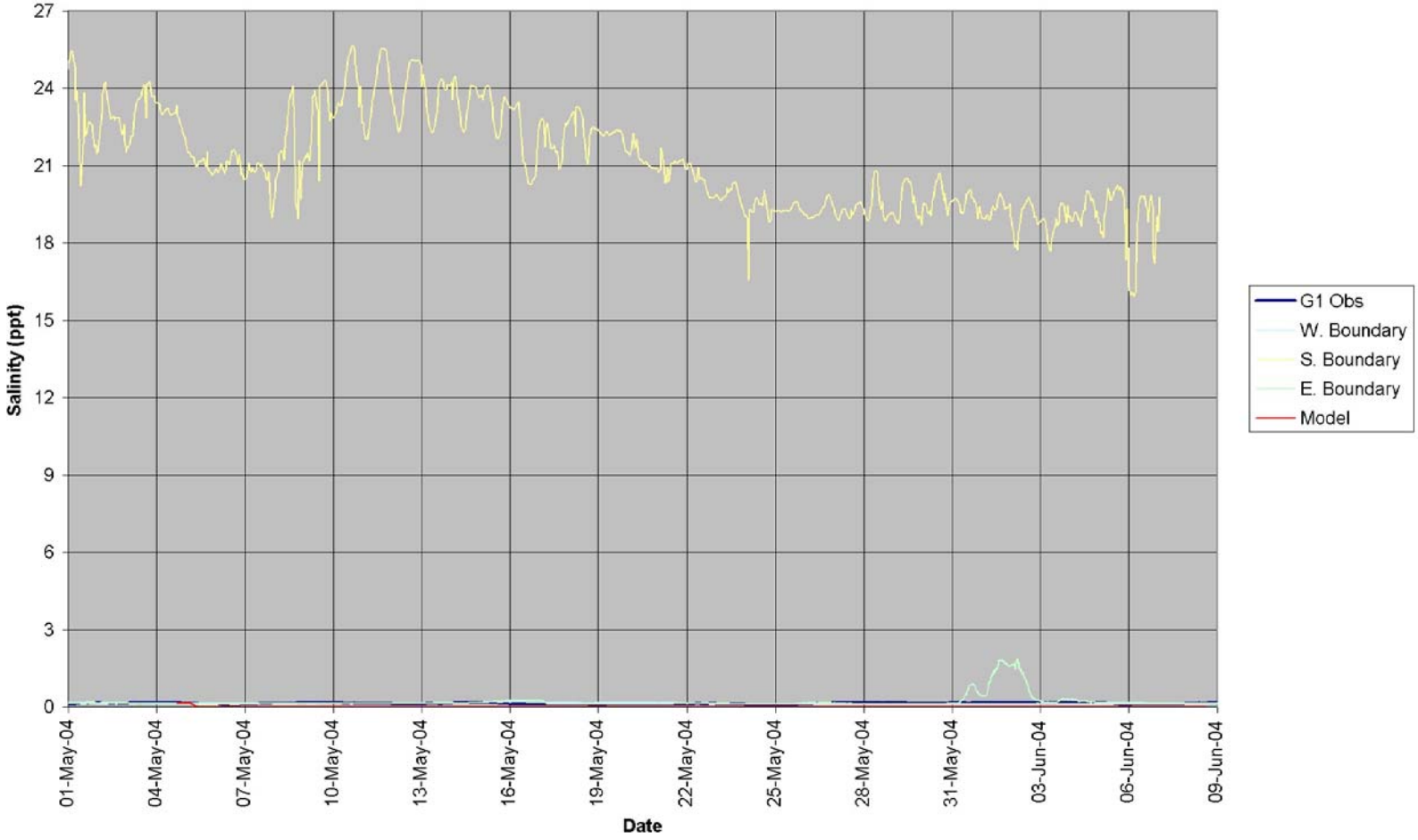

Figure B.1. Final RMA-11 Salinity Calibration (Gage 1).

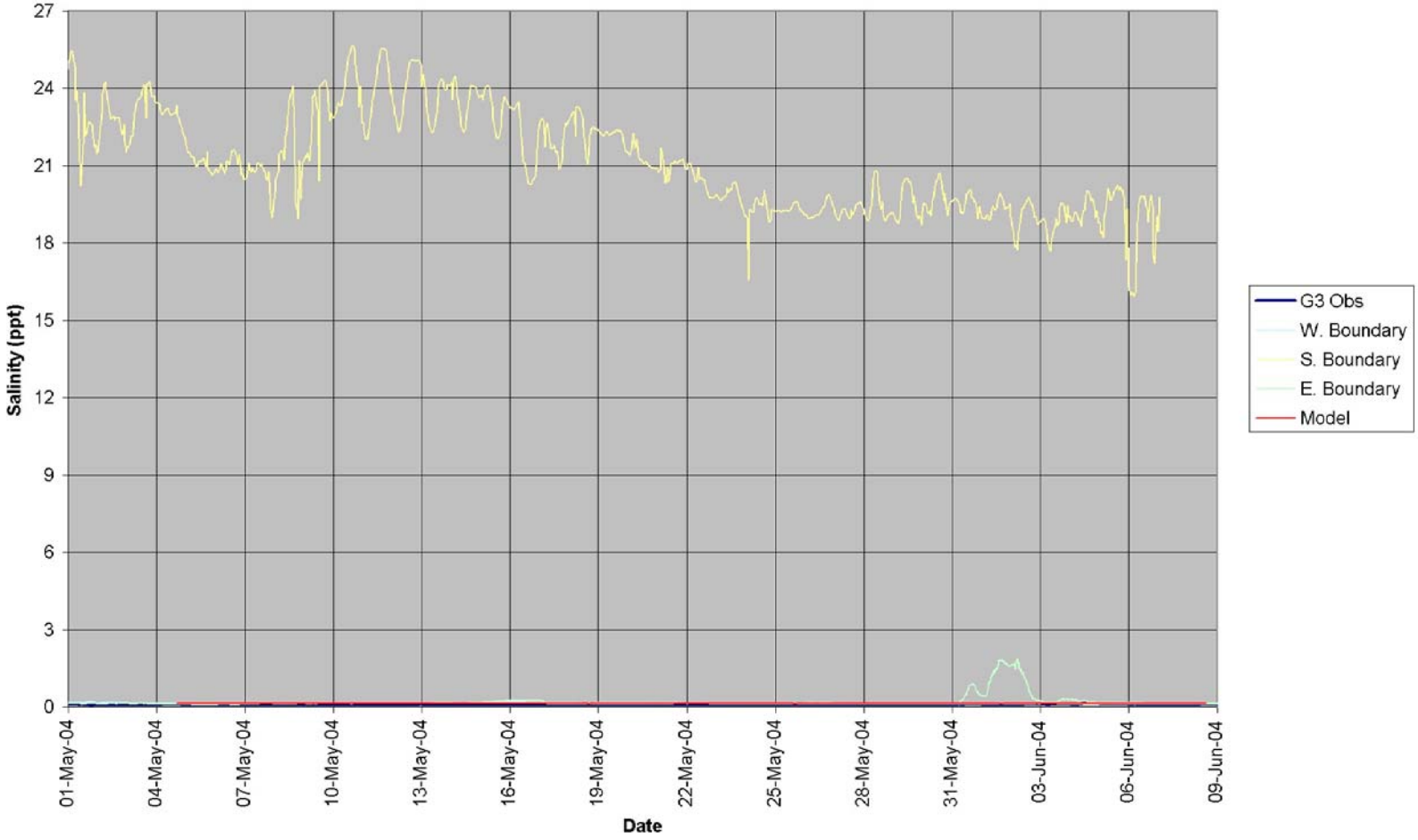

Figure B.2. Final RMA-11 Salinity Calibration (Gage 3).

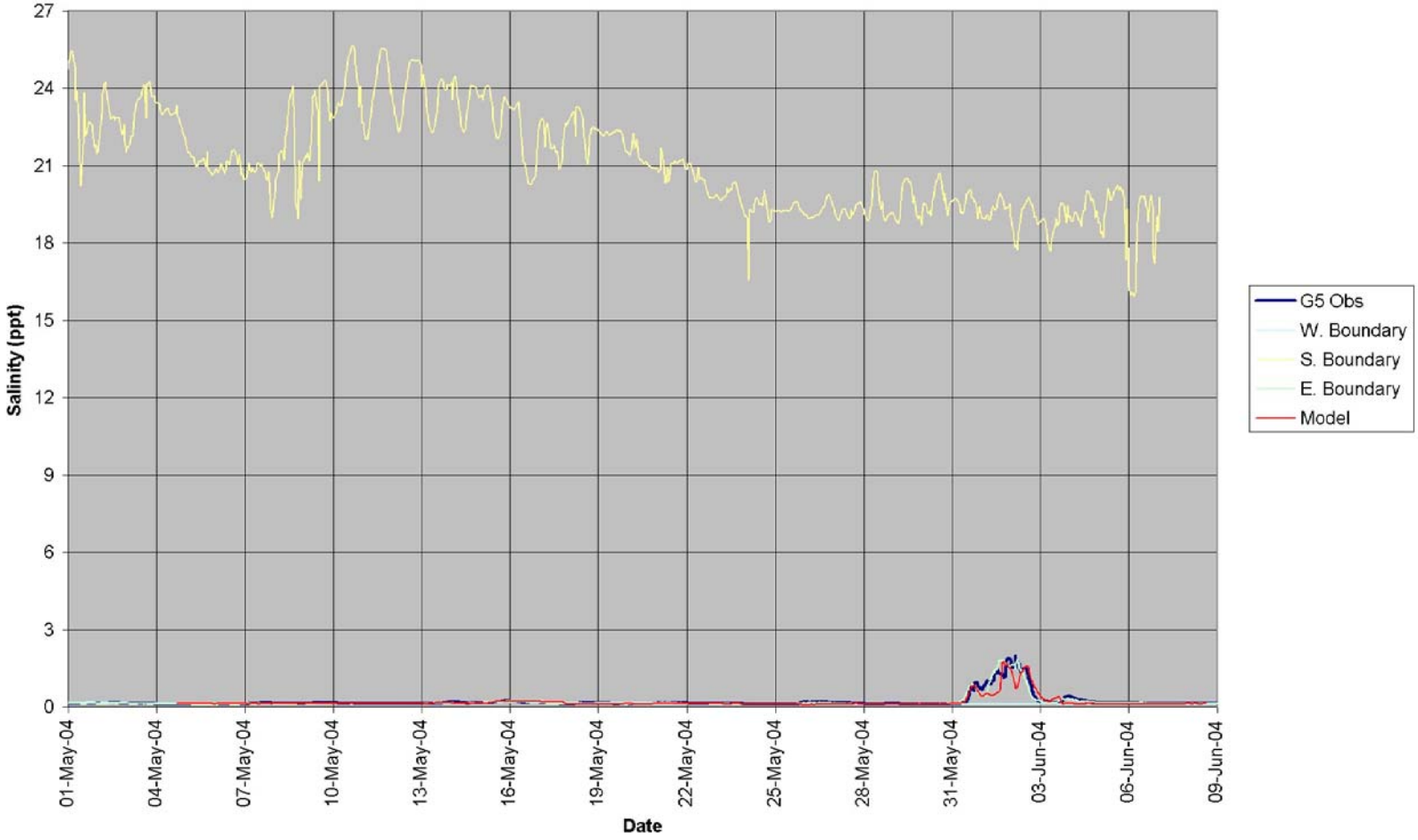

Figure B.3. Final RMA-11 Salinity Calibration (Gage 5).

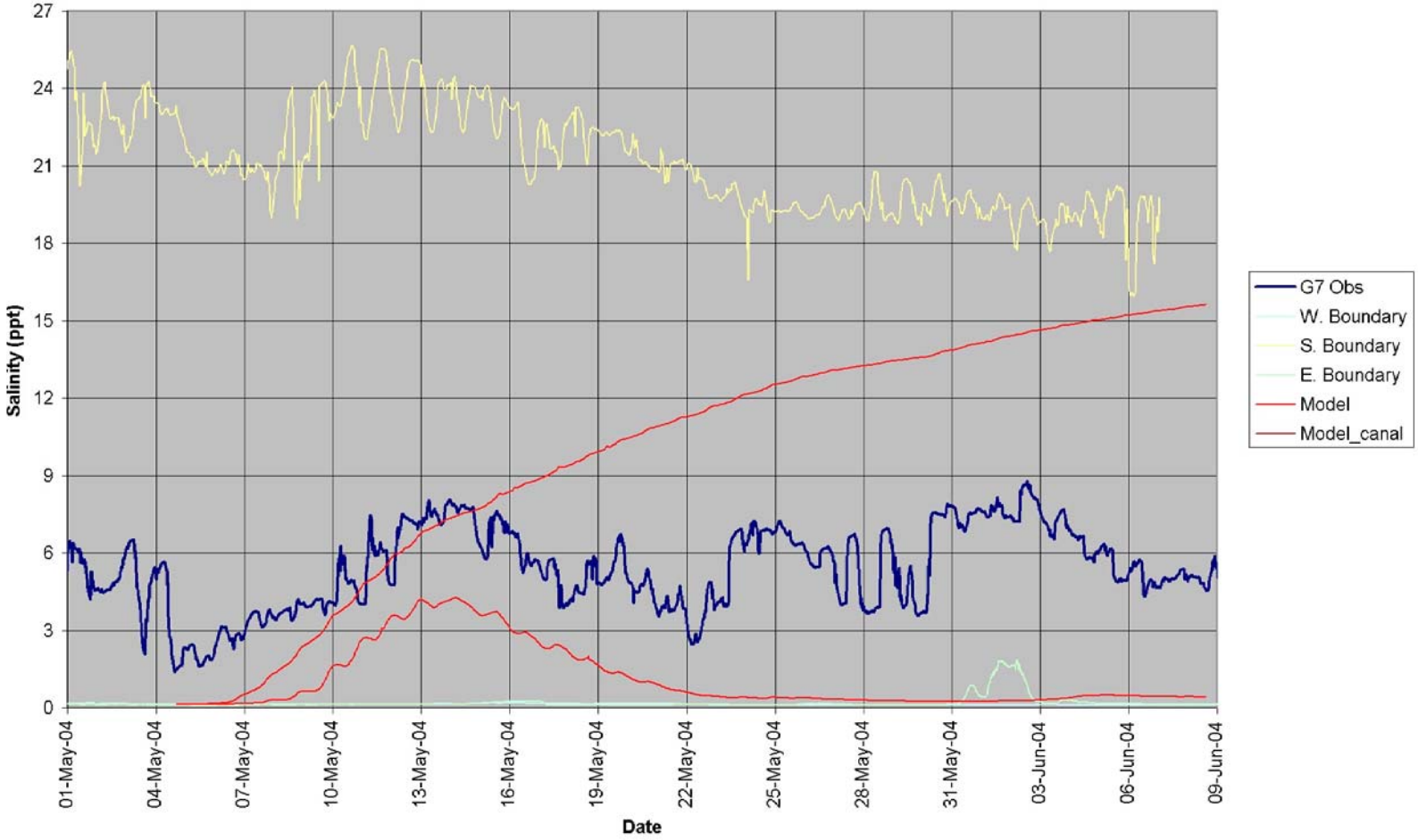

Figure B.4. Final RMA-11 Salinity Calibration (Gage 7).

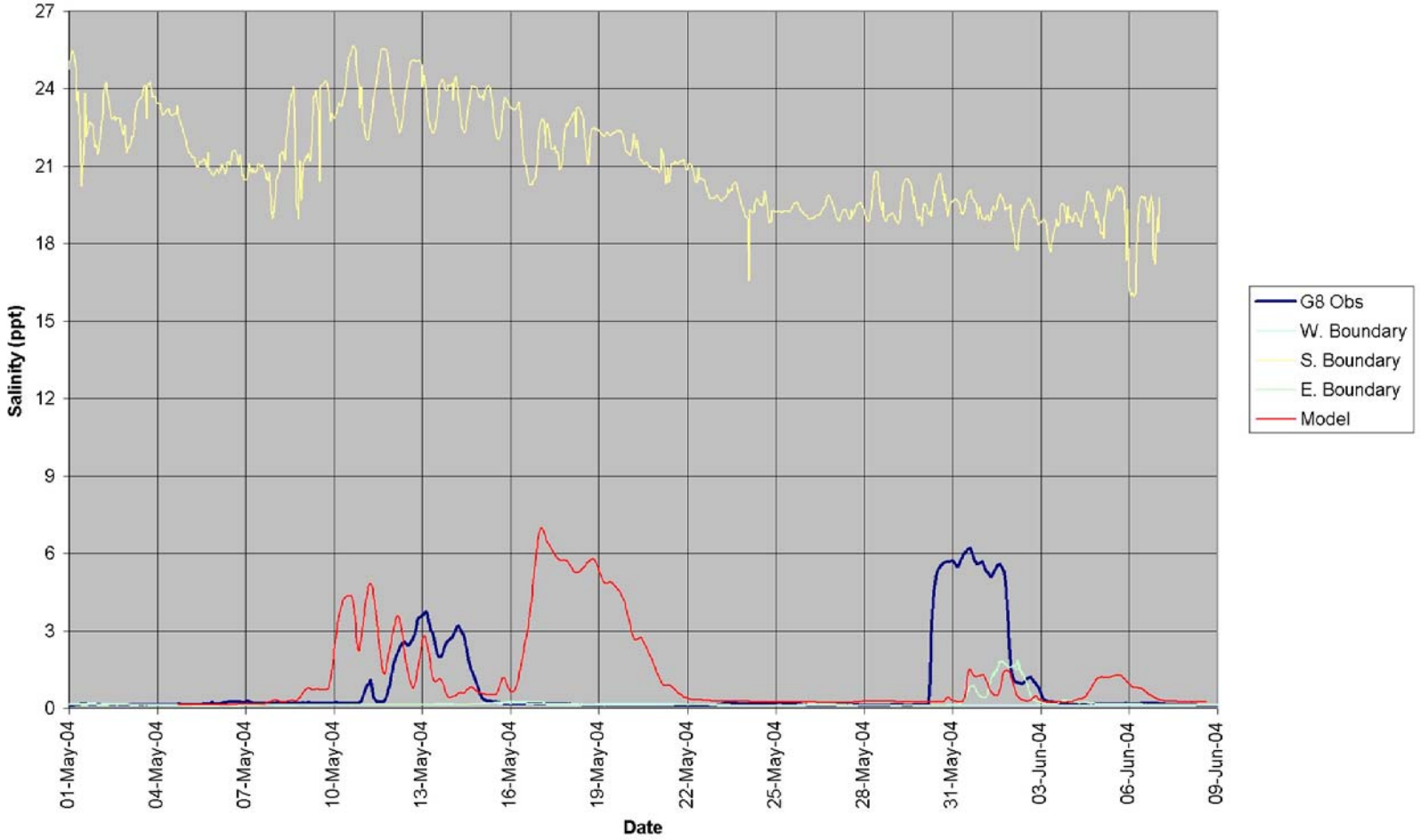

Figure B.5. Final RMA-11 Salinity Calibration (Gage 8).

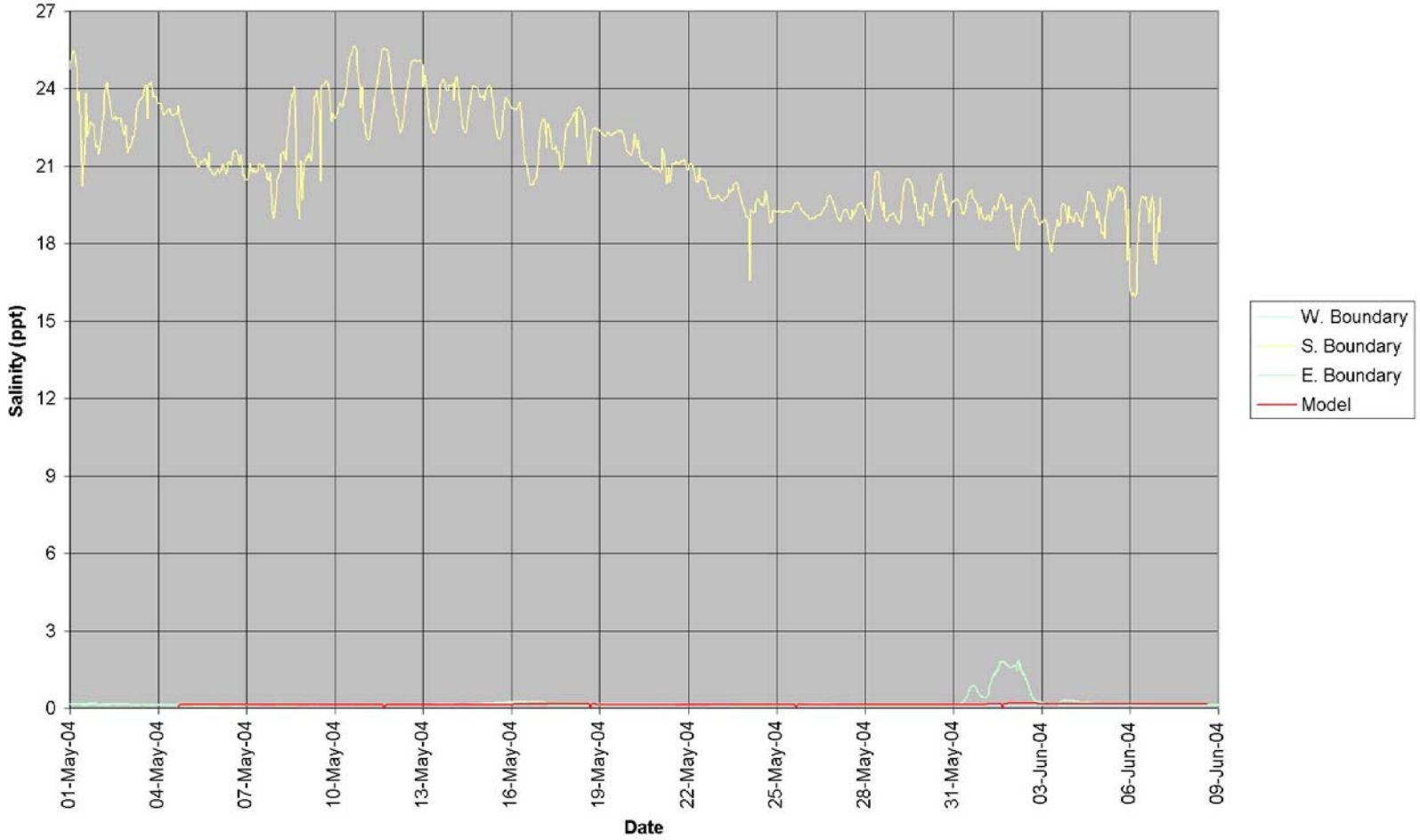

Figure B.6. Final RMA-11 Salinity Calibration (Gage 10).

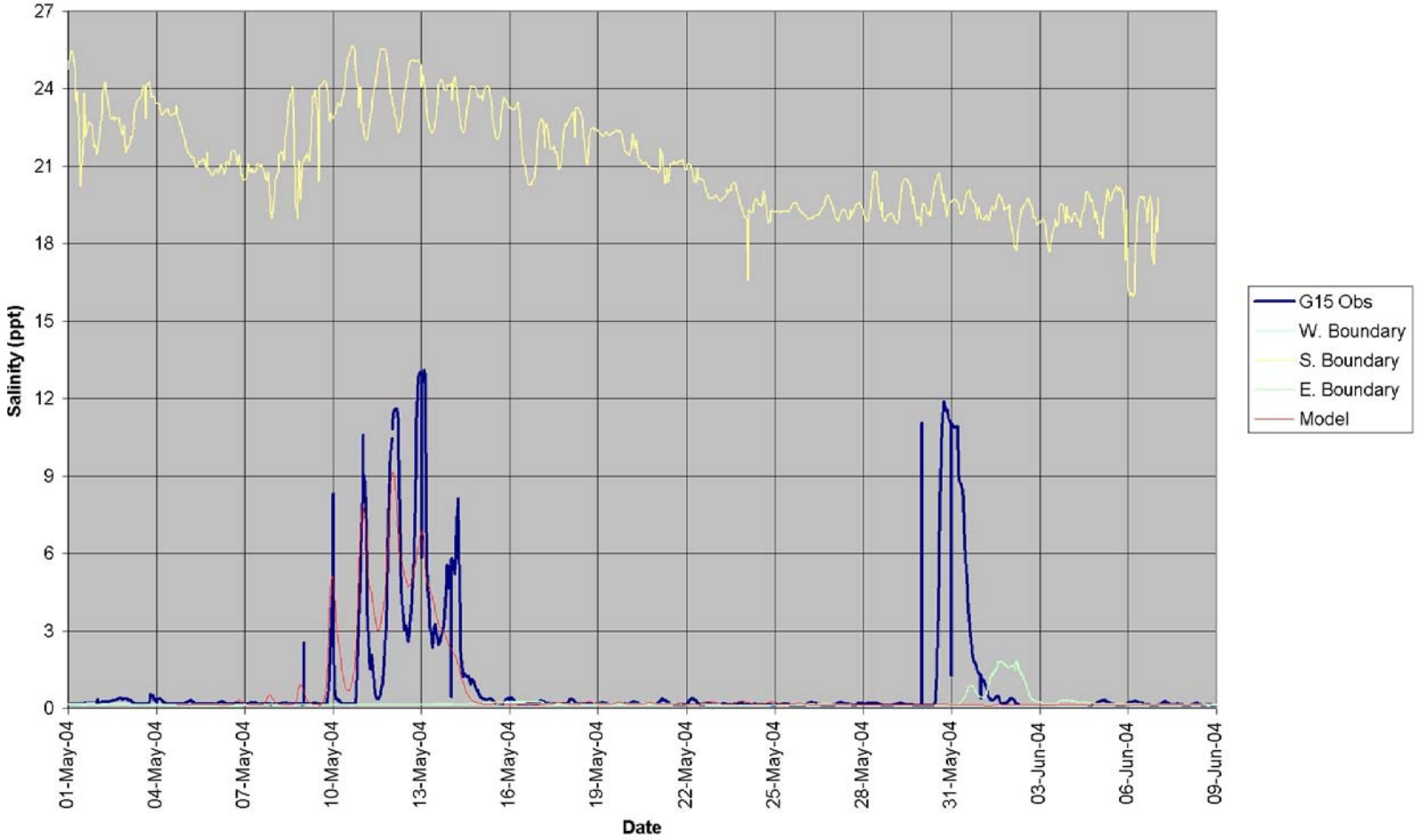

Figure B.7. Final RMA-11 Salinity Calibration (Gage 15).

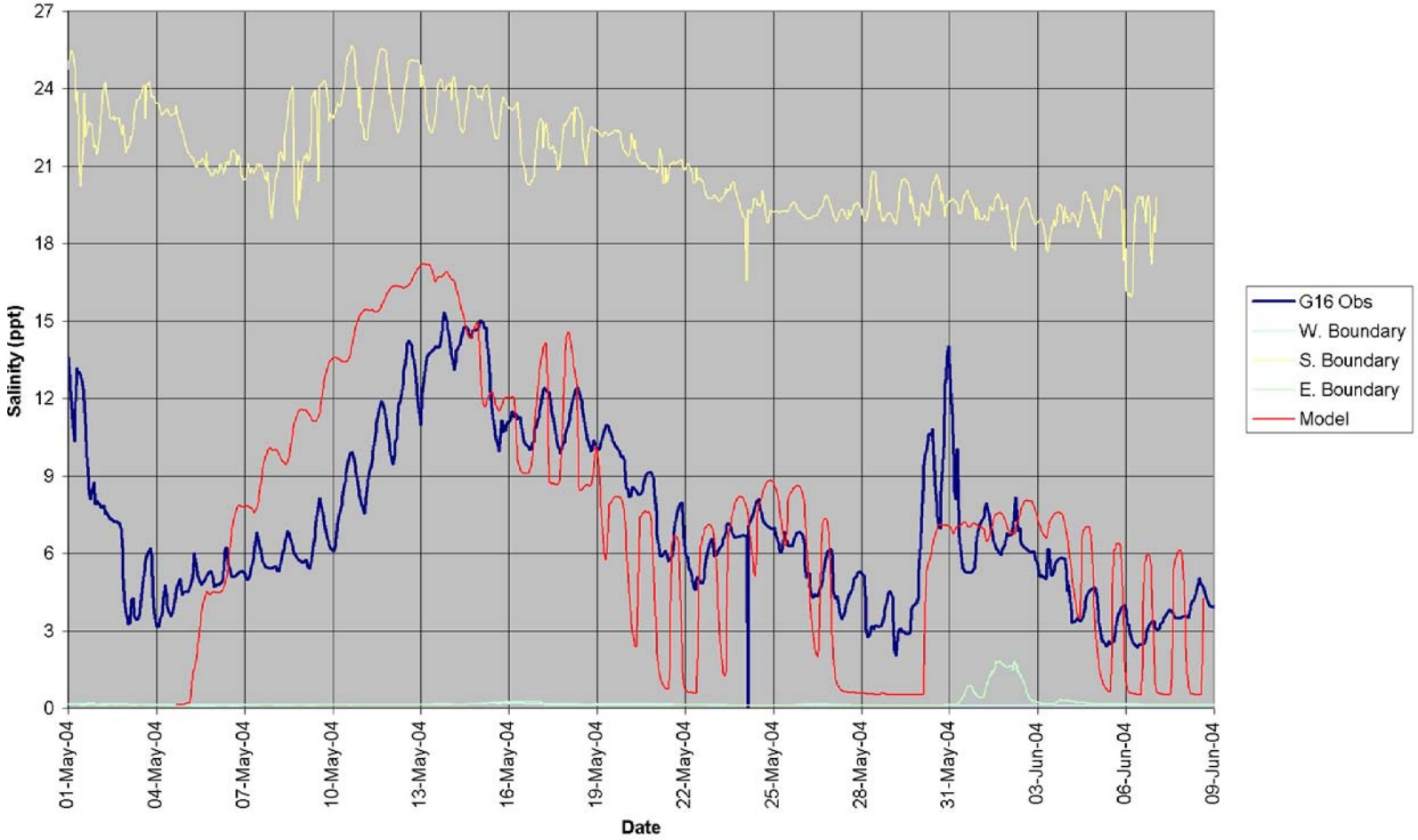

Figure B.8. Final RMA-11 Salinity Calibration (Gage 16).

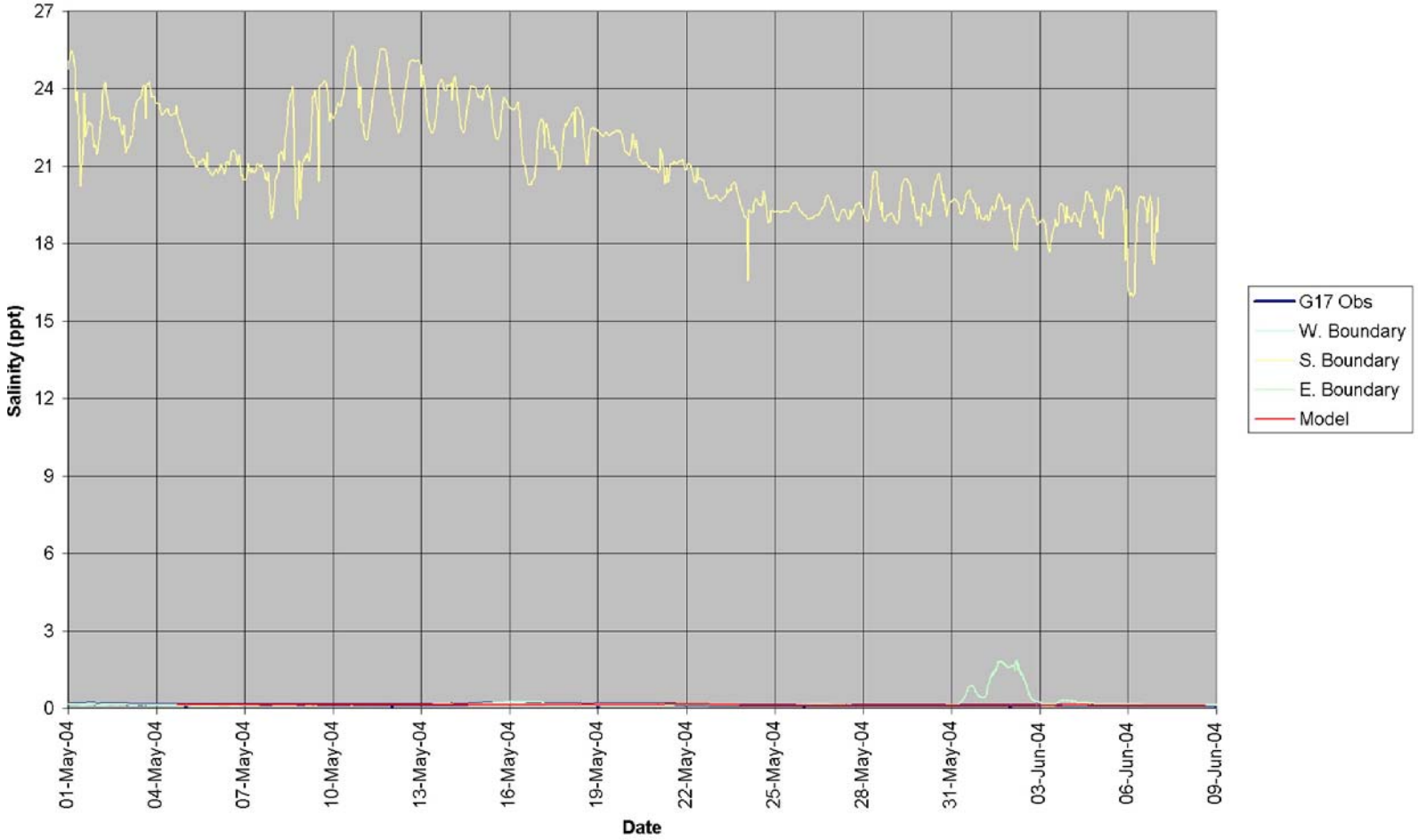

Figure B.9. Final RMA-11 Salinity Calibration (Gage 17).

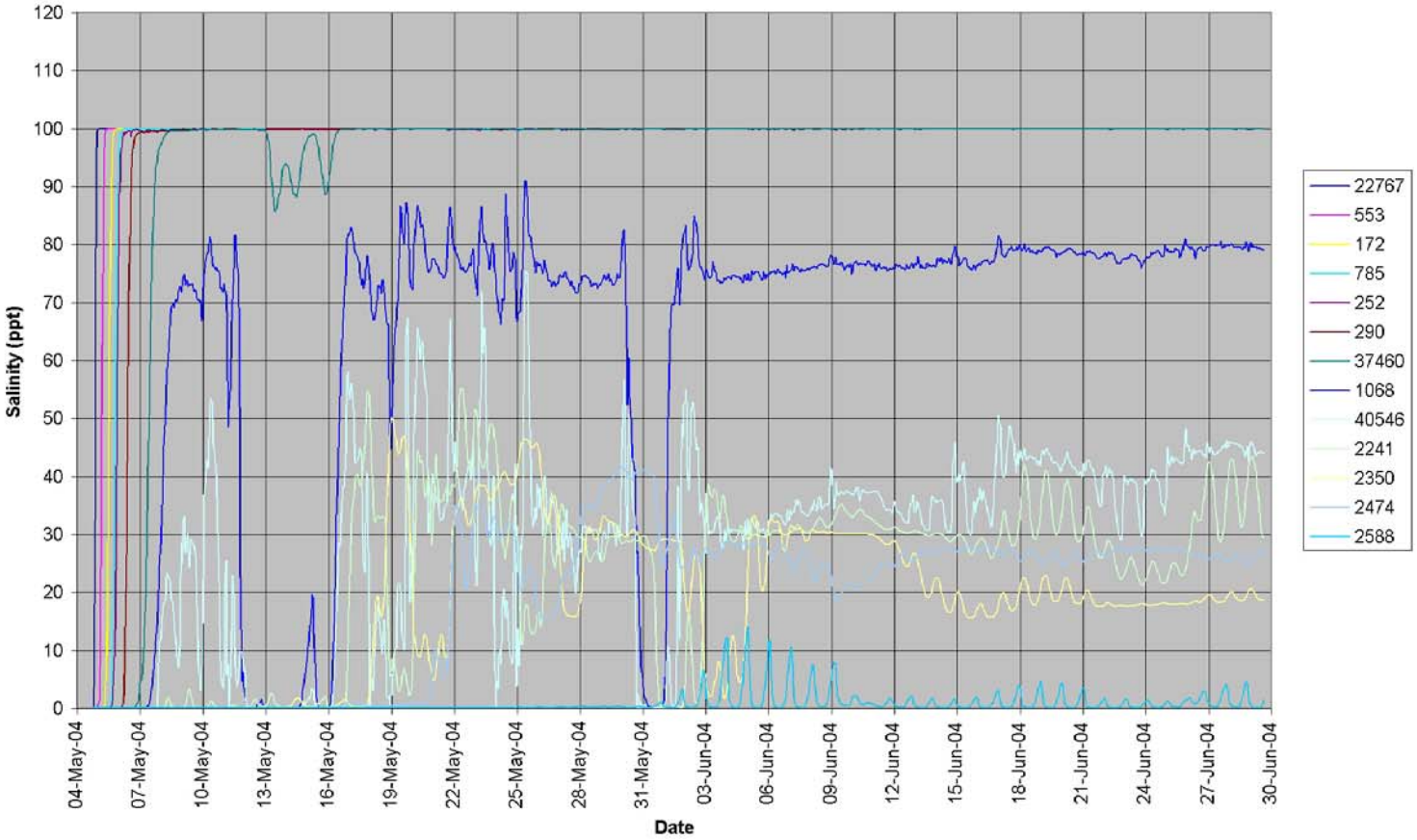

Figure B.10. Tracer time series in Bayou Lafourche for 1,000 cfs diversion.

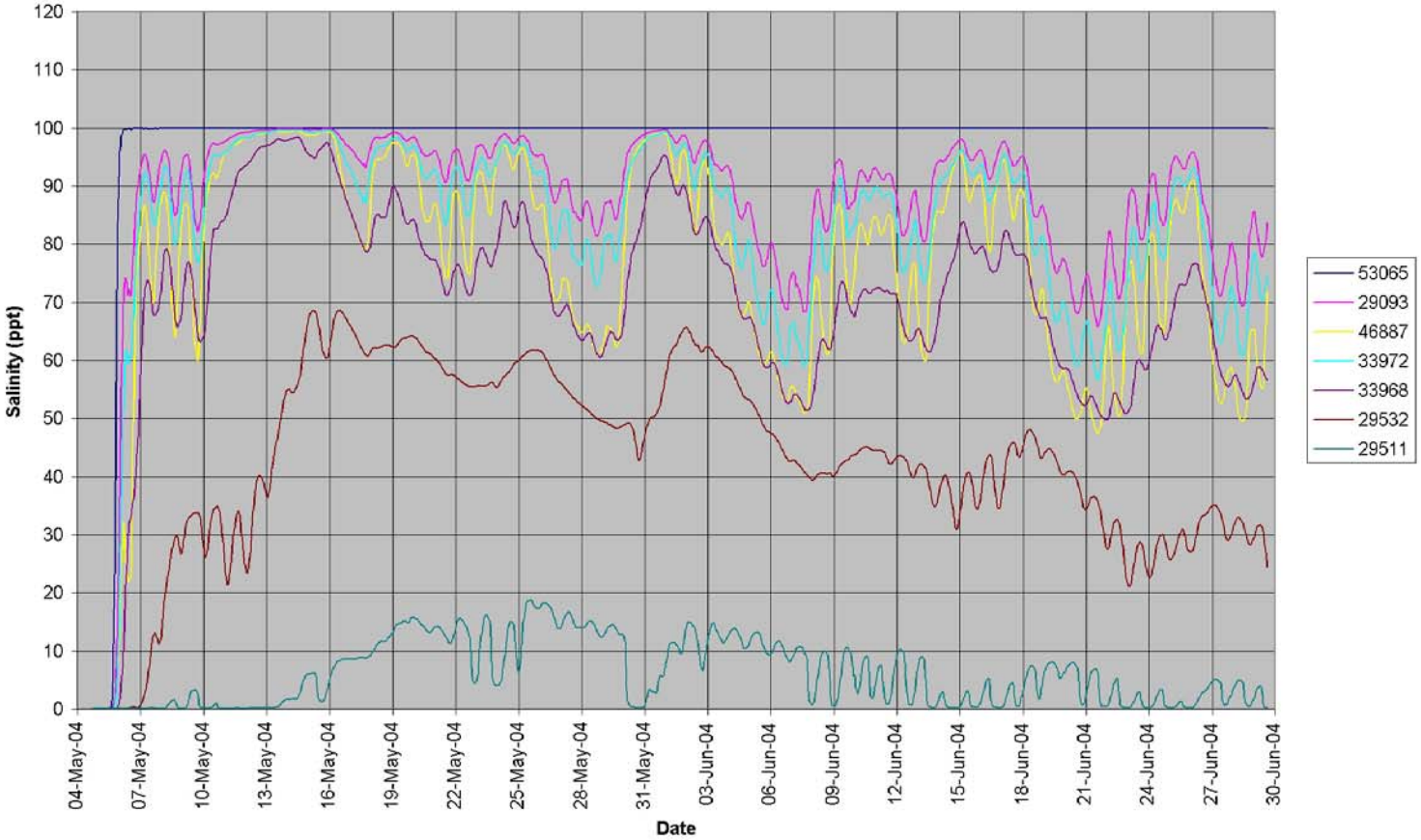

Figure B.11. Tracer time series in Company Canal for 1,000 cfs diversion.

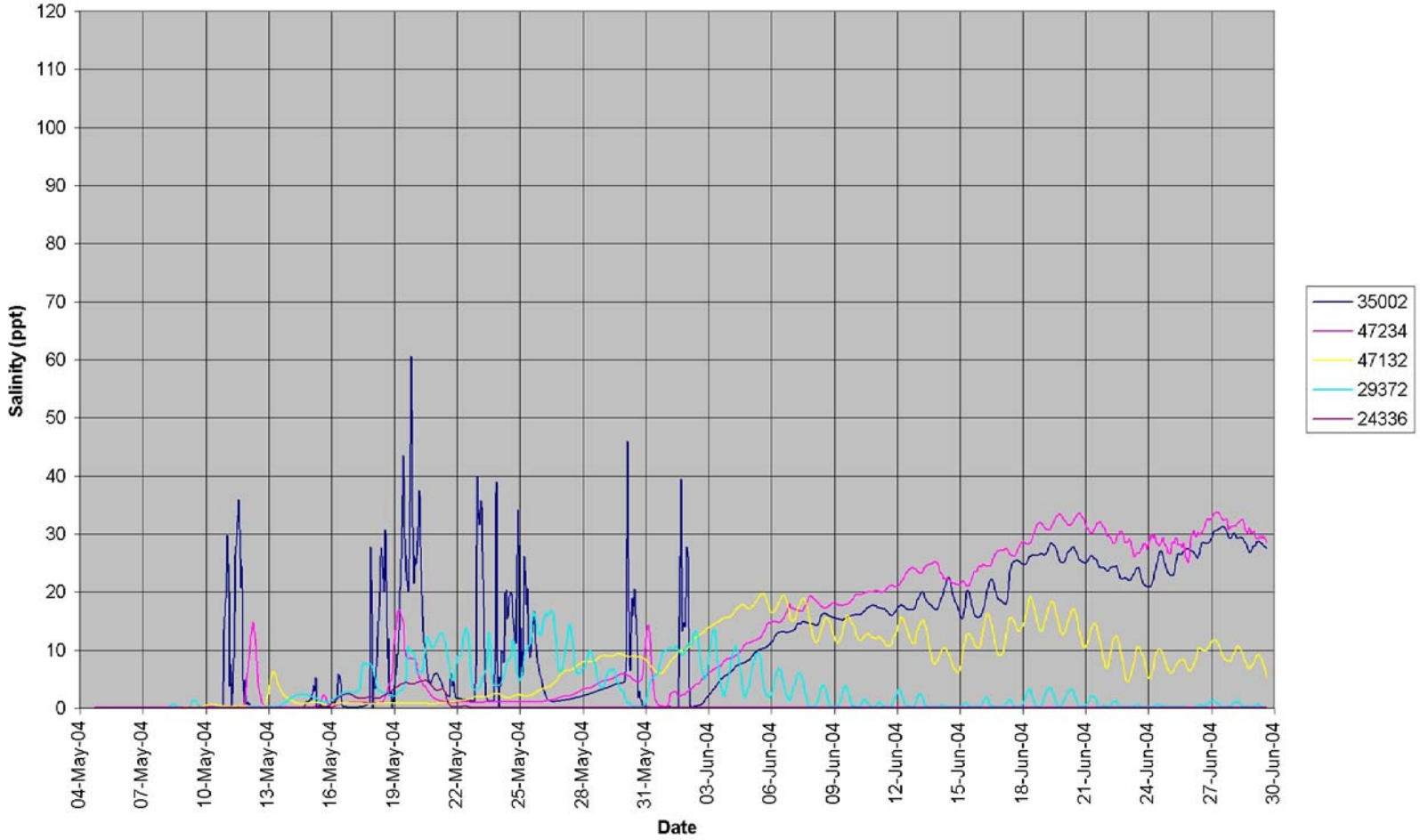

Figure B.12. Tracer time series in GIWW for 1,000 cfs diversion.

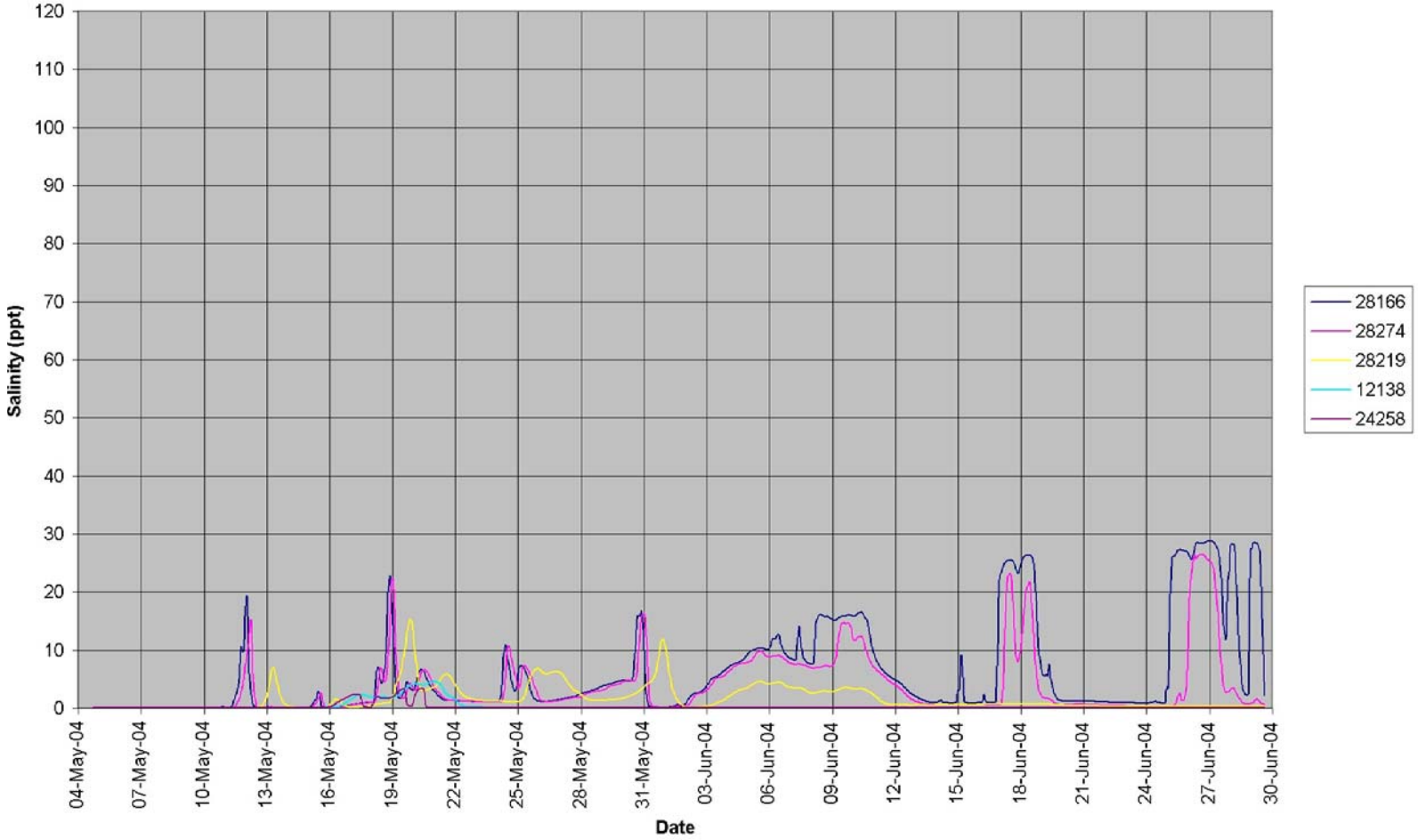

Figure B.13. Tracer time series in HNC and Grand Bayou for 1,000 cfs diversion.

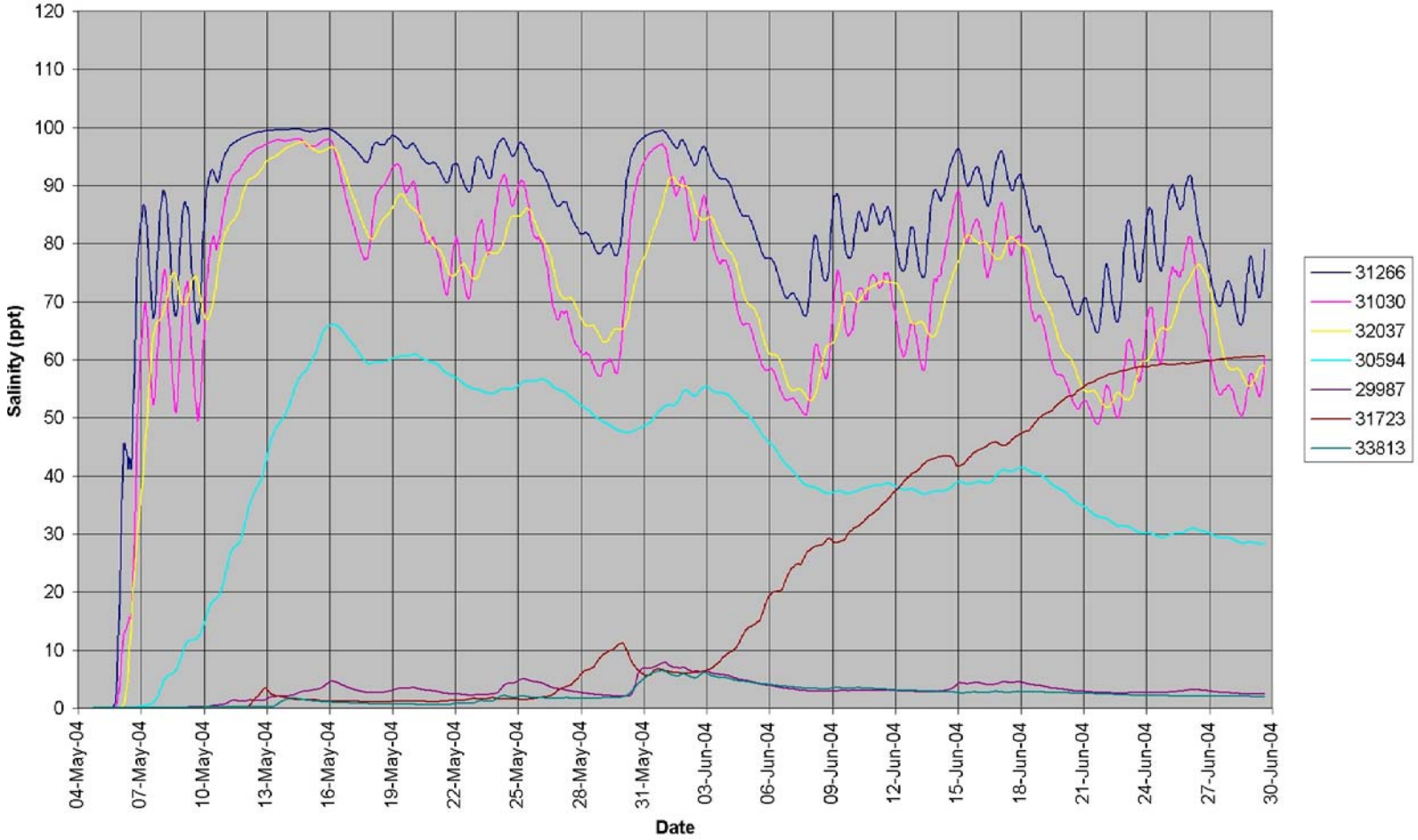

Figure B.14. Tracer time series in selected marshes for 1,000 cfs diversion.

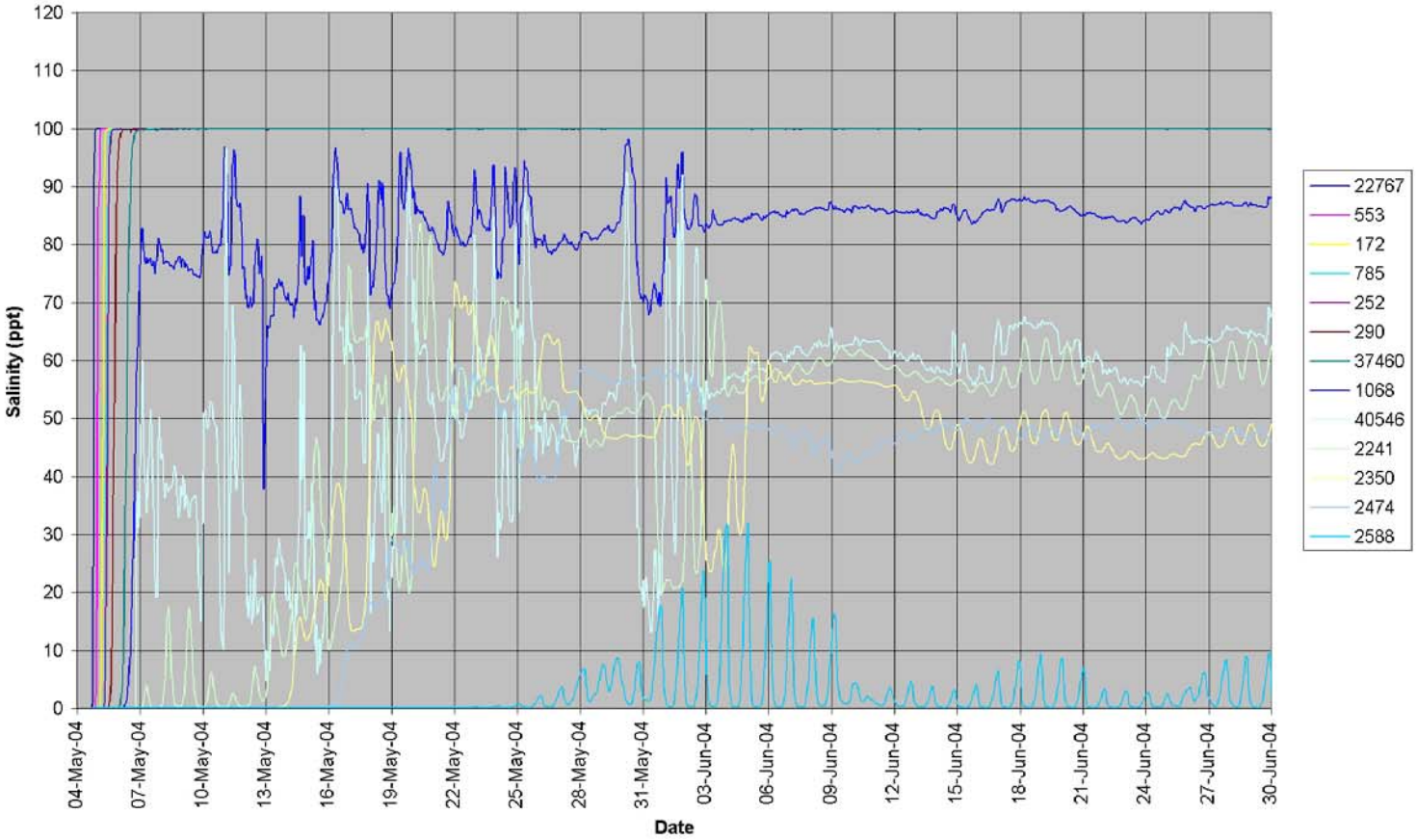

Figure B.15. Tracer time series in Bayou Lafourche for 2,000 cfs diversion.

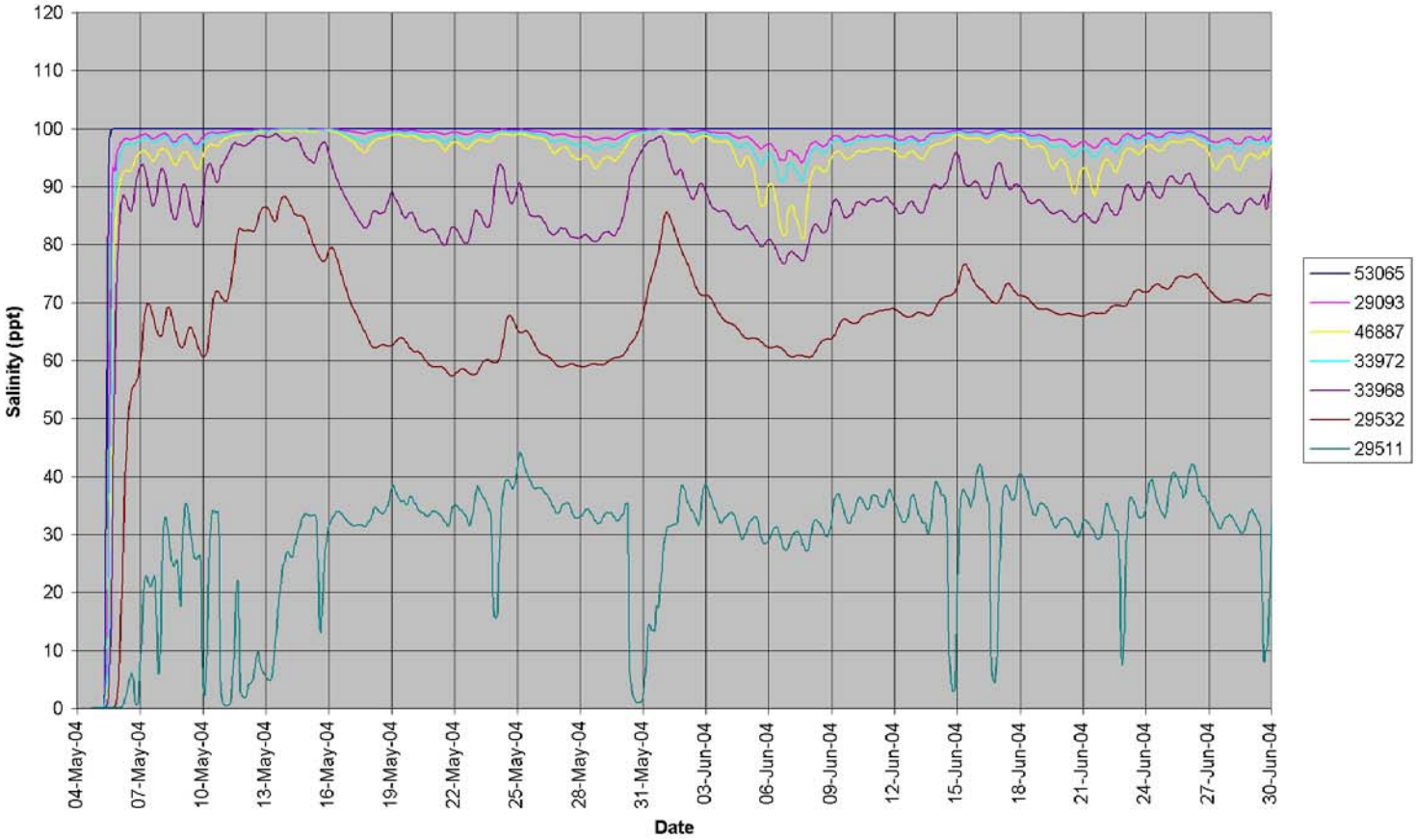

Figure B.16. Tracer time series in Company Canal for 2,000 cfs diversion.

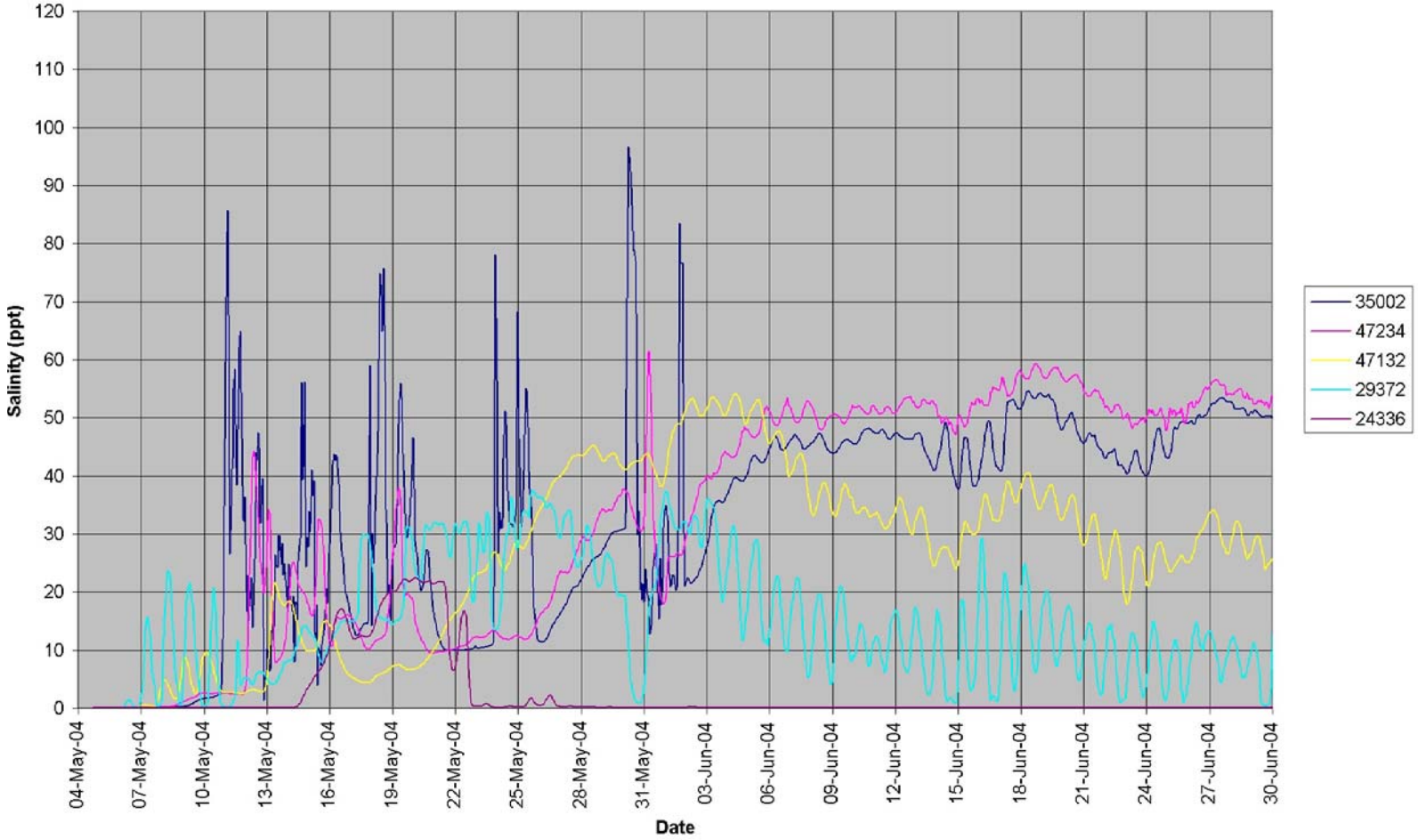

Figure B.17. Tracer time series in GIWW for 2,000 cfs diversion.

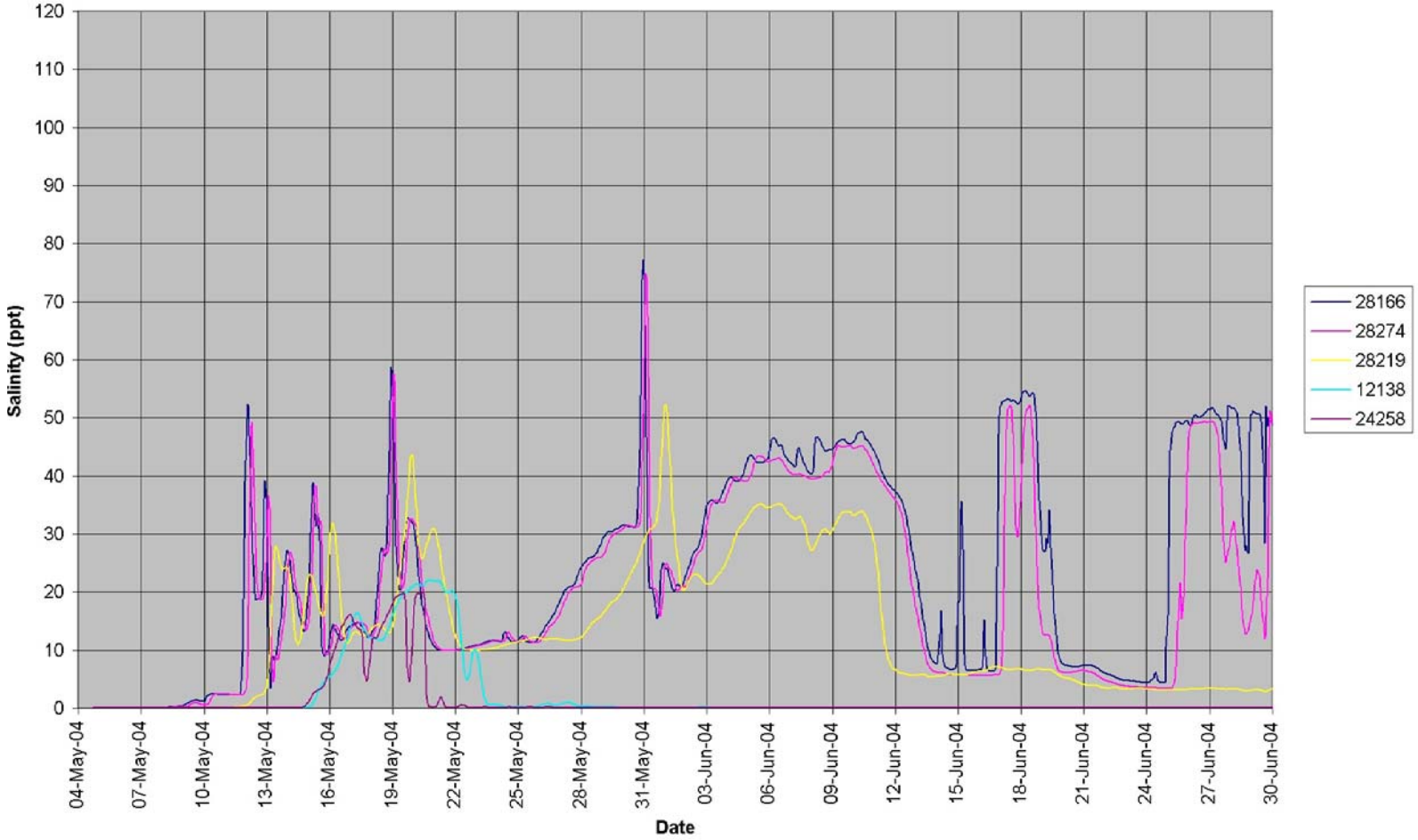

Figure B.18. Tracer time series in HNC and Grand Bayou for 2,000 cfs diversion.

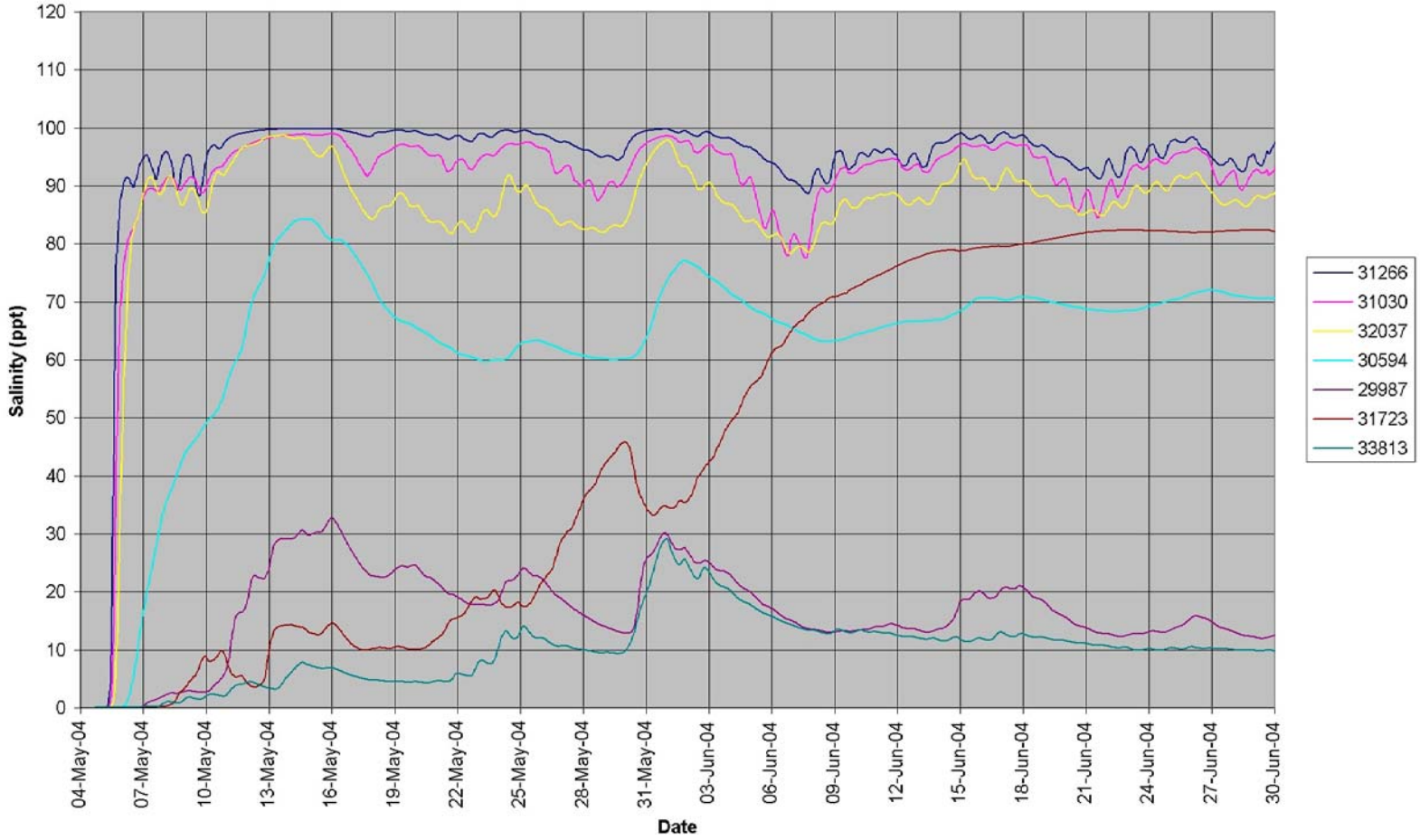

Figure B.19. Tracer time series in selected marshes for 2,000 cfs diversion.

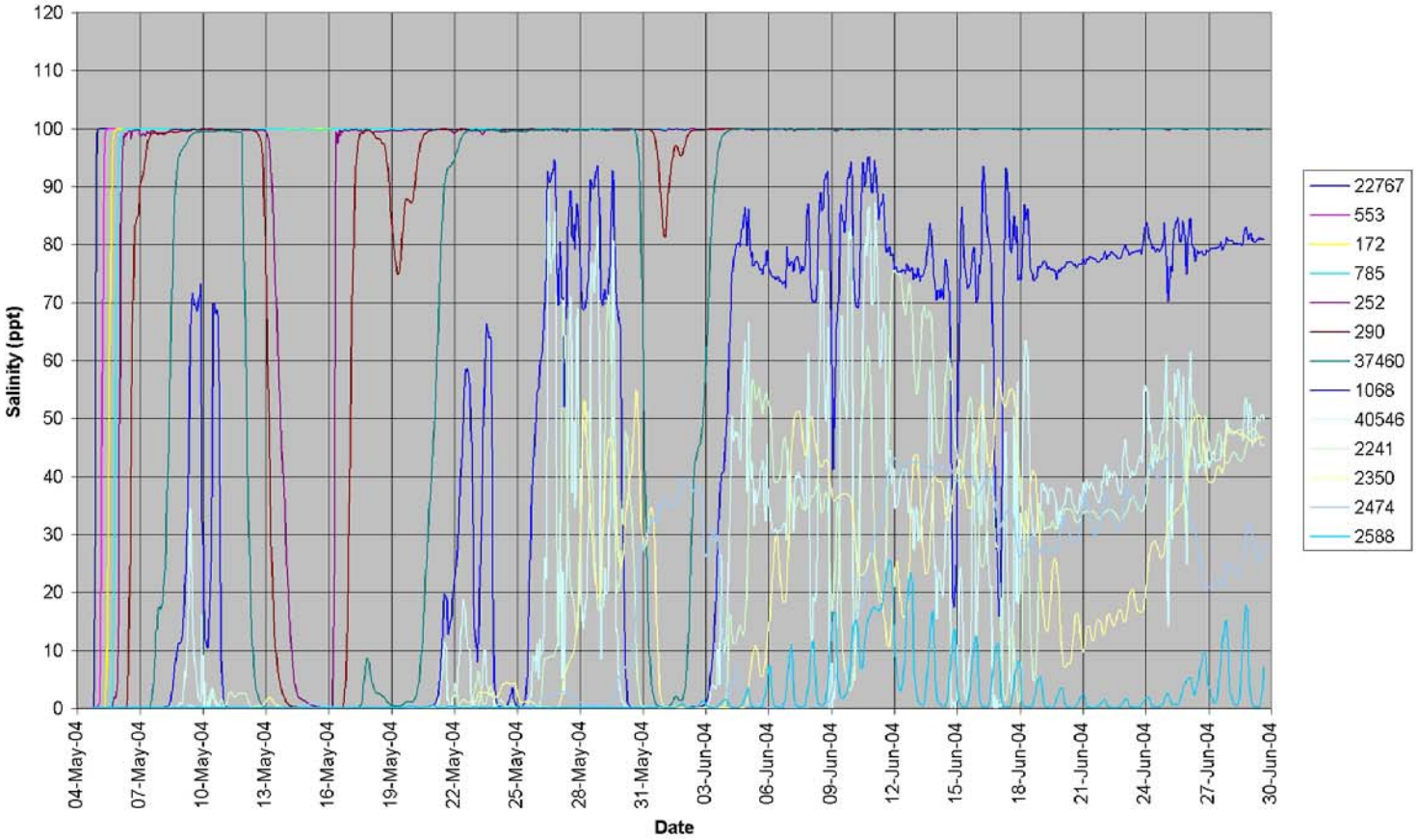

Figure B.20. Tracer time series in Bayou Lafourche for 1,000 cfs diversion with westerly GIWW flows.

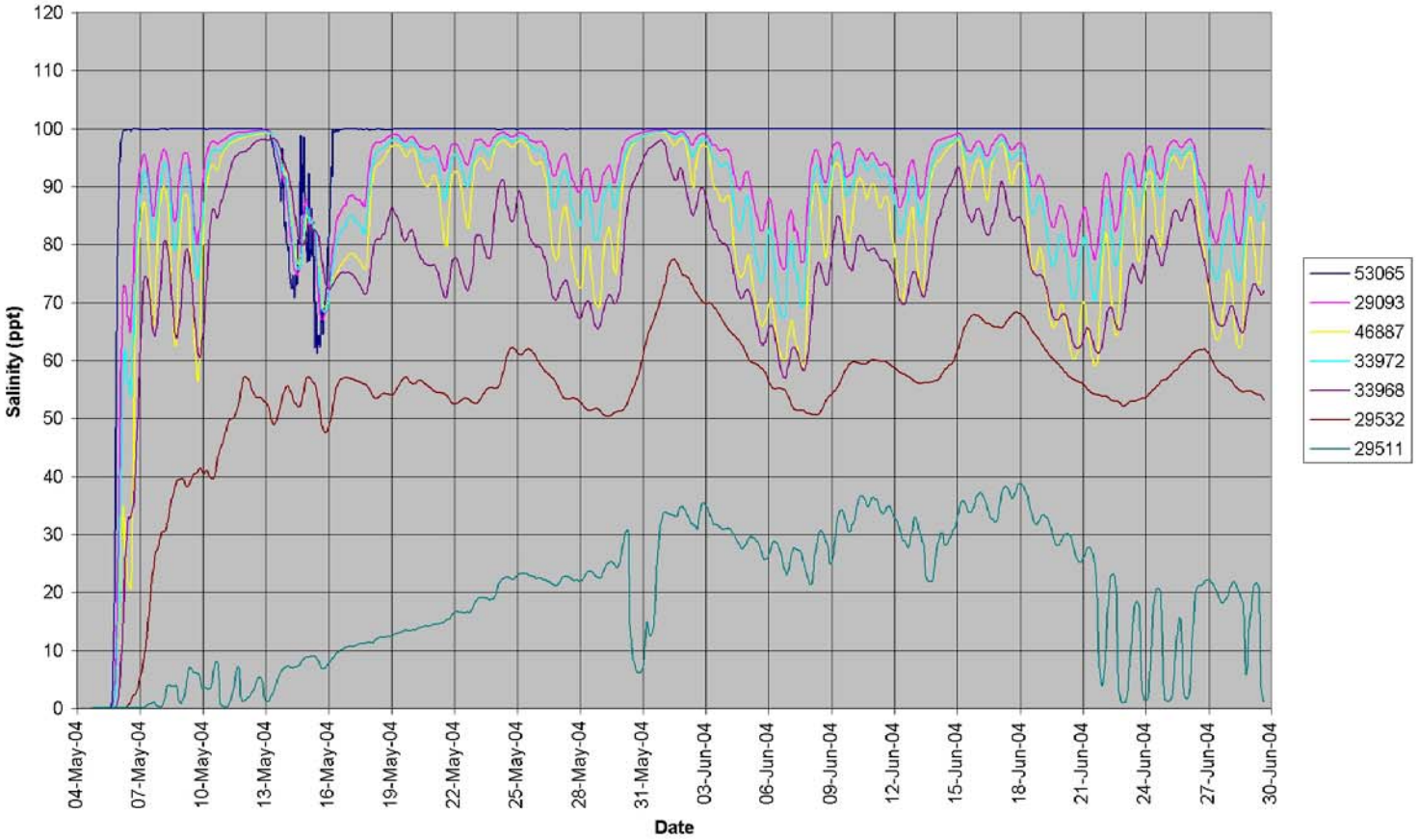

Figure B.21. Tracer time series in Company Canal for 1,000 cfs diversion with westerly GIWW flows.

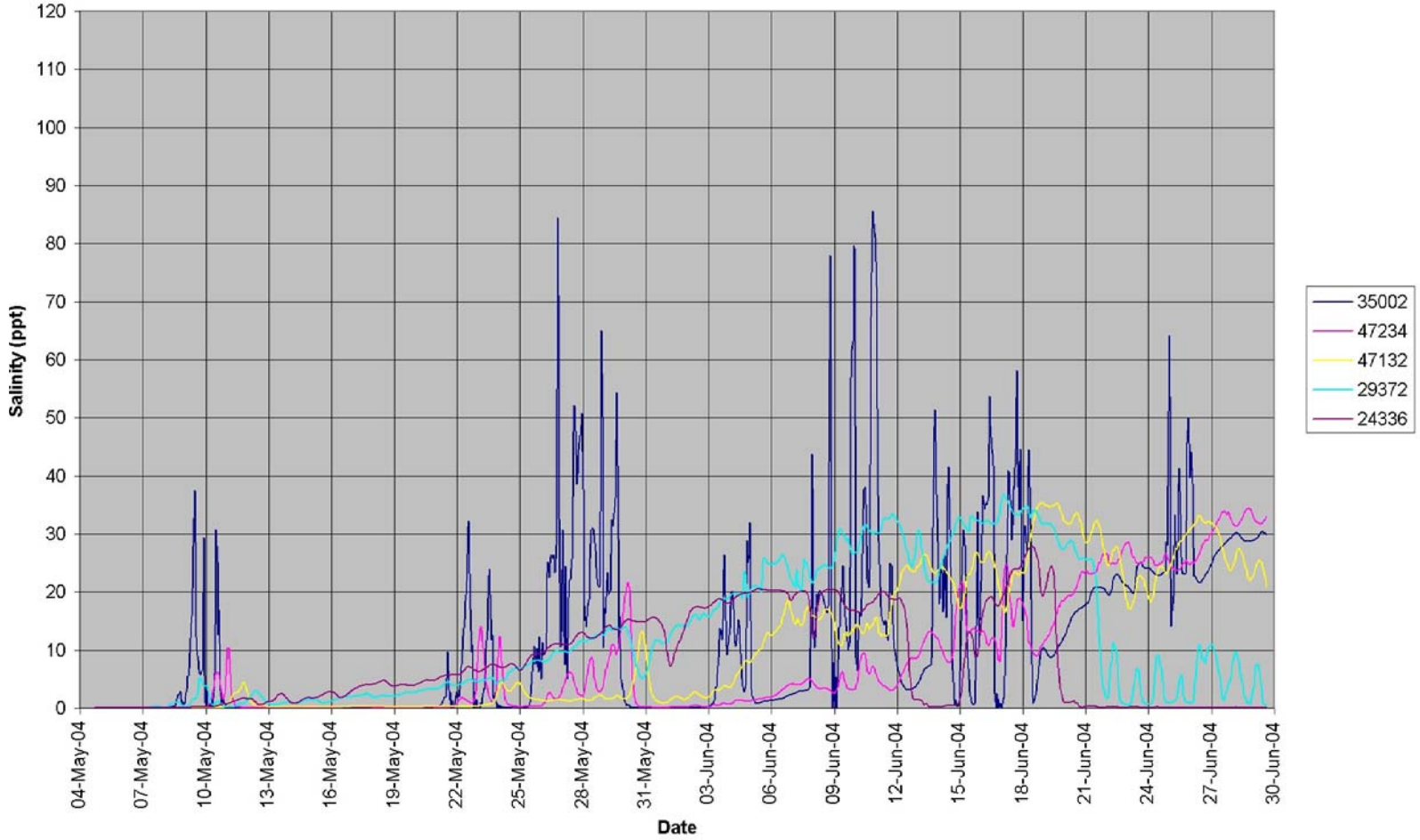

Figure B.22. Tracer time series in GIWW for 1,000 cfs diversion with westerly GIWW flows.

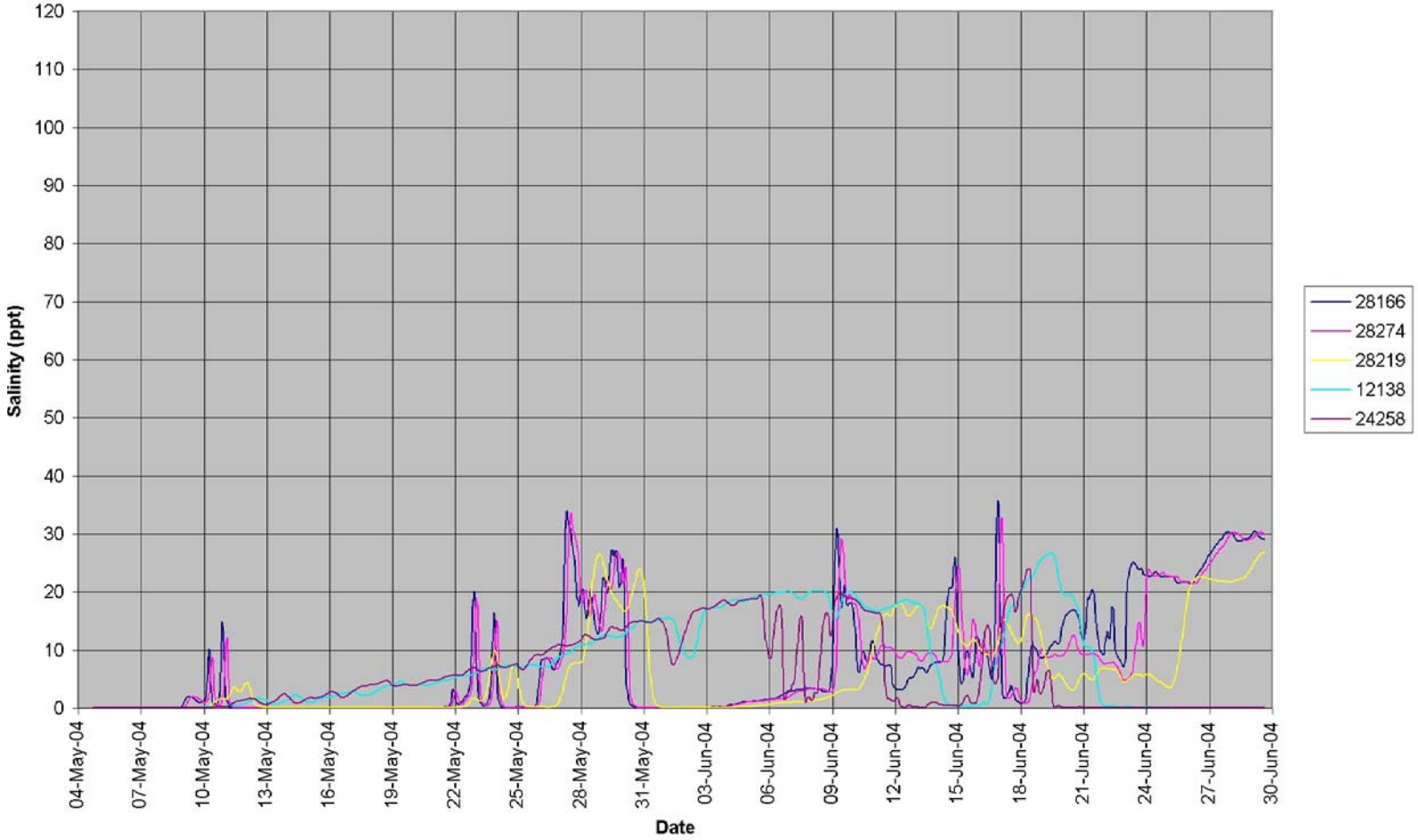

Figure B.23. Tracer time series in HNC and Grand Bayou for 1,000 cfs diversion with westerly GIWW flows.

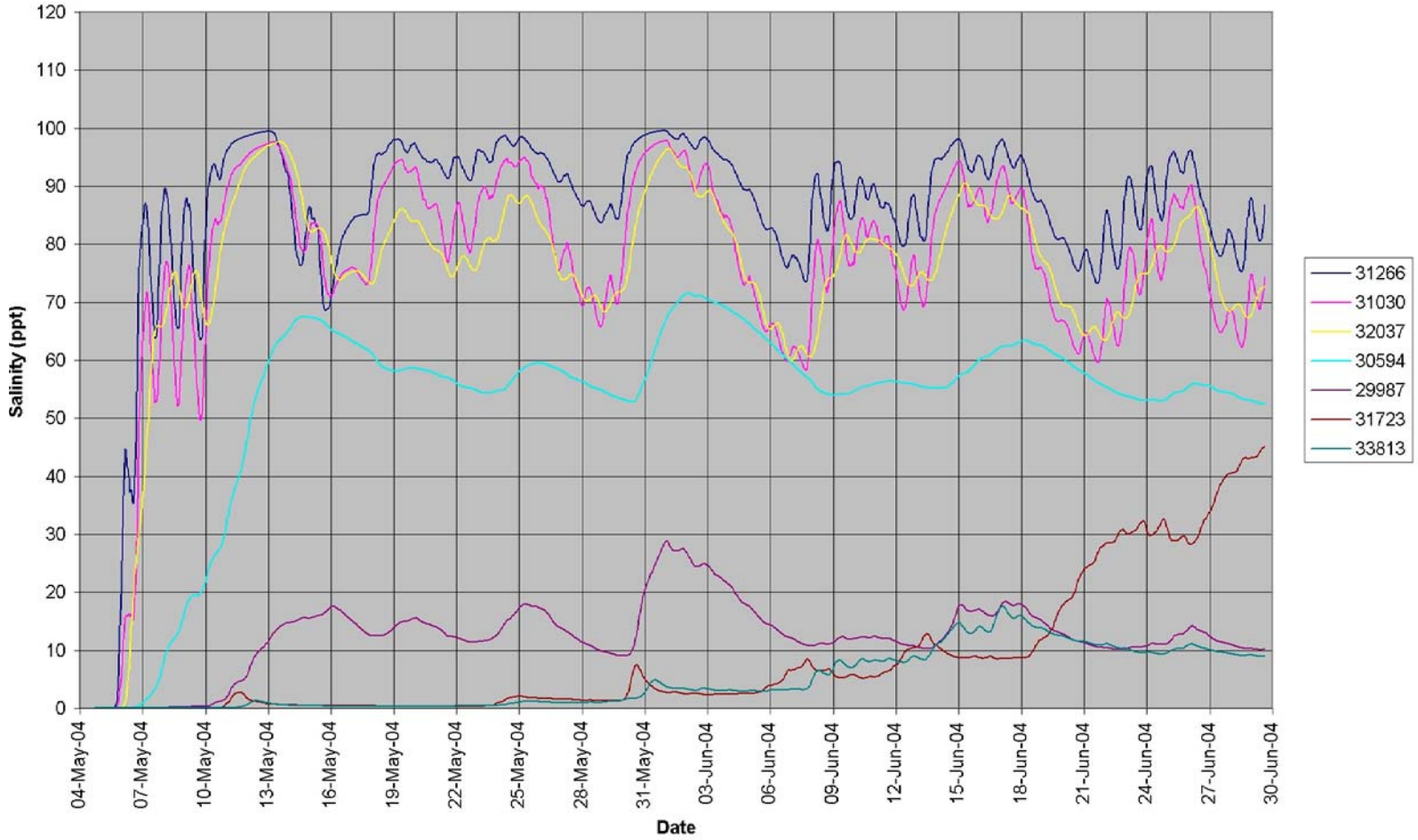

Figure B.24. Tracer time series in selected marshes for 1,000 cfs diversion with westerly GIWW flows.

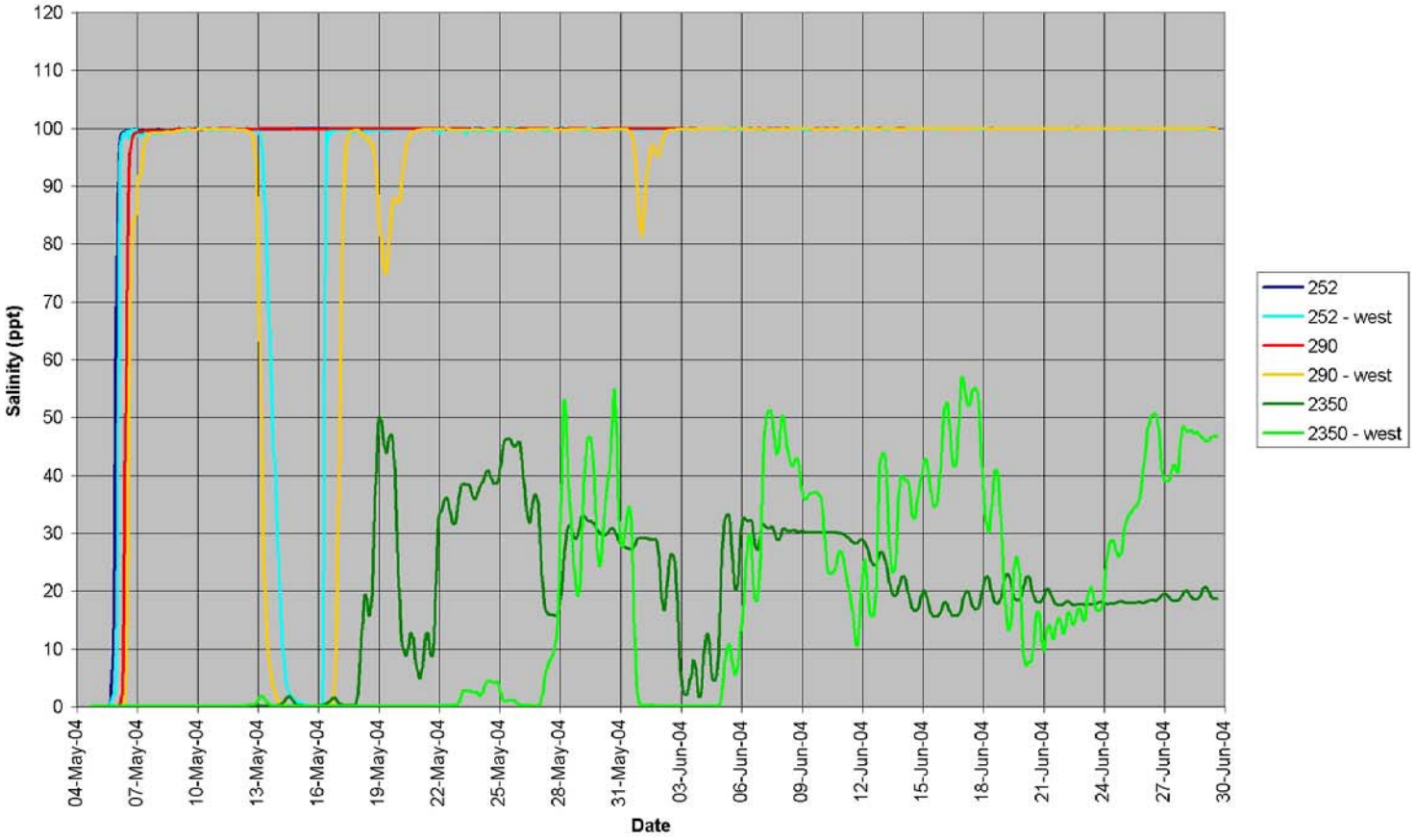

Figure B.25. Comparison of tracer time series in Bayou Lafourche for 1,000 cfs diversion with easterly (Run 1) and westerly (Run 5) GIWW flows.

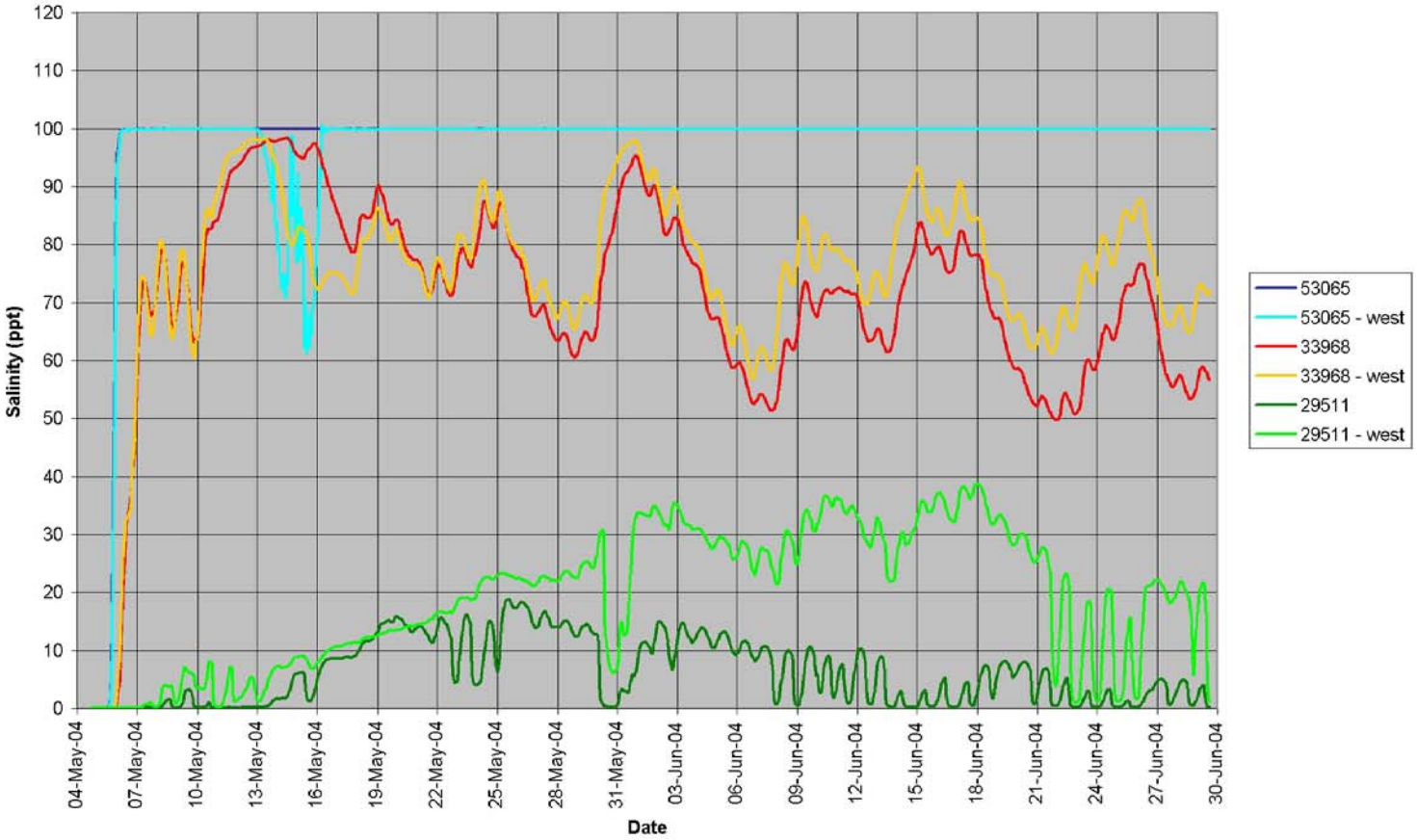

Figure B.26. Comparison of tracer time series in Company Canal for 1,000 cfs diversion with easterly (Run 1) and westerly (Run 5) GIWW flows.

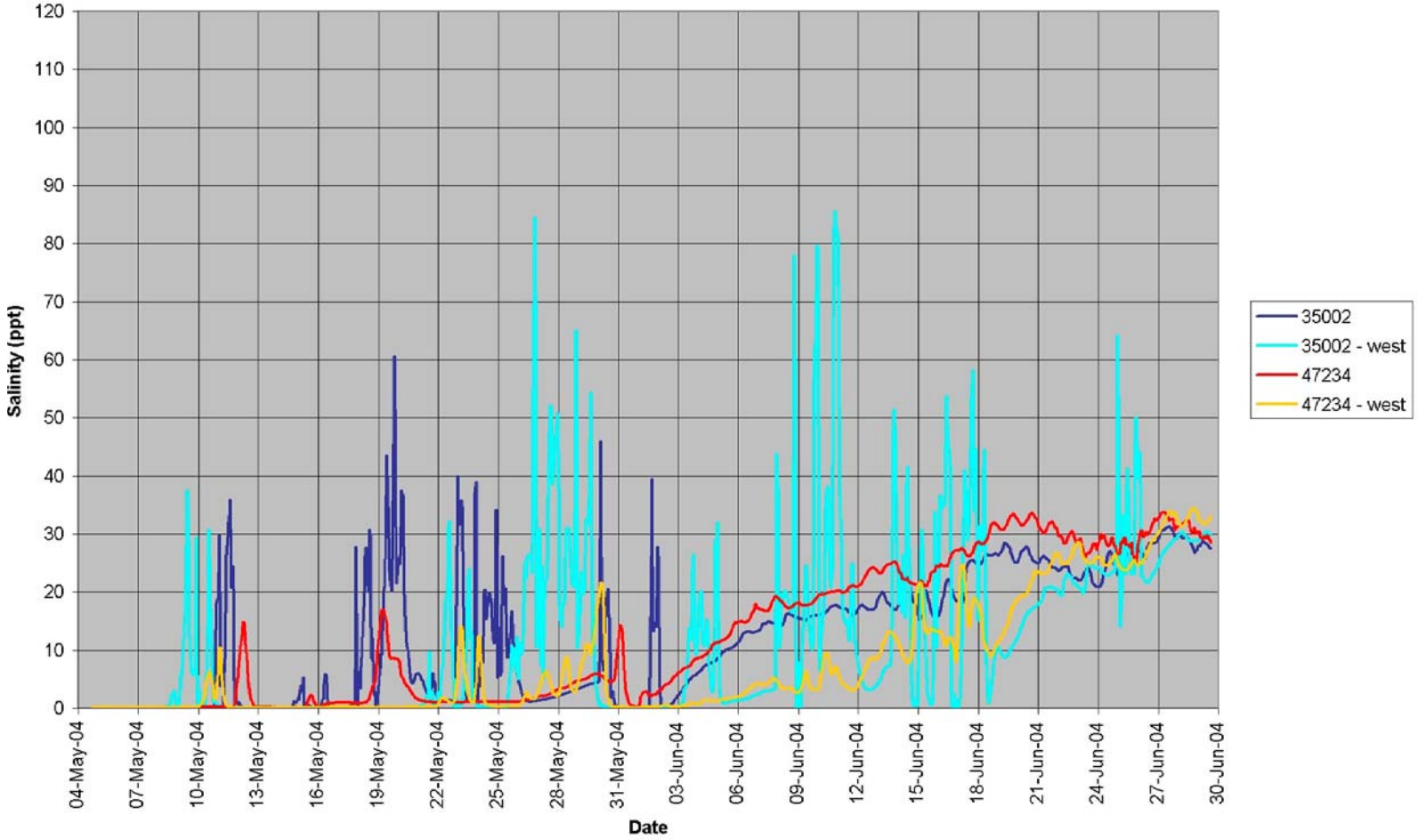

Figure B.27. Comparison of tracer time series in GIWW for 1,000 cfs diversion with easterly (Run 1) and westerly (Run 5) GIWW flows (Node Set 1).

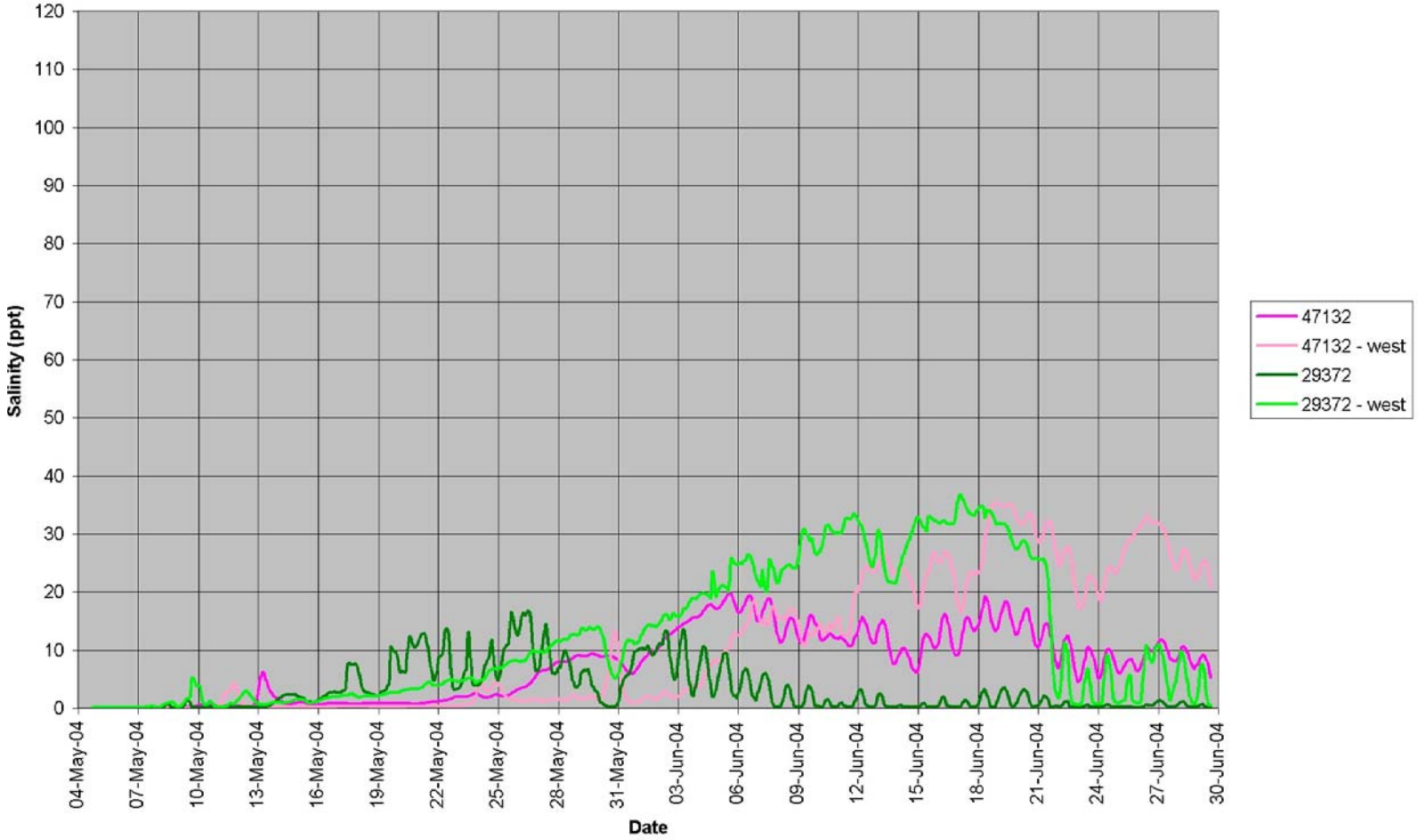

Figure B.28. Comparison of tracer time series in GIWW for 1,000 cfs diversion with easterly (Run 1) and westerly (Run 5) GIWW flows (Node Set 2).

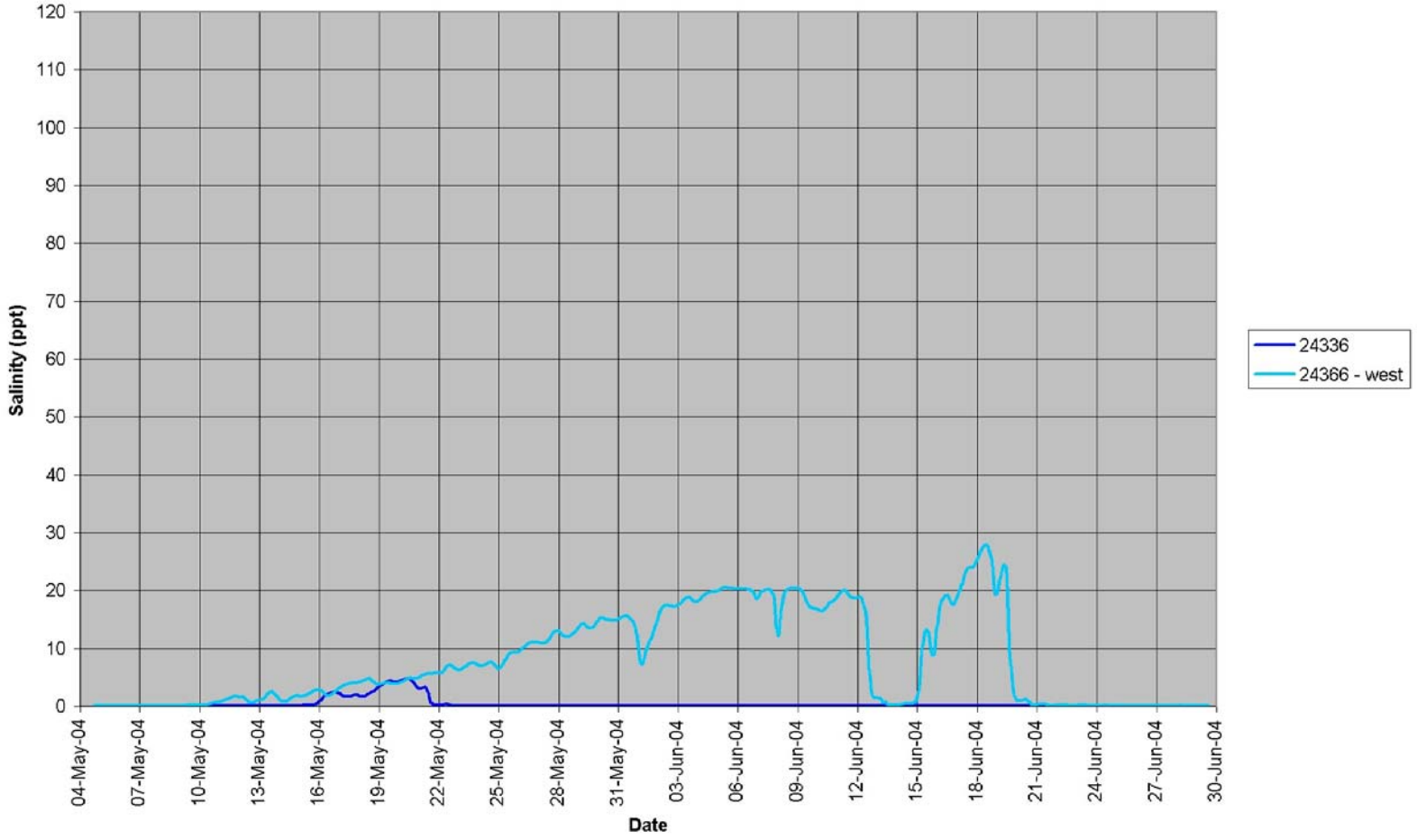

Figure B.29. Comparison of tracer time series in GIWW for 1,000 cfs diversion with easterly (Run 1) and westerly (Run 5) GIWW flows (Node Set 3).

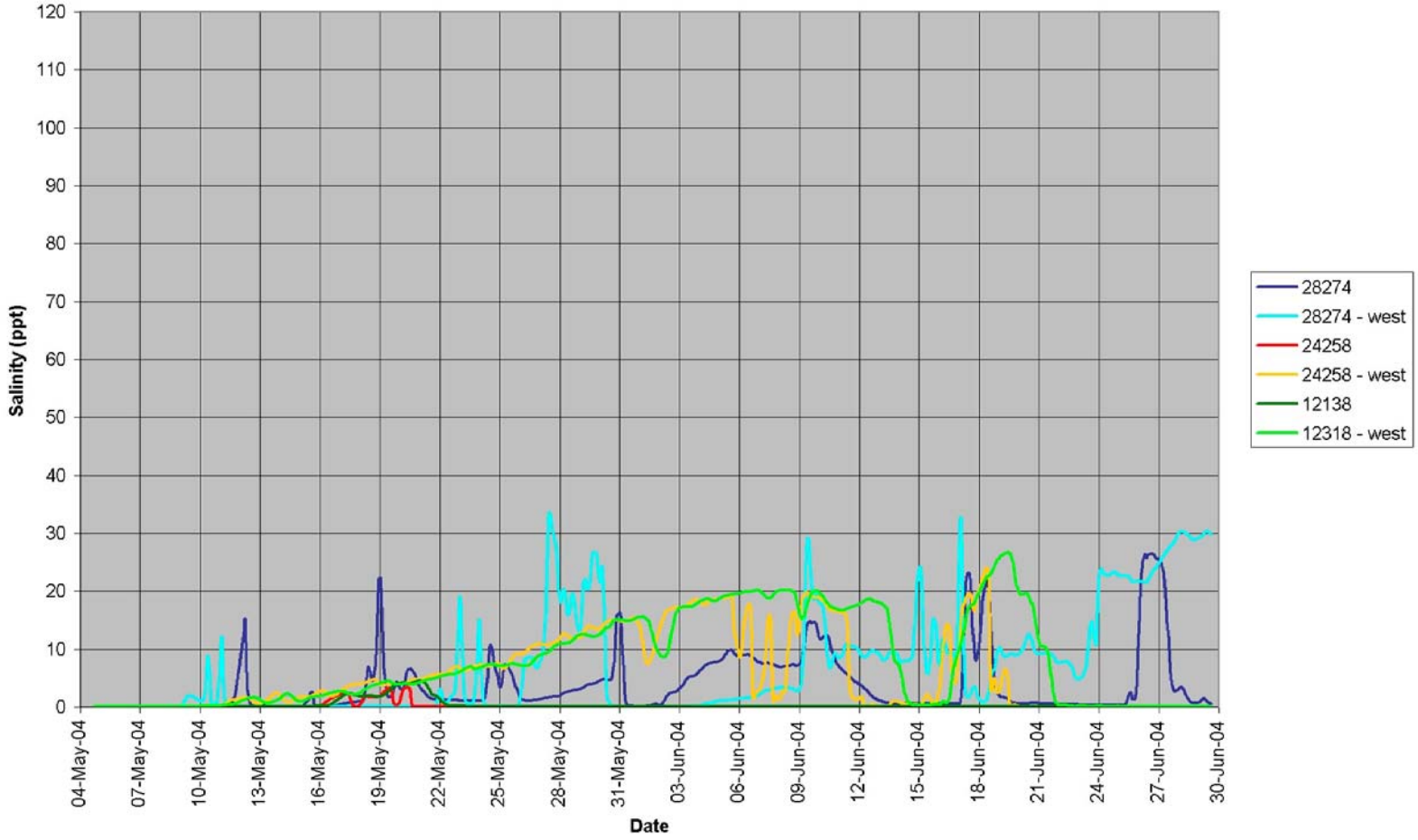

Figure B.30. Comparison of tracer time series in HNC and Grand Bayou for 1,000 cfs diversion with easterly (Run 1) and westerly (Run 5) GIWW flows.

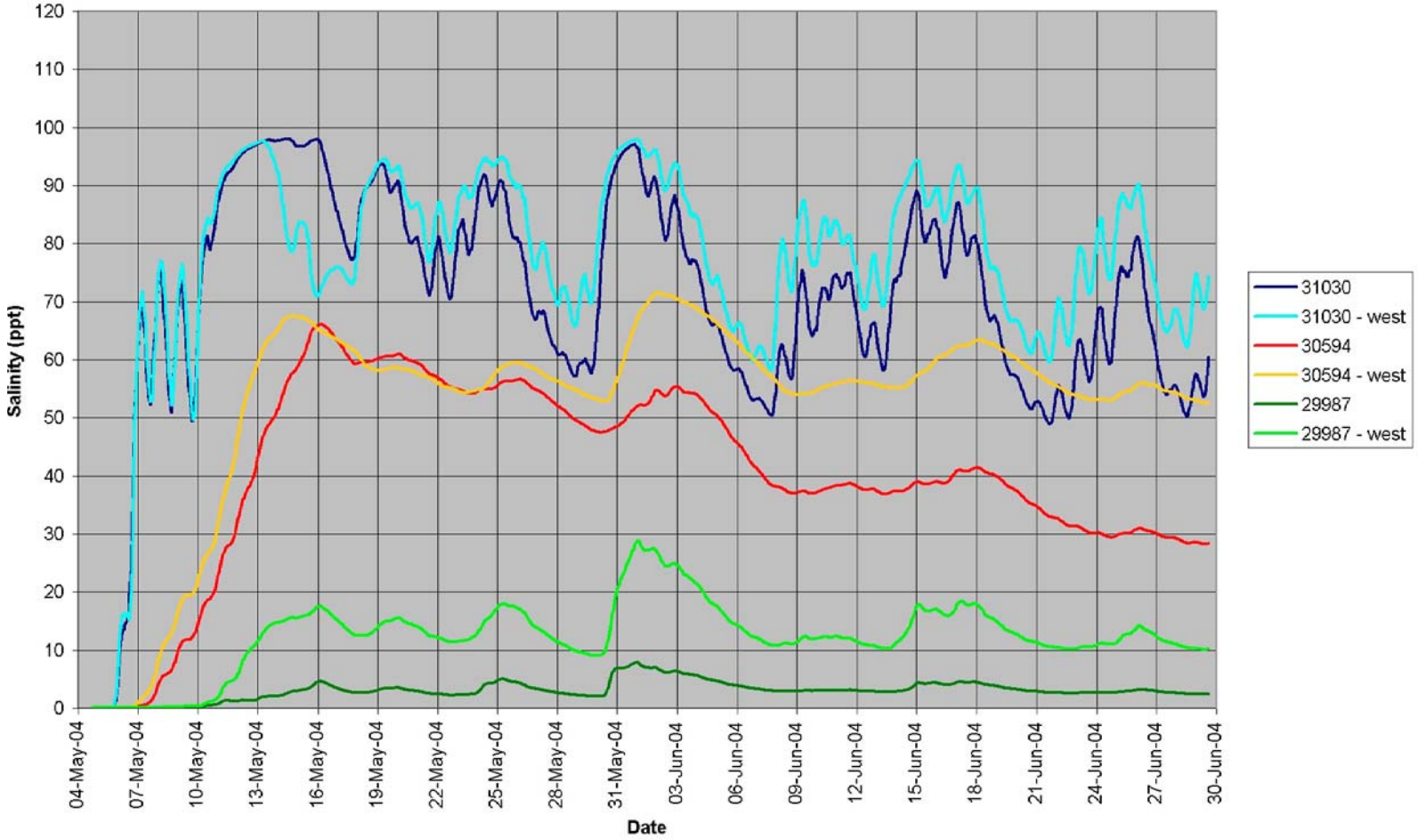

Figure B.31. Comparison of tracer time series in some marshes for 1,000 cfs diversion with easterly (Run 1) and westerly (Run 5) GIWW flows (Node Set 1).

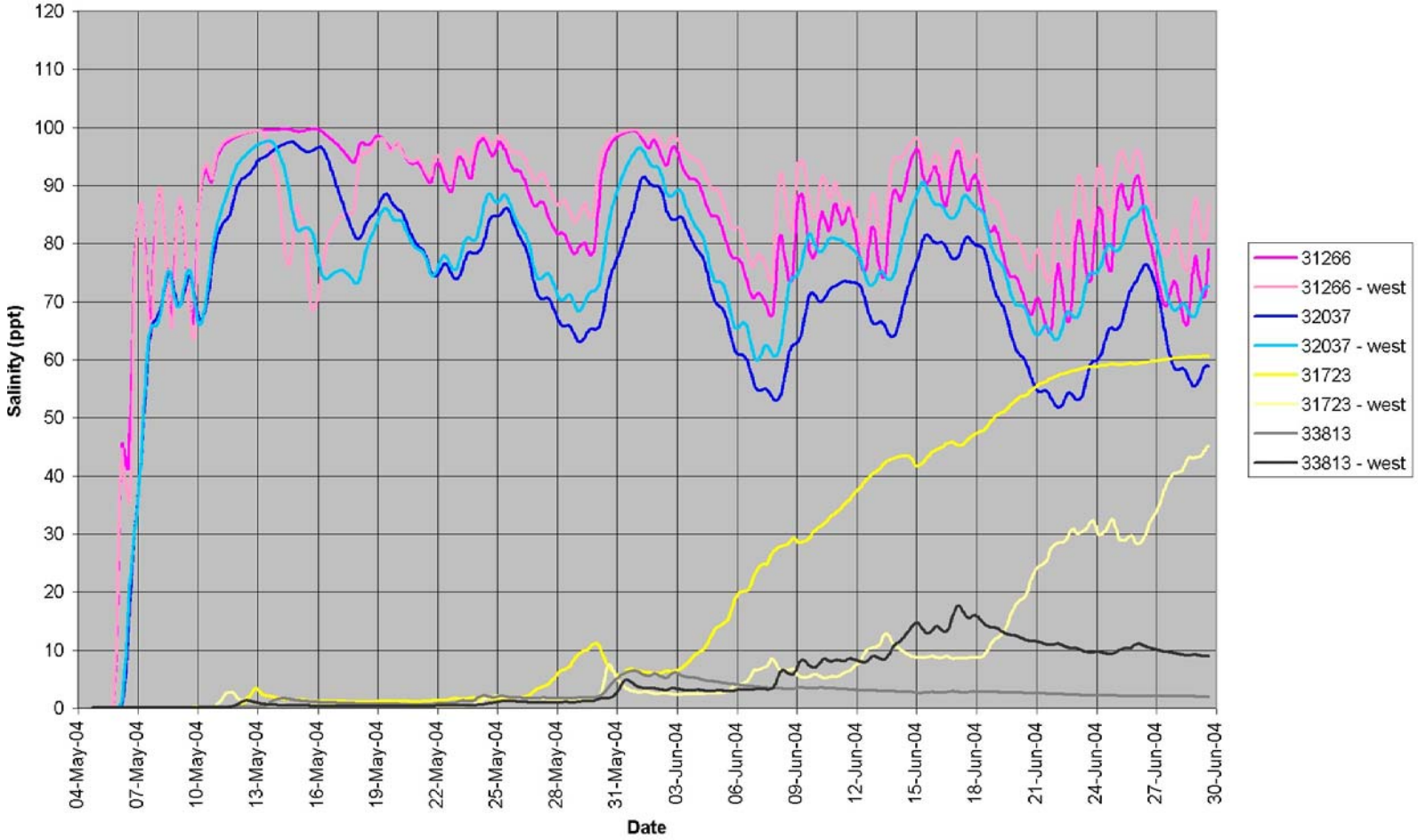

Figure B.32. Comparison of tracer time series in some marshes for 1,000 cfs diversion with easterly (Run 1) and westerly (Run 5) GIWW flows (Node Set 2).

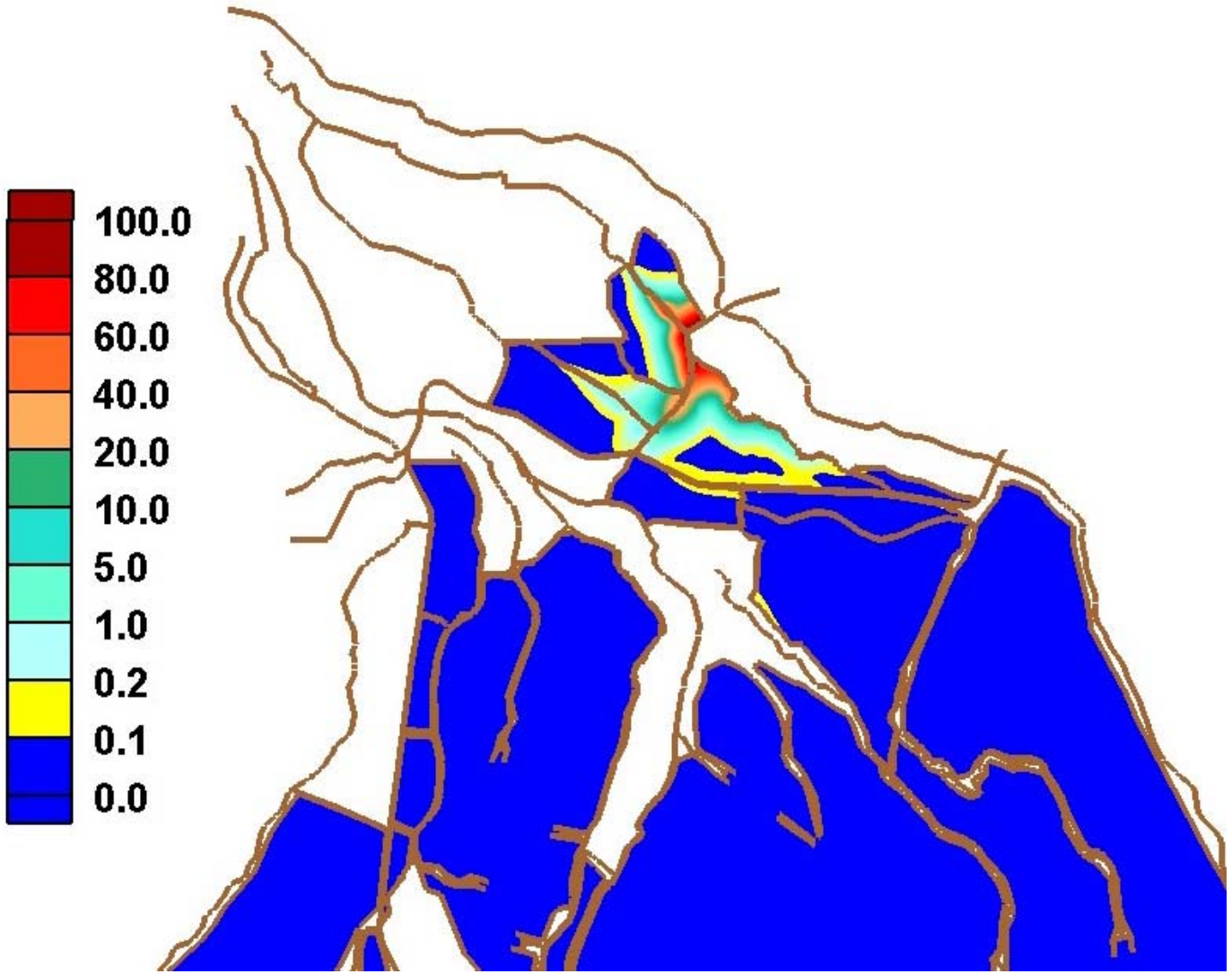

Figure B.33. Tracer distribution in the system for 1,000 cfs by the end of week 1.

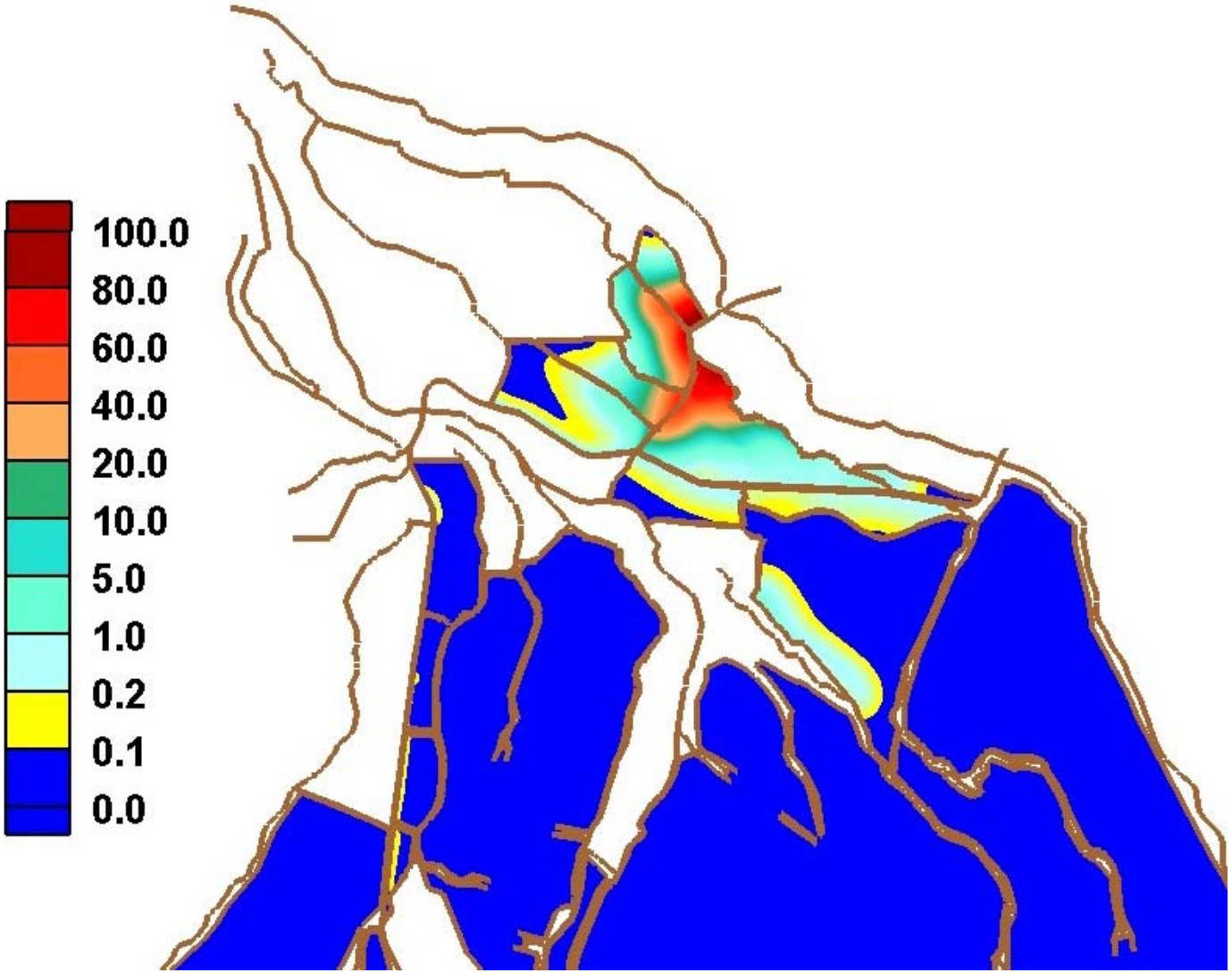

Figure B.34. Tracer distribution in the system for 1,000 cfs by the end of week 2.

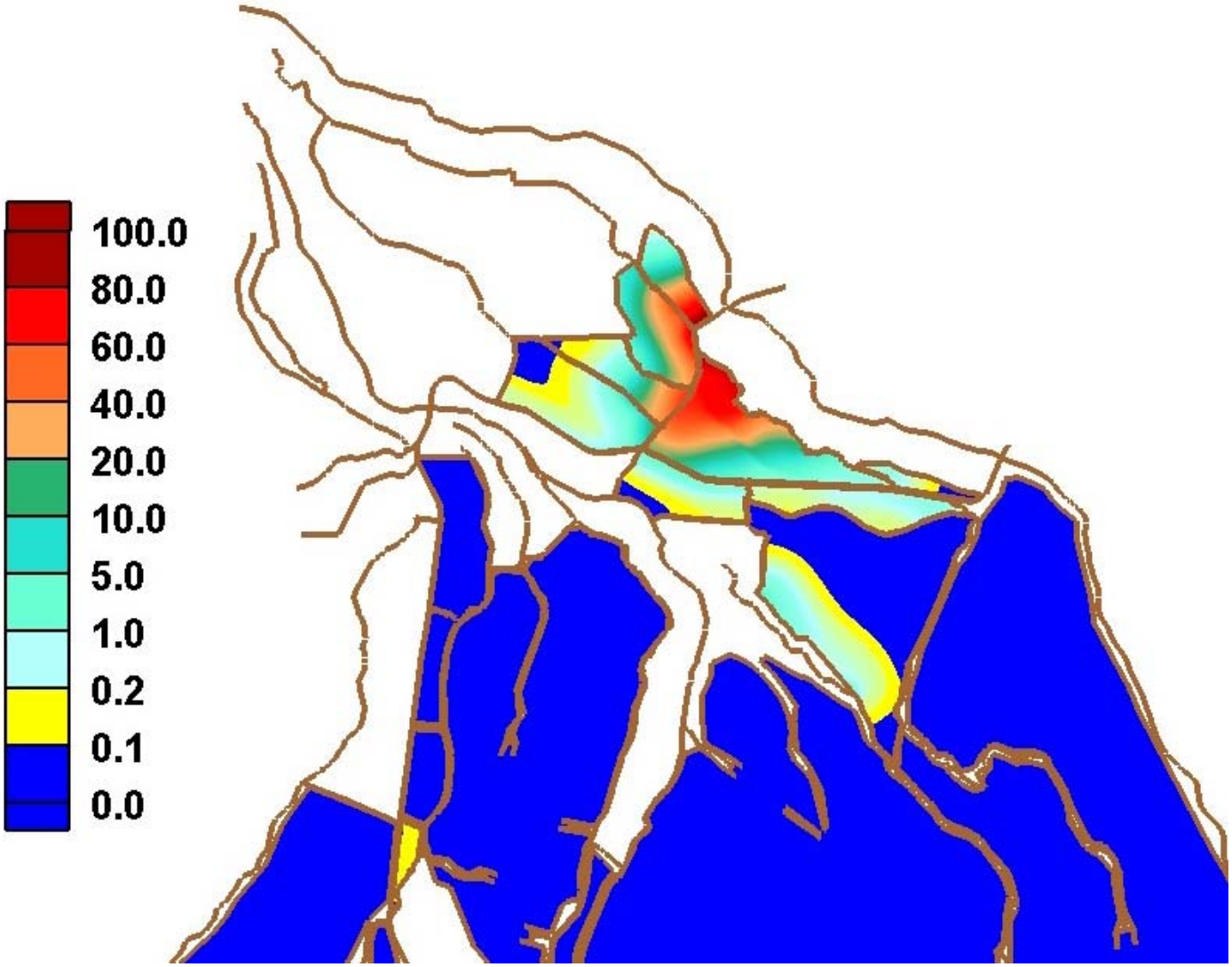

Figure B.35. Tracer distribution in the system 1,000 cfs by the end of week 3.

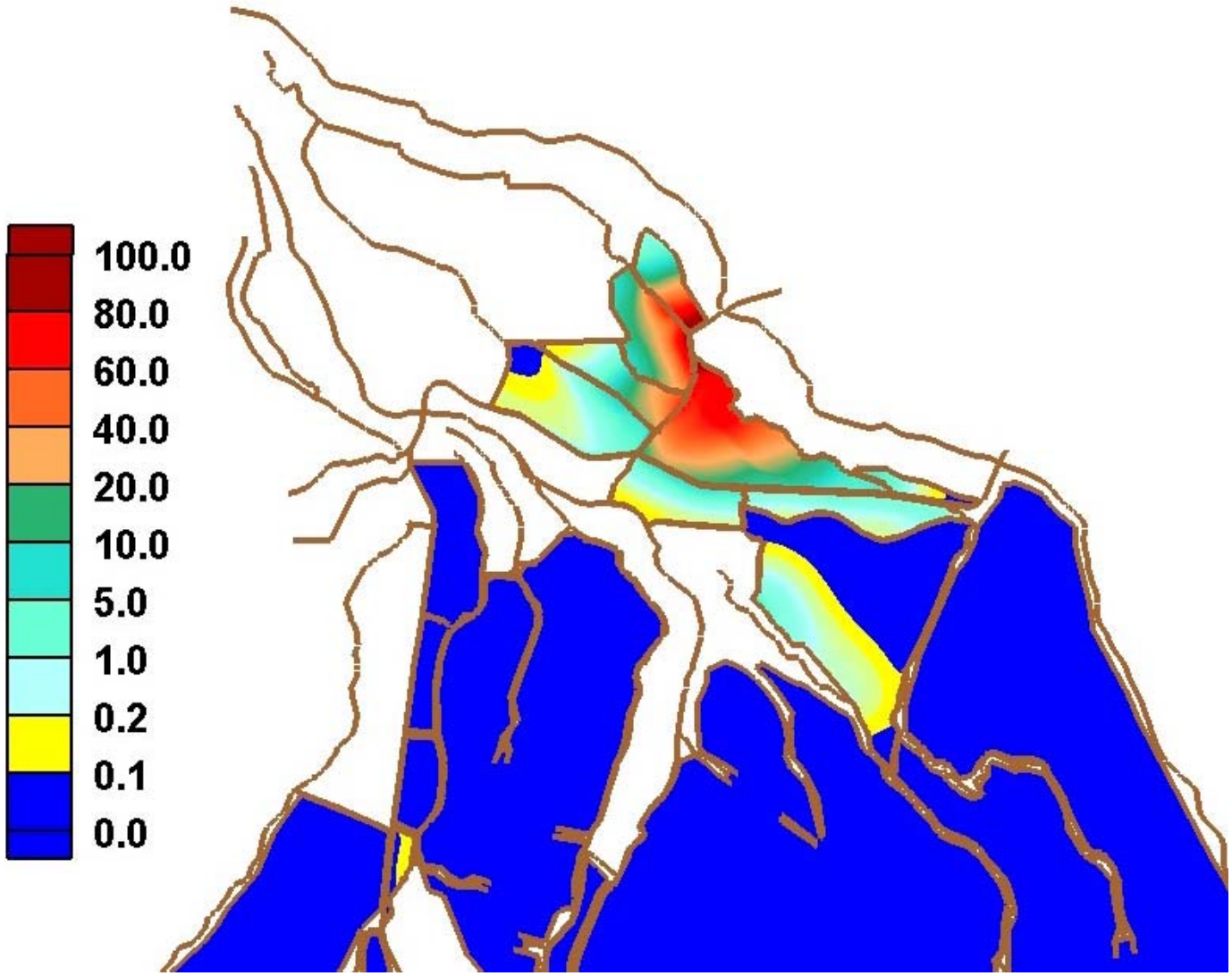

Figure B.36. Tracer distribution in the system for 1,000 cfs by the end of week 4.

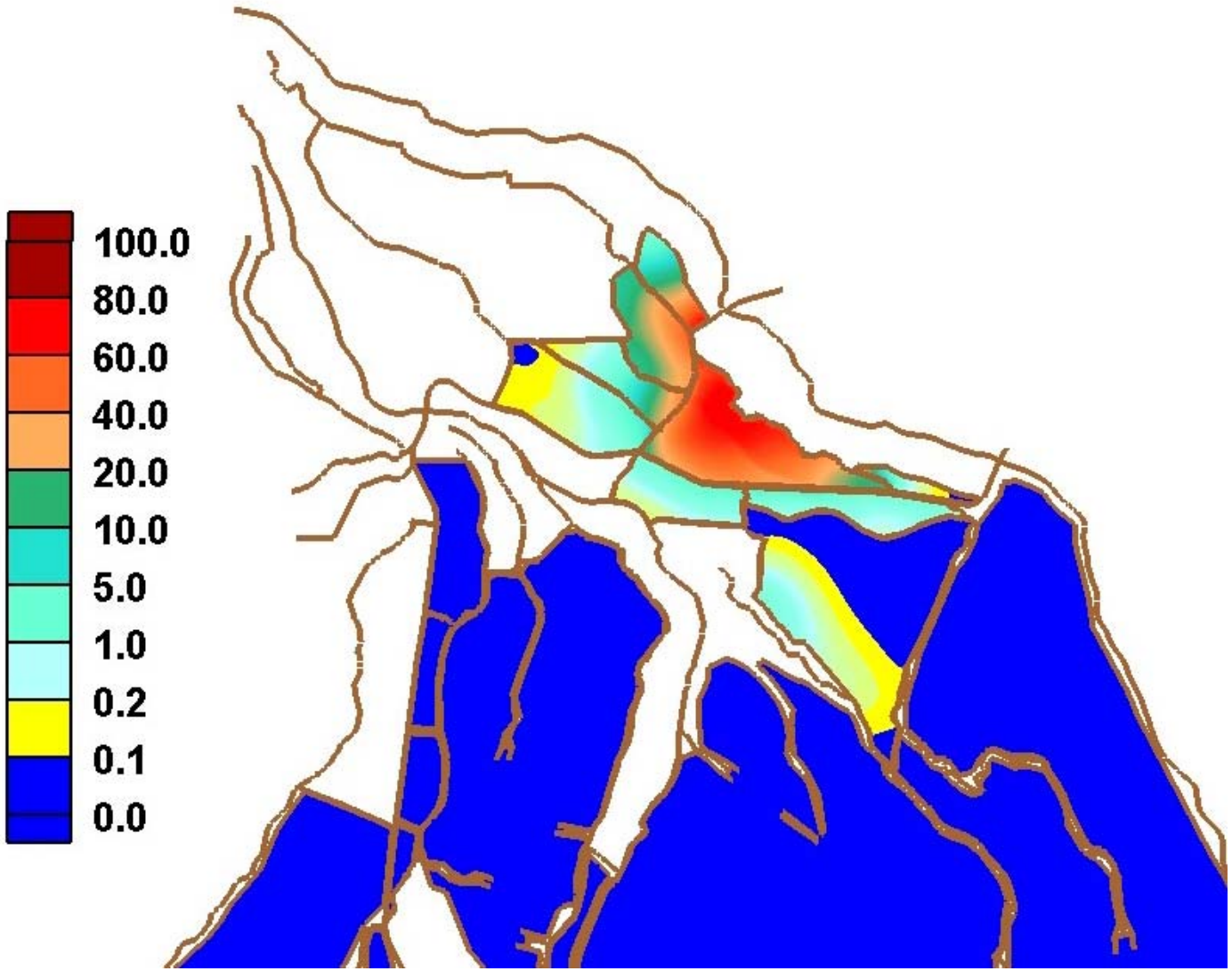

Figure B.37. Tracer distribution in the system for 1,000 cfs by the end of week 5.

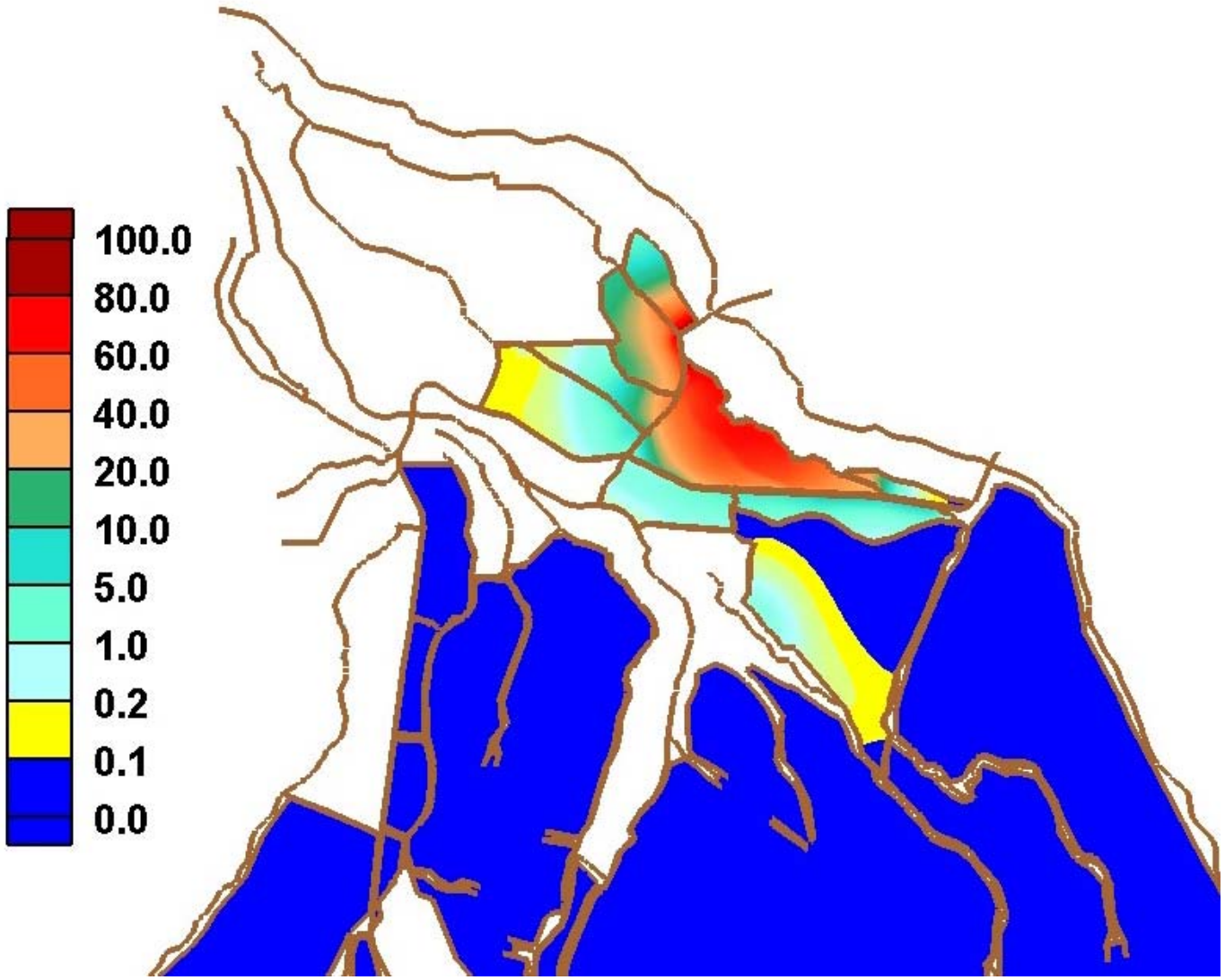

Figure B.38. Tracer distribution in the system for 1,000 cfs by the end of week 6.

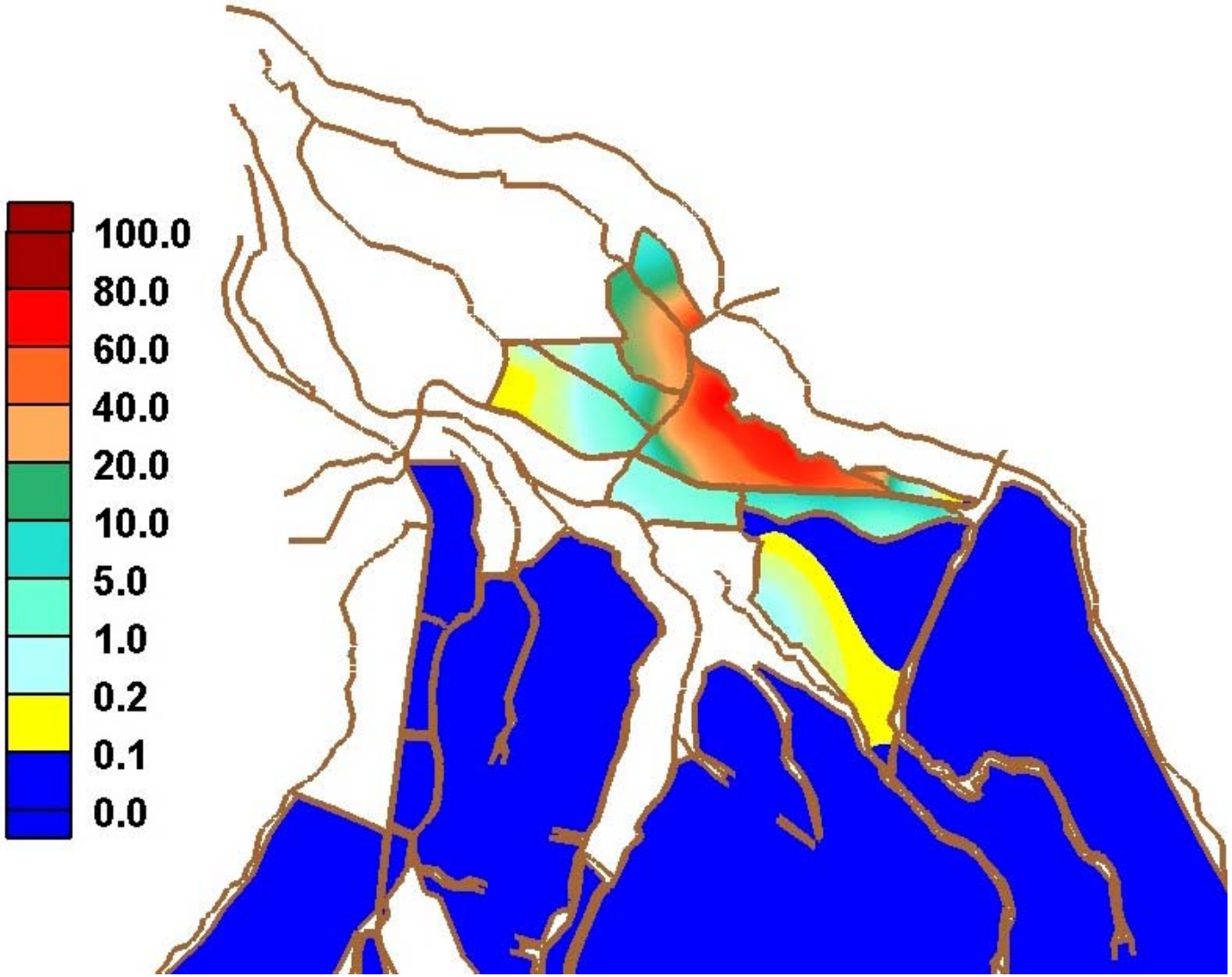

Figure B.39. Tracer distribution in the system for 1,000 cfs by the end of week 7.

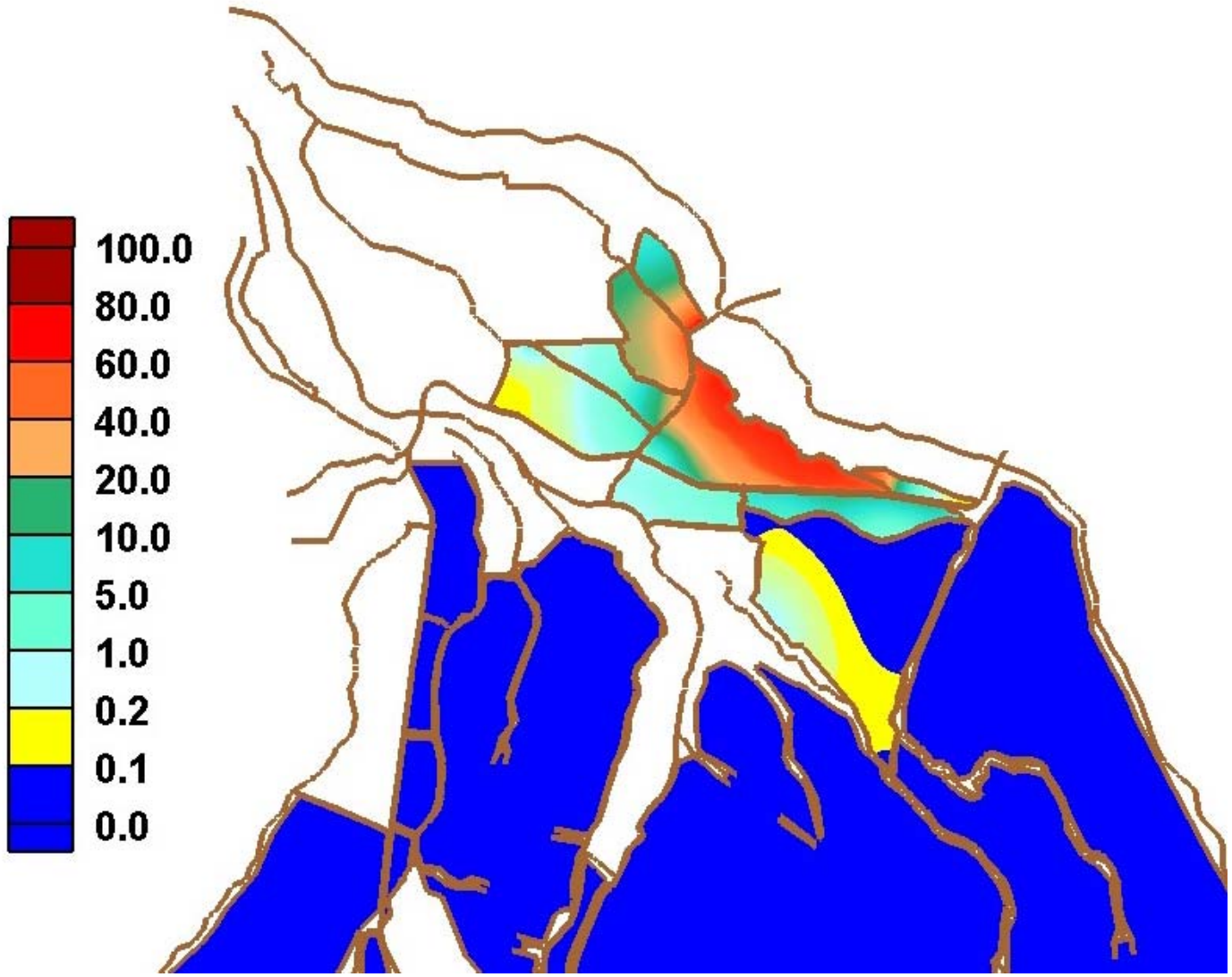

Figure B.40. Tracer distribution in the system for 1,000 cfs by the end of week 8.

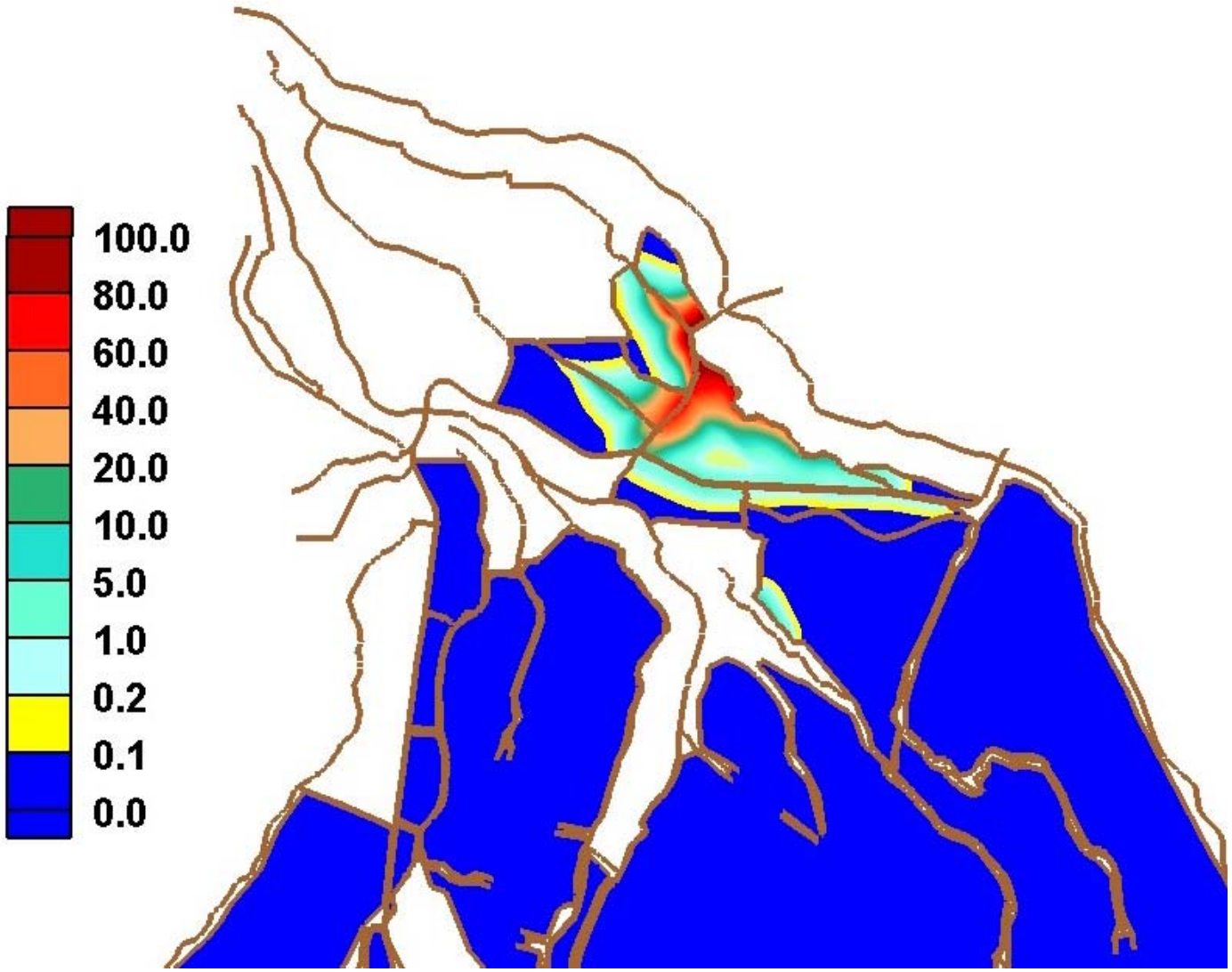

Figure B.41. Tracer distribution in the system for 2,000 cfs by the end of week 1.

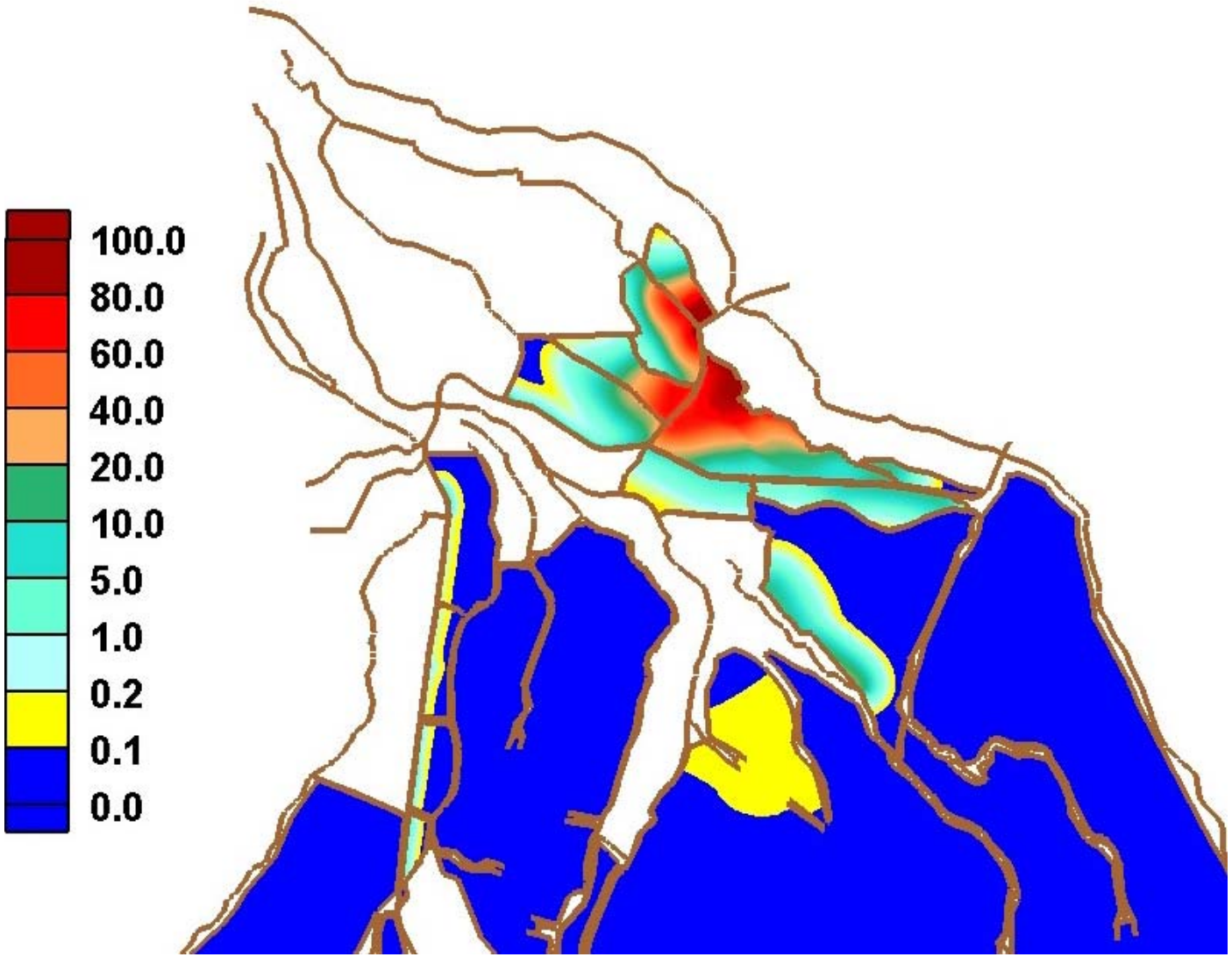

Figure B.42. Tracer distribution in the system for 2,000 cfs by the end of week 2.

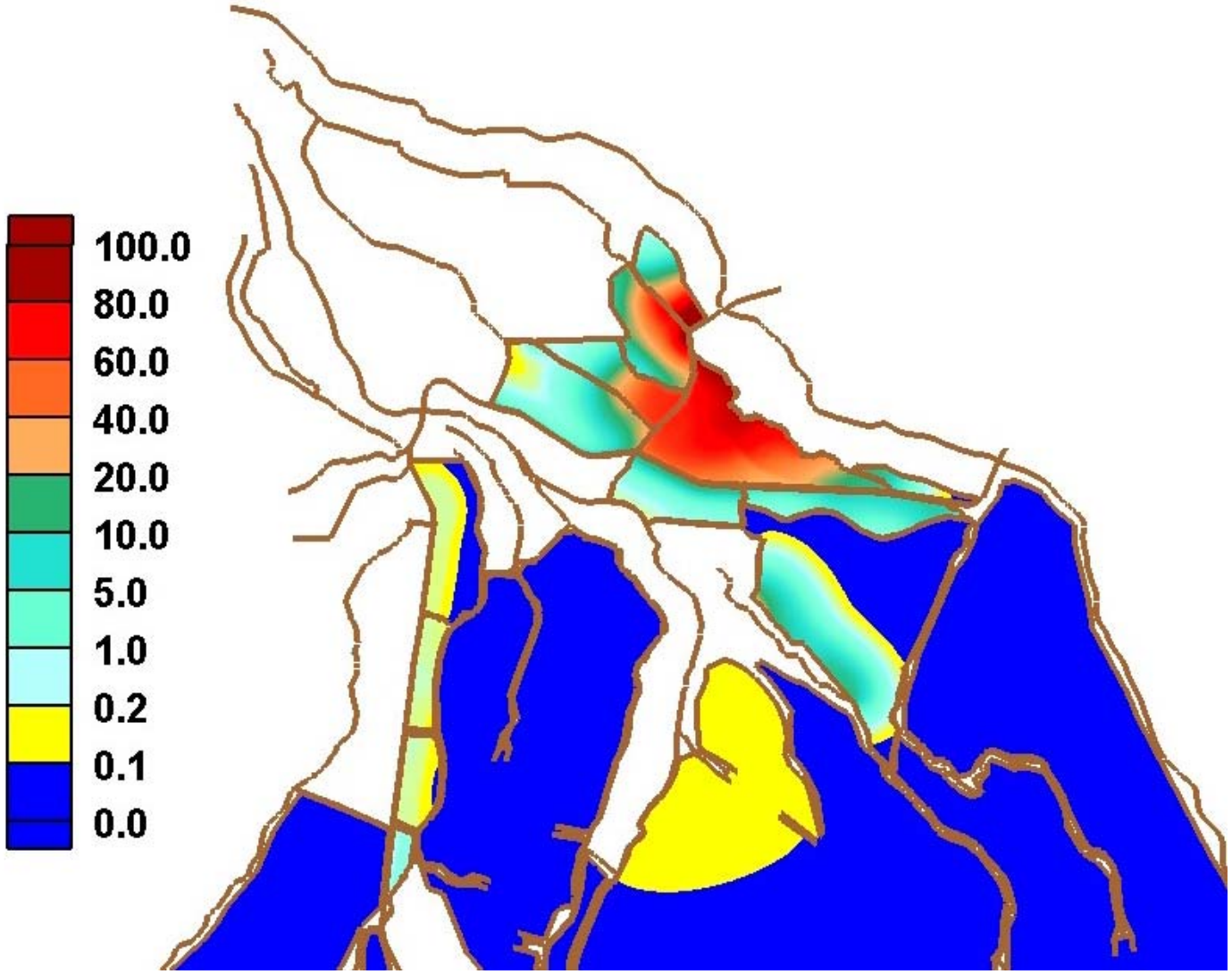

Figure B.43. Tracer distribution in the system for 2,000 cfs by the end of week 3.

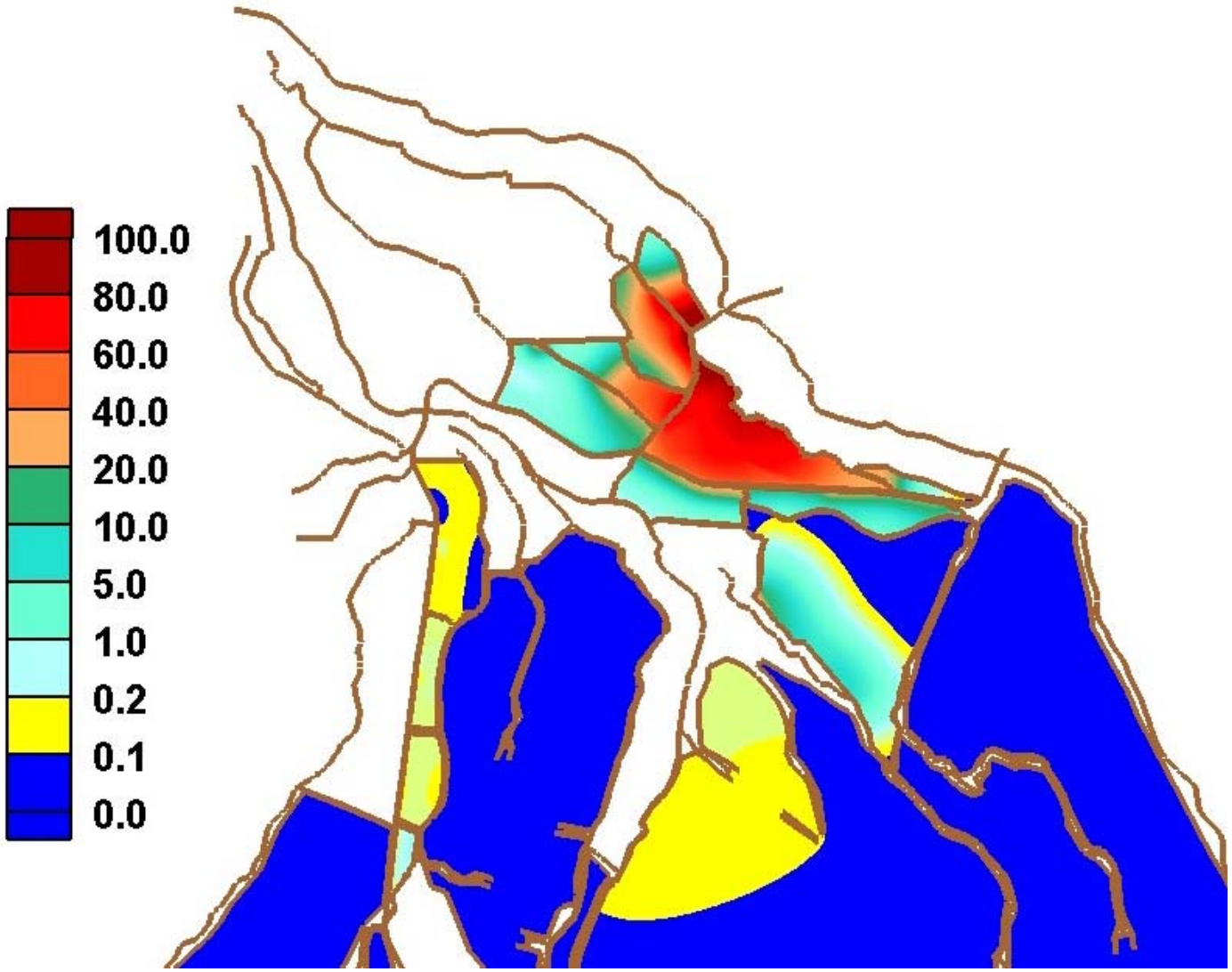

Figure B.44. Tracer distribution in the system for 2,000 cfs by the end of week 4.

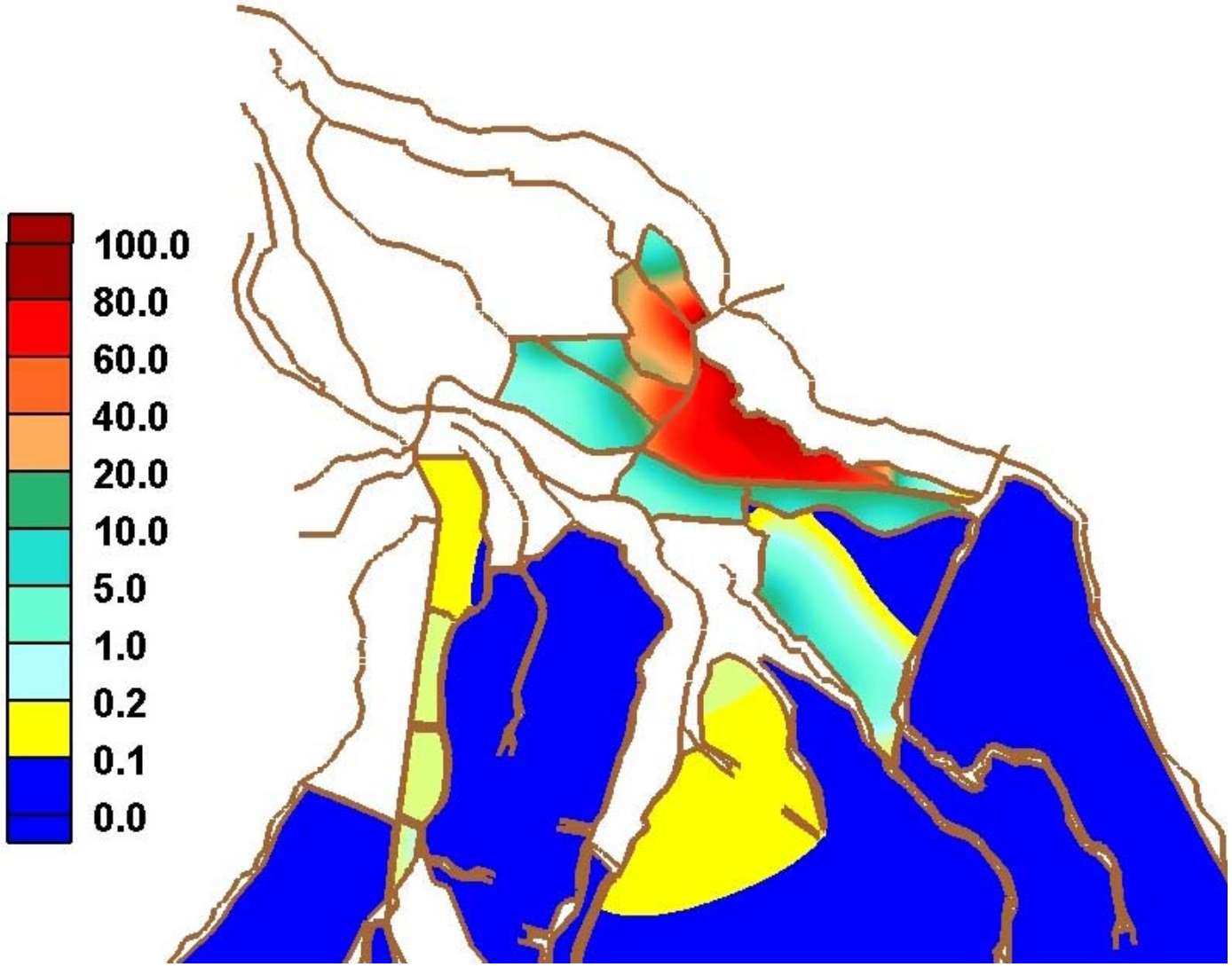

Figure B.45. Tracer distribution in the system for 2,000 cfs by the end of week 5.

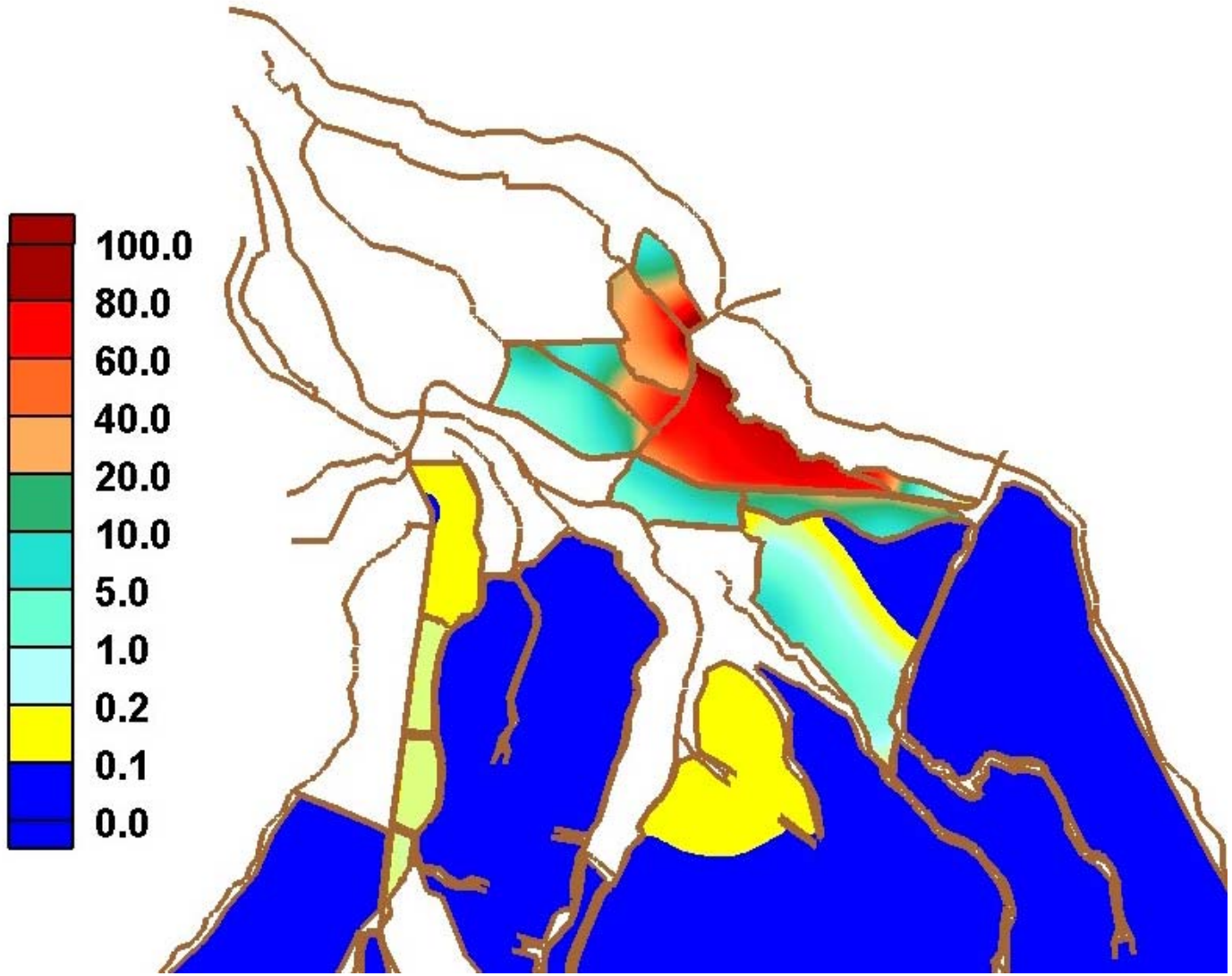

Figure B.46. Tracer distribution in the system for 2,000 cfs by the end of week 6.

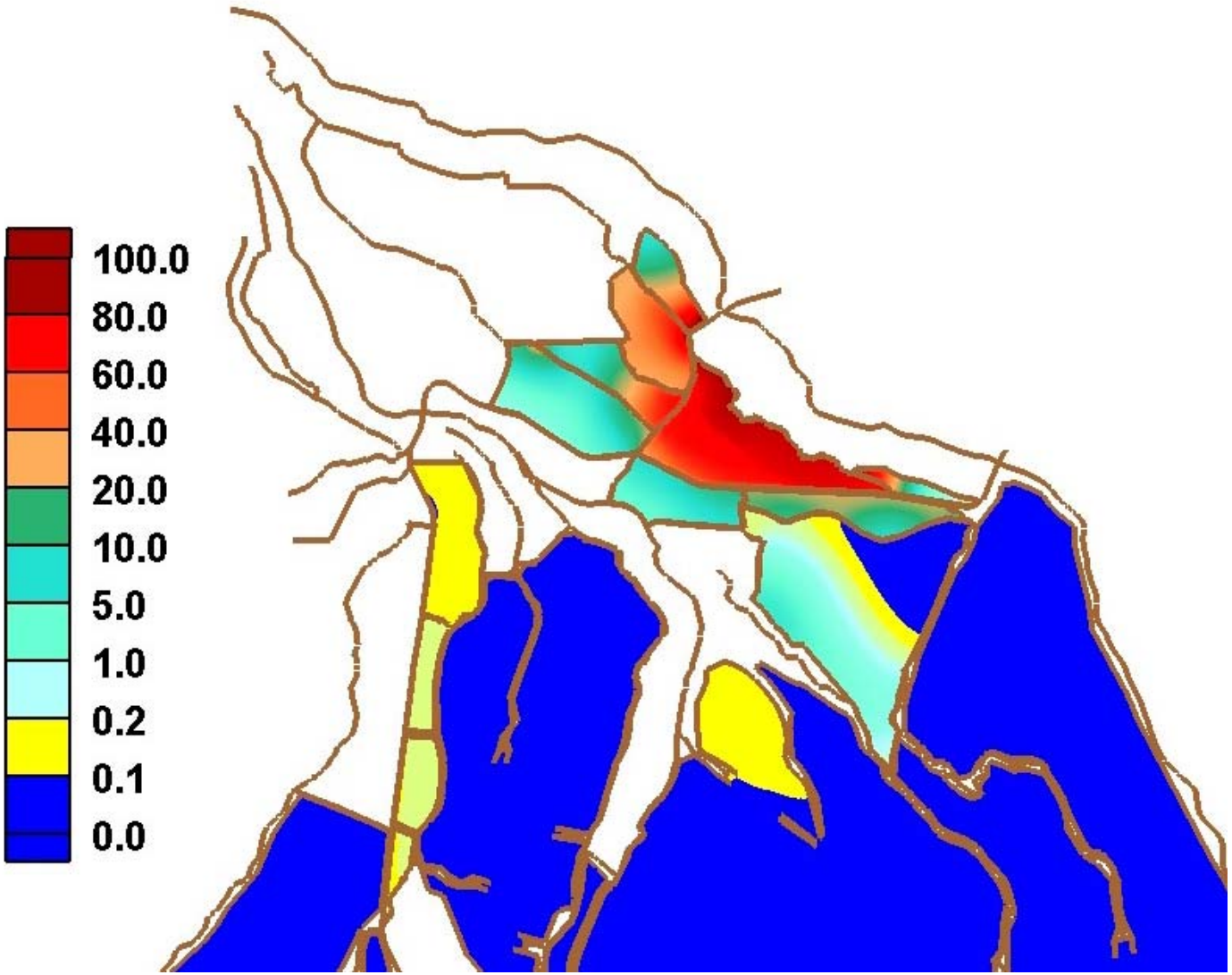

Figure B.47. Tracer distribution in the system for 2,000 cfs by the end of week 7.

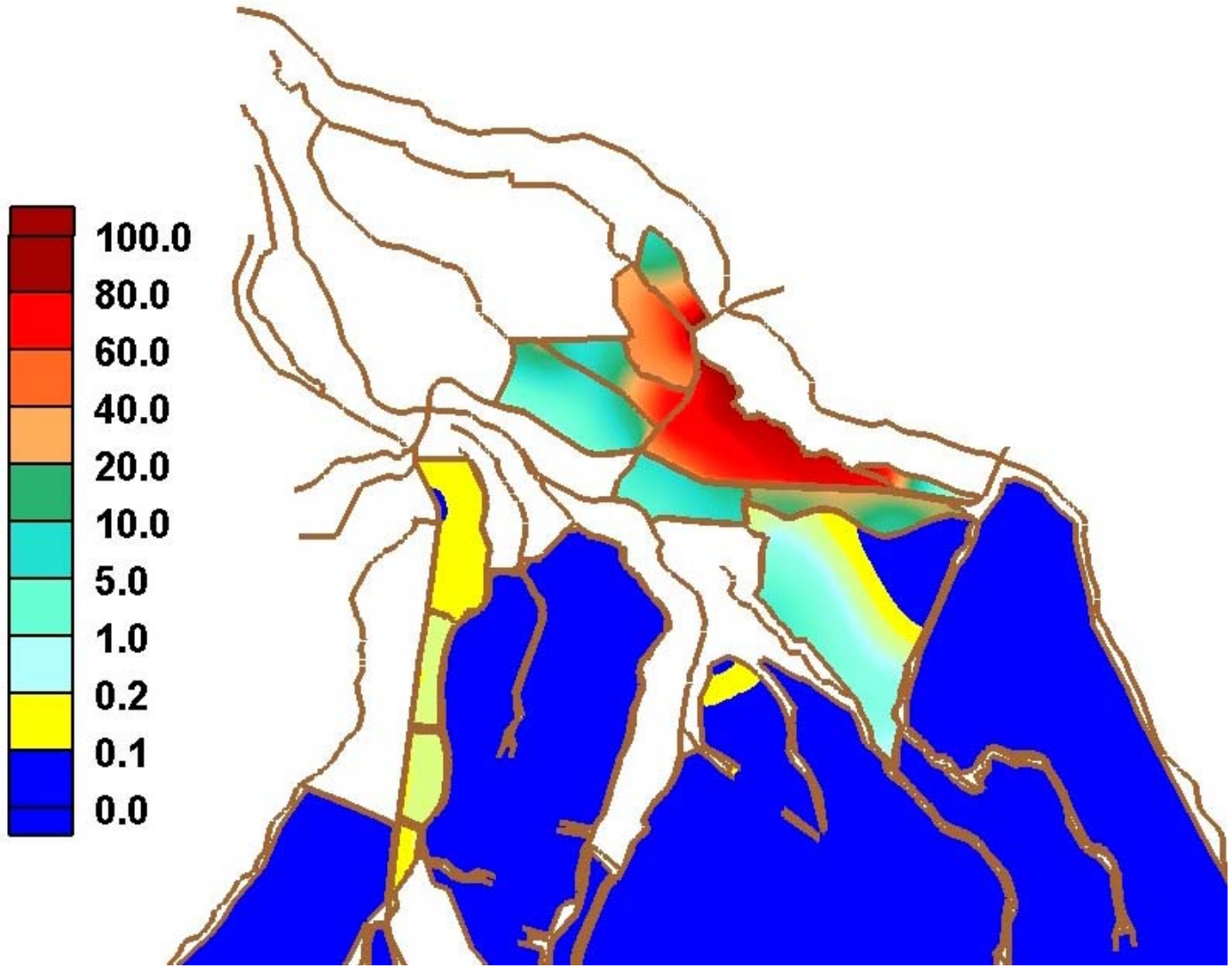

Figure B.48. Tracer distribution in the system for 2,000 cfs by the end of week 8.

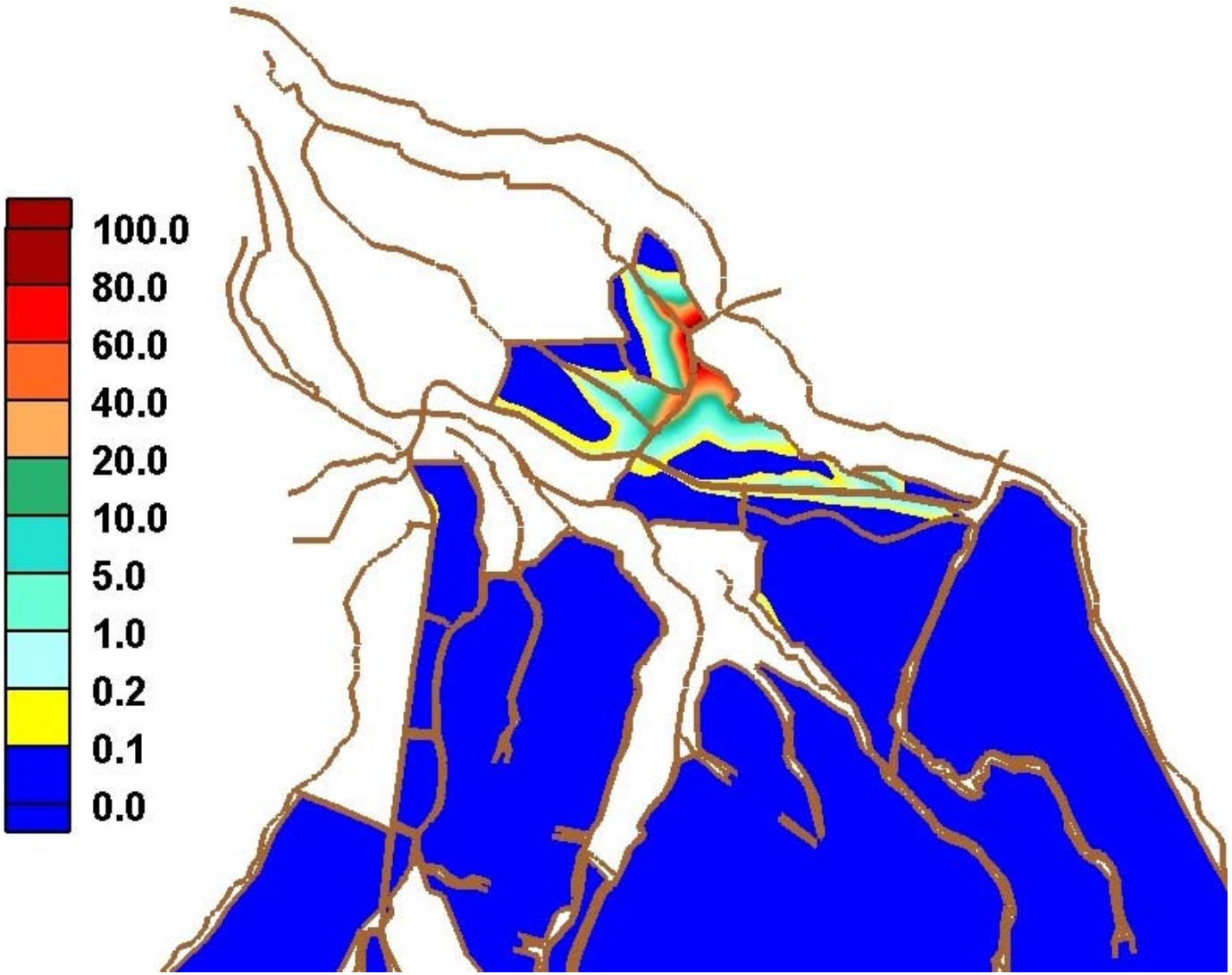

Figure B.49. Tracer distribution in the system for 1,000 cfs by the end of week 1 with westerly GIWW flows.

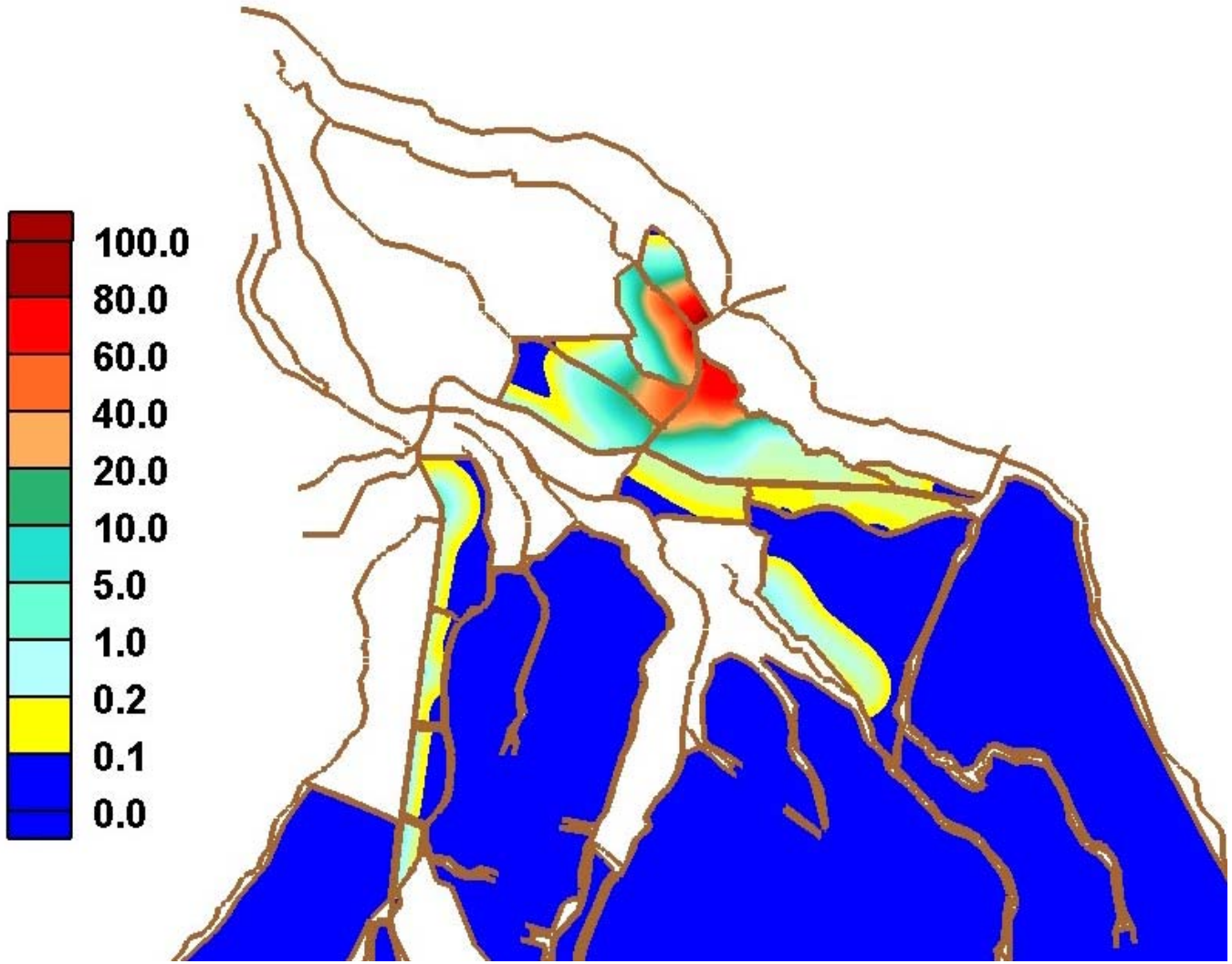

Figure B.50. Tracer distribution in the system for 1,000 cfs by the end of week 2 with westerly GIWW flows.

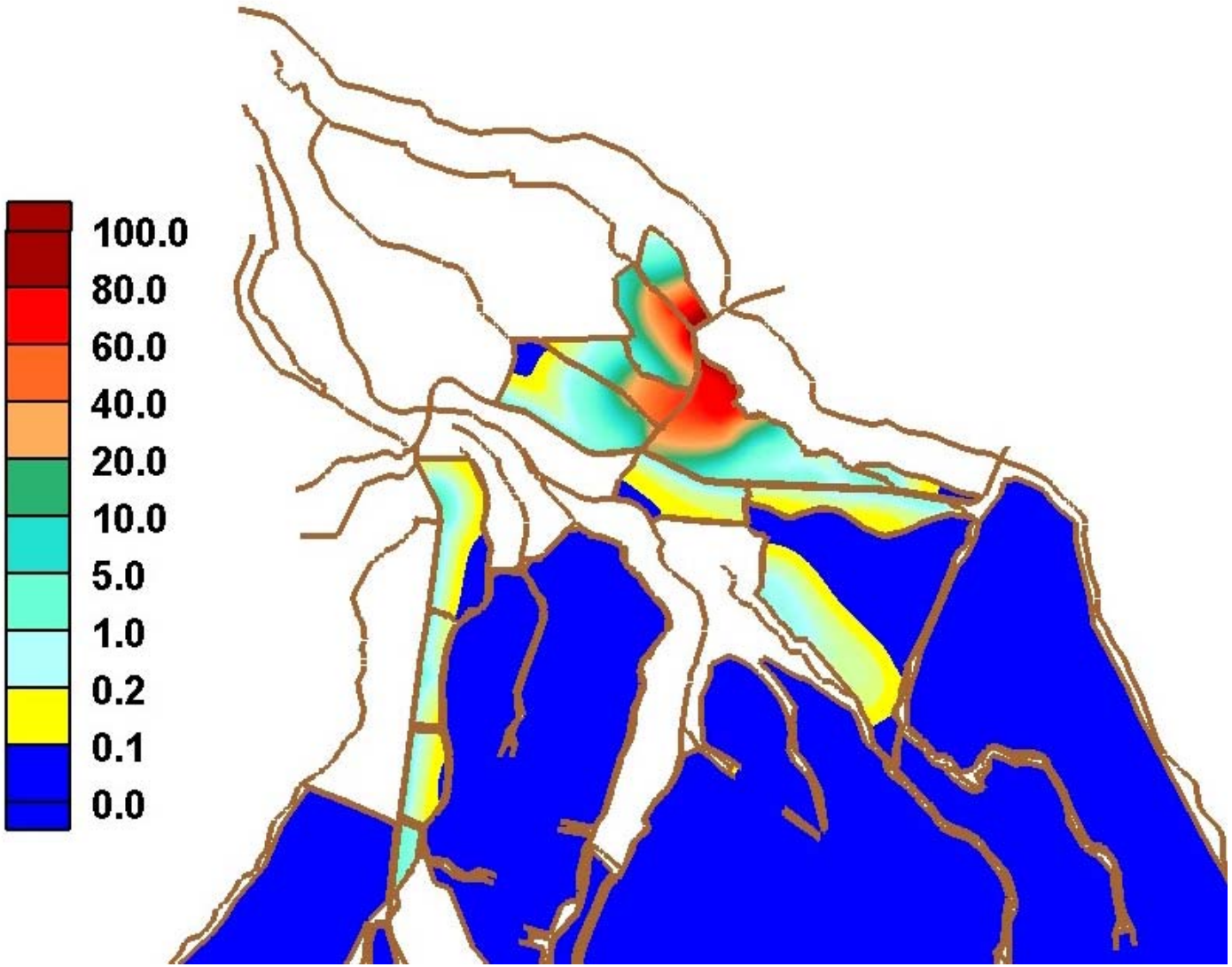

Figure B.51. Tracer distribution is the system for 1,000 cfs by the end of week 3 with westerly GIWW flows.

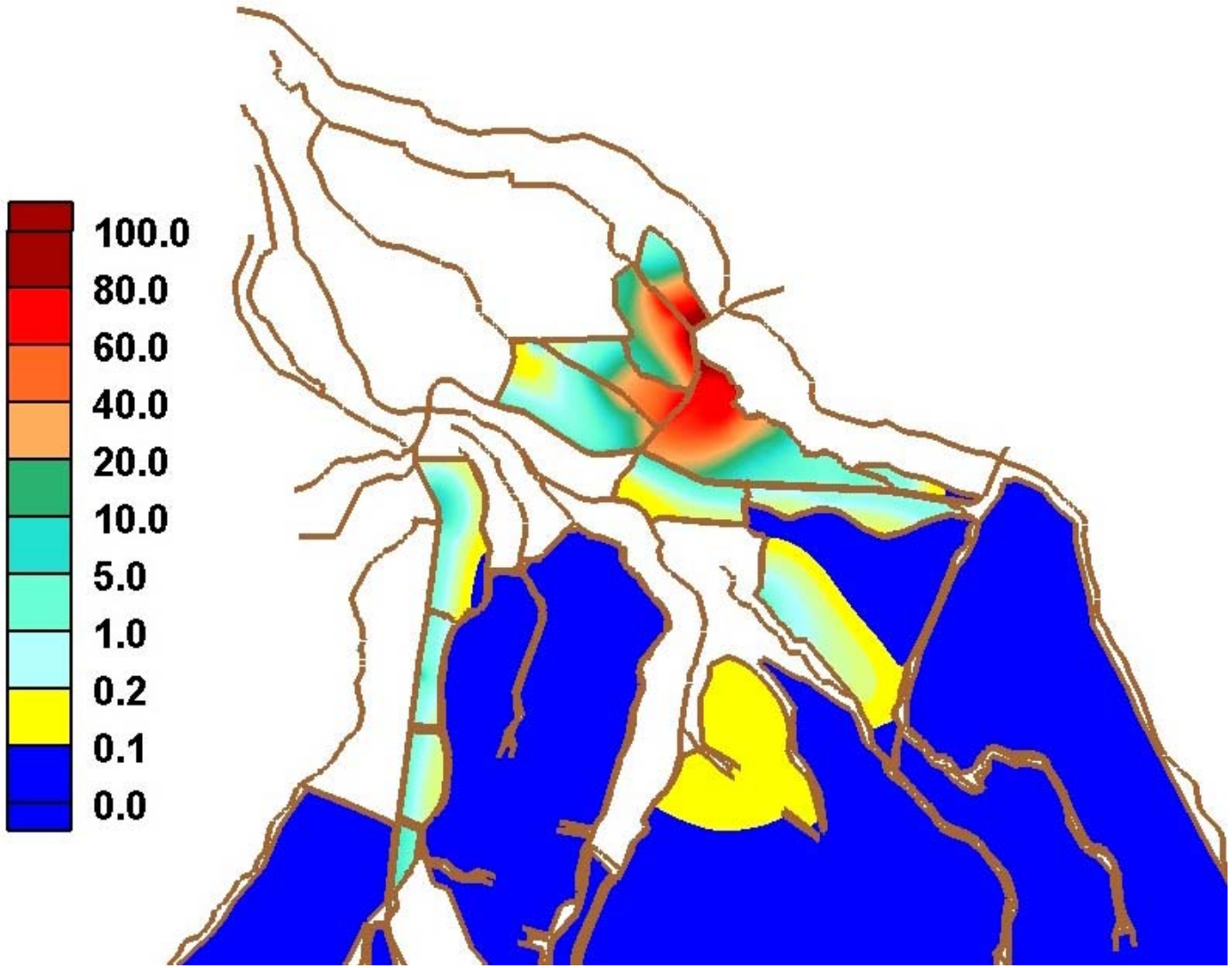

Figure B.52. Tracer distribution in the system for 1,000 cfs by the end of week4 with westerly GIWW flows.

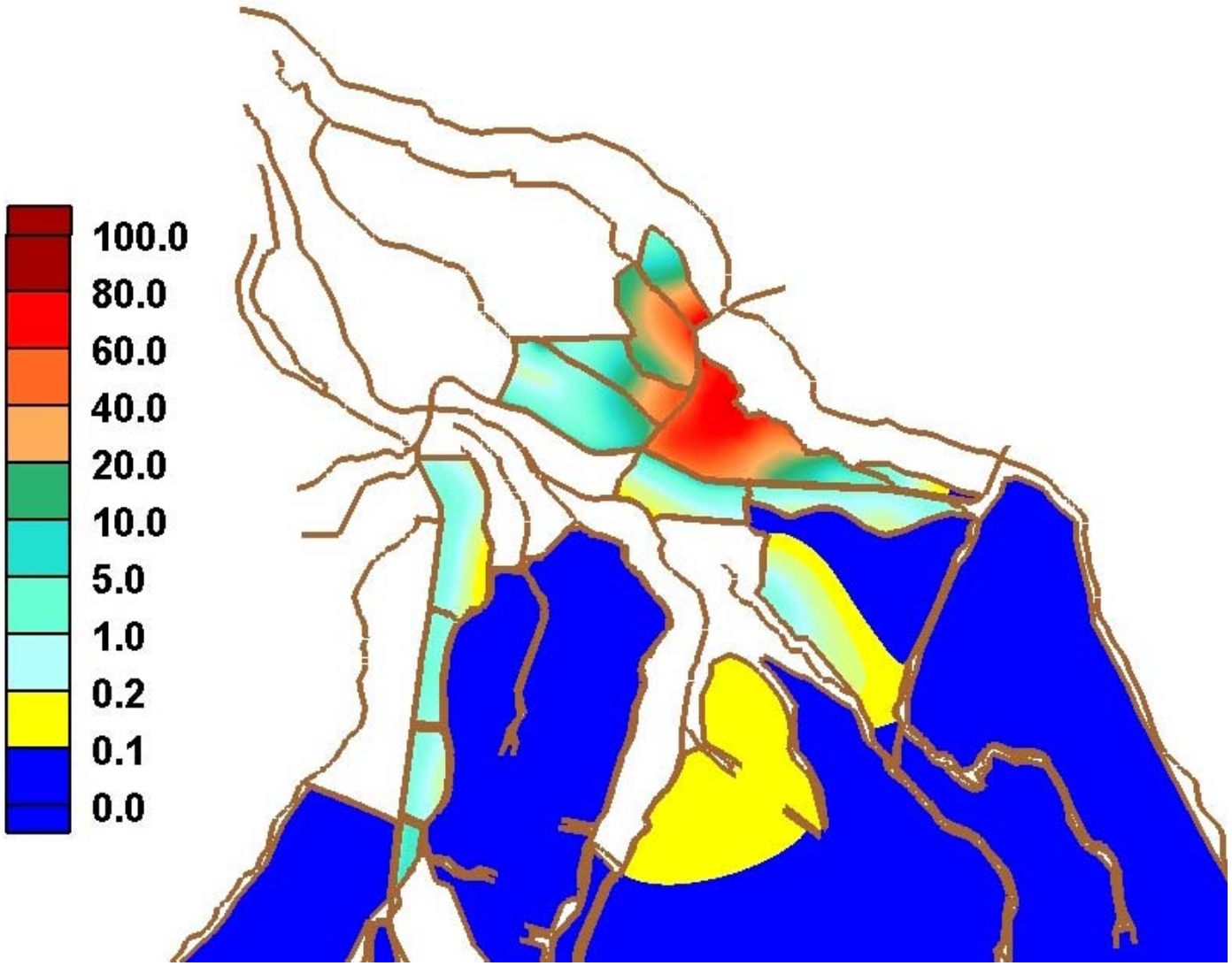

Figure B.53. Tracer distribution in the system for 1,000 cfs by the end of week 5 with westerly GIWW flows.

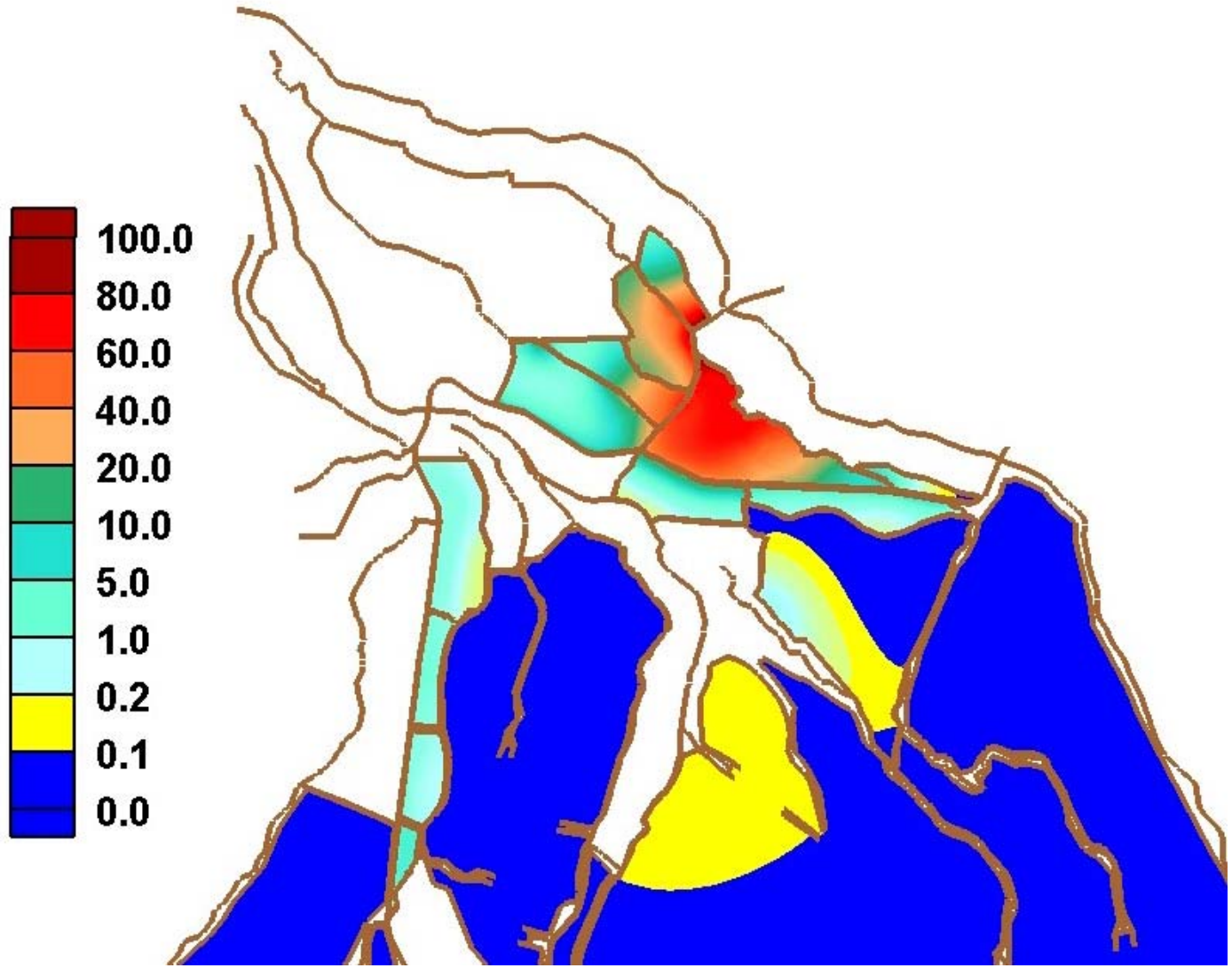

Figure B.54. Tracer distribution in the system for 1,000 cfs by the end of week 6 with westerly GIWW flows.

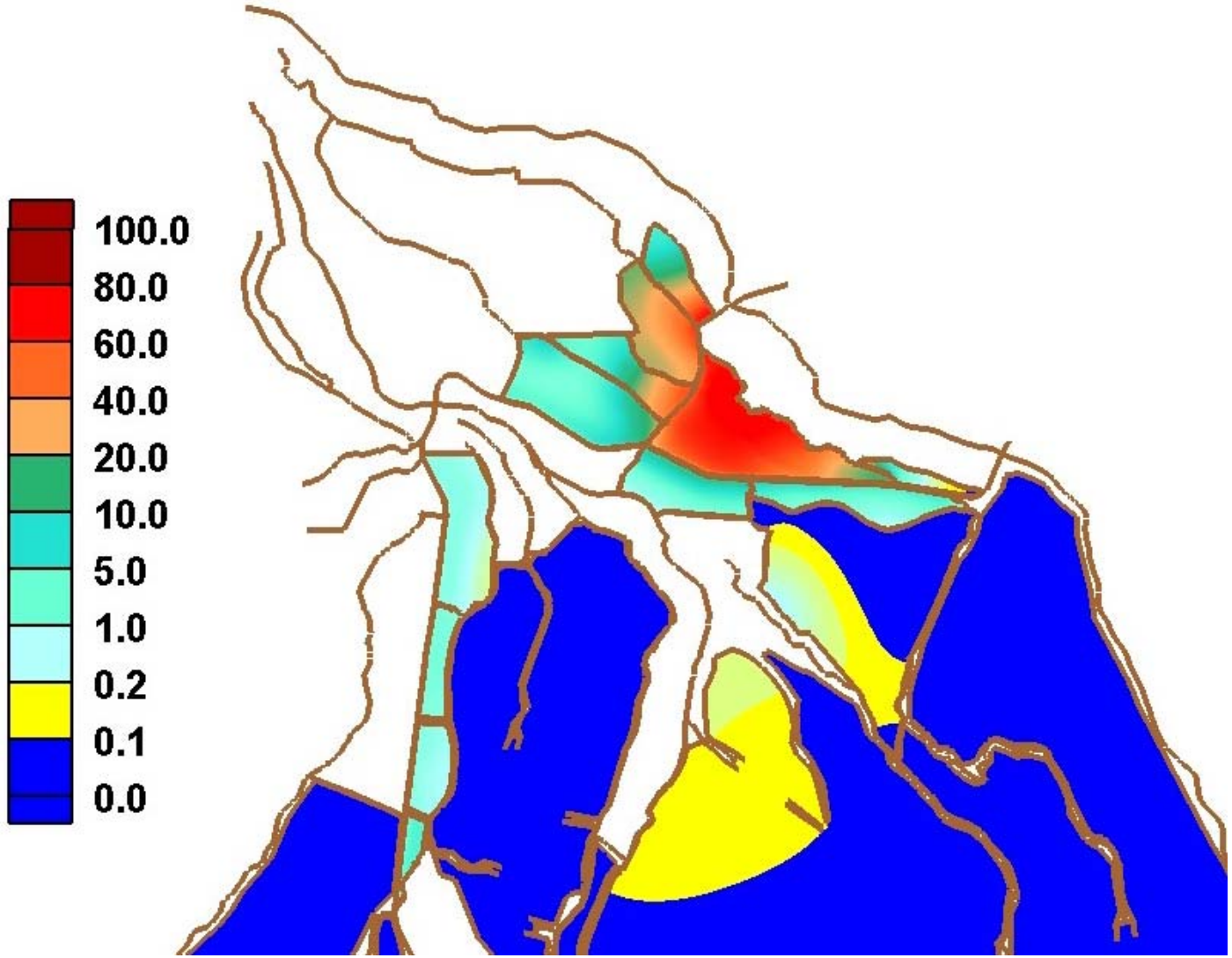

Figure B.55. Tracer distribution in the system for 1,000 cfs by the end of week 7 with westerly GIWW flows.

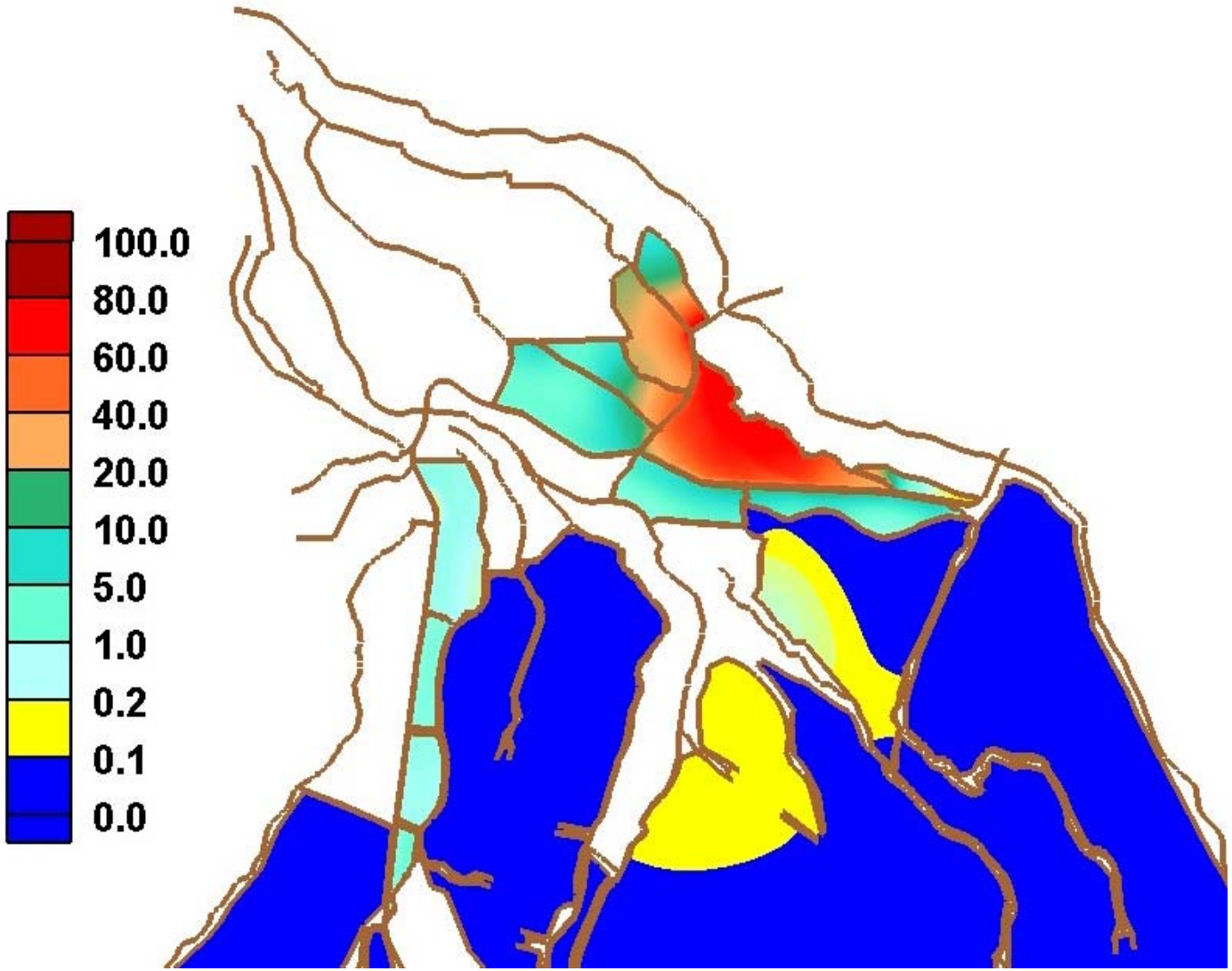

Figure B.56. Tracer distribution in the system for 1,000 cfs by the end of week 8 with westerly GIWW flows.